THE UNIVERSITY OF QUEENSLAND

AUSTRALIA

Reliability Impacts of Increased Wind Generation in the Australian National Electricity Grid

Mehdi Mosadeghy

B.Sc., M.Sc.

A thesis submitted for the degree of Doctor of Philosophy at

The University of Queensland in 2015

School of Information Technology and Electrical Engineering

Abstract

Wind power penetration has been consistently growing and it has been rapidly becoming a significant generation technology in many countries. However, the intermittent and variable nature of wind energy is a major barrier in wind power commitment. Wind speed fluctuations and unpredictability can affect the operation and reliability of power systems. Therefore, the impact of integrating large volume of wind generators on the system reliability needs to be carefully investigated and the reliability contributions of wind farms require to be evaluated for better integration of wind energy sources.

Because of intermittency and variability of wind energy, conventional reliability evaluation methods are not applicable and different techniques have been developed to model wind generators. However, most of these methods are time-consuming or may not be able to capture time dependency and correlations between renewable resources and load. Therefore, this research intends to improve the existing reliability methods and proposes a faster and simpler approach. In this approach, wind power and electricity demand are being modelled as time-dependent clusters, which not only can capture their time-dependent attributes, but also is able to keep the correlations between the data sets. To illustrate the effectiveness of this framework, the proposed methodology has been applied to the IEEE reliability test system. In addition, the developed technique is validated by comparing results with the sequential Monte Carlo technique.

Due to an increase in the wind power penetration level in Australia, this research also investigates the contribution of wind power in the Australian power system from reliability point of view. In order to calculate the reliability contribution of wind power, the proposed framework is implemented on the national electricity market at two different reliability assessment levels: generation and composite system levels. Moreover, the impacts of strategies such as coordinating hydro units with wind farms on the reliability of wind energy are investigated. Similar to wind energy, photovoltaic (PV) penetration level is increasing in the Australian power system, which can affect not only the reliability of the power system, but also the reliability benefit of wind farms. Therefore, in this thesis the impacts of solar energy on wind load carrying capability under different scenarios are also assessed.

Declaration by author

This thesis is composed of my original work, and contains no material previously published or written by another person except where due reference has been made in the text. I have clearly stated the contribution by others to jointly-authored works that I have included in my thesis.

I have clearly stated the contribution of others to my thesis as a whole, including statistical assistance, survey design, data analysis, significant technical procedures, professional editorial advice, and any other original research work used or reported in my thesis. The content of my thesis is the result of work I have carried out since the commencement of my research higher degree candidature and does not include a substantial part of work that has been submitted to qualify for the award of any other degree or diploma in any university or other tertiary institution. I have clearly stated which parts of my thesis, if any, have been submitted to qualify for another award.

I acknowledge that an electronic copy of my thesis must be lodged with the University Library and, subject to the policy and procedures of The University of Queensland, the thesis be made available for research and study in accordance with the Copyright Act 1968 unless a period of embargo has been approved by the Dean of the Graduate School.

I acknowledge that copyright of all material contained in my thesis resides with the copyright holder(s) of that material. Where appropriate I have obtained copyright permission from the copyright holder to reproduce material in this thesis.

Publications during candidature

Peer-reviewed Journal Papers:

1. Mehdi Mosadeghy, Ruifeng Yan and Tapan K. Saha, "Impact of PV Penetration Level on the Capacity Value of South Australian Wind Farms" *Renewable Energy (Elsevier)*, Accepted 25 July 2015, DOI:10.1016/j.renene.2015.07.072.
2. Mehdi Mosadeghy, Ruifeng Yan and T.K. Saha, "A Time Dependent Approach to Evaluate Capacity Value of Wind and Solar PV Generation" *IEEE Transactions on Sustainable Energy*, early access, DOI: 10.1109/TSTE.2015.2478518.
3. Ruifeng Yan, Tapan K. Saha, Nilesh Modi, Nahid Al-Masood and Mehdi Mosadeghy, "The combined effects of high penetration of wind and PV on power system frequency response" *Applied Energy (Elsevier)* 145 (2015) 320–330.

Peer-reviewed Conference Papers:

1. Mehdi Mosadeghy, Ruifeng Yan and Tapan K. Saha, "The Impact of Interconnectors on the Reliability Benefits of Wind Farms" Asia-Pacific Power and Energy Engineering Conference 2015, 15-18 November, 2015, Brisbane, Australia.
2. Mehdi Mosadeghy, Tapan K. Saha, Ruifeng Yan and Simon Bartlett, "Reliability Evaluation of Wind Farms Considering Generation and Transmission Systems" 2014 IEEE Power and Energy Society General Meeting, 27-31 July, 2014, Washington, DC, USA.
3. Mehdi Mosadeghy, Tapan K. Saha and Ruifeng Yan, "Increasing Wind Capacity Value in Tasmania Using Wind and Hydro Power Coordination" IEEE Power and Energy Society General Meeting, 21-25 July, 2013, Vancouver, British Columbia, Canada.

Peer-reviewed Conference Papers *(NOT INCLUDED IN THIS THESIS):*

4. Andres A. Recalde, Tapan K. Saha, and Mehdi Mosadeghy. "Reliability evaluation with wind turbines and photovoltaic panels." 2014 IEEE/PES Transmission and Distribution Conference and Exposition (T&D-LA 2014), Medellin, Colombia. 10-13 September 2014.

Abstract Conference paper *(NOT INCLUDED IN THIS THESIS):*

1. Mehdi Mosadeghy, Ruifeng Yan and Tapan K. Saha, "A New Methodology to Model Photovoltaic Systems in Reliability Assessment" 2015 Asia-Pacific Solar Research Conference, 8-10 Dec 2015, Brisbane, Australia.

Publications included in this thesis

1. Mehdi Mosadeghy, Ruifeng Yan and Tapan K. Saha, "Impact of PV Penetration Level on the Capacity Value of South Australian Wind Farms" Renewable Energy (Elsevier), Accepted 25 July 2015, DOI:10.1016/j.renene.2015.07.072.

   This paper is incorporated in Chapter 6.

Contributor	Statement of contribution
Mehdi Mosadeghy	Simulation and modelling (100%) Result interpretation and discussion (80%) Paper writing (80%)
Ruifeng Yan	Result interpretation and discussion (15%) Paper writing and review (15%)
Tapan K. Saha	Result interpretation and discussion (5%) Paper writing and review (5%)

2. Mehdi Mosadeghy, Ruifeng Yan and T.K. Saha, "A Time Dependent Approach to Evaluate Capacity Value of Wind and Solar PV Generation" IEEE Transactions on Sustainable Energy, early access, DOI: 10.1109/TSTE.2015.2478518.

   This paper is incorporated partially in Chapters 5 & 6 and mainly in Chapter 4.

Contributor	Statement of contribution
Mehdi Mosadeghy	Simulation and modelling (100%) Result interpretation and discussion (80%) Paper writing (80%)
Ruifeng Yan	Result interpretation and discussion (15%) Paper writing and review (15%)
Tapan K. Saha	Result interpretation and discussion (5%) Paper writing and review (5%)

3. Ruifeng Yan, Tapan K. Saha, Nilesh Modi, Nahid Al-Masood and Mehdi Mosadeghy, "The combined effects of high penetration of wind and PV on power system frequency response" *Applied Energy (Elsevier)* 145 (2015) 320–330.

   This paper is incorporated in Chapter 5.

Contributor	Statement of contribution
Ruifeng Yan	Simulation and modelling (70%) Result interpretation and discussion (40%) Paper writing and review (40%)
Tapan K. Saha	Result interpretation and discussion (20%) Paper writing and review (20%)
Nilesh Modi	Result interpretation and discussion (20%) Paper writing and review (15%)
Nahid Al-Masood	Simulation and modelling (20%) Result interpretation and discussion (10%) Paper writing (15%)
Mehdi Mosadeghy	Simulation and modelling (10%) Result interpretation and discussion (10%) Paper writing (10%)

4. Mehdi Mosadeghy, Ruifeng Yan and Tapan K. Saha, "The Impact of Interconnectors on the Reliability Benefits of Wind Farms" Asia-Pacific Power and Energy Engineering Conference 2015, 15-18 November, 2015, Brisbane, Australia.

   This paper is incorporated partially in Chapter 4 and mainly in Chapter 5.

Contributor	Statement of contribution
Mehdi Mosadeghy	Simulation and modelling (100%) Result interpretation and discussion (80%) Paper writing (80%)
Ruifeng Yan	Result interpretation and discussion (15%) Paper writing and review (15%)
Tapan K. Saha	Result interpretation and discussion (5%) Paper writing and review (5%)

5. Mehdi Mosadeghy, Tapan K. Saha, Ruifeng Yan and Simon Bartlett, "Reliability Evaluation of Wind Farms Considering Generation and Transmission Systems" 2014 IEEE Power and Energy Society General Meeting, 27-31 July, 2014, Washington, DC, USA.

   This paper is incorporated in Chapter 5.

Contributor	Statement of contribution
Mehdi Mosadeghy	Simulation and modelling (100%) Result interpretation and discussion (80%) Paper writing (80%)
Tapan K. Saha	Result interpretation and discussion (10%) Paper writing and review (10%)
Ruifeng Yan	Result interpretation and discussion (5%) Paper writing and review (5%)
Simon Bartlett	Result interpretation and discussion (5%) Paper writing and review (5%)

6. Mehdi Mosadeghy, Tapan K. Saha and Ruifeng Yan, "Increasing Wind Capacity Value in Tasmania Using Wind and Hydro Power Coordination" IEEE Power and Energy Society General Meeting, 21-25 July, 2013, Vancouver, British Columbia, Canada.

   This paper is incorporated partially in Chapter 4 and mainly in Chapter 5.

Contributor	Statement of contribution
Mehdi Mosadeghy	Simulation and modelling (100%) Result interpretation and discussion (80%) Paper writing (80%)
Tapan K. Saha	Result interpretation and discussion (10%) Paper writing and review (10%)
Ruifeng Yan	Result interpretation and discussion (10%) Paper writing and review (10%)

Contributions by others to the thesis

"No contributions by others."

Statement of parts of the thesis submitted to qualify for the award of another degree

"None"

Acknowledgements

Though only my name appears on the cover of this dissertation, many people have contributed to its production. I owe my gratitude to all the people who have made this work happen while a few words cannot express my appreciation for their help and support.

Firstly, I would like to express my sincere gratitude to my advisors Prof. Tapan Saha and Dr Ruifeng Yan for their continuous support during my PhD study, for their patience, motivation, and immense knowledge. Their guidance helped me in all time of research and writing of this thesis. I could not have imagined having better advisors and mentors for my PhD study.

I would like to acknowledge the financial support from my principal adviser Prof Tapan Saha and University of Queensland through UQI Scholarship. I would also thank my principal advisor and the School of ITEE for all supports including funding for attending conferences. I also acknowledge all the industry partners for their help and provision of data.

I thank my fellow officemates for the stimulating discussions, for the sleepless nights we were working together before deadlines, and for all the fun we have had in the last three years. Thanks to Ms. Maureen Shields and Ms. Mandeep Waraich for their help and hospitality. Thanks to Mr. Steve Wright for proofreading my thesis. I would also like to thank all of my friends especially Nadali, Jalil, Kapila and Ali who supported and incentivized me to strive towards my goal.

Special thanks go to my family. Words cannot express how grateful I am to my mother and father for all of the sacrifices that they have made for me. Their prayer for me was what sustained me thus far. I would also like to thank my sister Razieh, my brother in law Morteza and my brother Reza. They were always supporting me and encouraging me with their best wishes.

Keywords

Australian National Electricity Market (NEM), effective load carrying capability (ELCC), Monte Carlo simulation method, power system reliability, renewable energy, time-dependent clustering, wind capacity value.

Australian and New Zealand Standard Research Classifications (ANZSRC)

ANZSRC code:

090607, Power and Energy Systems Engineering (excl. Renewable Power), 50%

ANZSRC code:

090608, Renewable Power and Energy Systems Engineering (excl. Solar Cells), 50%

Fields of Research (FoR) Classification

FoR code: 0906, Electrical and Electronic Engineering, 100%

Table of Contents

List of Figures

List of Tables

Abbreviations

AEMC	Australian Energy Market Commission
AEMO	Australian Energy Market Operator
ARMA	Auto-regressive Moving Average
COPT	Capacity Outage Probability Table
DG	Distributed Generators
DNS	Demand Not Supplied
EENS	Expected Energy Not Supplied
ELCC	Effective Load Carrying Capability
FCM	Fuzzy C-means
FOR	Forced Outage Rate
HLI	Hierarchical Level I
HLII	Hierarchical Level II
IEEE	Institute of Electrical and Electronics Engineers
IEEE-RTS	IEEE Reliability Test System
LDC	Load Duration Curve
LOEE	Loss of Energy Expectation
LOLE	Loss of Load Expectation
LOLP	Loss of Load Probability
MCS	Monte Carlo Simulation
MTTF	Mean Time to Failure
MTTR	Mean Time to Repair
MW	Megawatt
NEM	National Electricity Market
NSW	New South Wales
PV	Photovoltaic
QLD	Queensland
RET	Renewable Energy Target
SA	South Australia
TAS	Tasmania
VIC	Victoria

Chapter 1

Introduction

1.1. Background and Problem Statements

1.1.1. Reliability Contribution of Wind Power

The use of wind energy is growing significantly and this clean energy continues to be the technology of choice in many countries around the world. Governmental support and policies are the most important motivations for the growth of the wind industry [1]. However, wind unpredictability and variability are the main barriers in its development and bring several challenges to power systems. Reliability, steady-state analysis, power system security and frequency regulation are some of the main technical issues that are influenced by wind integration [2]. The growth of wind energy in the electricity grid with its specific characteristics may add too much uncertainty to the system's reliability and affects its ability to supply electricity demand. Thus, it is important to understand the reliability contribution of wind farms and evaluate their actual capability to supply demand.

Reliability of an electric power system and its ability to supply electricity demand as continuously as possible is an important challenge and system operators and planners always attempt to improve it. There are three levels in reliability assessment studies: generation, transmission and distribution [3]. Hierarchical level 1 (HLI) is related to the sufficiency of the generation system to serve electric load. Hierarchical level 2 (HLII), which is also known as composite system level, studies the reliability of systems considering inadequacy and outages in both generation system and transmission network. In hierarchical level 3 (HLIII), the ability of power system facilities from the generation point to supply electricity demand is evaluated. However, because of the extreme scale of this level, HLIII is usually conducted only in the distribution facilities zone. The research described in this thesis focuses on the generation system and composite system studies.

Reliability assessment of power systems in the presence of wind generators is a main concern. As the characteristics of wind units are different from conventional generators, different approaches should be taken to model them and to evaluate their reliability contributions. Several probabilistic

and analytical methods have been developed in recent years to model wind power in reliability studies and to calculate their reliability benefits [4]–[9]. Negative load and time series [4], [5], multistate unit [6]–[8] and probabilistic distribution [9] are some of the popular models recently in use. The first group utilizes chronological techniques for reliability assessment. These techniques are capable of keeping correlations between wind and demand. However, their main drawback is extensive evaluation time, especially in the composite system studies. On the other hand, multistate and probabilistic models [6]–[9] are fast but may not be able to keep the chronological features and correlations between datasets. Although some studies presented techniques to keep the relevancies between wind generation and load data [10]–[14], these methods still face difficulties in modelling for systems with a large number of renewable units. For example, wind farms and demand data are modelled as three dimensional clusters in [12] to keep the correlations between them. However, by increasing the number of wind farms, the size of the matrix will grow and calculations will become complicated. Moreover, some of these approaches such as the non-iterative method presented in [14] are applicable only at the generation level and have not addressed the reliability assessment at the composite system level.

Therefore, to address the deficiencies of the previous studies and improve the existing methods, a time-dependent clustering approach is developed in this thesis. This methodology is capable of keeping the correlations and time dependency features of data sets and can be used to model both wind and solar generation. In addition, since this technique is using clustered data, it is efficient in the use of computational time and does not require a large amount of historical data. Another advantage of this method is its simplicity, even in networks with a large number of wind farms and solar units it will remain simple and fast. Furthermore, this framework is applicable to analyse the contribution of renewables at both generation and composite system levels.

1.1.2. Reliability Benefit of Wind Power in The Australian Market

Similar to other countries, renewable energy contribution in the Australian National Electricity Market (NEM) has been increasing. From all renewable energy resources, the share of wind power is the highest in the NEM. Total installed capacity of wind in this market by the end of 2014 was more than 3GW and is expected to increase to 11GW by 2020 [15]. Since the share of wind energy in the NEM is rising, its role in this electricity market is becoming more significant and will affect the reliability of this system. Therefore, comprehensive studies are required to investigate the impact of wind power on the reliability of the NEM network. Furthermore, to have a reliable system in the future, an accurate estimation of wind farms capability to supply electricity demand in this power system is crucial.

In order to calculate the reliability contribution of wind in NEM, a time-dependent approach is utilized to model wind power, electricity demand and exchanged power through interconnections. The main reason for applying this methodology is its advantages mentioned before. In particular, its time efficiency in the transmission level studies of large power systems in the Australian NEM, where the sequential methods might not be explicitly applicable and need significant computational time.

1.1.3. Impact of Solar Power on the Reliability Contribution of Wind

Moreover, solar photovoltaic (PV) penetration level has also been increasing in many power systems. The integration of solar units affects the demand profile and overall reliability level, and as a result the reliability contribution of wind farms will be affected. Several studies have proposed models for PV generators in reliability assessment and have evaluated electric system reliability in the presence of solar energy [16]–[18]. However, these works haven't considered wind generation in their studies and the reliability assessment has been performed for just PV panels.

In the case of studying the impact of solar energy on wind contribution, a few works have addressed the reliability of systems with wind and solar PV generators [13], [19]. However, they have considered both wind and PV together and have not studied the impact of PV generation on the reliability benefits of wind farms. Moreover, they have done the assessment only for small test systems. To our best knowledge, little or no study has evaluated the reliability benefit of wind and solar for a large scale realistic power system, and the influence of solar generation on the reliability contribution of wind energy has not yet been analysed.

To address these gaps and investigate the influence of solar energy on reliability benefits of wind generators, the South Australia (SA) power system has been selected as a case study. This system has the highest level of wind generation in Australia and also has a high penetration level of solar energy [20]. The time-dependent clustering methodology is applied to model wind, solar power and load data. Then the reliability contribution of solar power in this power system is evaluated and a sensitivity analysis is conducted to assess the influence of PV integration level on the reliability level of SA. In addition, the impact of PV panels on the reliability benefit of wind farms is analysed and the contribution of renewables in the future of this electricity network is investigated.

1.2. Thesis Objectives

This research aims to assess the impacts of integrated wind farms on the reliability of the Australian power system. The following objectives are investigated in this thesis:

1. Proposing a time-dependent clustering approach to address the drawbacks of current techniques in calculating the reliability contribution of wind farms.
2. Validating the proposed methodology and verifying its effectiveness by applying it on a standard test system and an Australian power system.
3. Studying the wind market in Australia and investigating the reliability contribution of wind power in the national electricity market at two different reliability assessment levels: generation system and composite system.
4. Investigating factors that can affect the reliability benefit of wind farms in different reliability assessment levels. Evaluating techniques such as hydro coordination to improve the reliability contribution of wind power.
5. Developing a method to analyse the influence of solar PV generators on the reliability benefit of wind farms. Verifying this method's effectiveness by applying it to an Australian power system. Validating its ability to capture seasonal impacts and the influence of correlations between wind regimes and solar pattern.

1.3. Thesis Structure

Following this chapter, the rest of the thesis is organized as follows:

Chapter 2 describes wind characteristics, power curve and capacity factor. A brief overview of global wind market was provided and the experiences of some leading countries in this industry are discussed and, government policies and supporting targets in these countries are reviewed. In addition, the current situation and the future of wind energy in the Australian NEM are presented and the importance of this research for NEM is explained.

Chapter 3 reviews reliability assessment models and techniques. Reliability assessment levels are defined and main reliability indices in these levels are described. Different models to simulate generating units, load and system risk in reliability studies are presented. The process of performing Monte Carlo simulation methods to estimate the reliability indices are explained using IEEE reliability test system (RTS).

Chapter 4 defines the capacity value term and reviews different techniques to calculate capacity value of wind power. Furthermore, several models to represent wind in reliability studies are

presented and their advantages and disadvantages are discussed. Then, the process of the proposed methodology to calculate the capacity value of wind power is explained and its effectiveness is examined for the IEEE-RTS system as a case study. Finally, outcomes have been compared with results of the sequential Monte Carlo technique to validate the accuracy of the developed approach.

Chapter 5 presents the capacity value of wind power in different regions of the Australian National Electricity Market. The reliability assessment has been conducted at generation and composite system levels. Furthermore, the impact of interconnections and interstate exchanged power on the capacity value of wind is evaluated. For this reason, the capacity value of wind farms in New South Wales and Victoria power systems, which have several interconnections, has been calculated in island and connected modes. Moreover, coordinating hydro units with wind farms in Tasmania to increase the capacity value of its wind power is investigated and different values are selected as the coordination capacity to analyse the impact of different coordination capacities on the reliability contribution of wind farms.

Chapter 6 provides an overview of solar energy in the NEM. Then, the proposed methodology to model solar power in reliability studies is explained. South Australia, which has high levels of wind and solar generation, is selected as the case study. The impact of solar PV on the capacity value of wind energy at the generation level of SA has been investigated. Furthermore, the contribution of renewable generators and the impact of solar energy in the future of South Australia are studied. In addition, seasonal impact and the influence of correlations between wind regimes and solar generation profile are analysed.

Chapter 7 provides a summary of the thesis findings and concludes the main contributions. In addition, possible future research is recommended in this chapter.

Chapter 2

Wind Energy

2.1. Introduction

Wind energy is becoming a matured technology and is growing dramatically all over the world. Governmental support and policies, which are established due to imperatives such as climate change, energy security and economic competitiveness, are the most important motivations for the growth in the wind industry [1]. For instance, the European Union (EU) has set a 20% renewable energy target in final energy consumption by 2020. The EU is also considering increasing it to 27% in the 2030 Climate and Energy package in order to meet the EU's greenhouse gas emissions reduction target. The Ministry of Energy in Japan started to support 50% of the cost of pre Environmental Impact Assessment (EIA) investigations. In Mexico the target is to have 9,500MW wind capacity by 2018 and 15,000MW by 2022 [21]. However, wind is unpredictable and variable in nature, which affects several aspects of power systems. Reliability, grid planning, steady-state analysis, power system security and frequency regulation are some of the technical issues that are influenced by wind integration [2]. The growth of wind energy in the electricity grid with its specific characteristics may add too much uncertainty to the system's reliability and affects its ability to serve a specific demand. Thus, it is important to understand the reliability contribution of wind energy and evaluate its real capability in supplying the demand.

In common with many other countries/regions, the penetration level of renewable generators in the Australian National Electricity Market (NEM) is growing rapidly. From all renewable energy resources, the role of wind power is expected to become more significant in NEM. Australia has seen an average 30% annual increase in installed wind power over the past decade and this trend is expected to continue [21]. The current installed capacity of wind power in NEM is around 3.8 GW [22]. Implementation of policies such as Renewable Energy Target (RET) [23] will be an important driver for renewable generation expansion over the next 10 years in Australia. The RET scheme aims to meet a renewable energy target of 33,000GWh by 2020, where for this purpose, an additional 6 GW renewable capacity in the NEM is required [24]. However, as the integration of wind power in this grid is increasing, more challenges are expected to rise in this power system and reliability is one of the main concerns [25]. Therefore, comprehensive studies are required to

investigate the impact of wind power on the reliability of the NEM. Furthermore, as wind turbines are going to replace conventional generators, accurate estimation of wind farms capability to supply the demand is crucial to having a reliable system in the future.

Therefore, in this chapter, the characteristics of wind power are described. Then an overview of global wind energy is provided and the experience of three different countries, namely: Denmark, Germany and USA, in integrating high levels of wind into the system is presented. Afterward, the current situation and the future of wind energy in the Australian National Electricity Market (NEM) are discussed and the importance of this research for NEM is explained.

2.2. Wind Characteristics

2.2.1. Wind Energy

The most obvious characteristic of wind is its fluctuation and unpredictability [26]. Variability is a main concern, especially for systems with a high level of wind generators, where the wind power fluctuations may become greater than the load and other generator variations. This variability will be different for different sites and depends on the wind regimes and the topography of the wind farm location. The relation between wind power and wind speed is nonlinear and therefore, the fluctuations in wind power is significantly different from that of wind speed [1].

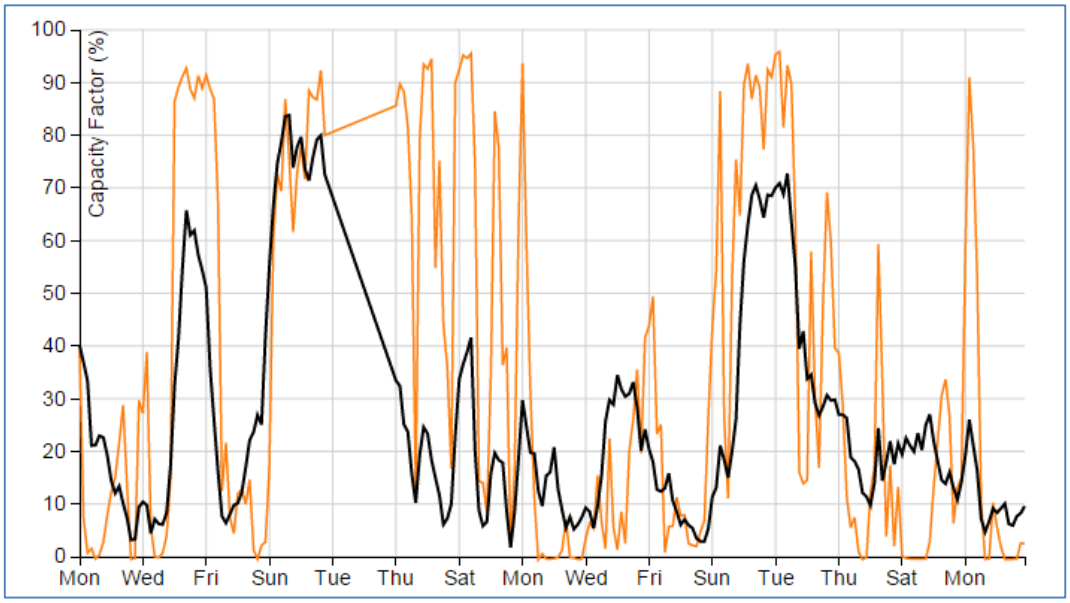

Figure 2.1.Variations in the generated power of an individual wind farm (Orange line) vs total wind generation in Australia (Black line) in June 2015.

Distributing wind turbines and aggregating wind farms across a large area may reduce the correlation between their wind patterns and hence, decrease the level of variability in the total output power of wind farms. Figure 2.1 displays the normalised variations of a sample wind farm

and total wind power in Australia for June 2015 [27]. It can be seen that the impact of aggregation is significant, and fluctuations in the total Australian wind generation is much lower than the output of the individual wind farm.

Unpredictability is also important and can affect power systems operation and reliability. Knowing the exact amount of power that wind farms are going to produce will make the operation and reliability maintenance of power systems much easier and more economical [15]. Forecasting over short time frames is not challenging as wind is relatively constant, even on an individual plant basis. However, providing an accurate long term prediction is a main concern. Aggregation over a large area will also improve forecasting performance [2].

2.2.2. Power Curve

The output power of a wind turbine is a function of wind speed and is related to specific values of wind speed and nominal capacity of the turbine. The relationship between generated power of a turbine and wind speed can be shown in a power curve. This curve depends on the characteristics of the wind turbine and values of cut-in, cut-out and rated wind speeds of the wind generator [26]. Figure 2.2 displays the power curve for a sample 3 MW wind turbine [28].

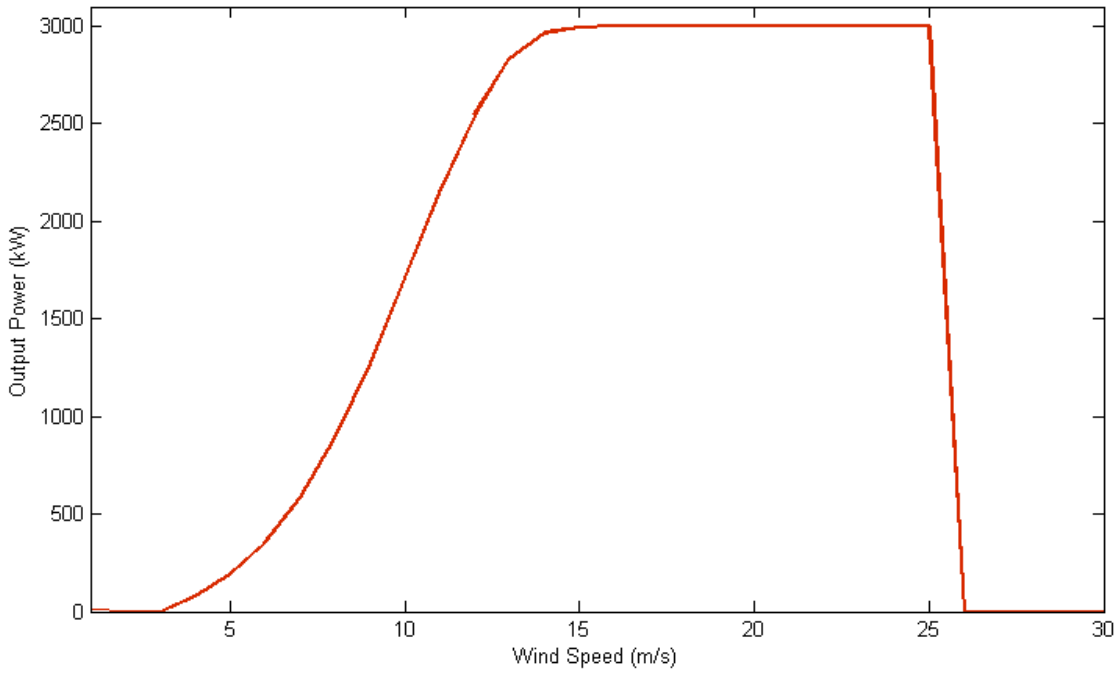

Figure 2.2. Power curve of a sample 3MW wind turbine

Cut-in wind speed is the speed at which the turbine starts to generate power. The wind turbine reaches its nominal capacity at the rated speed and stops generating power when the wind speed is blowing faster than the cut-out value. For the power curve demonstrated in Figure 2.2, the cut-in, rated and cut-out wind speeds are 3 m/s, 14 m/s and 25 m/s, respectively.

2.2.3. Capacity Factor

Capacity factor is the ratio of the mean power generated by a wind turbine in a period of time, to the installed capacity of the turbine [26]. This value depends on the wind regime and the type of the turbine. Capacity factor normally lies in the range of 25% to 40% [26] and can be different for different seasons or even different years [1]. The capacity factor of wind farms is lower than the one of conventional power plants like gas or coal generators.

This value can be calculated by means of (2.1) where, P_m denotes the mean power, x represents the available power production, $f_p(x)$ is the probability density function of total wind power and C_I is the total installed capacity of the wind farm.

$$CF = \frac{P_m}{C_I} = \frac{\int_0^{C_I} x f_p(x) dx}{C_I} \tag{2.1}$$

Another method to calculate the capacity factor is to divide the total amount of energy generated by a wind farm during a period of time by the maximum possible amount of energy it could have produced with its nominal capacity. The formula to calculate annual capacity factor of a wind farm using this method is given in (2.2).

$$CF = \frac{\sum_{t=1}^{8760} x_t}{C_I \times 8760} \tag{2.2}$$

where, x_t is the average output power of wind farm at hour t.

2.3. International Increase and Overview of Wind Energy

Wind power penetration in electricity grids has been increasing considerably and wind turbines are becoming one of the major electricity producers. Since the advent of these generators, every year more wind farms are integrated into the power system. 2014 was a record year for the wind industry and the wind market grew by almost 51 GW in this year. This growth was mainly driven by China, Germany and the US [21]. It was a significant growth in comparison to 2013, when universal installations were lower than 2012 and was just over 35.6 GW. The previous record belonged to 2012, when almost 45 GW of new wind farms were installed worldwide. Global annual installed wind capacity is displayed in Figure 2.3 [29].

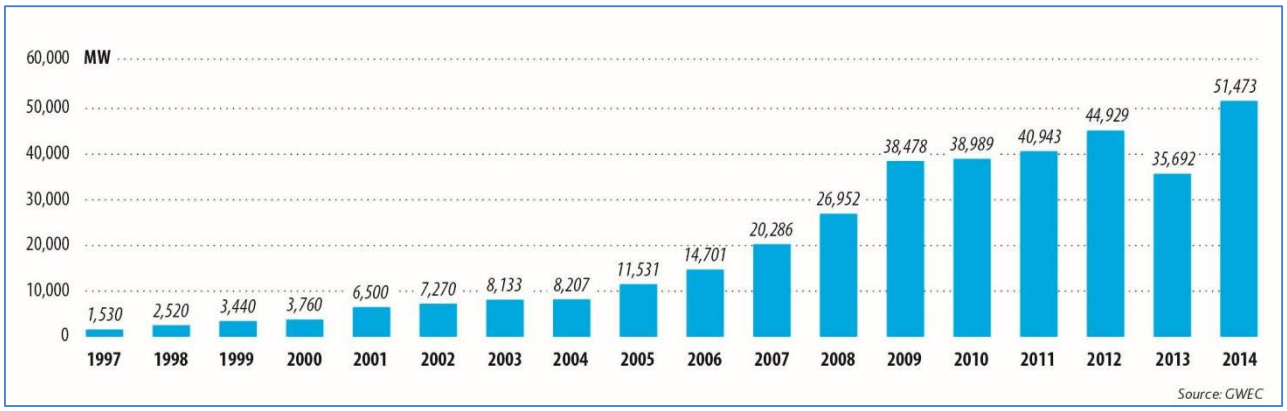

Figure 2.3. Global annual installed wind capacity 1997-2014 [29]

The global installed wind capacity is shown in Figure 2.4. It can be seen that in less than two decades, the contribution of wind energy in producing electricity has grown significantly from less than 8 GW in 1997 to around 370 GW by the end of 2014. This exponential trend is expected to continue and the universal cumulative wind capacity is expected to double by 2020 in a moderate scenario and rise to more than 700 GW [30].

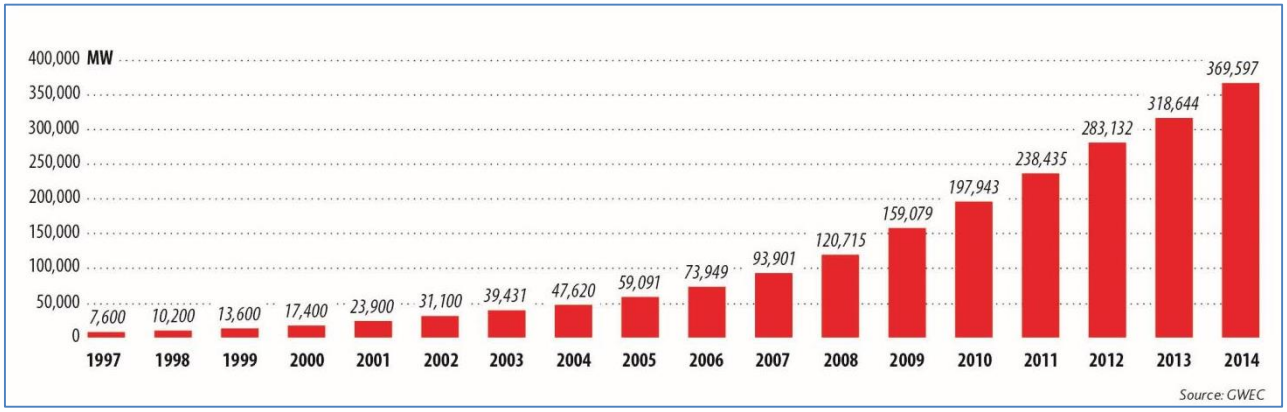

Figure 2.4. Global cumulative installed wind capacity 1997-2014 [29]

This increment in wind integration is a universal trend, however different countries have a different share of universal wind energy. The cumulative wind power capacity of the top ten countries in the world is given in Figure 2.5 [21]. It can be seen that China and USA together have almost 50% of total installed wind power in the world. Germany is in third place with more than 39 GW of wind farms and Spain, India, UK, Canada, France, Italy and Brazil are next in order. The total share of these ten countries in wind generation was more than 80% of the globally installed wind capacity at the end of 2014.

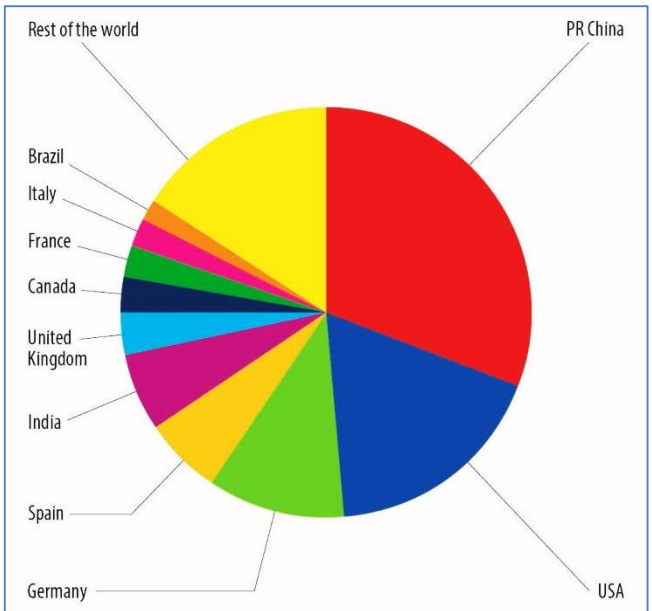

Country	MW	% SHARE
PR China	114,609	31.0
USA	65,879	17.8
Germany	39,165	10.6
Spain	22,987	6.2
India	22,465	6.1
United Kingdom	12,440	3.4
Canada	9,694	2.6
France	9,285	2.5
Italy	8,663	2.3
Brazil*	5,939	1.6
Rest of the world	58,473	15.8
Total TOP 10	**311,124**	**84.2**
World Total	**369,597**	**100**

** Projects fully commissioned, grid connection pending in some cases* *Source: GWEC*

Figure 2.5. Top 10 countries with highest installed wind capacity at Dec 2014 [21]

Details of regional installed wind generators in the world at the end of 2014 is provided in Table 2.1 [21]. It shows that in 2013, Europe had the highest wind capacity with more than 120 GW of wind farms. However, in 2014, wind energy in Asia increased significantly and by adding 26 GW of new wind turbines in this year, Asia reached first place with 141 GW of wind power by the end of 2014. This growth was mainly due to the huge installation of new wind farms in China, which led all countries in that year. China installed more than 23 GW of new wind farms in 2014, the highest annual added capacity for any country ever. The goal of China is to increase its wind capacity to 200 GW by the end of 2020. North America is ranked third in the size of its wind industry with 78 GW and other regions are following at a distance. By the end of 2014, Latin America & the Caribbean had 8.5 GW, Pacific region 4.4 GW and the size of total wind farms in Africa & the Middle East was around 2.5 GW [21].

Table 2.1: Global installed wind power capacity (MW) – Regional distribution [21]

		End 2013	New 2014	Total (End 2014)
AFRICA & MIDDLE EAST	Morocco	487	300	787
	South Africa	10	560	570
	Egypt	550	60	610
	Tunisia	245	-	245
	Ethiopia	171	-	171
	Cape Verde	24	-	24
	Other [1]	115	14	129
	Total	**1,602**	**934**	**2,535**
ASIA	PR China	91,413	23,196	114,609
	India	20,150	2,315	22,465
	Japan	2,669	130	2,789
	Taiwan	614	18	633
	South Korea	561	47	609
	Thailand	223	-	223
	Pakistan	106	150	256
	Philippines	66	150	216
	Other [2]	167	-	167
	Total	**115,968**	**26,007**	**141,964**
EUROPE	Germany	34,250	5,279	39,165
	Spain	22,959	28	22,987
	UK	10,711	1,736	12,440
	France	8,243	1,042	9,285
	Italy	8,558	108	8,663
	Sweden	4,382	1,050	5,425
	Portugal*	4,730	184	4,914
	Denmark	4,807	105	4,883
	Poland	3,390	444	3,834
	Turkey	2,958	804	3,763
	Romania	2,600	354	2,954
	Netherlands	2,671	141	2,805
	Ireland	2,049	222	2,272
	Austria	1,684	411	2,095
	Greece	1,866	114	1,980
	Rest of Europe [3]	5,715	835	6,543
	Total Europe	**121,573**	**12,858**	**134,007**
	of which EU-28 [4]	117,384	11,829	128,790
LATIN AMERICA & CARIBBEAN	Brazil**	3,466	2,472	5,939
	Chile	331	506	836
	Uruguay	59	405	464
	Argentina	218	53	271
	Costa Rica	148	50	198
	Nicaragua	146	40	186
	Honduras	102	50	152
	Peru	2	146	148
	Carribean [5]	250	-	250
	Others [6]	55	28	83
	Total	**4,777**	**3,749**	**8,526**
NORTH AMERICA	USA	61,110	4,854	65,879
	Canada	7,823	1,871	9,694
	Mexico	1,917	634	2,551
	Total	**70,850**	**7,359**	**78,124**
PACIFIC REGION	Australia	3,239	567	3,806
	New Zealand	623	-	623
	Pacific Islands	12	-	12
	Total	**3,874**	**567**	**4,441**
	World total	**318,644**	**51,473**	**369,597**

Source: GWEC

1 *Algeria, Iran, Israel, Jordan, Kenya, Libya, Nigeria*
2 *Bangladesh, Mongolia, Sri Lanka, Vietnam*
3 *Bulgaria, Cyprus, Czech Republic, Estonia, Finland, Faroe Islands, FYROM, Hungary, Iceland, Latvia, Liechtenstein, Lithuania, Luxembourg, Malta,Norway, Romania, Russia, Switzerland, Slovakia, Slovenia, Ukraine*
4 *Austria, Belgium, Bulgaria, Cyprus, Croatia, Czech Republic, Denmark, Estonia, Finland, France, Germany, Greece, Hungary, Ireland, Italy, Latvia, Lithuania, Luxembourg, Malta, Netherlands, Poland, Portugal, Romania, Slovakia, Slovenia, Spain, Sweden, UK*
5 *Caribbean: Aruba, Bonaire, Curacao, Cuba, Dominica, Guadalupe, Jamaica, Martinica, Granada, St. Kitts and Nevis*
6 *Bolivia, Colombia, Ecuador, Venezuela*

Note:
Project decommissioning of approximately 523 MW and rounding affect the final sums
*** Provisional figure**
**** Projects fully commissioned, grid connection pending in some cases**

2.3.1. Denmark

Denmark is one of the leading countries in the contribution of wind power in supplying total demand. In 2014, around 39% of the electricity load in Denmark was served by wind power. By the end of 2014, this country had 4,883 MW of installed wind turbines. Electricity demand in Denmark varies between 2,100 MW and 6,300 MW, and the share of wind power in supplying load is expected to go up to 60% by 2021. This system also has 4,200 MW of central power stations, 2,300 MW of combined heat and power (CHP) units and 575 MW of Solar PV systems. Around 75% of Denmark's wind farms are onshore (3,612 MW) and 1,271 MW of its wind capacity is from offshore plants. Figure 2.6 displays the development of onshore and offshore wind farms and the contribution of wind energy in total energy consumption from 1990 until 2014 and expectations till 2021. It can be seen that the share of wind is expected to grow further and the contribution of offshore wind farms will increase.

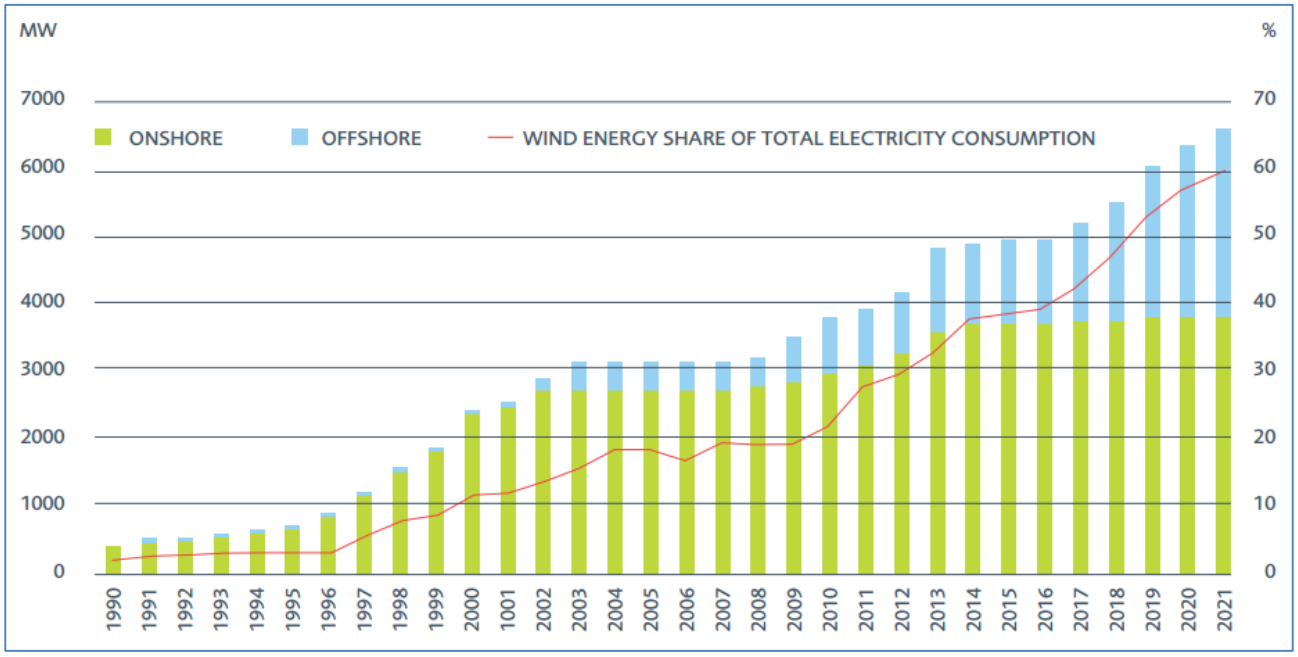

Figure 2.6. Development of Danish wind energy [31]

These values are the average, indeed in some occasions generated wind power may exceed demand in Denmark. For instance, at 3am on 10 July 2015, wind farm production was as high as 140% of the Danish domestic demand and therefore, a significant share of it was exported to Germany, Norway and Sweden through interconnectors [32].

2.3.1.1. Latest Policy and Future Wind Energy Development in Denmark

Around 200MW of onshore wind farms are expected to be installed by 2015, while there will be no more offshore wind farms in Denmark before the period of 2017-2020 [21]. The wind energy target for Denmark, established in March 2012, is to supply 50% of its electricity consumption from

wind energy by 2020. With current wind generation in the Danish power system, this goal is expected to be reached well before the target date of 2020. The long term plan for Denmark is to serve 100 % of its total energy demand by renewable energy by 2050 [33].

The main challenge in the future of the Danish grid will be to provide an adequate technical and regulatory framework for the continuation of the integration of wind energy in the system. This framework should include the construction of new interconnectors to neighbouring countries and implementing more wind power in the district heating system [21].

2.3.2. Germany

Germany has the highest installed wind capacity in Europe and third place globally. Its wind generation capacity at the end of 2014 was 39,165 MW, of which more than 5,000 MW was installed in 2014 [21]. The majority of Germany's wind farms are onshore and the size of its offshore plants in 2014 was 1,049 MW. The German grid has a maximum peak load of 82 GW [34]. Renewables supplied more than 25% of electricity demand in Germany in 2014, where the share of wind power was around 9% [21]. In 2014, for the first time renewable energy has been the major source in Germany's electricity generation with around 83 GW of installed capacity. During several days in 2014, renewables made up nearly 75% of peak power demand in Germany [35]. Fossil fuel generators were the second source of electricity with the capacity of about 82 GW. This power system also has more than 10 GW of hydro generators and 12 GW of nuclear power plants [34].

Total installed wind capacity in Germany for the last fourteen years is illustrated in Figure 2.7. It shows that the wind industry has experienced a significant growth in this period and wind power in Germany has gone up sevenfold. It can also be observed that the growth rate in 2014 was the highest and this year was a record in integrating new wind farms.

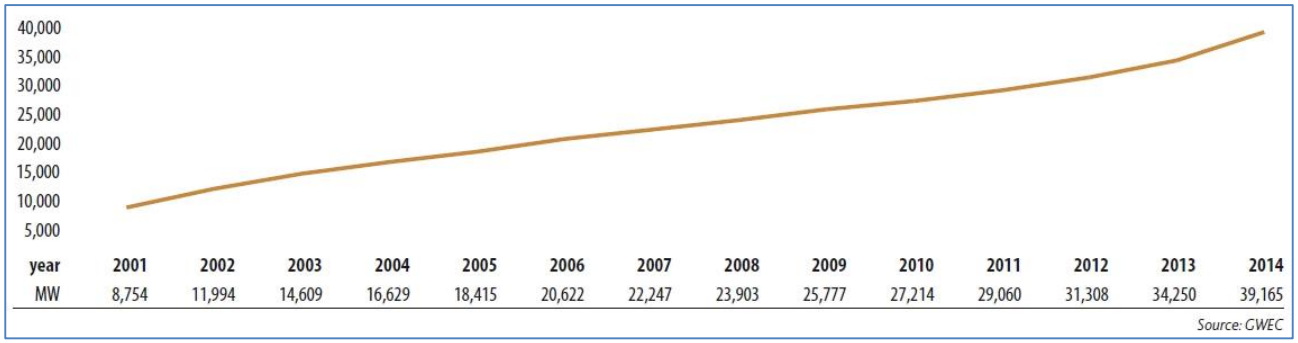

Figure 2.7. Total installed wind capacity in Germany [21]

2.3.2.1. Latest Policy and Future Wind Energy Development in Germany

The Renewable Energy Sources Act (EEG), which was introduced in 2000, provides support for wind energy in Germany. In 2014, the EEG was revised and new targets for renewables were

defined. The new target is to achieve a 40 to 45% share of renewables by 2025, and 55 to 60% by 2035 and a minimum of 80% by 2050 [30].

In 2015, around 3,500 MW to 4,000 MW of new wind farms are expected to be installed in Germany and almost half of this will be offshore wind farms. Although installation levels will stay high, the growth rate is expected to slow down in 2016 and future developments will depend on the timing and improvements in the German system [21].

The main barrier in the future growth of wind power in Germany is system optimisation and transmission network development, especially for offshore wind. Technical and environmental regulatory issues, such as rare species and turbine locations have delayed some wind farm construction projects [21].

2.3.3. USA

Currently, the United States has the second highest installed wind power capacity in the world with more than 65 GW of wind farms at the end of 2014. This clean source of energy has become one of the main electricity producers in the US market due to a significant development in recent years [21]. Although the US has a high level of wind energy, fossil fuel generators are still the major electricity producer with more than 870 GW capacity. Nuclear power and conventional hydro with about 104 GW and 79 GW capacity respectively have the next places in the US generation mix [36]. The share of wind power in total electricity production of USA is around 5.5%. This is almost equal to 8% of the maximum peak demand in 2014, which was around 770 GW [36]. However, as a result of continued technological improvement and domestic manufacturing, wind has become one of the most affordable sources of electricity in the US and its share in electricity production is growing rapidly. Figure 2.8 depicts the development of wind energy in the USA since 2001. From 2005 to 2012, due to supporting policies the wind industry grew dramatically and saw 800% growth in this period and average annual growth was around 31%. The record in wind energy expansion belongs to 2012, when more than 13GW of new wind farms were installed [21].

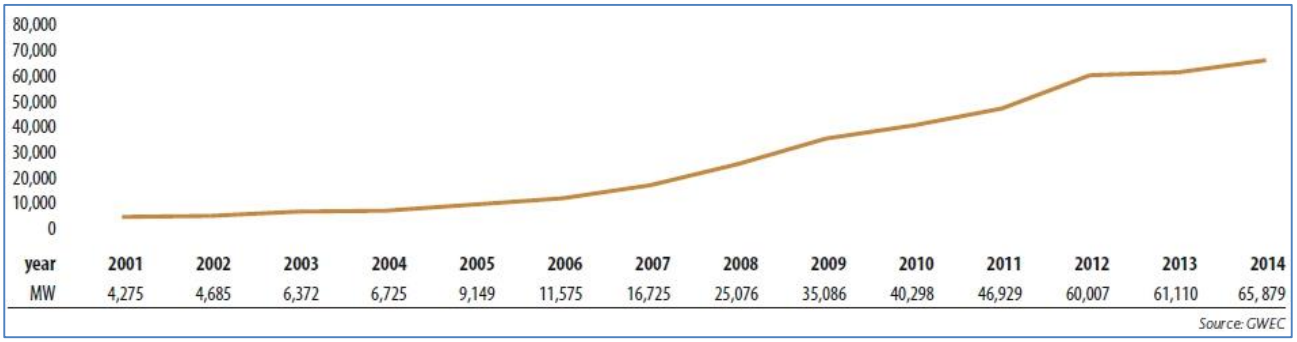

Figure 2.8. Total installed wind capacity in USA [21]

The share of different states in total wind capacity of the US is different. Texas with more than 15 GW has the largest wind industry in the USA. The size of the wind market in all states is displayed in Figure 2.9 [37]. After Texas, California and Iowa are the leading states in producing electricity from wind with 6,018 MW and 5,708 MW wind capacity, respectively.

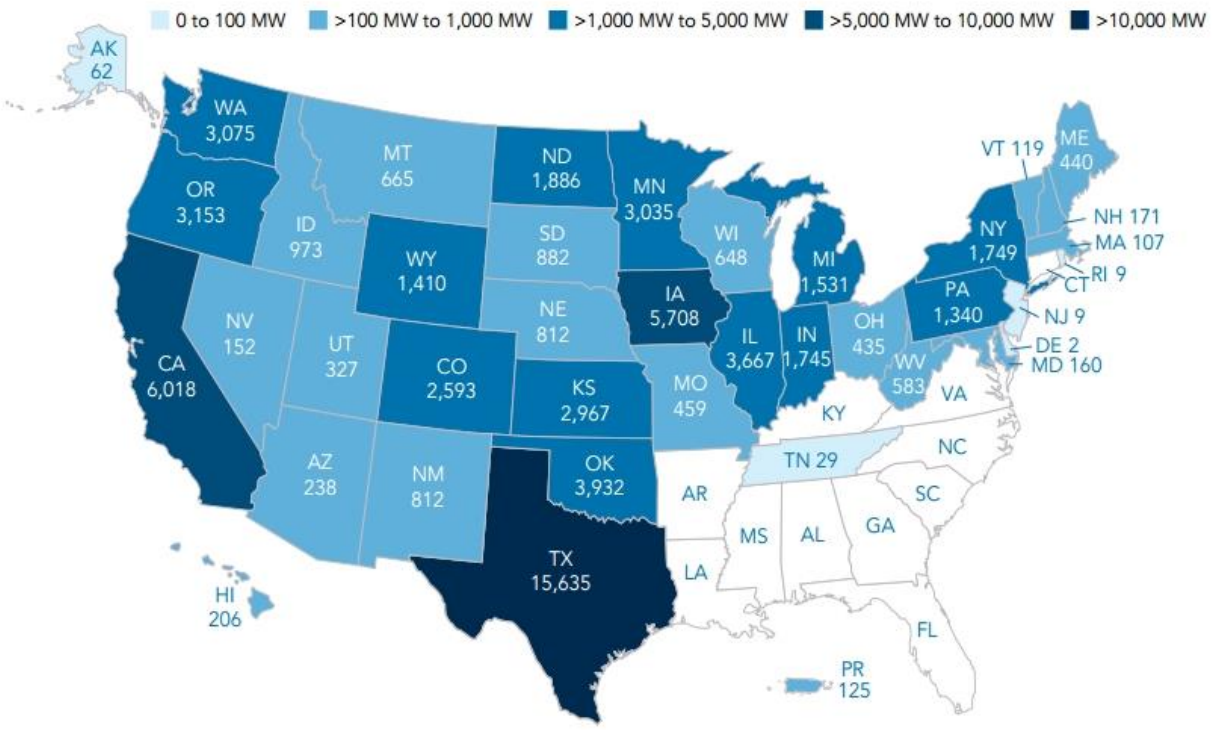

Figure 2.9. USA wind power installation by state [37]

2.3.3.1. Latest Policy and Future Wind Energy Development in USA

The federal Production Tax Credit (PTC) which has reduced the cost of wind is the main incentive policy in the US. However, this credit usually expires and is extended for one and two years. Therefore, the uncertainty and the frequent expirations in the PTC have affected the growth rate in the US wind development. In 2015, the US Department of Energy released its Wind Vision report which claims that the capacity of wind power can supply 10% of the US electricity consumption by 2020, and then its contribution should double and become 20% by 2030. It also predicts that wind energy can supply 35% of the electricity demand by 2050 [38].

2.4. Wind Power in The Australian National Electricity Market

The Australian National Electricity Market's (NEM) electricity grid is operated by Australian Energy Market Operator (AEMO) and includes the Eastern and South Eastern states of Australia: New South Wales (NSW), Queensland (QLD), South Australia (SA), Victoria (VIC) and Tasmania (TAS). This network is primarily dominated by Alternating Current (AC) with some High Voltage

Direct Current (HVDC) interconnections. Like other countries, the contribution of wind power in some Australian states (e.g. South Australia) is growing and it is becoming one of the major electricity producers. In this section, a brief overview of the NEM is presented and the current role of wind energy in this market and the future of wind power in Australia are discussed.

2.4.1. National Electricity Market

Currently, coal is the main source of electricity in Australia and gas is the second highest source of generation. Total generation capacity of NEM in 2014 was about 48 GW, whereas the share of these fossil fuels together was more than 75 per cent. Amongst clean technologies, hydro and wind had the highest generation capacities with 7,987 MW and 3,144 MW respectively [39]. Although the contribution of solar energy in the generation system and high voltage network was small, the share of this renewable source at the distribution level was significant and at the end of 2014, there were more than 4,100MW of rooftop photovoltaic systems in Australia [40].

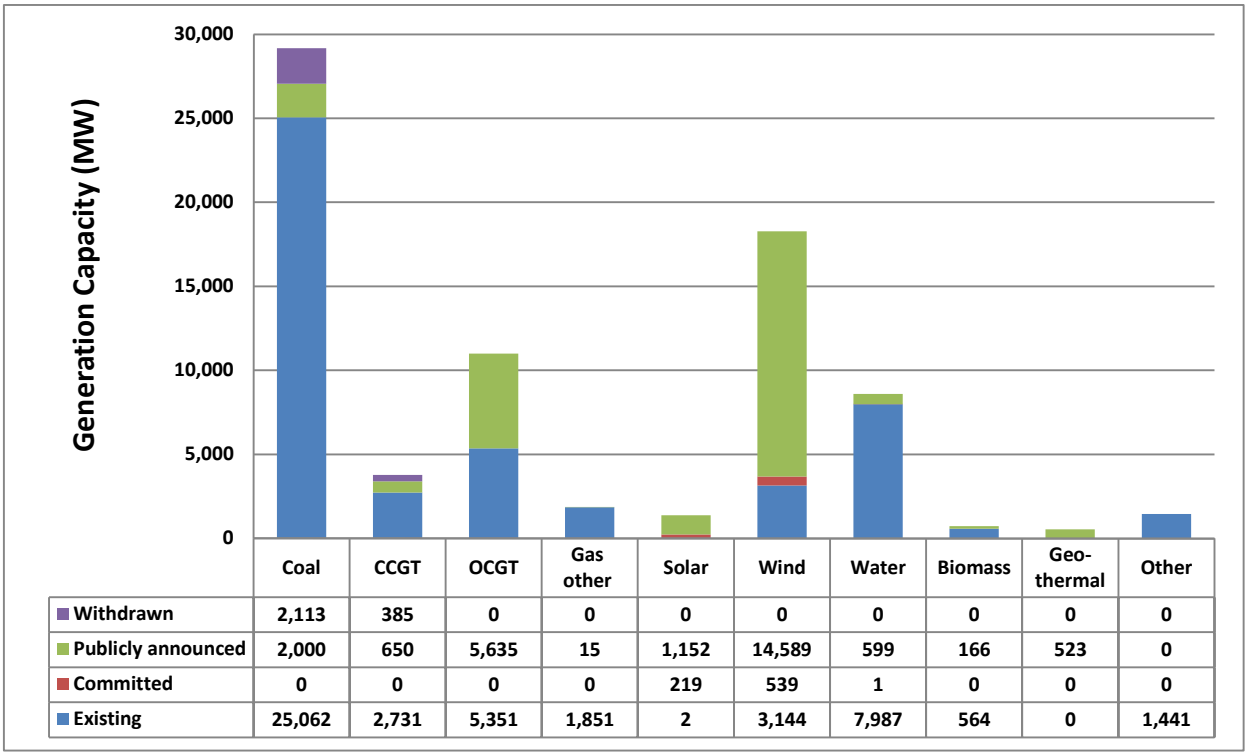

	Coal	CCGT	OCGT	Gas other	Solar	Wind	Water	Biomass	Geo-thermal	Other
Withdrawn	2,113	385	0	0	0	0	0	0	0	0
Publicly announced	2,000	650	5,635	15	1,152	14,589	599	166	523	0
Committed	0	0	0	0	219	539	1	0	0	0
Existing	25,062	2,731	5,351	1,851	2	3,144	7,987	564	0	1,441

Figure 2.10. Generation capacity of National Electricity Market in 2015 [39]

The generation mixture of NEM at the end of 2014 is presented in Figure 2.10. This graph shows the share of all energy sources in this market and the changes in their future contributions including new installations and withdrawn projects. As can be seen from this graph, most of the committed projects which, will be added to NEM in the near future, belong to renewables. A new project is defined as committed if it meets all of the following AEMO criteria [25]:

- All land has been acquired.
- Contracts for supply of major components are finalised.

- All planning and environmental approvals have been obtained.
- Financing arrangements are finalised.
- Project construction has commenced or a date for commencing construction has been set.

Publicly announced proposals represent generation at an early stage of development that has satisfied less than three commitment criteria [25].

As the capacity of renewables is growing in Australia, conventional fossil fuel generators are expected to be mothballed and replaced by clean technologies. Coal power plants are the first nominees for retirement as they are highly pollutant and disperse harmful gases into the air. In the National Transmission Network Development Plan [41], the following coal plants are projected to be retired by 2020.

Table 2.2: Retired power plants in NEM by 2020 [41]

Region	Fuel Type	Capacity (MW)
QLD	Black coal	190
NSW	Black coal	1,644
VIC	Brown coal	884
SA	Brown coal	240
Total		2,958

Electricity demand growth in Australia has decreased in recent years due to several reasons such as lower manufacturing activities due to higher labour cost, after effect of global financial crisis, usage of energy efficiency technologies by most sectors and the integration of solar panels. However, maximum load is predicted to increase again in the near future [42]. The maximum value of electricity loads for different regions of NEM for the last three years are given in Table 2.3. In all states, the maximum peak demand happens during the summer except Tasmania, where the maximum load occurs in the winter. New South Wales has the highest demand and for many years Victoria had been following that. However, since 2014 Queensland has taken over the second place and is expected to keep this place for several years [42].

Table 2.3: Maximum demand of NEM regions from 2012 till 2015 [42]

	New South Wales	Queensland	South Australia	Tasmania	Victoria
2012 – 2013	13,892	8,479	3,095	1,599	9,774
2013 – 2014	12,027	8,374	3,281	1,683	10,313
2014 – 2015	11,883	8,831	2,872	1,656	8,626

As the wind generation in the NEM is developing fast, the share of wind farms in supplying demand will increase. Indeed, in South Australia currently there are some hours when generated wind power exceeds the instantaneous demand [15]. These hours are expected to increase as the wind level in SA is expected to grow by around 70% by 2020. Similar to SA, Tasmania will face the same issue in the near future, i.e. expecting to face occasions where the wind generation becomes higher than the electricity load. However, other states; NSW, VIC and QLD, are not expected to experience this exceedance until after 2030 [15].

2.4.2. Wind Power in NEM

Wind energy is maturing in Australia and its total wind capacity has increased from around 73 MW in 2001 to over 3,800 MW at the end of 2014.. This growth has been consistent and every year Australian wind generation has increased around 30%. The increment in total installed capacity of wind power in Australia is drawn in Figure 2.11.

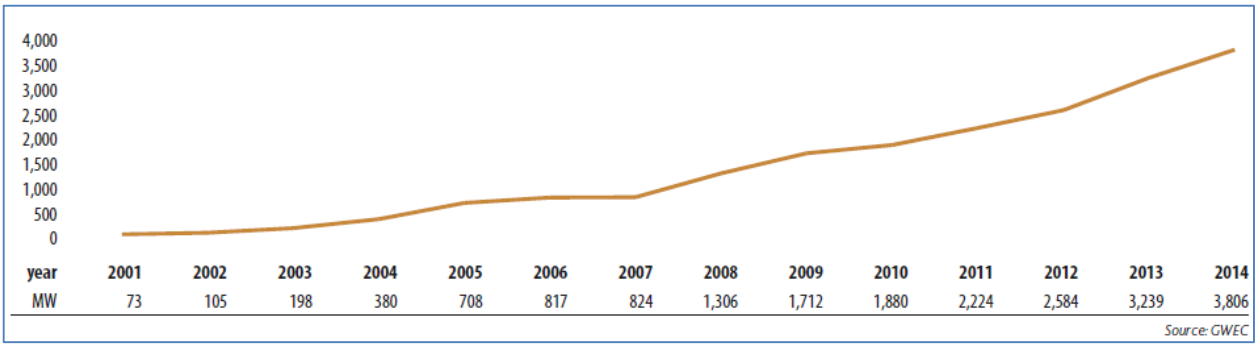

Figure 2.11. Total installed wind capacity in Australia [21]

It can be seen that Australia's wind industry had a strong year in 2014 with the addition of 567 MW of new wind farms. This was the second largest annual growth compared to 2013, where 655 MW of new wind projects were completed [21].

Australian wind farms are mostly distributed along its Southern coastline and to the West, which are the regions with the most favourable wind resources. Predicted wind speed in Australia is demonstrated in Figure 2.12 [43]. It shows that Australia has an excellent wind resource, particularly in Tasmania, South Australia and Western Australia.

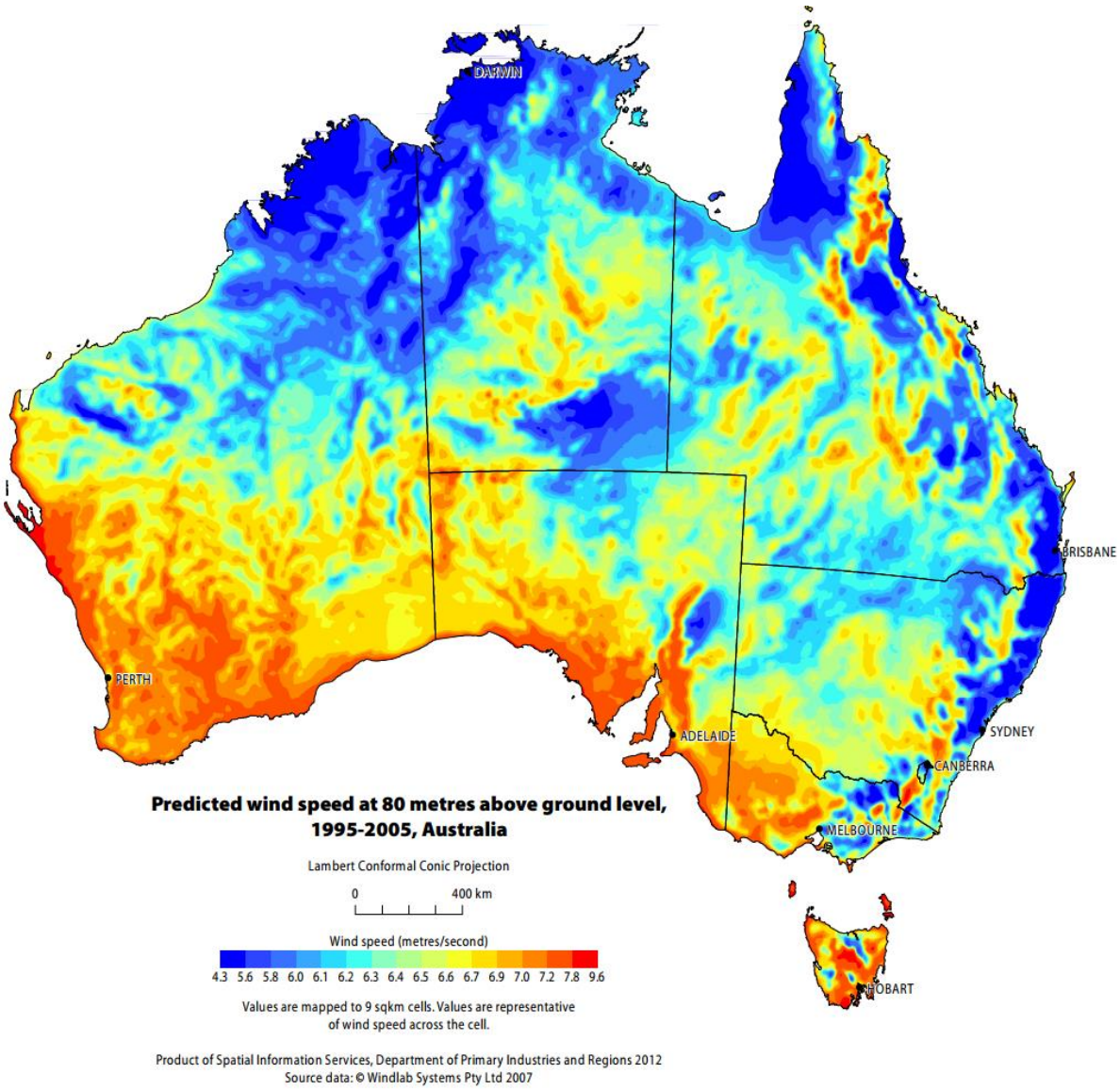

Figure 2.12. The potential of wind energy in Australia [43]

At the end of 2014, there were more than 3,200 MW wind farms in NEM, and South Australia accounts for almost half of the share of this market [25]. This state generated more than 33% of its electricity from wind energy between 2013 and 2014 [15]. All the regions in NEM have several wind farms except Queensland, which has only one small wind farm. The capacity of other regions and their wind generation levels is different. Victoria has the second largest wind capacity in Australia and is expected to become the largest one by 2020 with about 5GW of wind farms. The share of NSW was not that high, however new wind farms were added to this state and its capacity rose to 559 MW by May 2015 [39]. Although the installed wind capacity in Tasmania is not that high in terms of megawatts, its contribution is almost equal to 20% of the maximum demand of this island. Details of the wind capacity of all states in NEM and the projected values in 2020 are given in Table 2.4.

Table 2.4: Installed wind capacity of NEM in 2014 and 2020 [39], [15]

Region	Existing Wind (MW)	2020 Wind (MW)
New South Wales	281	2,382
Queensland	12	266
South Australia	1,473	2,555
Tasmania	308	1,368
Victoria	1,070	4,974

2.4.2.1. Latest Policy and Future Wind Energy Development in Australia

The Australian Government's Renewable Energy Target (RET) is a national scheme supporting investment in renewable energy technologies [23]. As wind power is one of the lowest cost technologies, it has been the dominant form of renewable generation to receive support under the RET. This target was introduced in 2001 to support renewable energy development [44]. At the beginning, the aim of this policy was to supply at least 20% or more than 41,000 GWh of Australia's electricity demand from renewable sources by 2020. Since then however, the electricity load growth rate has decreased and it seems that with this target by 2020 the share of renewable resources may overshoot the 20 percent [21]. In 2015, this policy was revised by the Australian Government and the new target is to provide 33,000 GWh in 2020. This means by 2020 around 23.5% of Australia's generation will be from renewables which is double in comparison to the current levels [23].

Recent changes in the RET have brought uncertainty to the wind industry and put investors at more risk. However, in the latest revision, it is agreed that the 33,000 gigawatt hour renewable energy will be required by 2020 to meet the target in the changed load growth scenario. This will give the renewable energy industry the certainty it needs to grow [23].

RET includes two main schemes: small-scale renewable energy scheme (SRES) and large-scale renewable energy target (LRET). The LRET provides financial incentives for large renewable energy power stations, such as wind and solar farms or hydro-electric power stations. While, the SRES scheme supports owners to install eligible small-scale renewable energy systems such as rooftop solar, solar water heaters, heat pumps, and small-scale wind and hydro systems [23].

2.4.3. The Importance of This Work for NEM

Since the integration level of wind power is increasing significantly, more uncertainty and risk is expected to be introduced to the system, in particular to system adequacy and reliability. The intermittent nature of wind energy may affect the ability of power systems to supply demand with high levels of confidence. For systems like Australia where conventional generators are expected to retire and be replaced with wind power plants it is especially so. Therefore, it is important to evaluate the capability of wind farms in supplying demand without reducing the reliability of the system. In other words, the equivalent amount of wind power to replace conventional fossil fuel generators should be estimated precisely in order to avoid generation inadequacy in the future.

Moreover, since wind farms are often located in remote areas and far from load centres, the impact of the transmission system on the added value of wind energy should be investigated. This is necessary not only for transmission expansion planning but also to have an appropriate estimation of how much load wind farms can serve considering grid constraints and outages. Hence, a proper model is required to study the reliability impacts of wind power plants at the transmission level. Modelling interconnections in reliability assessment is crucial and can affect the results. In addition, because of significant growth in solar generation the load pattern of NEM's regions is changing. As a result of this change, the reliability contribution of wind farms may vary.

Therefore, this research is investigating the reliability impacts of wind farms on the national electricity market. The ability of wind farms in the NEM to supply the demand without increasing the unreliability of this power network is evaluated. Furthermore, the impact of the transmission system is assessed and different models are considered to study the influence of the interconnectors between the NEM's regions. In addition, the influence of solar generation on the reliability benefits of wind power in the national electricity market is evaluated.

2.5. Summary

In this chapter, wind characteristics were described, and power curve and power factor terms were defined. A brief overview of the global wind market was provided and the experiences of some leader countries in this industry, namely Denmark, Germany and USA were discussed. Government policies and supporting targets are the main drivers for wind development in these countries and some technical developments are required for their future networks where high levels of wind are expected to be integrated.

The Australian wind industry is rapidly developing as well, and according to the Australian Government RET scheme, renewables are expected to generate 33,000 GWh electricity by 2020.

This means more than 23% of demand in NEM will be served by clean generators and wind will have the highest share in the near future. As more and more wind generation is integrated into the grid, more conventional generators will be retired. This replacement will need to be managed carefully to ensure the adequacy and reliability of the power system. Therefore, the actual capability of wind farms to supply demand reliably should be evaluated. Furthermore, the impact of several factors, such as transmission system constraints and changes in load pattern due to rooftop photovoltaic systems, on the reliability benefits of wind energy should be investigated.

Because in most cases generation adequacy assessment is conducted using reliability measures and indices, evaluation of wind load carrying capability using reliability techniques is the most accurate and recommended calculation method. In the next chapter basics of power system reliability are provided, important reliability indices are described and different methods to calculate these indices are explained.

Chapter 3

Reliability Assessment

3.1. Introduction

Due to the failure of equipment and network elements in power systems, the electricity network may not be able to fulfil its main function, which is to supply electricity demand with an acceptable degree of reliability and as economically as possible. Failure of power system components is usually outside of the control of system engineers and can lead to interruptions, which can affect a wide range of customers from small residential loads to major industrial/commercial demands [45]. Therefore, reliability of an electric power system and its ability to supply electricity demand as continuously as possible is an important challenge, and system operators and planners try to improve it. Thus, power system reliability assessment has been widely developed and a wide range of indices and methodologies have been proposed to evaluate the reliability level of a power system.

Reliability evaluation of power systems can be divided into two main classes of system adequacy and system security [45]. System adequacy assessment is related to the sufficiency of the system facilities to supply the electricity demand, which includes the capability of generation units to produce enough electricity and the ability of transmission and distribution networks to deliver the generated power to the load point. System security, on the other hand, indicates the ability of the system to respond to disturbances arising within the system and is associated with system dynamic and transient disturbances.

There are two main techniques to evaluate the system adequacy: analytical and simulation [46]. Analytical methods construct mathematical models for a system and calculate the reliability indices by means of mathematical solutions. Simulation techniques, such as Monte Carlo, on the other hand estimate the system insufficiency by simulating the real process and system behaviour using statistical approaches. Simulation methods simulate the system in a series of experiments. Both of these methodologies have advantages and disadvantages. Analytical methods are more accurate and more efficient in small grids, however they may become complex for large systems [47]. While, in Monte Carlo simulation techniques the number of samples to obtain an accurate result is independent of the size of the system and is suitable for large systems. Moreover, analytical

techniques (Section 3.2.1.5), unlike simulation methods, are not capable of simulating probability distribution of element failure and repair activities [47].

Reliability assessment studies can be classified in three levels according to the functional zones of a power system; generation, transmission and distribution [3]. Hierarchical level 1 (HL I) is related to the generation system adequacy and the sufficiency of electricity producers to serve the load is evaluated regardless of the constraints and limitations of the transmission networks. Hierarchical level 2 (HL II) considers the inadequacy and outages of both generation system and transmission network together. HLII is also known as composite system level. In hierarchical level 3 (HL III), the ability of power system facilities from the generation point to the customer load point, including power plants, transmission lines and distribution systems, in delivering electricity and supplying the demand is evaluated. However, due to the extreme scale of this level in real power systems, this level is usually conducted in the distribution facilities zone. These functional zones can be combined in adequacy assessment studies as hierarchical levels illustrated in Figure 3.1. The research described in this thesis focuses on the HLI and HLII studies.

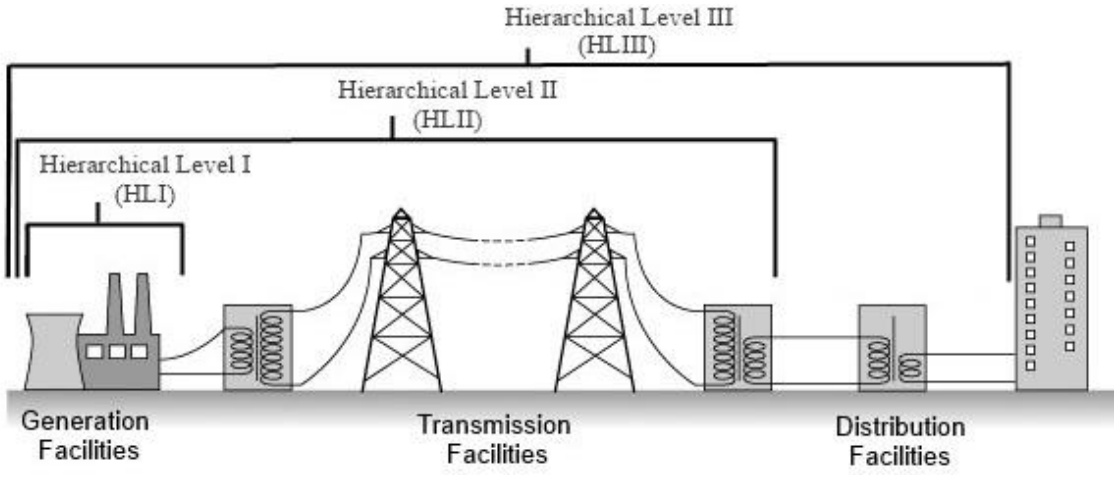

Figure 3.1. Hierarchical levels in the power system reliability studies [45]

3.2. Reliability Evaluation for Adequacy Assessment

3.2.1. Generation System (HLI)

In generation system level studies, all the generators and loads of a system are accumulated into the same bus and the system is modelled as a single bus system which is shown in Figure 3.2. The transmission system is not a part of the analysis at this level, therefore, the limitations, outages and contingencies of transmission lines are not considered in the HLI studies.

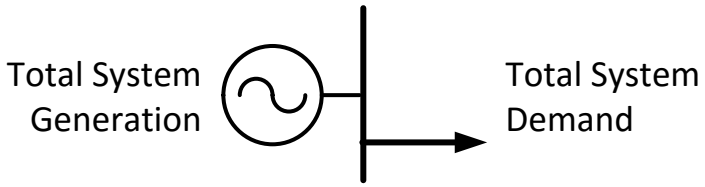

Figure 3.2. Power system model in hierarchical level 1 (HLI)

The basic concern in the HL I studies is to determine the generating capacity sufficient to supply the demand, considering the uncertainty in load variation, generator failures, maintenance and repairs. In order to avoid unserved demand, a generation capacity higher than the peak demand is required, in which the difference of the two is very often measured by the capacity reserve. There are several deterministic and probabilistic methods to estimate the capacity reserve of the system. However, deterministic methods do not distinguish the random nature of generator failures and the uncertainty in demand and consequently are not capable of assessing the actual system risk. Therefore, probabilistic methods, which are able to capture the random behaviour of units and load fluctuations, have replaced deterministic approaches and are widely being used to evaluate the system adequacy [48].

The general model of power system in generation adequacy (HLI) studies is shown in Figure 3.3. This model consists of three main parts: generation, load and risk models [45]. Both analytical and simulation techniques use this concept, however, they use different methods to model load, generation and risk of the system. Although HLI is to evaluate the generation system shortages and there is no transmission system model in it, limited tie-line considerations can be included in this level. Interconnections between neighbouring systems and remote generating units are these considerations.

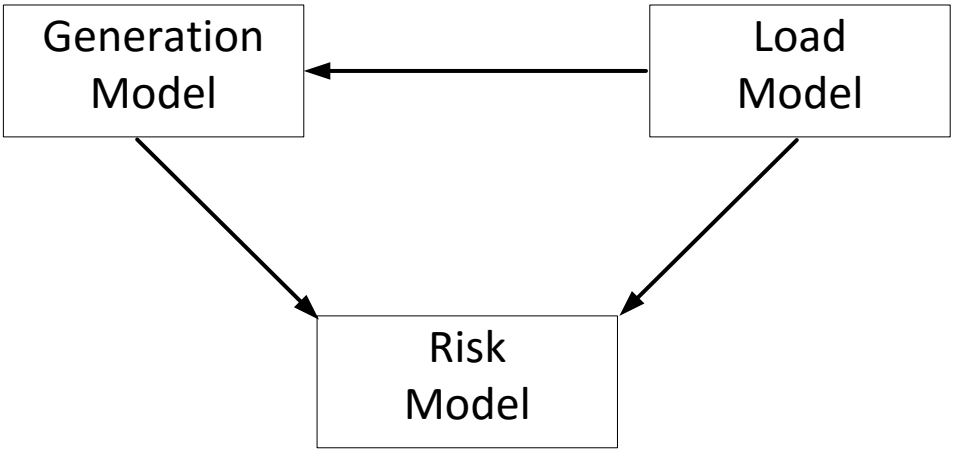

Figure 3.3. Power system model in hierarchical level 1

As it can be seen in this figure, generation and load models should be constructed separately and then being combined together in order to obtain the risk model and assess the system adequacy. These models are described in the following sub-sections.

3.2.1.1. Generation Model

The most important part of adequacy assessment in HLI is generation unit modelling. This model can provide an artificial historical operation cycle for the generator. A generating unit in a power system can be represented by multi-state Markov models. A conventional two-state model [49], which is shown in Figure 3.4 [50], represents a generator that is working in the fully functional state, or in the forced out of service state. The generating unit transits between these two states with the transition rates λ (failure rate) and μ (repair rate), as is depicted in Figure 3.4.

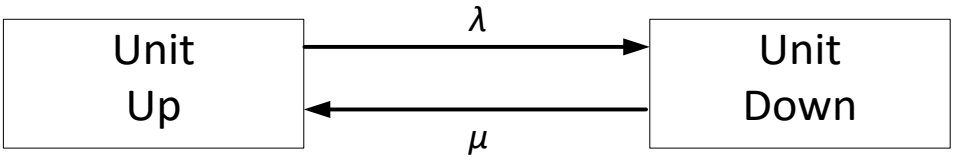

Figure 3.4. Two-state model for a generating unit

The mean time to failure (MTTF) is the average time a unit spends in the "Up" state, and is equal to the reciprocal of the failure rate λ. The mean time to repair (MTTR) is the average time taken to repair a unit and is equal to the reciprocal of the repair rate μ. By having MTTF and MTTR for each unit and using random variables, an up-and-down cycle model for each generator can be produced.

The two-state model is usually used to represent base load generators which have long operating cycles. These units can also be in a derated state, where they operate with a reduced-capacity in addition to the up-state and down-state modes [50]. For these units a three-state Markov model which is shown in Figure 3.5 can be used, where λ_{ij} is the transition rate from state *i* to state *j*.

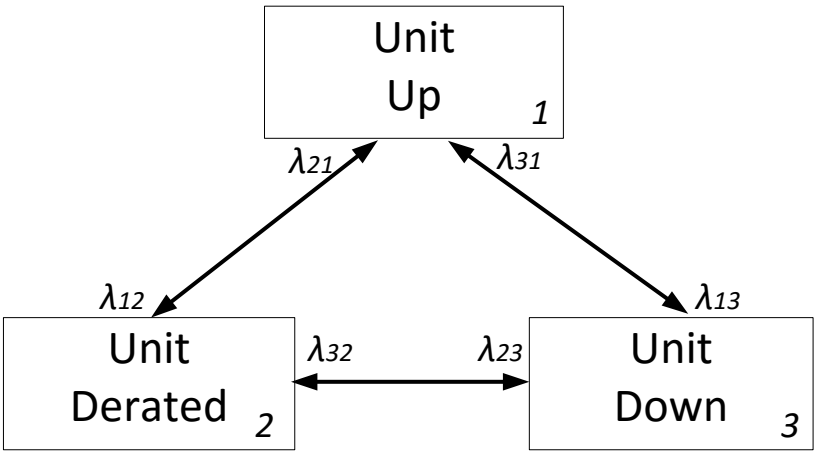

Figure 3.5. Three-state model for a generating unit

The duration of the generating unit working in the up-state can be obtained using (3.1) and (3.2).

$$T_{up1} = -\frac{1}{\lambda_{12}} \ln U_1 \qquad (3.1)$$

$$T_{up2} = -\frac{1}{\lambda_{13}} \ln U_2 \tag{3.2}$$

where, T_{up1} is the up-state duration if the system goes to down-state and T_{up2} is the sampling value of the up-state duration when the system transits to the derated mode, and U_1 and U_2 are uniformly distributed random numbers. Therefore, the sampling value of up-state duration can be calculated by means of (3.3).

$$T_{up} = \min(T_{up1}, T_{up2}) \tag{3.3}$$

T_{up} can also be used to determine the next state of the unit. For example, if $T_{up}= T_{up1}$, the unit will transit to the derated state. By using the state durations, an operating cycle can be created for the generating unit.

Peaking units are different from base units and have short operating cycles. Therefore, two-state or three-state models may not be appropriate to represent them. Figure 3.6 displays the four-state model proposed by the IEEE Task Group on Models for Peaking Service Units [51].

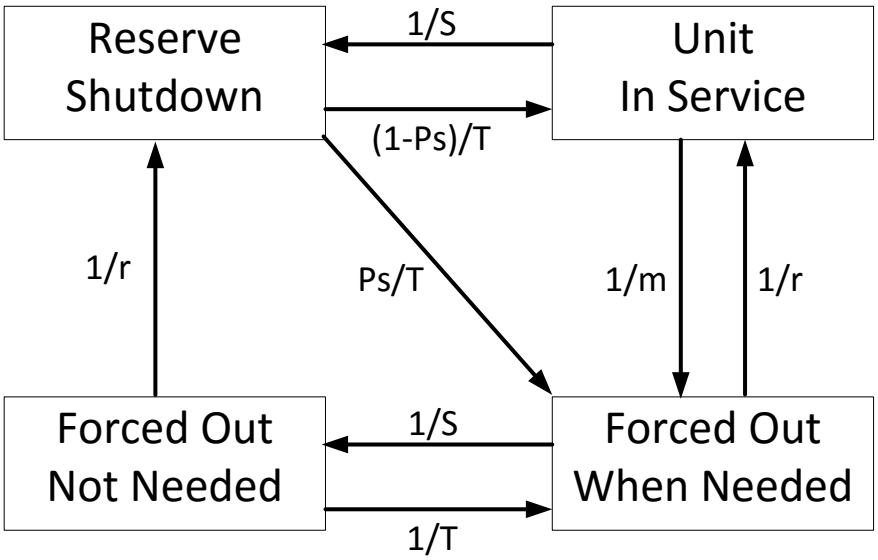

Figure 3.6. IEEE four-state model for a peak generating unit

Where *m* and *r* represent mean time to failure and mean time to repair, respectively. *T* is average reserve shutdown time between periods of need, *S* denotes the average in service time per occasion of demand and P_s represents probability of starting failure.

Peaking units are in service only when they are needed and their starting up duration is so short that they can be neglected in assumptions. In order to create an operation cycle for these units, first a uniformly distributed random number in the interval of [0, 1] is produced. If this number is

smaller than P_s the unit fails to start up, otherwise, it starts. Then the sampling values drawn for m and r are used to indicate the next state of the generator and the duration of each state.

3.2.1.2. Load Model

There are several methods to model load in reliability studies.

1) Fixed load: The simplest way is to consider the peak demand as a fixed load level for the entire period of the study [47].
2) Chronological load: Another simple and popular method to model load in reliability assessment is chronological load model. This model shows the hourly variations of the system demand and can also be used to determine the annual peak demand or the minimum load level. A chronological hourly load model for a sample power system in Australia is shown in Figure 3.7. It can be seen that the annual maximum demand for this system is around 12,000MW and the demand can drop to less than 6,000MW. The load level can also be presented in per-unit values to model different peak demand scenarios for the system.

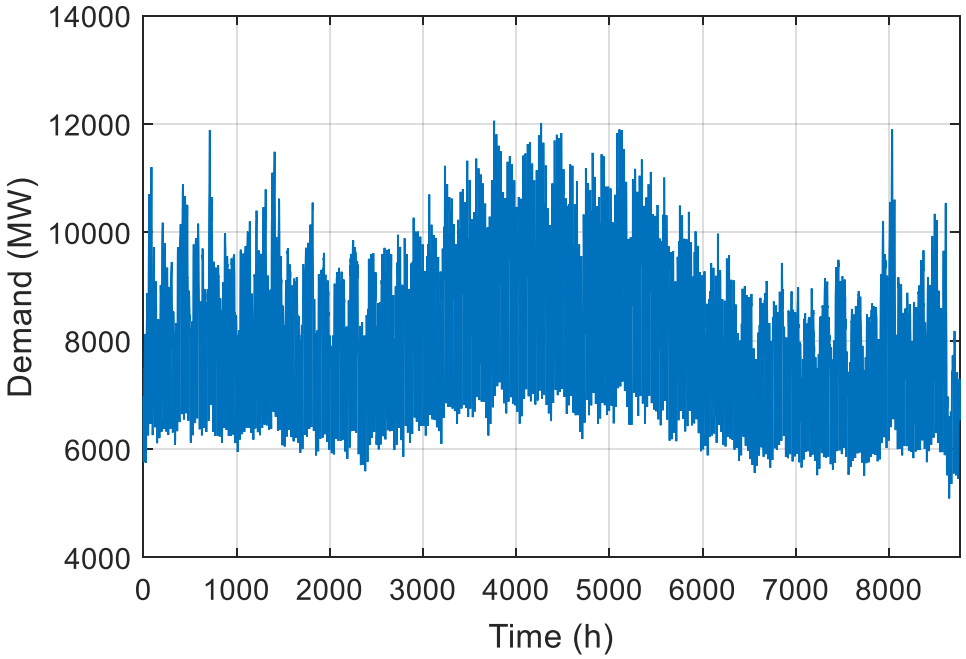

Figure 3.7. Hourly load model for an Australian sample system

3) Load duration curve (LDC): LDC is also a popular method to represent demand in the adequacy assessments in HLI. This model displays the relationship between generating capacity requirements and capacity utilization. It is similar to the hourly load model but in the LDC load is ordered in descending order of magnitude, rather than chronologically. In other words, LDC model is the hourly load curve rearranged from chronological order into an order based on magnitude [52]. The area under the load duration curve model

indicates the total annual energy requirement of the system. The load duration curve for a sample power system in Australia is illustrated in Figure 3.8. This model can also be drawn in per-unit values.

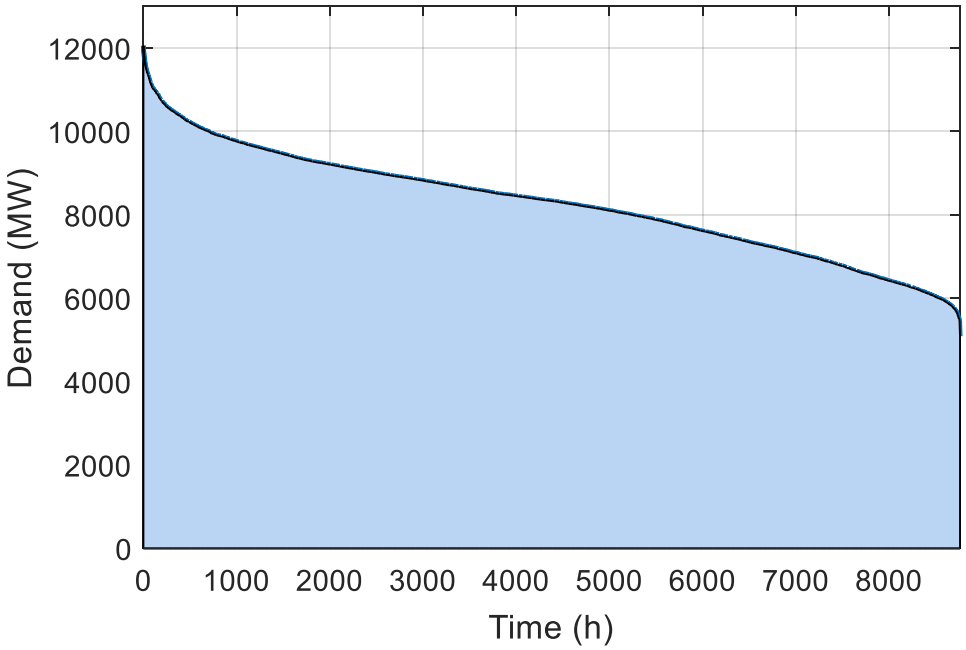

Figure 3.8. Load duration curve for a sample system

4) Clustered model: Load clustering is another approach to model load data. Clustering is a useful method to classify a set of data into a set of groups. Each cluster is a collection of load data objects with similar attribute values [53]. The clustering technique can be used to create a multistep model of the annual load duration curve. There are several clustering techniques and two of them are widely being used in power system reliability assessments: K-means [53] and Fuzzy-C means (FCM) [54].

The K-means algorithm is a method to classify N data points into K clusters. Each cluster is parameterized by a mean vector (M_i). The hourly load data points are denoted by L_n where the superscript n is from 1 to the number of hourly data points N. For instance, N for 1 year hourly load data is 8760. The distance from each hourly load point to each cluster mean value (D_{in}) can be calculated using (3.4).

$$D_{in} = | M_i - L_n | \tag{3.4}$$

Then load points are classified in the closest cluster and new cluster centres are determined by means of (3.5).

$$M_i = \frac{\sum_{n \in IC} L_n}{C_i} \tag{3.5}$$

where, C_i denotes the number of load points in the i_{th} cluster and *IC* is the set of the load points in the i_{th} cluster. This process is repeated until all the cluster means are fixed between iterations.

Another clustering method is Fuzzy-C means (FCM). This method is one of the most popular clustering techniques [55]. Unlike K-means algorithm, final clustered centres in this method are not related to the initial mean values [56]. The objective function of FCM method is to minimize the distance between data points and centre of clusters and can be formulated as (3.6) [54]:

$$J(U,V)=\sum_{m=1}^{M}\sum_{c=1}^{C}(\mu_c(i))^m\left\|X_i-V_c\right\|^2,\quad 1\le m<\infty \tag{3.6}$$

where, U is fuzzy partition matrix for C clusters and V denotes the matrix for centre of clusters. M is the total number of input data, m represents the index of fuzziness and μ_c is the membership value as a weighing exponent between data vector (X_i) and centre of cth cluster (V_c).

FCM is an iterative method; first the estimated membership values should meet Equation (3.7). Then, by means of (3.8) the vector of cluster centres for kth iteration can be computed.

$$\sum_{c=1}^{C}\mu_c(i)=1,\quad \forall i\in 1,...,M \tag{3.7}$$

$$V_c=\frac{\sum_{m=1}^{M}\left(\mu_c(i)^{(k)}\right)^m X_i}{\sum_{m=1}^{M}\left(\mu_c(i)^{(k)}\right)^m} \tag{3.8}$$

The membership values for all input data are updated using (3.9) in each iteration.

$$\mu_c(i)^{(k)}=\frac{1}{\sum_{j=1}^{C}\left[\frac{\left\|X_i-V_c\right\|}{\left\|X_i-V_j\right\|}\right]^{\frac{2}{m-1}}} \tag{3.9}$$

The iterative process will continue until (3.10) is met. where, ε is a small value for convergence tolerance.

$$\left\|\mu_c(i)^{(k)}-\mu_c(i)^{(k-1)}\right\|<\varepsilon \tag{3.10}$$

It should be noted that the clustering technique may result in multi-solutions. Therefore, selecting an appropriate number of clusters to obtain a proper model is very important [57]. A 20-step load model which is accurate enough to represent a sample Australian power system load data is shown in Table 3.1. This table shows the value of load levels in per-unit (p.u.), which is the load

level value in MW divided by the peak demand (12,000MW), and their probability of occurrence. It can be seen that the probabilities of high demand levels are low.

Table 3.1: The 20-step load model of a sample System

Step No.	Load Level (p.u.)	Probability	Step No.	Load Level (p.u.)	Probability
1	0.3044	0.0214	11	0.5065	0.0645
2	0.3363	0.0479	12	0.5234	0.0655
3	0.3607	0.0668	13	0.5424	0.0580
4	0.3820	0.0686	14	0.5630	0.0518
5	0.4025	0.0663	15	0.5869	0.0441
6	0.4219	0.0724	16	0.6180	0.0357
7	0.4401	0.0718	17	0.6576	0.0257
8	0.4573	0.0675	18	0.7205	0.0149
9	0.4737	0.0729	19	0.8003	0.0108
10	0.4903	0.0673	20	0.8928	0.0061

3.2.1.3. Risk Model

Risk is a combination of a probability for an accident occurrence and resulting negative consequences [46]. The extent of consequences in the power system can represent the amount of unserved demand in a specific time interval or a number of affected customers, etc. The risk criterion is a term that may distinguish between what is considered as an acceptable level of reliability and what is not [46]. A wide range of related measures or indices can be utilized to model and determine the risk of the system. The system risk model in generation adequacy studies is related to generation and load models and is obtained by combining these two models, as was shown in Figure 3.3. The risk model can be utilized to obtain the system risk indices. Some widely used indices in generation system assessment level (HLI) are presented in the following subsection.

3.2.1.4. Adequacy Indices in HLI

There is a variety of indices to measure the adequacy of the generation system. Some of the most popular indices in HLI studies are loss of load probability (LOLP), loss of load expectation (LOLE) and loss of energy expectation (LOEE). These indices are related to the unserved load in the system and can be calculated using different techniques. Loss of load occurs whenever the system load

exceeds the available generating capacity and these indices can be obtained according to the probability, severity, duration and frequency of the shortages.

The LOLP is defined as the probability of the system load exceeding available generating capacity [46]. The LOLP represents the insufficiency of installed available capacity and expresses an expected percentage of hours or days per year of capacity deficiency.

The LOLE is the expected number of hours or days in a year that the loss of load may happen. This index is closely related to the term LOLP. The difference between them is that LOLE is expressed in the time units while LOLP is in percentage values [46].

The LOEE is the expected energy that will not be supplied by the generating system due to generation inadequacy. This index incorporates the effect of inadequacies as well as their probability. Normalized LOEE index, which is the energy not supplied divided by the total energy demand, can be used to compare the reliability level of different systems.

Different analytical and Monte Carlo simulation techniques can be implemented to calculate the capacity shortage and these adequacy indices. As mentioned in the introduction of this chapter, these methods have their own advantages and disadvantages. Therefore, the appropriate method should be selected based on the type of evaluation and the particular system problems.

3.2.1.5. Analytical Methods

The easiest approach to calculate the reliability indices in analytical methods is to represent the generation system with a capacity outage probability table (COPT). In the COPT, the combinations of available and unavailable generating units and their associated probabilities of existence are ordered in rows [46]. This table is also presented as a cumulative outage probability of having capacity shortage. The method to create COPT for a sample system with one 70MW and two 30MW generators and 98% availability for all generating units is illustrated in Table 3.2. In this table A denotes availability and U represents unavailability.

The COPT can be combined with the LDC load model to calculate the LOLP and LOLE of system. The method of combining the different system capacity states in a generation model with the load duration curve to make the system risk model and to calculate reliability indices is demonstrated in Figure 3.9.

Table 3.2: A sample a capacity outage probability table

Capacity Outage	Available Capacity	Availability	Cumulative success probability
0	130	A×A×A	0.941192
30	100	U×A×A	0.019208
30	100	A×U×A	0.019208
60	70	U×U×A	0.000392
70	60	A×A×U	0.019208
100	30	U×A×U	0.000392
100	30	A×U×U	0.000392
130	0	U×U×U	0.000008

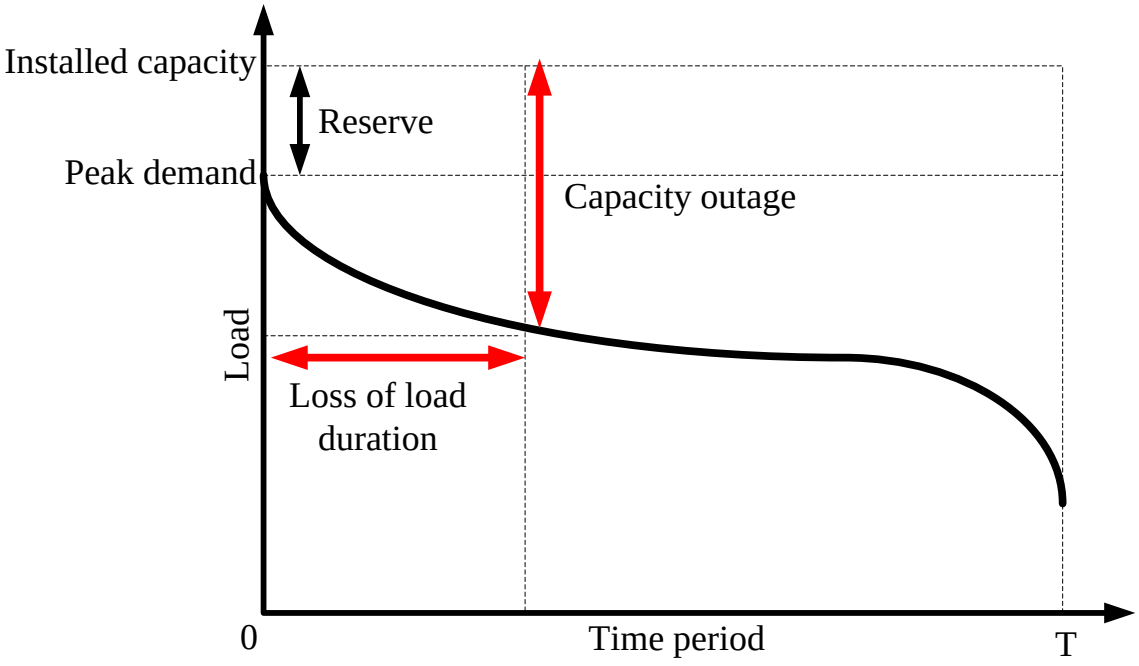

Figure 3.9. Loss of load concept

Loss of generators causes the expected risk of loss of power supply *E(t)*, which is also known as mathematical expectation and is given in (3.11).

$$E_i(t) = p_i t_i \tag{3.11}$$

where, p_i is the probability of loss of capacity in system state i, and t_i is the duration of loss of capacity in percent. LOLP is defined as a sum of all expectations for all n system states associated with loss of load.

$$LOLP = \sum_{i=1}^{n} p_i t_i \tag{3.12}$$

The formula to calculate LOLE is given in (3.13), where t_i is the duration of state i in hours or days.

$$LOLE = \sum_{i=1}^{n} p_i t_i \tag{3.13}$$

As mentioned earlier, the area under the LDC represents the systems' required energy. Therefore, the combination of COPT and this area can be utilized to calculate the loss of energy expectation index. The process of obtaining the amount of curtailed energy due to a capacity outage in state i is displayed in Figure 3.10.

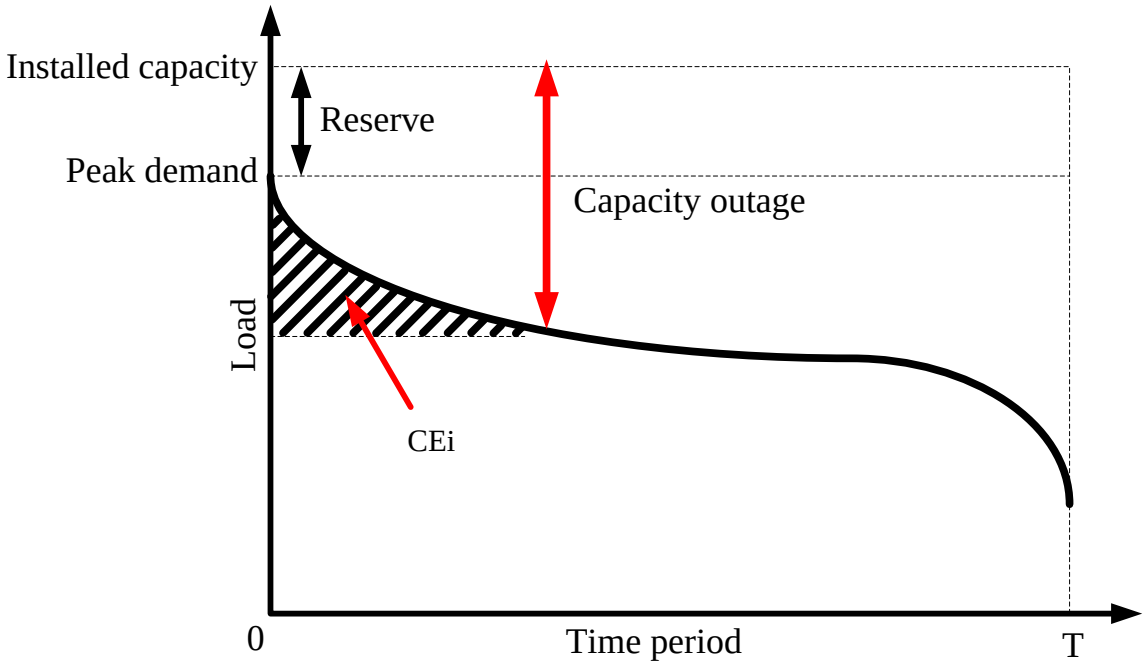

Figure 3.10. Loss of energy expectation method

Equation (3.14) can be used to calculate LOEE in a year, where CE_i is the curtailed energy in the system state i.

$$LOEE = \sum_{i=1}^{n} CE_i p_i \tag{3.14}$$

The analytical approaches use mathematical models and assume a simplified system operation [58]. These methods are accurate to model small systems. However, they do not have the flexibility to represent system variables such as time-varying loads and renewables' variations, and can become very complicated in evaluating the adequacy of complex power systems with variable energy resources such as wind and solar [59]. Another disadvantage of analytical methods is that

the distribution of various indices cannot be determined by them, which can easily be generated by MCS [59]. For reliability assessment of large systems or to evaluate the reliability contribution of renewable energy sources, the Monte Carlo simulation techniques are more appropriate.

3.2.1.6. Monte Carlo Simulation Technique

A popular method used for power system reliability assessment is Monte Carlo Simulation (MCS). There are two different MCS methods: Sequential and non-sequential MCS. In the sequential technique, system states are sequentially sampled over time according to the system operation history. While in the non-sequential method, system states are randomly sampled, regardless of the chronological behaviour of the system [60]. Both of these methods are capable of calculating the expected value of main indices and can be effectively used to evaluate the reliability of power systems [61].

The state sampling method is relatively simple and requires basic reliability data such as the component-state probabilities [47]. In this method, instead of sampling a distribution function, random numbers are generated to simulate the system's state. The main drawback of non-sequential technique is its incapability to calculate the frequency of load curtailments precisely [47]. The sequential MCS can determine a comprehensive set of reliability indices including the frequency and duration of interruptions. However, this technique needs a larger computational effort compared to the state sampling method and requires chronological hourly load data at each bus, which may not be available [61].

In this research, for reliability assessment at composite system level, the state sampling MCS is utilised since it is faster and requires less input data. While for generation adequacy level sequential technique is applied. Both MCS techniques and the process of calculating generation adequacy indices using these methods are explained in the following subsections using IEEE reliability test system (RTS) [62]. Details of IEEE-RTS system are provided in Appendix A.

3.2.1.6.1. Sequential Monte Carlo Simulation

State duration sampling or sequential MCS method is based on simulating the chronological state transition processes by sampling. First, the sequential state transition model for all system elements is simulated. Then by combining them the chronological system state transition process is constructed. The process of state duration sampling method to calculate reliability indices for IEEE-RTS is described in the following:

In first step, the operation cycle for each generator is created using their MTTF and MTTR and random numbers. For this reason, time to failure (TTF) and time to repair (TTR) for each unit are

generated using (3.15) and (3.16), where U_1 and U_2 are uniformly distributed random variables between [0,1].

$$TTF = -MTTF\ Ln(U_1) \tag{3.15}$$

$$TTR = -MTTR\ Ln(U_2) \tag{3.16}$$

Then, regarding the sampling values of TTF and TTR, operating histories for each generator is produced. Figure 3.11 shows the available capacity model and up and down cycles of a 12MW unit of IEEE-RTS in a sample year.

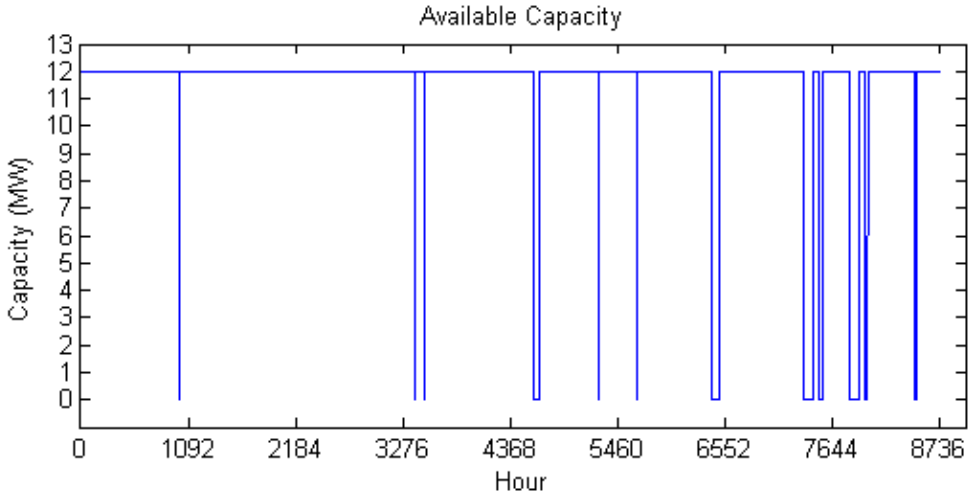

Figure 3.11. Available capacity model in a sample year for a 12MW generator

In the next step, system available capacity is constructed using the operating cycles of all generators. All generators capacity models are combined together and the system total generation capacity model is obtained. The system available capacity of IEEE-RTS for a sample year is displayed in Figure 3.12.

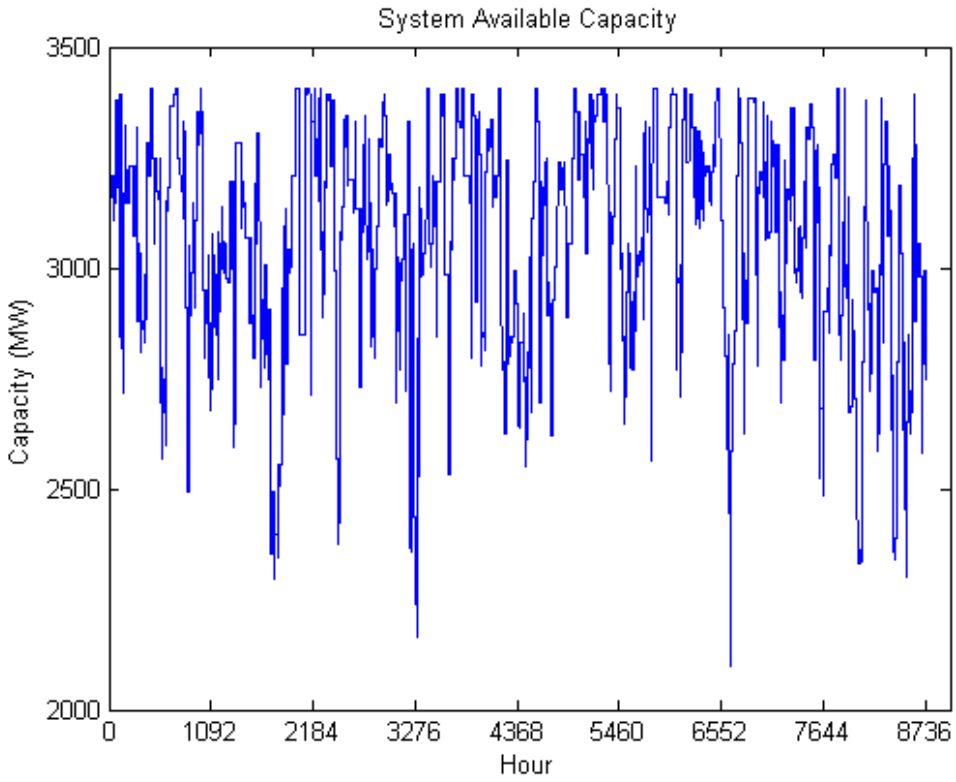

Figure 3.12. System available generation capacity for a sample year

To calculate the system insufficiency, the system generation capacity and load models should be compared and the occasions when demand exceeds generation capacity should be obtained. Figure 3.13 depicts the chronological load model of the IEEE-RTS.

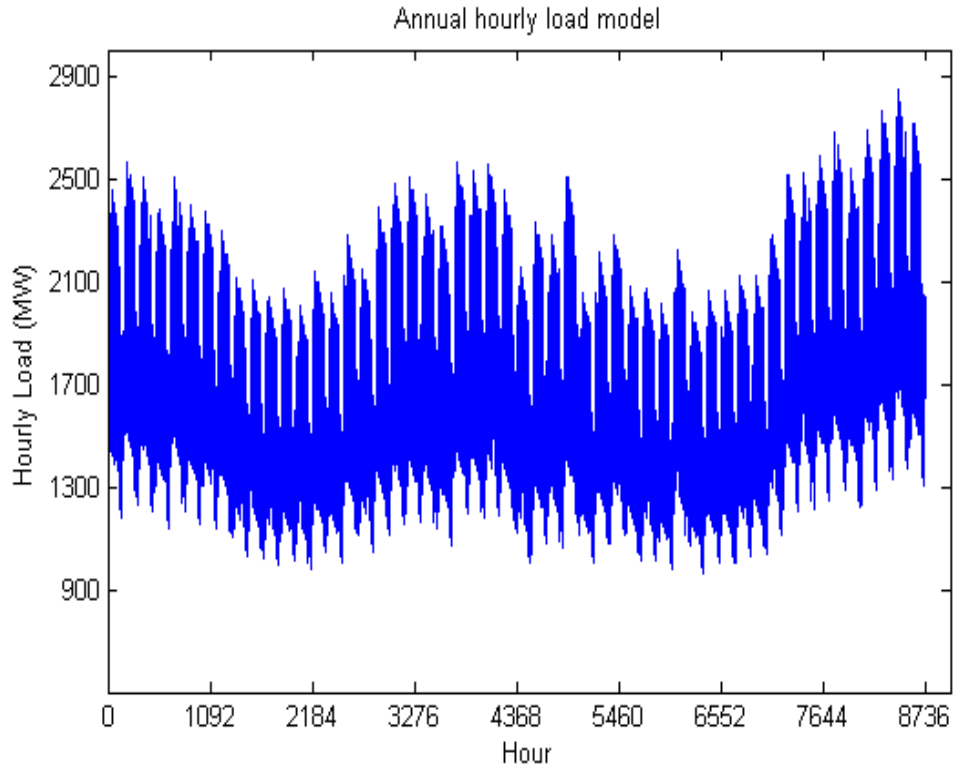

Figure 3.13. Chronological hourly load model for the IEEE-RTS

By deducing load model from generation capacity model, a system available margin model is created, which is shown in Figure 3.14. This model represents the difference between the system demand and the generation available capacity. When demand is higher than generation, system margin will become a negative value which indicates the amount of demand not supplied at that time.

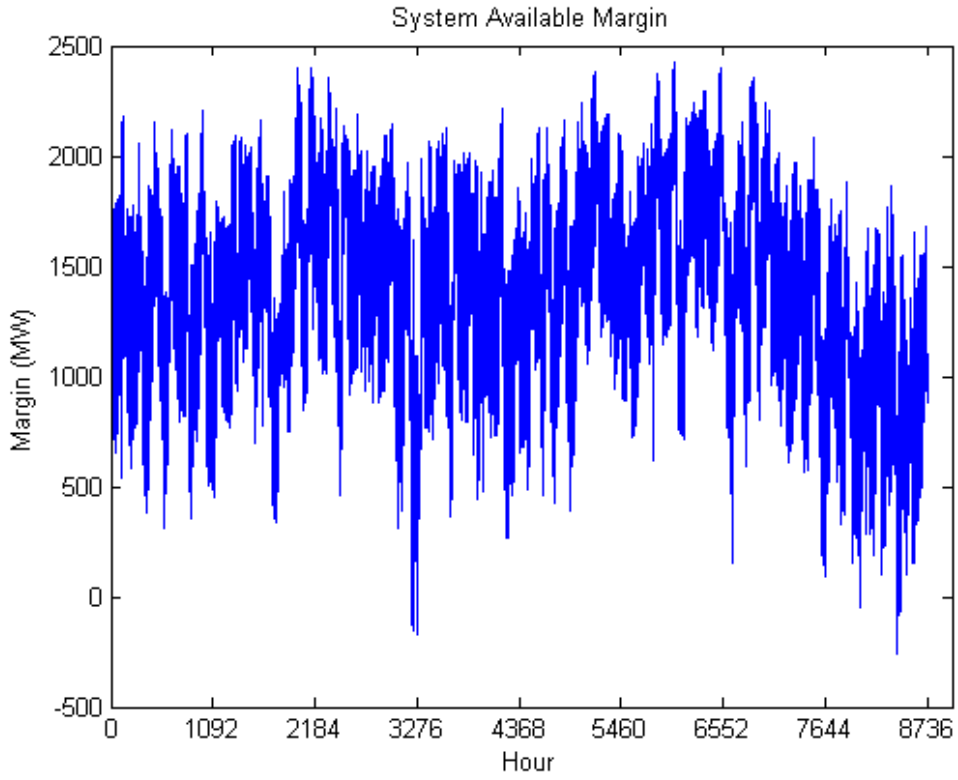

Figure 3.14. System available margin model for IEEE-RTS in a typical sample year.

Finally, by recording the amount of these losses of load values and their duration from the system margin model, reliability indices of the system can be estimated. Equations (3.17) and (3.18) show the formulas to calculate LOLE and LOEE by taking the average value of loss of load duration (LLD) and energy not supplied (ENS) for *N* sample iterations.

$$LOLE = \frac{\sum_{i=1}^{N} LLD_i}{N} \text{ (hr/yr)} \tag{3.17}$$

$$LOEE = \frac{\sum_{i=1}^{N} ENS_i}{N} \text{ (MWh/yr)} \tag{3.18}$$

Reliability indices of IEEE-RTS system obtained by using Monte Carlo state duration sampling method for 3000 sample years are shown in Figures 3.15 and 3.16. In these figures, the blue line represents the value of index calculated by MCS method and the red line is the analytical answer.

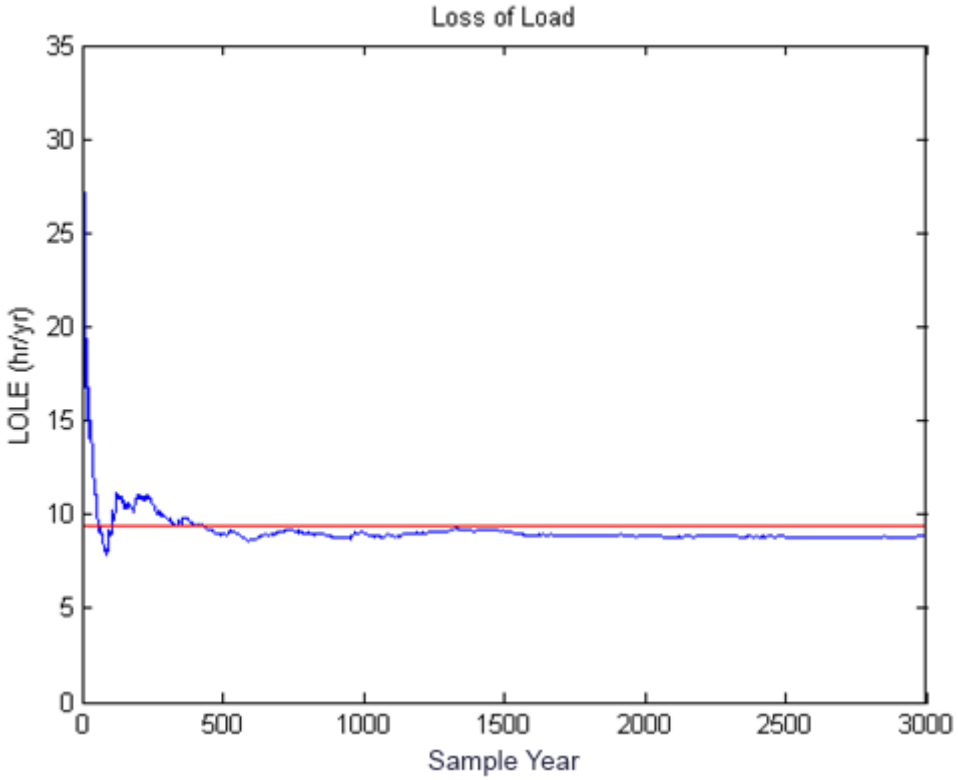

Figure 3.15. LOLE vs. the number of sample years

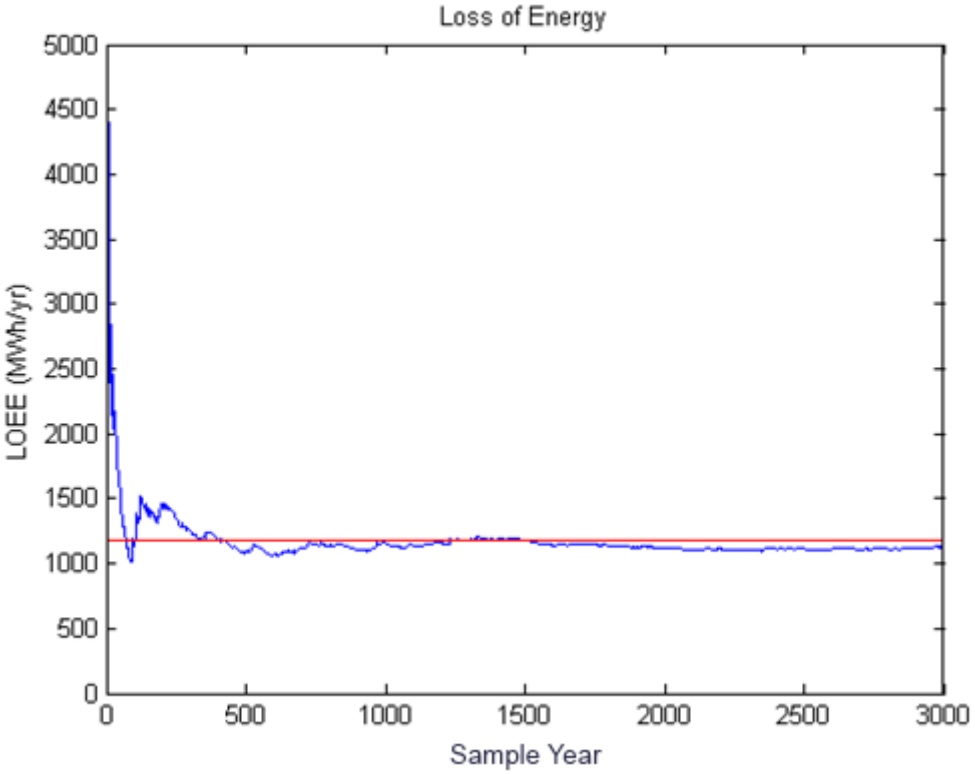

Figure 3.16. LOEE vs. the number of sample years

Reliability indices for the IEEE-RTS system obtained by sequential technique and analytical values are compared in Table 3.3. It can be seen that the estimated results obtained from this method have an acceptable accuracy.

Table 3.3. Reliability indices for IEEE-RTS using sequential MCS and Analytical method

Reliability Index	Sequential MCS	Analytical	Error
LOLE (hr/yr)	9.2	9.38	1.9 %
LOEE (Mwh/yr)	1169	1174	0.4%

3.2.1.6.2. **Non-Sequential Monte Carlo Simulation**

In non-Sequential MCS, the state sampling approach is used, in which case random selection of time intervals are used to create a non-chronological system state model. In this method the behaviour of generating units is modelled by means of generator forced outage rate (FOR) and uniformly random numbers. The state of the i_{th} generator is indicated using (3.19) and a random variable (U_i) between [0, 1].

$$S_i = \begin{cases} 0 \quad (up\ state) & if\ U_i \geq PF_i + PD_i \\ 1 \quad (down\ state) & if\ PF_i \leq U_i < PF_i + PD_i \\ 2 \quad (derated\ state) & if\ 0 \leq U_i < PD_i \end{cases} \tag{3.19}$$

where, PF_i is the probability of down state and PD_i represents the probability of the derated state.

Then by determining the state of all generators, the state of system with n generating units can be obtained by a vector S = (S_1, S_2, ..., S_i, ..., S_n). The total available generation capacity in each system state can be calculated regarding the state of all generating units in that state. In the next step, the amount of demand not supplied (DNS) is computed by deducing the system's equivalent demand from the total generation capacity. This can be calculated by means of (3.20), where, D is total demand and G_{lk} denotes the available capacity of unit l in the k_{th} iteration and n is the number of generators.

$$DNS_k = \max\left\{0, D - \sum_{l=1}^{n} G_{lk}\right\} \tag{3.20}$$

The formula to calculate the annualized loss of energy expectation for N sample years based on the DNS value is given in (3.21).

$$LOEE = \frac{\sum_{k=1}^{N} DNS_k \times 8760}{N} \tag{3.21}$$

And the LOLE index can be obtained by using (3.22).

$$LOLE = \frac{\sum_{k=1}^{N} I_k(DNS_k) \times 8760}{N} \tag{3.22}$$

where I_k is an indicator which is shown in (3.23).

$$I_k = \begin{cases} 0 & if \quad DNS_k = 0 \\ 1 & if \quad DNS_k \neq 0 \end{cases} \tag{3.23}$$

Reliability indices for the IEEE-RTS system obtained by state sampling method Monte Carlo for 5000 samples are given in Table 3.4.

Table 3.4. Reliability indices for IEEE-RTS using non-sequential Monte Carlo method

Reliability Index	Non-Sequential MCS	Analytical	Error
LOLE (hr/yr)	9.63	9.38	2.6 %
LOEE (Mwh/yr)	1190	1174	1.3%

Although the errors of the non-sequential method in comparison with sequential results are higher, these indices are still accurate, whereas, the computation time of this method is much lower than the sequential MCS.

3.2.2. Composite System Adequacy Assessment (HLII)

To analyse the impact of transmission system constraints on the system reliability, adequacy evaluation should be conducted in the hierarchical level II (HLII). Adequacy evaluation at HLII is also known as bulk system evaluation because it includes both the generation system and the transmission network [50]. Figure 3.17 depicts a sample composite system.

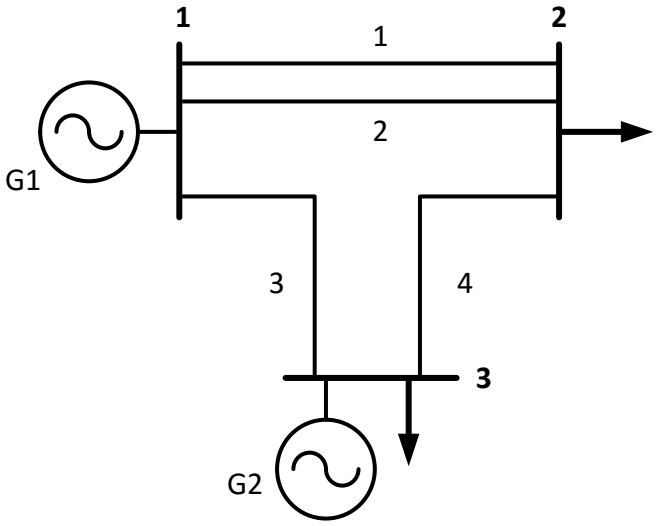

Figure 3.17. A sample composite power system for HLII studies

Besides generation capacity shortages, insufficiency of the transmission capacity or transmission line outages may also result in load curtailment and can cause reduction in reliability level of the system. Therefore, at this level, the adequacy of both generation and transmission systems is being evaluated. Reliability assessment at HLII involves many activities, such as load flow analysis, contingency analysis, generation rescheduling, load curtailment philosophy, etc [45]. The general process to assess the reliability of a composite system is presented in Figure 3.18 [63]. First a system state is generated based on generator and line outages. Then, a load flow analysis is conducted to check if the security constraints (line flow limits and voltage limits) are violated in that state or not. If yes, corrective actions such as generation rescheduling should be taken to avoid load curtailment. However, in some states, to meet system security limits load shedding is inevitable. In these scenarios, methods such as linear programming are utilized to optimize the load curtailment. At the end, reliability indices of the composite system are calculated based on the amount of curtailed load. The steps of HLII reliability evaluation process is described in Section 3.2.2.2.

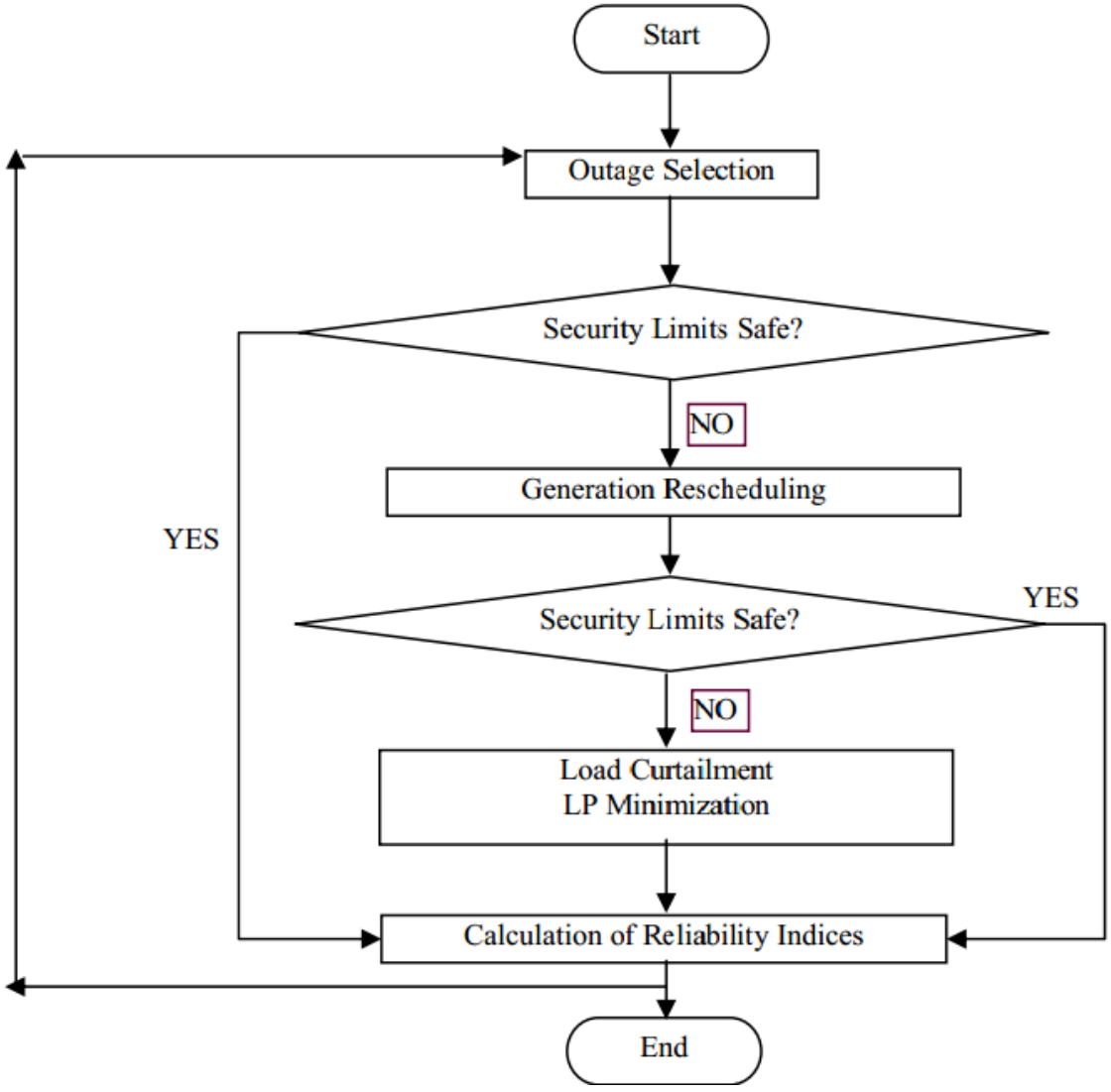

Figure 3.18. Adequacy assessment process for HLII studies [63]

In the composite system studies, a two state model, which was illustrated in Figure 3.4, can also be utilized to model transmission lines and transformers which are the main components of the transmission system. To simulate generating units, load and risk of the system, models presented in generation system level can be applied in the HLII studies as well. However, adequacy assessment indices of the composite system are different from the HLI indices.

3.2.2.1. Adequacy Indices in HLII

Similar to the generation adequacy assessment, there is a variety of risk indices available to determine the system reliability in HLII. These indices in the composite system studies can be divided in two sets. The first one is load point index which shows the reliability level at an individual load bus, and the second one is the overall system indices. Both load point and system indices can be utilized to assess the reliability of the composite system. However, load point indices are usually used to determine unreliable buses in the system, while system indices are utilized to provide a global assessment of the system [63]. Some of the main indices in the HLII studies are presented in the following, where p_i denotes the probability of the i_{th} failure state, C_i represents the amount of load curtailments in state i and S is the set of all system states with load shedding. These indices can be calculated for either whole system or each bus.

Probability of Load Curtailment (PLC)

$$PLC = \sum_{i \in S} p_i \tag{3.24}$$

Expected Duration of Load Curtailment (EDLC)

$$EDLC = PLC \times 8760 \quad hrs / yr \tag{3.25}$$

Expected Demand Not Supplied (EDNS)

$$EDNS = \sum_{i \in S} C_i p_i \quad MW \tag{3.26}$$

Expected energy not supplied (EENS)

$$EENS = \sum_{i \in S} 8760 C_i p_i \quad MWh / yr \tag{3.27}$$

The HLII reliability indices can be calculated in two ways based on the load model [64]. If the annual load is used in the reliability calculations, the result will be annual indices. If a fixed peak load model is considered for the whole period of the study, the annualized indices will be the outcome. The process of calculating annualized indices requires less computational time, however, annual indices are more useful and more appropriate to model system risk as they consider the

actual load profile [64]. Therefore, in the HLII studies of this research all the reliability indices are annual values.

3.2.2.2. Reliability Assessment Method in HLII

State sampling Monte Carlo method [61] has been applied in this research to assess the reliability of the composite system. This method was explained in section 2.2.1 for generation system adequacy assessment. The process of state sampling MCS for composite system level can be described as follow [65] :

1. A clustered model is constructed for system load and each load level has its probability of occurrence which is used as a weighting factor to obtain annual indices.
2. The state sampling MCS method is performed for each load level. Component states (up, down or derated) are simulated using random numbers, and a system state vector $S = (S_1, S_2, ..., S_l, ..., S_t)$ is created. This vector represents the state of a system of *t* elements, containing generators, transmission lines, transformers, etc. Generally, generator states are simulated using multiple-state model (3.19) and the two-state (up and down) model (3.28) is utilized to simulate transmission line states.

$$S_i = \begin{cases} 0 \quad (up\ state) & if\ \ U_i \geq FOR_i \\ 1 \quad (down\ state) & if\ \ 0 \leq U_i < FOR_i \end{cases} \tag{3.28}$$

3. Perform a contingency analysis, if there is no contingency and all component states are zero, system state is normal and no load curtailment is required. However, when there is an element outage or more outages, demand not supplied may exist.
4. In some contingency states Generation rescheduling may be required to avoid load shedding. Optimal load flow analysis approach is used to conduct the contingency analysis and to determine the load shedding requirements in failed system states. In this work, MATPOWER [66] has been utilized to run AC load flow, calculate transmission lines power flow and to obtain the amount of load curtailment due to any component outage(s) in composite system studies.
5. If load curtailment is inevitable, the amount of curtailed load in system state *i* (C_i) should be measured. The HLII indices are calculated based on the load shedding events and equations (3.24) to (3.27).

This process is applied to the IEEE reliability test system and annual reliability indices of this system are presented in Table 3.5.

Table 3.5: Annual system indices for the IEEE-RTS

Indices	Annual Value
PLC	0.00206
EDLC (hrs/yr)	18.04
EDNS (MW)	0.281
EENS (MWh/yr)	2461.56

3.3. Summary

The basics of reliability assessment models and techniques are briefly presented in this chapter. There are three levels in reliability adequacy studies: generation, generation and transmission composite system and distribution levels. In the first level (HLI) the sufficiency of generation system in supplying demand is evaluated. In HLII, generation and transmission systems are studied together and the adequacy of the system considering contingencies in generators and transmission lines is assessed. The third level (HLIII) evaluates the adequacy of all the components from the production level to the delivery point. In this research HLI and HLII are taken into consideration as wind farms are connected to these high voltage levels.

Different models to simulate generating units, load and system risk in HLI and HLII studied are presented and main reliability indices in these levels are described. Different models can be applied depending on the reliability assessment method. There are two main adequacy assessment techniques: analytical and Monte Carlo simulation. Analytical methods are simple and use mathematical models to calculate the reliability indices, while MCS techniques are based on random variables and can be divided into two categories: sequential or non-sequential. The sequential MCS method can recognize the chronology and the correlation between subsequent events, however, it needs a large computational time. On the other hand, the non-sequential approach is incapable of keeping the chronology of the system but is time efficient. The process of performing MCS methods to estimate the reliability indices are explained using IEEE-RTS system. Reliability indices of HLI and HLII levels are used in the following chapters to measure the impacts of wind power on the reliability of power systems and to calculate their load carrying capability.

Chapter 4

Capacity Value of Wind Power

4.1. Introduction[1]

Participation of renewable technologies, particularly wind turbines, to supply electricity demand is increasing in many power systems all over the world. Although these clean energies bring many benefits and opportunities, fluctuations and uncertainty of these resources pose challenges to electricity grids. Reliability assessment of electricity networks in the presence of these green technologies is one of the challenges. As the nature of these power supplies is different from conventional generators, different techniques are required to model these units and to evaluate their reliability contribution in power systems. In the reliability studies, the term capacity value is commonly used to assess the reliability contribution of renewable resources.

Several probabilistic and analytical methods have been developed to evaluate the reliability of power systems with wind generators and to model wind power in reliability assessment [4]–[9]. Negative load [4], [5], multistate generator [6]–[8] and probabilistic distribution [9] are some of the proposed models. Negative load models require chronological techniques like sequential Monte Carlo [67] for reliability assessment. This technique is effective in modelling wind and keeping correlation between wind and demand. However, an extensive evaluation time is the main drawback of this method, especially in composite system studies where the transmission system insufficiency should be considered in the reliability evaluation. Unlike sequential methods, multistate and probabilistic models [6]–[9] are fast and time efficient but may not be able to capture the chronological nature and the correlation between wind power, solar energy and demand data. Although some studies presented techniques to keep the relevance between wind farms and load [10]–[12] or even wind, PV and load data [13], these methods will face difficulties in modelling and

[1] This chapter has materials from the following references published by the PhD candidate.

- Mehdi Mosadeghy, Ruifeng Yan and T.K. Saha, "A Time Dependent Approach to Evaluate Capacity Value of Wind and Solar PV Generation" IEEE Transactions on Sustainable Energy, early access, DOI: 10.1109/TSTE.2015.2478518.
- Mehdi Mosadeghy, Tapan K. Saha and Ruifeng Yan, "Increasing Wind Capacity Value in Tasmania Using Wind and Hydro Power Coordination" IEEE Power and Energy Society General Meeting, 21-25 July, 2013, Vancouver, British Columbia, Canada.

may become complicated when the number of wind farms or solar generators increases. For instance, in [12] wind farms and load data are being modelled as three dimensional clusters to keep the dependencies among them. However, this method is effective for systems with a small number of wind farms and by increasing them, the size of the matrix will grow and calculations will become complicated. Furthermore, non-iterative techniques in [14], [68] are faster than chronological techniques but they have some drawbacks as well. For instance, the method proposed in [68] cannot capture the correlation between the renewable sources and load, which can cause errors in estimating the reliability benefits of them. Although the evaluation technique in [14] is capable of keeping the correlations, it will become complicated as the number of renewable generators increases because this method uses an available capacity probability table. Moreover, this approach is applicable in generation level studies and hasn't addressed the reliability assessment of renewable energy considering transmission system outages and constraints. In addition, in these methods a huge amount of historical data is required to create probabilistic models.

Therefore, a time-dependent clustering approach is developed in this thesis in order to addresses the deficiencies of the previous studies. The proposed framework can be applied to assess the reliability of systems with wind and PV units and is capable of keeping the correlations and time dependency features of data sets. In this approach, renewable generation units and demand data are modelled as time-dependent clusters. Therefore, as this technique is using clustered data, it is efficient in the use of computational time and does not require large amounts of historical data. In addition, this method will not lose its simplicity even in networks with a large number of wind farms and PV systems. Another benefit of this technique is its capability of analysing the contribution of renewables not only in generation adequacy, but also in composite systems reliability, where the transmission system constraints and outages should be taken into consideration.

In this chapter, the capacity value term is defined and different techniques to calculate capacity value are described. Furthermore, several models to represent wind in reliability studies are presented and their advantages and disadvantages are discussed. Then, the process of the proposed methodology to calculate the ELCC of wind power is explained and its effectiveness is examined on the IEEE reliability test system (RTS) as a case study. The reliability assessment has been conducted in both hierarchical level I (HLI) and hierarchical level II (HLII). Two wind farms with different generation profiles and several aggregated PV systems have been added to this testing network and their reliability contribution under several scenarios have been investigated. Finally, outcomes have been compared with results of the sequential Monte Carlo technique to validate the accuracy of the developed approach.

4.2. Capacity Value of Wind Power

Due to outages and uncertainties, the ability of a generator to supply loads at some time in the future is not guaranteed. An important index to measure the capability of a generator in supplying demand is its capacity value (also known as capacity credit) or effective load carrying capability (ELCC). This value can quantify risks associated with generators, especially for intermittent units like wind farms [69]. ELCC is the amount of extra load that can be met by renewable generators while the reliability level of a system remains unchanged [5]. The capacity value of wind generators ranges from 5 to 40 % [2] and depends on several factors such as capacity factor of wind farms, wind profile, correlations between wind and electricity load, wind power penetration level, etc. [10]. Higher wind power generation during peak demand time and high capacity factors will result in a higher capacity credit [69]. ELCC as a percentage of installed wind capacity has a reverse relation with wind penetration level and decreases with increasing wind capacity, because at higher wind capacities the possibility of very low output becomes more important on a system scale. Also since the correlation between wind generators increases, the installation of additional capacity does not compensate for the low wind hours; in this case, while additional installed capacity would increase the MW capacity value, the capacity value as a percentage of rated capacity would decrease [2]. However, this does not mean that less conventional capacity can be replaced by wind energy, but rather that a new wind farm added to a system with large installed wind capacity will substitute less than the first wind farm in the system [2]. Generation profile and other units' maintenance and forced outage rates can also affect the ELCC of wind farms [69]. Therefore, considering these factors in the capacity credit calculation to obtain an accurate estimation is crucial. There are several techniques to determine the capacity value of wind generators [2], [4], [5], [69]–[77]. Some of the popular methods in calculating ELCC are described in the next section.

4.3. Current Techniques to Evaluate Capacity Value of Wind

To determine generation adequacy, each unit is assigned a capacity value, which represents the capability of the generator when it is needed. Since all units are subject to outages, a probabilistic framework to estimate the ELCC is appropriate, in particular for units with stochastic nature such as wind generators. The capacity value of a wind farm can be calculated in two ways: Reliability-based technique and Approximation method [2].

4.3.1. Reliability-Based Method

Generation adequacy evaluation is often based on reliability indices such as loss of energy expectation (LOEE), loss of load expectation (LOLE) or loss of load probability (LOLP), which represent the probability of generation insufficiency or load curtailment at a given time [2]. Using these metrics, the capacity value or the effective load carrying capacity of wind, which is the amount of extra demand that can be supplied with wind generation at a fixed reliability level, can be calculated. The level of a system's reliability is often expressed in terms of the amount of unserved demand or the percentage or maximum hours per year that demand exceeds power production.

The reliability-based method requires a large amount of historical data and complicated analysis to calculate the capacity value of wind energy. For example, in Ref. [5] it is shown that for Irish wind farms at least four or five years of data with hourly resolution are required to keep the deviations in the ELCC result under 10%. There are some alternative approaches in the case where sufficient data is not available. One method is to use prediction models and weather data to produce wind speed and convert them to large scale wind power generation [2]. Another solution is to implement techniques such as auto regressive moving average (ARMA) to simulate wind generation for several years retaining its time-dependent characteristics based on historical data [10], [70]. Probability distribution is another reliability-based technique to compute the ELCC of wind farms [71]–[74]. In this approach wind speed time series are converted into probability distributions, which are then combined with conventional generator distributions to calculate the capacity value of wind energy. These simulation methods have been explained in Section 4.4.

The standard reliability-based framework to calculate the capacity value of wind energy is explained in [4]. Figure 4.1 can be used to briefly describe this ELCC evaluation process for a sample wind farm in a power system.

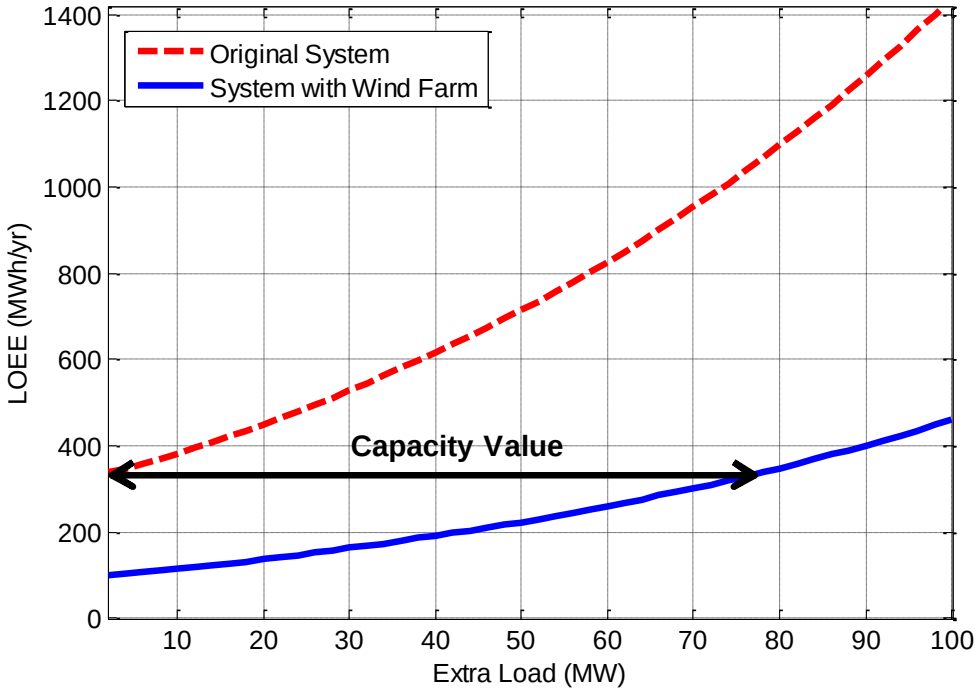

Figure 4.1. Capacity value calculation for a sample wind farm

The red dashed line is the LOEE of the original system without any wind generator. It can be seen that the LOEE of this system is around 380 MWh/yr and by adding extra loads this value is increasing and the system is becoming less reliable. The blue line is the LOEE index for this system in the presence of a 250MW wind farm for different levels of extra loads. It shows that with this wind plant, the LOEE value stays under the original level (380 MWh/yr) for up to 77 MW added load. Therefore, this value can be considered as the capacity credit of the wind farm.

The reliability-based approach is rigorous, data-driven, and can precisely determine the capacity value of different generators. However, this approach needs excessive datasets that are not always available and is related to many system characteristics. For these reasons and others, approximation techniques have been proposed.

4.3.2. Approximation Method

Because of the potential difficulty of assembling the appropriate database to use for the ELCC calculation, interest in simpler methods has emerged over the past several years. The approximation techniques can be classified into two categories: risk-based or time-period-based [4]. Risk-based categories develop an approximation to the utility's LOLP curve throughout the year. Time-period-based methods attempt to capture risk indirectly, by assuming a high correlation between hourly demand and LOLP. A further limitation of time-period-based methods is that they cannot capture the potential system risks [4]. However, these methods are much simpler and allow the avoidance of a reliability model. Some of the main ELCC approximation methods are as follow:

4.3.2.1. Garver Approximation Based Methods

One of the well-known risk-based approximation methods than can be used to estimate the capacity value of wind is the Garver technique [75]. This approach is a graphical approximation method to calculate the capacity value of an additional generator [4]. Garver method estimates the decreasing exponential risk function (LOLP in each hour, LOLE over a specific time). The ELCC value of a wind farm can be calculated using (4.1). In this approach, wind power is modelled as a multi-state unit with *i* levels, where the capacity of each level is ω_i and p_i represents the probability of each state.

$$ELCC = -\frac{1}{m}\ln\left[\sum_i p_i e^{-m\omega_i}\right] \tag{4.1}$$

where, *m* is Garver's constant and can be determined after a simple reliability assessment run. This technique has been a popular method in the estimation of ELCC but has been superseded by advances in computing power [4].

4.3.2.2. Annual Peak Calculations

Some power systems use loss of load probability at time of annual peak demand as a risk criterion to calculate the ELCC of wind generators [76]. In this approximation method, instead of considering reliability index for the whole year, the impact of wind plants on the risk index is studied at the time of annual peak. Since this specific time happens once a year, the available data is limited [4]. There are two methods to estimate the capacity value of wind during annual peak: 1) considering the entire peaking season 2) considering hours where demand is within a specific percentage of the annual peak. The drawback of this method is that it is limited to a specific period and does not consider load curtailments at other times of the year [4].

4.3.2.3. Peak-Period Capacity Factor

One of the most straightforward methods is to calculate the wind capacity factor (average output) over several periods of peak demand [2], [77]. This approach is not as accurate as the reliability-based method, but might be useful as a quick screening method since it does not require rigorous calculations and excessive datasets. The main deficiency of this method is its incapability to capture the short term or annual fluctuations of wind energy, or the correlation between wind power and electricity demand.

4.4. Modelling Wind in Reliability Studies

There are several methods to model wind energy in the reliability assessment. Wind energy simulated from these models then is utilized in the reliability studies to calculate the capacity value of wind. Different models may result in different capacity values for wind energy. Hence, to have accurate results in reliability evaluation, implementing a proper method to model wind is essential.

Wind speed data generated from the following modelling methods are utilized to obtain wind power output. Wind power generation then is implemented in reliability evaluation as chronological data or a multi-state generator [6]–[8]. Chronological hourly wind data produced by these methods is used in a sequential Monte Carlo simulation to calculate the ELCC [78]. The hourly wind power is considered as a negative load and the system's demand at a specific time is equal to the original load minus the wind generation at that moment [4], [5]. On the other hand, the multi-state wind generator model is similar to conventional generators with derated states, where wind power is represented with partial capacity outage states with associated probabilities. Analytical methods or a Monte Carlo state sampling technique are suitable to determine the capacity credit of wind power when it is presented as a multi-state model [6], [79], [80].

Some of the popular models to represent wind in reliability evaluations are presented in this section and their advantages and disadvantages are described.

4.4.1. Observed Data

Directly using observed historical wind data repetitively in the reliability assessment procedure is one of the easiest and most straightforward methods. In this approach, generated wind power obtained from historical wind speed data is modelled as a negative load or as a multi-state generator and reliability evaluation is conducted according to the modelled wind power [4], [5].

However, the main issue with the observed wind data is the missing data. Because of equipment failures or extreme weather conditions, some data points may not be recorded and are required to be estimated before creating the wind models [78]. Moreover, reliability indices calculated based on the observed data are highly related to the wind regimes in the years considered in the assessment, especially when the size of data sets are limited [78].

4.4.2. Time Series

Time series models such as auto regressive moving average (ARMA) [70], [78], [80]–[83] are one of the most popular methods to simulate wind in reliability studies. The ARMA model is based on historical wind speed data and can represent wind speed fluctuations [70]. Reliability indices

obtained from an ARMA model based on a small number of historical data are similar to those calculated based on a large number of years of data [78]. The ARMA models are different for different locations due to the difference in their wind regimes [80].

To create an appropriate ARMA model for a wind farm, the methodology described in [70] can be utilized. In this method, the simulated wind speed SW_t is computed by implementing the average value (μ_t) and standard deviation (σ_t) of wind data at time t into the(4.2).

$$SW_t = \mu_t + \sigma_t y_t \tag{4.2}$$

where y_t represents the data series value and can be calculated from observed wind data (OW_t) and using (4.3).

$$y_t = (OW_t - \mu_t) / \sigma_t \tag{4.3}$$

Then an ARMA(n,m) time series model of a wind farm can be created by means of (4.4).

$$y_t = \sum_{i=1}^{n} \phi_i y_{i-1} + \alpha_t - \sum_{j=1}^{m} \theta_j \alpha_{t-j} \tag{4.4}$$

where, ϕ is the auto-regressive parameter, θ denotes the moving average element and α_t indicates white noise with a normal independent distribution.

For example, an ARMA(4,3) model of Musselroe wind site in Tasmania, which is created using historical wind data from 2007 until 2012, is presented in (4.5).

$$\begin{aligned} y_t &= 1.0148 y_{t-1} + 0.7822 y_{t-2} - y_{t-3} + 0.1934 y_{t-4} + \alpha_t \\ &\quad - 0.2404 \alpha_{t-1} - 0.8924 \alpha_{t-2} + 0.3196 \alpha_{t-3} \\ \alpha_t &\in NID(0\ ,\ 0.12633^2) \end{aligned} \tag{4.5}$$

Wind speed data created by the ARMA method can be more comprehensive in reliability evaluation than the observed wind speed model [78]. In addition, the ARMA model is the most proper model to represent wind in the sequential Monte Carlo simulation method [80].

4.4.3. Markov Chain

Markov Chain model can incorporate the probability, frequency and duration characteristics of wind speed [78]. In this model, wind speed or the output power of a wind turbine is represented as a multi-states Markov chain [9], [79]. These states are created based on the available observed wind data. In this model, transition rates between wind states (λ_{ij}) are required to simulate wind energy. In the Markov model, an exponential distribution is considered for state residence times of wind,

and states' frequencies are close to those of the historical wind data [78]. A Markov model for a sample 2MW wind turbine is shown in Figure 4.2 [79].

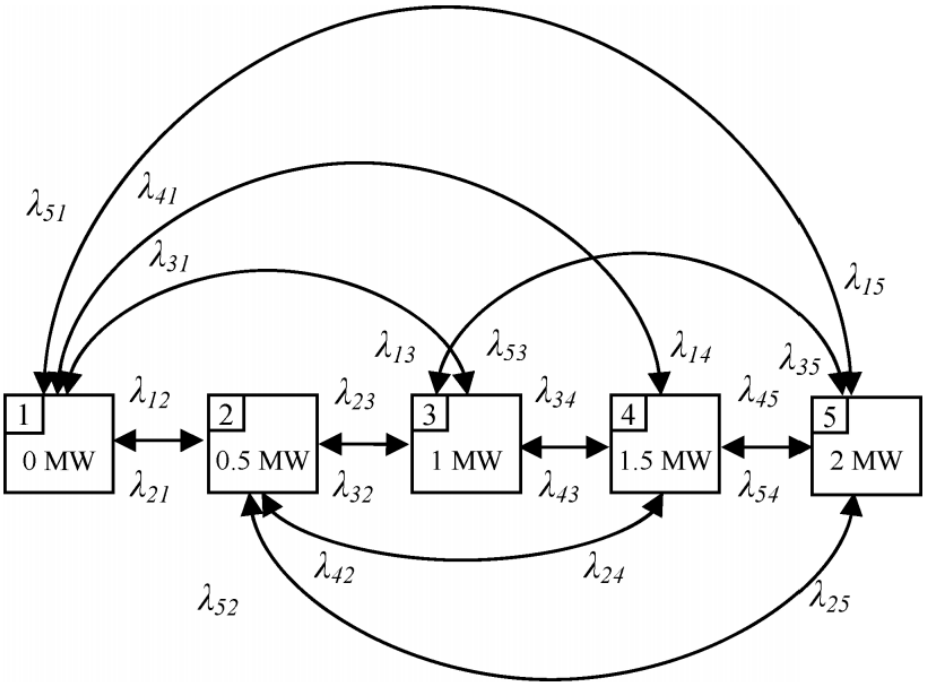

Figure 4.2. Markov model for generated power of a 2MW wind turbine [79].

There are several deficiencies associated with the Markov model. In this model, state probabilities of the simulated wind data are sometimes different from those of the historical data. The differences may lead to differences in the generated wind power and will cause noticeable errors in the ELCC estimations [78]. Moreover, since wind speed is used to create Markov model for wind turbines, when the number of turbines in a wind farm is large or there are several wind farms in the study, these models become complicated and face significant difficulties [79]. Also these models may generate a large number of states for wind farm output power, which is not desirable for reliability assessments. Furthermore, Markov chain models may not be able to keep the correlations and may lose the load following capability, which will result in different reliability indices [78].

4.4.4. Probabilistic Distribution

Several studies have utilized probability distribution functions to model wind speed in reliability assessments. The probability density functions of some popular models that have been proposed for wind speed modelling are presented in Table 4.1. Parameters in these formulas are as follows: α is shape parameter, β denotes size parameter, γ is location parameter and k represents inequality parameter. μ is the average and σ is the standard deviation of the logarithm of random variable.

Table 4.1: Probability density functions of popular distributions to model wind speed [71]

Distribution	Probability density function	Reference
Burr	$\alpha k\left(\frac{x}{\beta}\right)^{\alpha-1} \Big/ \beta\left(1+\alpha\left(\frac{x}{\beta}\right)\right)^{k+1}, \quad -\infty < x < \infty;\ 0 \text{ otherwise}$	[84]
Gamma	$\left(\frac{1}{\beta\Gamma(\alpha)}\right)\left(\frac{x-\gamma}{\beta}\right)^{\alpha-1} e^{(-(x-\gamma)/\beta)},\ \gamma < x < \infty;\ 0 \text{ otherwise}$	[85]
Inverse Gaussian	$\sqrt{\left(\frac{\beta}{2\pi(x-\gamma)^3}\right)} e^{(-\beta(x-\gamma-\alpha)^2/2\alpha^2(x-\gamma))}, \quad \gamma < x < \infty;\ 0 \text{ otherwise}$	[86]
Lognormal	$\frac{e^{-0.5\left(\frac{\ln(x-\gamma)-\mu}{\sigma}\right)^2}}{(x-\gamma)\sigma\sqrt{2\pi}}, \quad \gamma < x < \infty;\ 0 \text{ otherwise}$	[87], [88]
Rayleigh	$\left(\frac{x}{\beta^2}\right) e^{-0.5\left(\frac{x}{\beta}\right)^2},\ 0 < x < \infty;\ 0 \text{ otherwise}$	[88]–[90]
Weibull	$\left(\frac{\alpha(x-\gamma)^{\alpha-1}}{\beta^\alpha}\right) e^{-\left(\frac{x-\gamma}{\beta}\right)^\alpha},\ \gamma < x < \infty;\ 0 \text{ otherwise}$	[13], [85], [90]–[92]

Amongst these distribution functions, the Weibull distribution is the most commonly recommended and adopted distribution to describe the distribution of wind speed as this distribution can give a good fit to the measured data [72], [93].

The main drawback of these models is that a large amount of wind speed data is needed to build proper probability distributions of wind speed [82]. Moreover, it is difficult to select an appropriate distribution, and none of these distributions is suitable to represent wind distributions for all wind regimes since different locations may have different distributions [94]. Also, because of extreme randomness of wind speed in both time and space, the estimated parameters for an assumed distribution may not fit historical wind speed data [71]. Furthermore, some of these distributions cannot capture the chronological nature and the hourly dependencies among data sets [78].

4.5. Proposed Methodology

Wind power data simulated from the above methods as mentioned earlier, are normally implemented in reliability assessment either as chronological data or multi-state models. However, there are some concerns with these methods. A major concern associated with the multi-state technique is the loss of wind and load correlation and the relations between wind farm variations [4]. Since the capacity value is affected not only by the mean wind power, but also the correlation between wind farms and the demand at each hour, this incapability may cause errors in the ELCC calculation [78]. Although some studies proposed methods to keep the correlations [10]–[14], these

methods will face difficulties in modelling and may become complicated when the number of wind farms increases. For instance, the method presented in [14] is capable of keeping the relevance between datasets, as this method utilizes the available capacity probability table, it will become complicated as the number of wind farms increases. Moreover, some of these approaches [13], [14] are applicable in the generation level assessment and haven't addressed the reliability assessment of renewables considering transmission system outages and constraints. On the other hand, sequential method is capable of keeping dependencies. However, this approach needs considerable computation time, particularly in reliability assessments for large generation and transmission systems [80], [83][95].

Therefore, a new framework is proposed in this research in order to address these deficiencies and to capture timely features and correlations between load and renewable power data sets, while keeping the reliability assessment simple and fast. For this reason, a time-dependent clustering technique has been developed. Several years of data points are clustered into hourly base groups. Then, by means of random numbers, values of the wind power and load for each hour are determined. Afterward, reliability indices of electric systems are obtained, and load carrying capabilities of renewable generators are calculated based on these indices. In this study, the fuzzy c-mean clustering method [54] has been applied to classify data sets, a correlated random number sampling technique is proposed to select the proper value from time-dependent clusters and state sampling Monte Carlo is used to calculate reliability indices. These steps are briefly described in the following subsections.

4.5.1. Fuzzy C-Means (FCM)

Clustering is the process of dividing data sets into classes so that elements in the same class have similar values. Fuzzy C-means (FCM) is one of the most widely used clustering methods [96]–[98]. The FCM algorithm was described in Chapter 3. As it was mentioned in that chapter, an appropriate number of clusters should be selected to obtain an accurate clustered model. Elbow technique is a popular method to find the proper number of clusters [99]. In this method, if the objective function value (difference between data points and cluster centres) is graphed on a y-axis and the number of clusters on an x-axis, it can be observed that the objective function value is reduced by selecting higher number of clusters; however, this reduction is not significant after the elbow point. Figure 4.3 displays the objective function of FCM to create hourly cluster model for the RTS hourly demand with a different number of clusters.

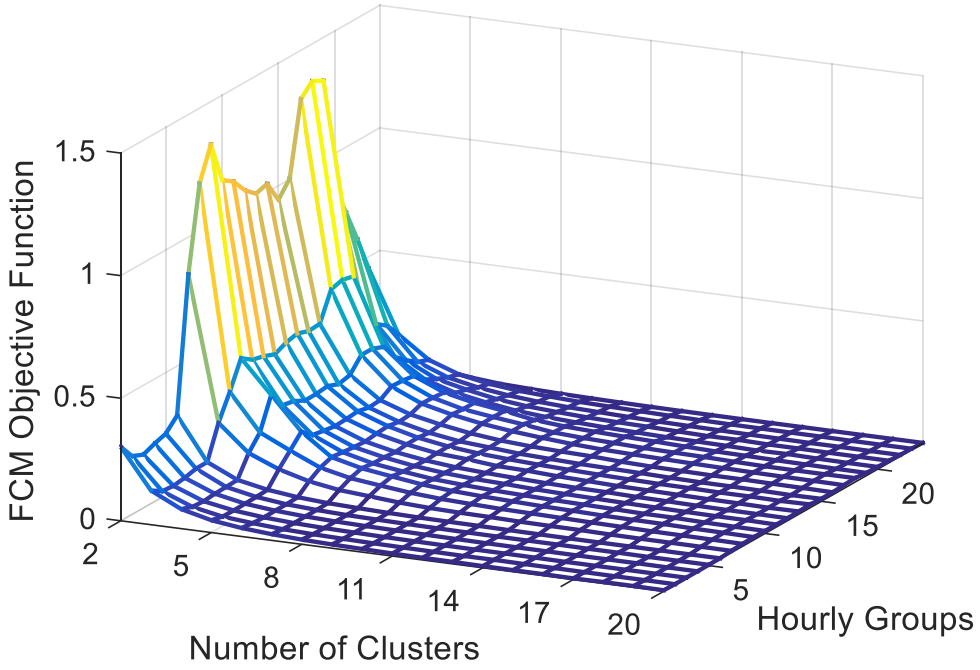

Figure 4.3. Number of clusters analysis

It can be observed that for all of the hourly data sets the objective function value can be reduced by selecting higher numbers of clusters. However, this reduction is not significant after selecting ten or more clusters, which is after the elbow point. An Hourly 10-step model of the per-unit demand of RTS is demonstrated in Figure 4.4. This model has retained the time dependency feature of the demand. It shows that the electricity demand can have 10 different states for each hour, while these values are low in the early morning and are high during the morning and evening peak times.

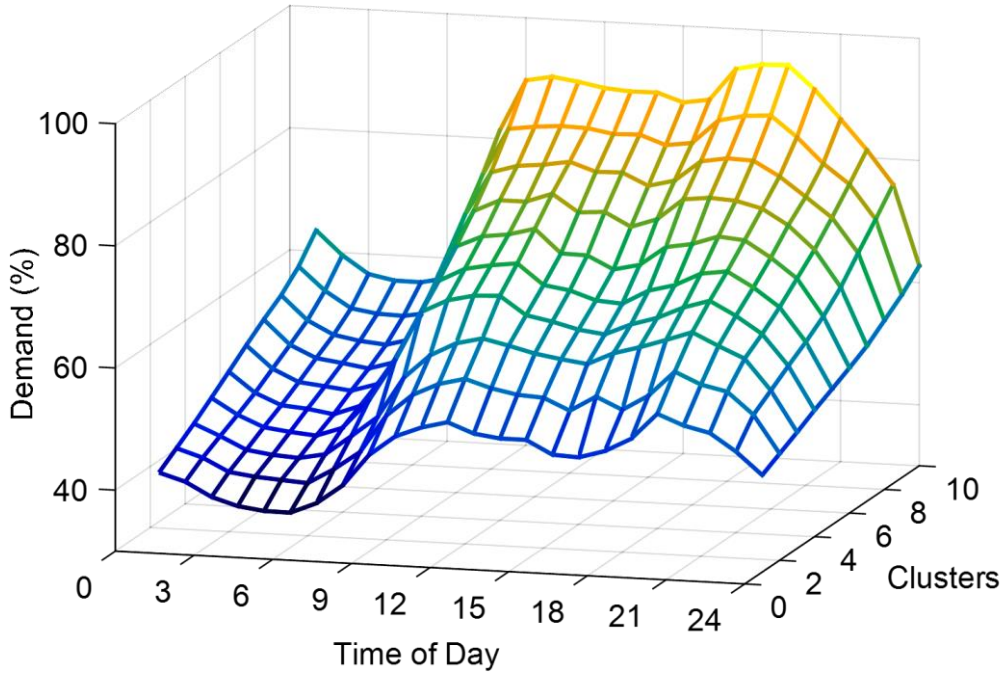

Figure 4.4. Time-dependent clustered model for the RTS demand

Each hourly state has a probability of occurrence P_j and these probabilities should meet (4.6).

$$\sum_{j=1}^{n} P_j = 1 \tag{4.6}$$

When a time-dependent cluster model is created, to determine the hourly value of wind or load in the reliability assessment, the sampling technique [45] is employed.

4.5.2. Sampling Technique

The probabilities of all clusters P_j are put consecutively in the interval [0, 1]. Then by generating a uniformly distributed random number in the same interval, a cluster centre will be selected for each sample according to the value of this random number [45]. Figure 4.5 shows this process which should be repeated for each hour to determine the value of data for that hour in each sample simulation.

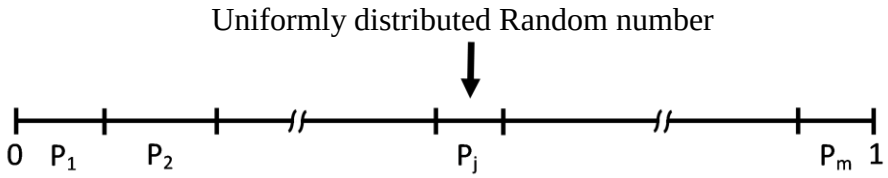

Figure 4.5. Explanation of how to sample clustered data

This process should be implemented on all wind farms output and load data sets. Figure 4.6 illustrates the RTS electricity load for a sample day created by this technique. Output value for each hour has been determined from time-dependent clusters using the sampling technique mentioned above.

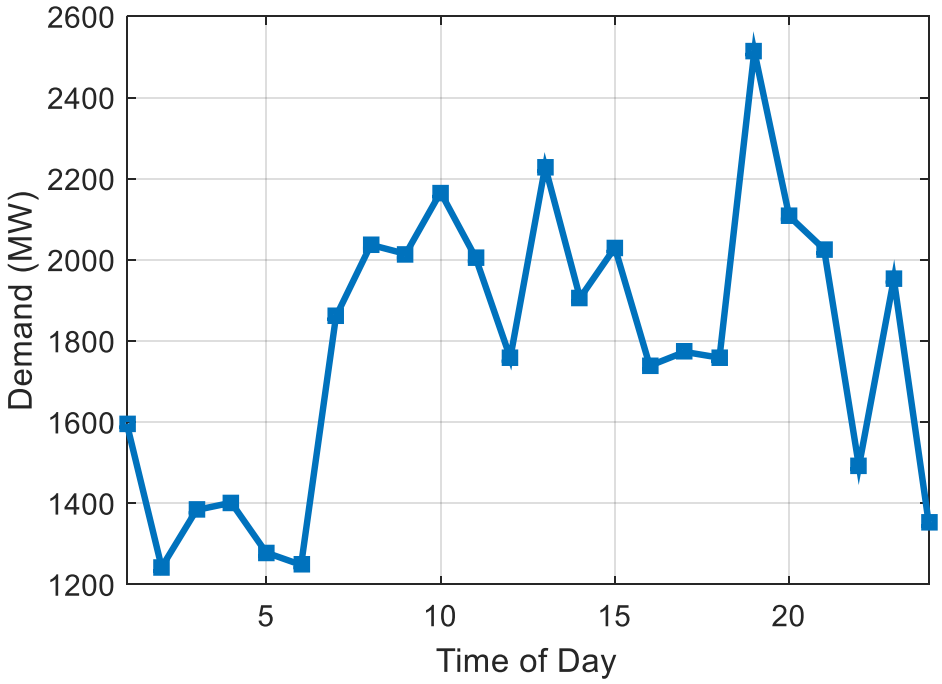

Figure 4.6. Hourly simulated demand for a sample day.

4.5.3. Correlation

The only problem with the sampling technique is the correlation between wind models. Although using independent uniformed random numbers for each cluster model may provide an accurate ELCC estimation in systems with uncorrelated wind farms, results may become different from chronological calculations if there are highly correlated wind plants in the power grid. Since a correlation among wind farms may exist, the problem with accuracy of the simulations arises when the output of several wind farms are simultaneously simulated [100]. To overcome this problem, a correlated random number selection process is proposed in this work.

Correlation matrix method is a conventional method to keep the relevance between wind regimes [100]–[102]. Cholesky decomposition (CD) technique [103] is one of the popular methods based on the correlation matrix, which is particularly useful for Monte Carlo simulations [104]. However the main drawback of this method is that it can just keep the correlation between normal distributions, while wind power usually does not follow this distribution [13], [74]. Therefore, the Cholesky decomposition is combined with distribution transformation techniques in the sampling process to deal with the correlations between random numbers. This can be conducted by means of the inverse transformation technique [45], [105], [106]. The correlated sampling process is explained in the following steps.

A) Creating a normal distributed random matrix

An independent random matrix *R* is created for all wind farms by using normal distributed variables. The size of this matrix depends on the number of wind plants and the number of sample years in the MCS reliability assessment.

B) Cholesky Decomposition

In order to generate correlated random variables (normal distributed) using CD, first, the correlation matrix of wind farms is required, which is a symmetric matrix and is shown in (4.7).

$$C = \begin{bmatrix} 1 & \rho_{12} & \rho_{13} & \cdots & \rho_{1n} \\ \rho_{12} & 1 & \rho_{23} & \cdots & \rho_{2n} \\ \rho_{13} & \rho_{23} & 1 & \cdots & \rho_{3n} \\ \vdots & \vdots & \vdots & \ddots & \vdots \\ \rho_{1n} & \rho_{2n} & \rho_{3n} & \cdots & 1 \end{bmatrix} \tag{4.7}$$

Then, with the correlation matrix *C*, a matrix *U* should be generated such that the equation (4.8) is met.

$$UU^T = C \tag{4.8}$$

Matrix U is a lower triangular matrix and U^T is upper triangular. The matrix U can be utilized to convert independent normal random values into dependent multi-normal variables. This matrix can be calculated by means of (4.9) [103].

$$U=\begin{bmatrix} 1 & 0 & 0 & \cdots & 0 \\ \rho_{12} & \sqrt{1-\rho_{12}^2} & 0 & \cdots & 0 \\ \rho_{13} & \frac{\rho_{23}-\rho_{12}\rho_{13}}{\sqrt{1-\rho_{12}^2}} & \sqrt{1-\rho_3 R_2^{-1}\rho_3^T} & \cdots & 0 \\ \vdots & \vdots & \vdots & \ddots & 0 \\ \rho_{1n} & \frac{\rho_{2n}-\rho_{12}\rho_{1n}}{\sqrt{1-\rho_{12}^2}} & \frac{\rho_{3n}-\rho_3^{*n}R_2^{-1}\rho_3^T}{\sqrt{1-\rho_3 R_2^{-1}\rho_3^T}} & \cdots & \sqrt{1-\rho_n R_{n-1}^{-1}\rho_n^T} \end{bmatrix} \tag{4.9}$$

where, $R_n=(\rho_{ij})_{ij=1}^{n}$ is a positive-definite correlation matrix, R^{-1} is its inverse and to simplify writing let $R_0^{-1}\equiv 1$. For j ≥ i , $\rho_i^{*j}=(\rho_{1j},\rho_{2j},\ldots,\rho_{1j})$, and $\rho_i\equiv\rho_i^{*i}$. For n ≥ j ≥ i+1 and i ≥ 1, equation (4.10) applies.

$$\rho_{i+1}^{*j}R_i^{-1}\rho_{i+1}^T=\sum_{k=1}^{i}\rho_{ki+1(1,\ldots,k-1)}\times\rho_{kj(1,\ldots,k-1)} \tag{4.10}$$

After creating matrix U, a correlated random numbers matrix (R_c) can be obtained from the uncorrelated random matrix (R) and using (4.11).

$$R_c=RU \tag{4.11}$$

C) Transformation

Inverse transform technique [45], [105] can be utilized to transform uniform or normal distributions to other distributions by using (4.12). For instance, in Ref. [13] this method is applied to transform normal values into Weibull distributions or in Ref. [74] normal distribution variables (N_i) are converted into different distributions such as Weibull, Burr, lognormal and gamma.

$$X_i=F_{X_i}^{-1}[\Phi(N_i)]\quad(i=1,\cdots,n) \tag{4.12}$$

where, X_i is non-normal distribution variables, $F_{X_i}^{-1}$ is the inverse of any cumulative distribution function F_{X_i}, and $\Phi(N_i)$ represents cumulative distribution function (CDF) of the standard normal variable N_i.

However, these techniques are useful in the Probabilistic Distribution wind models (Section 4.4.4.) where, as mentioned earlier, the complexity increases as the number of wind farms with different distribution functions increases. While in the proposed time-dependent method the purpose of transformation is to convert normal distributed random numbers into uniformly distributed ones for all wind farms. Therefore, the simplest method is utilized to perform this transformation which

is using the cumulative distribution function Φ of normal random variables. For N_i with a standard normal distribution N(0,1), the CDF can be calculated from (4.13) [106].

$$\Phi(N_i) = \frac{1}{\sqrt{2\pi}} \int_{-\infty}^{N_i} e^{-\frac{t^2}{2}} dt = \frac{1}{2}\left[1 + erf\left(\frac{N_i}{\sqrt{2}}\right)\right], \qquad N_i \in \mathbb{R} \tag{4.13}$$

where, *erf*, is the error function. Then the new random variable *U*, defined by U=Φ(N), is uniformly distributed into [0, 1] [106]. This CDF can be easily generated in MatLab by using *normcdf(x)* function. Since just the CDF is used to transform normal into uniform distribution, equation (4.12) and the complicated transformation methods presented in [13], [74] are not required.

To clarify the process of random number selection and the significance of the correlations between wind farms, four neighbouring sample wind farms with high relevance are selected and the result of different simulation methods are presented. The correlation coefficients matrix between these four sample wind farms (W1, W2, W3 and W4) and their distribution functions are illustrated in Figure 4.7.

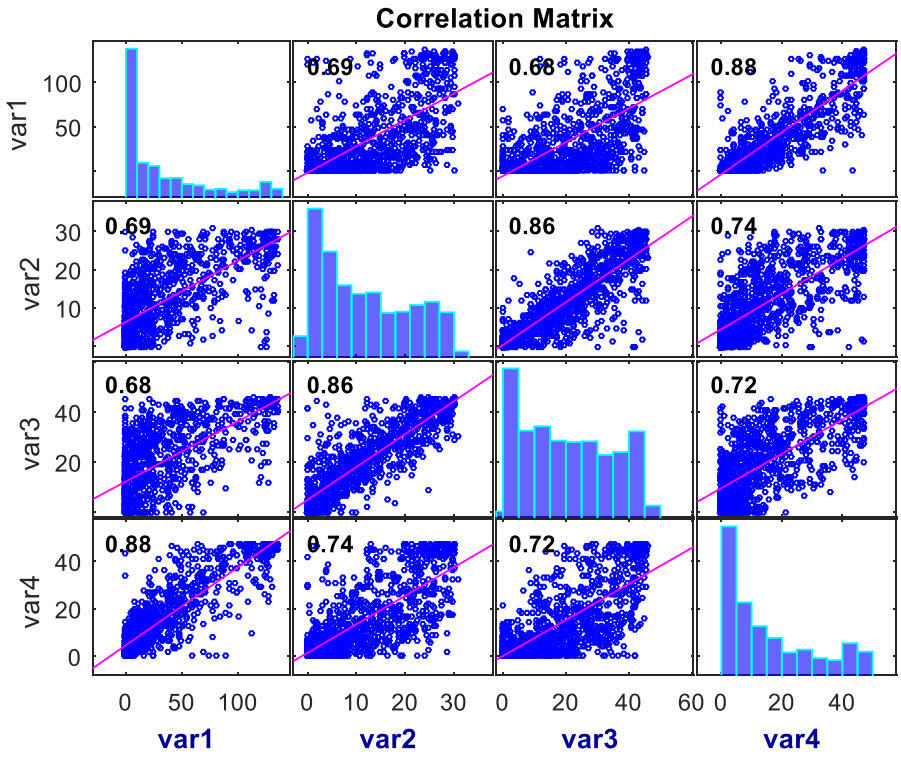

Figure 4.7. Correlations between wind farms based on historical data.

It shows that there are high relevancies between generated powers of these plants. The highest correlation (0.88) exists between W1 and W4, and the relevance between W1 and W3 is the lowest (0.68). Statistical data of the produced power of these wind plants and the total generated power of

them are provided in Table 4.2. It shows that amongst these wind systems W1 has the highest mean value and the highest deviation.

Table 4.2: Statistical data of four sample wind farms and their total wind generation

	W1 (140MW)	W2 (30MW)	W3 (47MW)	W4 (48MW)	W_{total}
Average (MW)	32.64	11.56	20.07	15.32	79.58
Standard Deviation (MW)	40.14	9.29	14.25	14.98	72.22

To show the importance of the dependencies among random variables, first, uniformly distributed random values without any correlation are utilized to select proper values from the time-dependent clustered models to represent wind. Results of this selection method without considering the correlations between wind farms are presented in Figure 4.8.

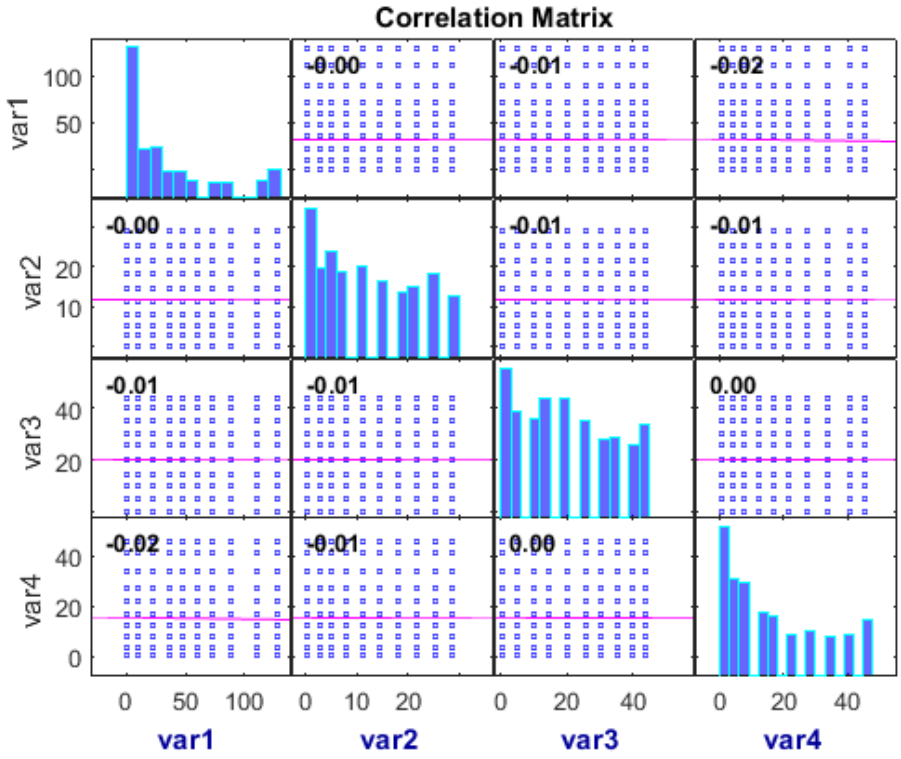

Figure 4.8. Correlations between wind farms using uniformly distributed random numbers.

As it can be seen from this figure, the model has captured the distribution of wind farms but it is incapable of retaining the dependencies. The average values and standard deviations of simulated wind farms and the errors between the standard deviations of simulated values and historical data are given in Table 4.3.

This method has produced individual wind powers with appropriate mean and deviation values. However, the main concern is the total wind power. Although the average value is close to the historical data but due to losing the correlations, the deviation is too far from the observed standard deviation and it has 37.15% error. Since this model cannot capture simultaneous variations between

these wind regimes, the total deviation is different. This total deviation is very crucial in capacity credit calculations. Because a smaller deviation means fewer fluctuations in the total wind power, the capacity value of wind will be overestimated and estimations will be higher than the real ELCC value.

Table 4.3: Statistical data of simulated wind farms and their total wind generation

	W1	W2	W3	W4	W_{total}
Average (MW)	31.52	11.71	20.18	15.29	78.71
Standard Deviation (MW)	39.75	9.28	14.29	14.94	45.39
Error (%)	0.97	0.14	0.23	0.25	37.15

In the second experiment, the Cholesky method has been applied to select correlated random values. The decomposition matrix is shown in (4.14) and simulation results are displayed in Figure 4.9.

$$U = \begin{bmatrix} 1.00 & 0.00 & 0.00 & 0.00 \\ 0.69 & 0.72 & 0.00 & 0.00 \\ 0.68 & 0.54 & 0.50 & 0.00 \\ 0.88 & 0.19 & 0.05 & 0.43 \end{bmatrix} \tag{4.14}$$

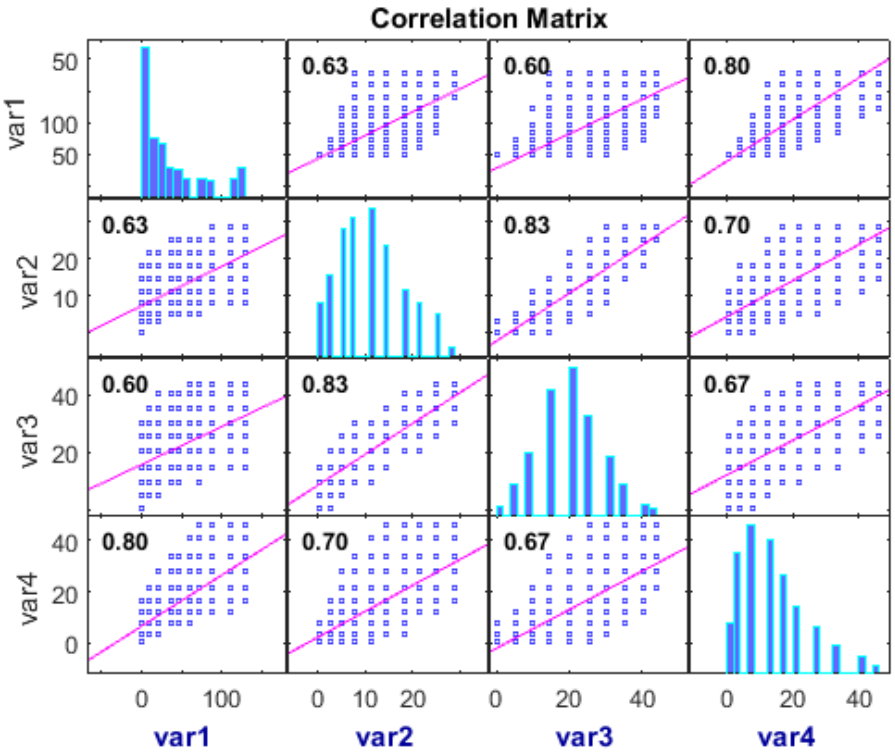

Figure 4.9. Correlations between wind farms using correlated normal random numbers.

This correlation matrix is close to the original one which was given in Figure 4.7. It shows that this method is effective in retaining the relevancies. However, since this method is just applicable

on normal distributed random numbers, it could not keep the distribution function of wind farm outputs. Therefore, the simulated results are not appropriate to represent these power plants in the reliability assessment. The main difference is in the deviation values of individual wind farms and total power production.

Table 4.4: Statistical data of simulated wind farms and their total wind generation

	W1	W2	W3	W4	W_{total}
Average (MW)	32.88	10.82	20.19	13.15	77.05
Standard Deviation (MW)	39.96	6.86	8.80	9.83	59.36
Error (%)	0.45	26.17	38.27	34.33	17.80

It can be seen that the statistical results of this method, presented in Table 4.4, have high errors in their deviations, which is mainly due to the differences between the distributions of the simulated wind powers and the original values.

In the final test, the proposed methodology, which is a combination of Cholesky and distribution transformation, is utilized to generate correlated uniformly distributed random numbers. As mentioned before, first the correlations are captured by using the Cholesky decomposition matrix, then, the normal distributed random variables are transformed into uniformly distributed values. Outcomes are provided in Figure 4.10 and Table 4.5.

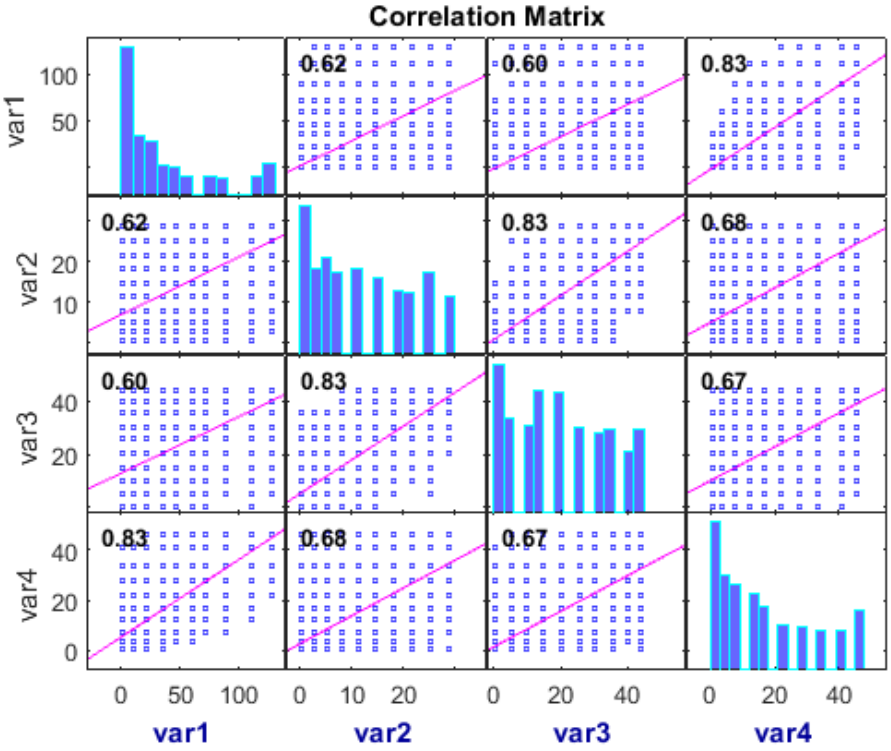

Figure 4.10. Correlations between wind farms using the proposed approach.

It can be observed that this method not only is successful in generating wind powers with accurate distributions but also has captured the dependencies among generated powers. The simulated wind farms have similar mean and standard deviation values and also the total average and deviation are close to the ones of the historical data with just 2.61% error. Therefore, it can be seen that the developed technique is a proper way to select random numbers and to determine the generated wind values from the time-dependent clustered models.

It should be mentioned that the differences in the shape of correlation coefficient diagrams of the clustered models from the historical data are because of the type of data sets. The generated power obtained from time-dependent clustered models are selected from ten cluster values while historical data can have any values from zero to the installed capacity. With more clusters the shape will be closer to the historical data shape. However, as mentioned earlier (Section 4.5.1), the main purpose of clustering is to reduce the size of data, and for wind data sets ten clusters are enough to represent the wind power and more clusters are not required.

Table 4.5: Statistical data of simulated wind farms and their total wind generation

	W1	W2	W3	W4	W_{total}
Average (MW)	32.98	11.59	19.96	15.50	80.03
Standard Deviation (MW)	40.08	9.29	14.16	14.92	70.34
Error (%)	0.17	0.07	0.66	0.38	2.61

4.5.4. Reliability Assessment

By determining all required values for each hour, the reliability index of a system for that moment is being calculated and the overall system index can be obtained by taking the average value of these indices. To calculate the reliability indices, the amount of unserved energy or curtailed load should be calculated. For this reason, the state sampling Monte Carlo Method [45] has been utilized. This technique estimates the generation capacity of the system and the status of transmission lines based on their forced outage rates and repair times. Then, the amount of unserved energy, as a system reliability index, is calculated for each hour of the day according to the system's available generation, transmission capacity and the value of load and wind production obtained from time-dependent clustered model.

As all data sets are being clustered on an hourly basis and reliability assessment is done for each hour separately based on the correlated random sampling, the time dependency attributes and the correlation between all these data sets will be automatically taken into account. The unserved energy of the system with and without renewable generators should be calculated using the

proposed approach and by comparing these indices, the capacity value of clean generators is evaluated.

The proposed framework is briefly described in the following steps:

- All wind farms output and load data sets are reshaped in 24 hourly groups.
- Proper numbers of clusters for all these hourly data sets are specified and elements in each hourly group are clustered using the Fuzzy C-mean technique.
- The probabilities of all clusters are put successively in the interval of [0, 1]. Then by means of correlated uniformly distributed random numbers, the value of wind power and electricity demand for each hour will be determined.
- Reliability of the system is evaluated by implementing these time-dependent cluster models into the state sampling Monte Carlo technique on an hourly basis. The overall system reliability index is obtained by taking the average value of these hourly indices.
- Capacity value of wind is evaluated by investigating the impact of wind generators on the system reliability indices and applying the reliability-based calculation method.

4.5.5. Generation System Level Study

In generation adequacy or hierarchical level I, different reliability indices have been implemented to calculate reliability benefits of renewable energies. Loss of load expectation (LOLE) [4]–[6], severity index (SI) [107] and at-risk and healthy state possibilities [108] are some of these indices. In this study, loss of energy expectation (LOEE) is adapted, because this index not only incorporates the effect of inadequacies but also includes their probabilities [45]. To calculate LOEE, firstly, Demand Not Supplied (DNS) should be computed by means of (4.15).

$$DNS_{s,t} = \max\left\{0, D_t - \sum_{j=1}^{g} G_{js}\right\} \tag{4.15}$$

Where g is the total number of generators and G_{js} represents the available capacity of the j_{th} generator in the S_{th} iteration. D_t denotes the total demand for each hourly cluster t and can be calculated using (4.16).

$$D_t = L_t + P_{\exp,t} - P_{imp,t} - P_{W,t} \tag{4.16}$$

where, L_t is the original system's load, $P_{exp,t}$ and $P_{imp,t}$ represent hourly exported and imported power to the system, respectively, and $P_{W,t}$ is the total wind power generation at time t. After calculating DNS, the annualized LOEE of each hourly cluster and for N iterations is calculated using (4.17).

$$LOEE_t = \frac{\sum_{s=1}^{N} DNS_{s,t} \times 8760}{N} \tag{4.17}$$

4.5.6. Composite System Level Study

Reliability assessment in the hierarchical level II includes generation and transmission systems adequacy. Therefore, reliability assessment results in this level can show the impact of transmission lines outages and insufficiencies on the capacity value of renewable generators. In this level, the amount of unserved energy can be calculated by running load flow for each system state and recording the unserved load in each iteration. In this work, MATPOWER [109] has been used to run load flow and record the total curtailed load due to any element outage(s).

An AC optimal power flow (OPF) is used to calculate the amount of unserved demand due to outages or insufficiencies. When a generator or a transmission line outage happens, the OPF model is applied to reschedule generations and reduce constraint violations. This generation rescheduling also tries to avoid or to minimize the total load curtailment. The objective function of the OPF model (4.18) is minimization of the total load curtailment while satisfying the AC power flow equations and line flow, voltage, and generation output limits, which are shown in equations (4.19) to (4.25).

$$\min \sum_{i \in n_l} C_i \tag{4.18}$$

Subject to

$$P_g^{i,\min} \le P_g^i \le P_g^{i,\max}, \qquad i = 1, \cdots, n_g \tag{4.19}$$

$$Q_g^{i,\min} \le Q_g^i \le Q_g^{i,\max}, \qquad i = 1, \cdots, n_g \tag{4.20}$$

$$V_m^{i,\min} \le V_m^i \le V_m^{i,\max}, \qquad i = 1, \cdots, n_b \tag{4.21}$$

$$\theta_i^{ref} \le \theta_i \le \theta_i^{ref}, \qquad i \in I_{ref} \tag{4.22}$$

$$\sum_{i \in n_g} P_g^i + \sum_{i \in n_l} C_i = \sum_{i \in n_l} P_d^i \tag{4.23}$$

$$0 \le C \le PD \tag{4.24}$$

$$|T(S_j)| \le T_{\max} \tag{4.25}$$

where, C_i is the curtailed load, $P_g{}^i$ and $Q_g{}^i$ are the real and reactive power injections, and $P_d{}^i$ denotes the load power. Voltage magnitude at bus i is shown with $V_m{}^i$ and θ_i is the reference bus angle. Total system demand is PD and C denotes the total unserved load. $T(S_j)$ represents the line flow vector under system state S_j, and T_{max} is the transmission lines limit. n_l, n_g and n_b are the number of generators, loads and total buses respectively, and I_{ref} is the set of indices at the reference bus.

The reliability indices are calculated based on the unserved load in selected system outage states and their probabilities of happening [65]. In this research, the amount of curtailed load and its probability of occurrence are utilized in (4.26) to calculate the hourly value of expected energy not supplied (EENS), which is an important index to represent the amount of unserved energy and is similar to LOEE in HLI.

$$EENS_t = \sum_{l \in S} c_l p_l \times 8760 \tag{4.26}$$

where, p_l is the probability and C_l denotes the amount of curtailed load in system state *l*. the overall EENS of the system is the mean value of these hourly indices. By comparing EENS indices of the system with and without renewable generators, the capacity value of these resources can be computed.

4.6. Implementation on IEEE Reliability Test System

To verify the efficiency of the developed approach, it has been implemented on the IEEE reliability test system. Reliability contribution of wind farms has been investigated at two different adequacy assessment levels: generation level (HLI) and composite system level (HLII). In order to investigate the impact of wind regime and penetration levels of wind, the developed method has been applied for different wind profiles and various levels of wind farms. Also reliability contribution of PV systems has been estimated using this technique to validate its effectiveness to model solar energy. In addition, reliability assessment of RTS with a significant amount of wind and PV has been conducted to evaluate the precision and simplicity of the proposed approach in modelling high levels of renewables.

The IEEE-RTS system is modified by adding wind generators. This system has 2,850 MW peak load and its generation capacity is 3,405MW. The details of this system can be found in Appendix A. Two wind farms with different wind regimes have been added to this system. Wind generation data for these two sites are measured from the real South Australian wind farms from 2012 till 2014 with hourly resolutions [110]. Wind power data for W1 is from the Mount Millar wind farm and data from the Clement Gap plant has been utilized for W2. Figure 4.11 (a) and (b) shows the average percentage value of generated power in these two wind farms.

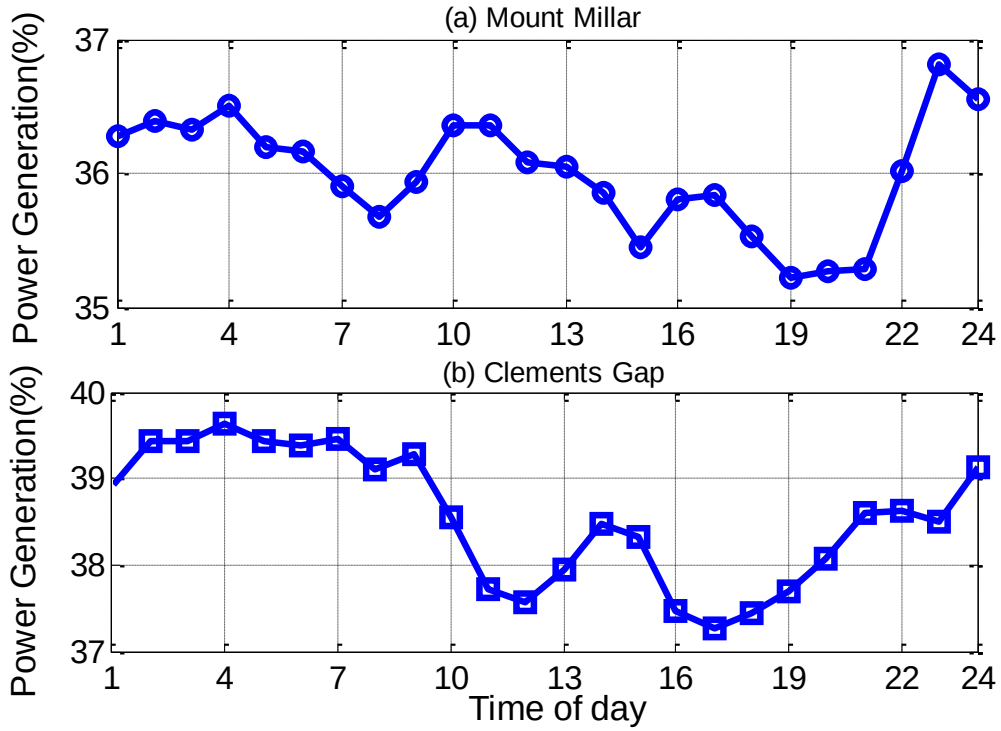

Figure 4.11. Average generated wind power for W1 and W2

Several photovoltaic systems with a sample generation profile have been added to IEEE-RTS. Figure 4.12 depicts the solar power generation pattern for two years. These PV data sets have hourly resolution and are aggregated values of measured data. It shows that the maximum PV generation is around 85% of the rated PV power (500MW), which happens during the summer time. In order to conduct a sensitivity analysis, PV systems with this profile and different installed capacity levels have been added to the RTS system.

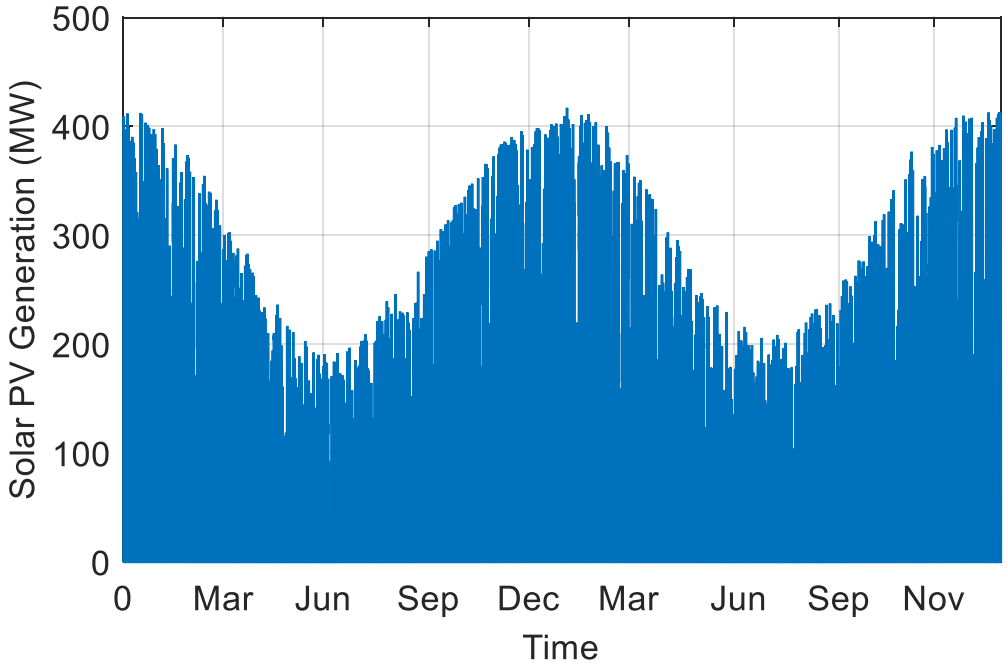

Figure 4.12. A sample PV generation pattern

After implementing the developed method on wind farms, PV units and load data, their time-dependent clustered models are created. Then by applying the sampling technique and implementing these models in the state sampling Monte Carlo, the hourly and total reliability indices of the RTS system at the HLI and HLII levels are calculated.

4.6.1. Results of HLI Assessment

In the first step, loss of load expectation of the original RTS system without renewables is calculated by using the time-dependent clustering model to represent its demand. Figure 4.13 shows the LOEE index of IEEE-RTS for each hour after 10,000 iterations. As this graph shows, the LOEE value is different for each hourly cluster and is expected to be higher during the peak period. The overall LOEE of this system is 1,132 MWh/yr, which is the average value of 24 hourly values.

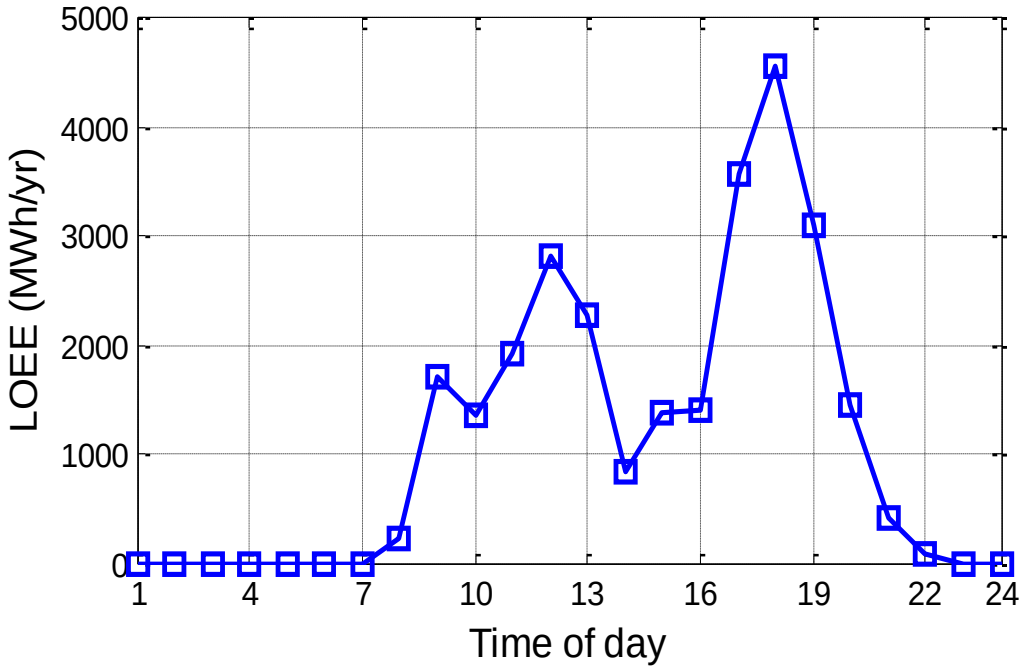

Figure 4.13. Loss of energy expectation value for hourly clusters

After obtaining the reliability index of the original system, the wind power model is added to the system and is utilized as a reference to calculate the capacity value of wind plants. Once again the reliability evaluation is conducted in the presence of wind and extra loads added to the system. The amount of extra load that can be supported with wind farms without exceeding the reliability level of the original system is considered as the ELCC of that wind farm. The ELCC calculation process for the W1 wind farm added to the RTS system is depicted in Figure 4.14.

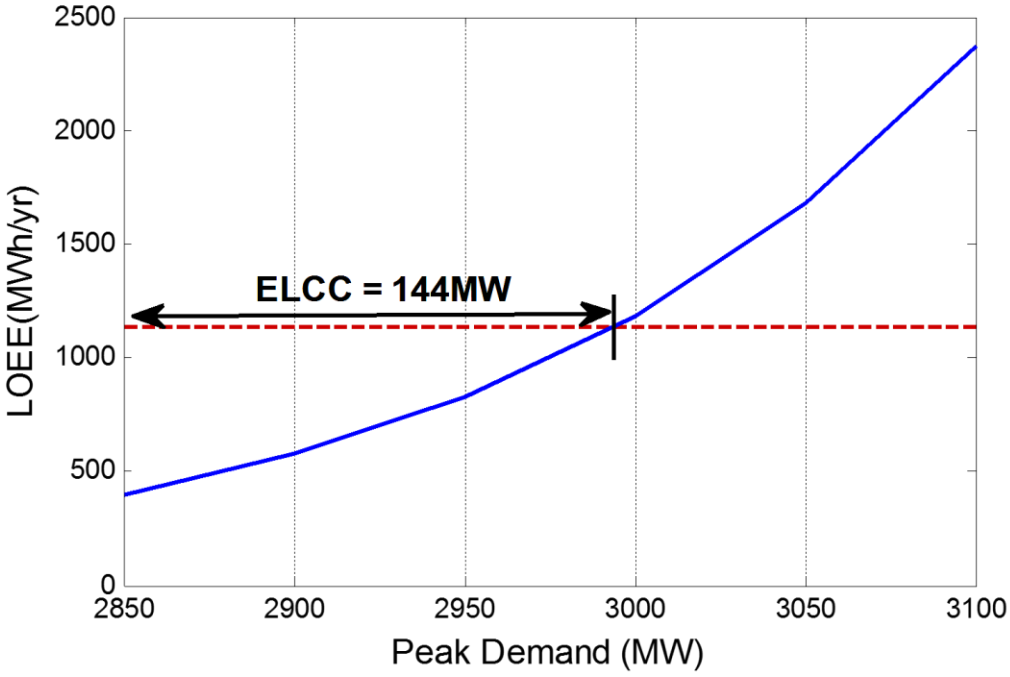

Figure 4.14. Capacity value of the W1 wind farm

The red dashed line is the LOEE of the original RTS system without any wind or PV generators and 2,850 MW peak demand. The blue line is the LOEE index for this system in the presence of the W1 wind farm with 500 MW installed capacity and for different levels of peak load. It shows that in the presence of W1, around 144 MW extra load can be added to the system, while the reliability level of the RTS system is maintained at the original level (1,132 MWh/yr).

Total results of this clustering technique and the sequential Monte Carlo are given in Table 4.6. It should be mentioned that all of the clustered models of wind and PV are generated by using two years of historical hourly data sets.

This table shows that in both techniques, the ELCC of W1 is higher than W2 and by increasing their installed capacity the percentage value of their load carrying capability will decrease. Table 4.6 also illustrates that the differences between the proposed approach and the sequential technique for these wind farms with two different wind regimes are small. In addition, estimated results obtained from the clustering method are acceptable for different levels of wind power. Thus, it can be concluded that the time-dependent approach can effectively estimate the ELCC of wind farms regardless of their wind regime and installed capacity.

Table 4.6: Capacity value of renewable energies for IEEE-RTS at generation level

Capacity Value	Sequential Monte Carlo		Time-dependent Cluster		Error
	MW	%	MW	%	%
Wind Regime 1 – 250MW	84	33.6	90	36.0	2.4
Wind Regime 1 – 500MW	144	28.8	141	28.2	0.6
Wind Regime 1 – 1000MW	230	23.0	211	21.1	1.9
Wind Regime 2 – 250MW	65	26.0	67	26.8	0.8
Wind Regime 2 – 500MW	104	20.8	110	22.0	1.2
Wind Regime 2 – 1000MW	145	14.5	157	15.7	1.2
250MW PV	60	24.0	55	22.0	2.0
500MW PV	98	19.6	91	18.2	1.4
500MW Wind+250MW PV	201	26.8	189	25.2	1.6
1000MW Wind+500MW PV	319	21.3	313	20.8	0.5

Furthermore, it can be seen that this method can also be applied in systems with high levels of PV and wind without losing its simplicity and accuracy. Moreover, simulation results for solar energy indicate that the time-dependent clustering technique is also applicable to model PV systems, and it can precisely estimate the reliability contribution of solar generators with various capacities. More details about the process of modelling solar PV units in reliability evaluation are presented in Chapter 7.

4.6.2. Results of HLII Assessment

In order to evaluate the time-dependent technique at HLII level, the same approach has been applied on the RTS composite system and results are presented in Table 4.7. The capacity values of these resources have decreased due to transmission system outages and congestions.

Table 4.7 shows that the time-dependent technique is also suitable to model wind and PV in the HLII studies. It can be used to estimate ELCC of wind and solar power, separately and combined, at the composite system level with an acceptable correctness.

From Tables 4.6 and 4.7 it can be observed that results of the proposed method in both reliability evaluation levels have an error of less than 2.5% compared to the results of the sequential Monte Carlo technique. However, this clustering technique is much faster as it just needs to be performed for 24 clusters in each sample year compared with 8760 hours in the sequential method. This time

efficiency is especially noticeable in the composite system assessment of large power systems, where load flow execution might be required for each simulation run.

Table 4.7: Capacity value of renewable energies in IEEE-RTS for HLII studies

Capacity Value	Sequential Monte Carlo		Time-dependent Cluster		Error
	MW	%	MW	%	%
Wind Regime 1 – 500MW	121	24.2	113	22.6	1.6
Wind Regime 2 – 500MW	80	16.0	88	17.6	1.6
250MW PV	49	19.6	43	17.2	1.4
500MW Wind + 250MW PV	151	20.1	145	19.3	0.8

The proposed methodology has been applied to an existing power system in Australia to demonstrate the effectiveness and speed of this technique in comparison with the sequential Monte Carlo method. The computational time and number of simulations to reach the stopping criterion in evaluating the reliability benefits of renewable generators in the composite system level of this system are given in Table 4.8. It should be mentioned that the LOEE coefficient of variation tolerance, which is 0.1, is utilized as the convergence criterion and the stopping rule is as follows: after reaching a given number of samples, the variation tolerance is checked to see if it is acceptable. If not, the number of samples is increased.

Table 4.8: Speed Comparison for composite system studies

Method	Number of Sample Years	Computation time (min)
Sequential Monte Carlo	2,000	2165.6
Time-dependent Cluster	50,000	118.55

From this table, it can be seen that the number of sample years to reach the proper tolerance error in clustering approach is higher than the sequential method. For the HLII studies, in the sequential Monte Carlo method 2,000 sample years were used while in the proposed method this number was 50,000. However, in the sequential Monte Carlo it should be simulated for 8,760 hours per sample year, while in the clustering methodology it just needs 24 simulations per year. Therefore, as it is shown, the computational time of the time-dependent clustering technique is much lower than the one of the sequential Monte Carlo method.

4.7. Summary

Because wind is uncertain and variable, it is important to determine the contribution of wind energy contribution to power demand adequacy. Capacity value or effective load carrying capability is a common term to demonstrate the reliability contribution of generators. In this chapter the definition of ELCC is presented and several methods from reliability-based and estimation methods to calculate this value are described. However, due to the characteristics of wind, conventional reliability evaluation methods are not applicable and different models have been developed to represent wind power in reliability assessment and ELCC calculations. Some of the most popular methods to model wind are presented in this chapter.

Most of these methods are time-consuming or may not be able to keep the time dependency and relevancies among renewable resources and load. Therefore, this research intends to improve the existing methods and proposes a fast and simple approach. In this approach, wind power, PV generation and electricity demand are being modelled as time-dependent clusters, which not only can capture their time-dependent attributes, but also is able to keep the correlations between these data sets. In addition, it can handle many wind farms in a large network without losing its time efficiency, simplicity and accuracy.

In this method, Fuzzy C-mean clustering algorithm has been utilized to create time dependant models to represent wind power, solar generation and load data. Then, a sampling method is developed based on the Cholesky decomposition and transformation approaches to select the proper hourly value from wind clusters while retaining the relevancies among wind farms. Afterward, the time dependant models are applied with the state sampling Monte Carlo to calculate the reliability indices of power systems with and without renewable generators. Then by means of these indices, capacity value of wind and PV is computed.

To illustrate the effectiveness of this framework, the proposed methodology has been applied on the IEEE-RTS system and the correctness of the results is validated. The validation test consists of comparing outputs of the developed technique with the results of the sequential Monte Carlo method. The proposed approach is implemented in the next chapters to calculate the capacity value of Australian wind farms at the generation and composite system levels.

Chapter 5

Capacity Value of Australian wind farms

5.1. Introduction[1]

Wind energy is growing fast in Australia and the total wind capacity of Australia has increased around 3GW in the last decade. Since the share of wind farms in electricity production is rising, their role in the Australian electricity market is becoming more significant. Therefore, in this chapter, the contribution of wind power in the Australian National Electricity Market (NEM) from a reliability point of view is investigated. NEM is an interconnected grid comprising several connected regional networks and approximately 48,000 MW of installed generation [39]. The NEM spot pool market is managed by the Australian Energy Market Operator (AEMO) and operates across the Eastern and Southern states. The NEM region incorporates Queensland (QLD), New South Wales (NSW), Australian Capital Territory (ACT), Victoria (VIC), South Australia (SA) and Tasmania (TAS). The regional map of NEM is shown in Figure 5.1.

The installed capacity of wind generation in the NEM at the end of 2014 was more than 3,100MW. Amongst all the states, South Australia has the highest wind capacity (1,473MW) and Victoria is in second place with almost 1GW wind capacity. However, new wind farms are

[1] This chapter has materials from the following references published by the PhD candidate.

- Mehdi Mosadeghy, Ruifeng Yan and T.K. Saha, "A Time Dependent Approach to Evaluate Capacity Value of Wind and Solar PV Generation" IEEE Transactions on Sustainable Energy, early access, DOI: 10.1109/TSTE.2015.2478518.
- Mehdi Mosadeghy, Tapan K. Saha and Ruifeng Yan, "Increasing Wind Capacity Value in Tasmania Using Wind and Hydro Power Coordination" IEEE Power and Energy Society General Meeting, 21-25 July, 2013, Vancouver, British Columbia, Canada.
- Ruifeng Yan, Tapan K. Saha, Nilesh Modi, Nahid Al-Masood and Mehdi Mosadeghy, "The combined effects of high penetration of wind and PV on power system frequency response" Applied Energy (Elsevier) 145 (2015) 320–330.
- Mehdi Mosadeghy, Ruifeng Yan and Tapan K. Saha, "The Impact of Interconnections on Reliability Contribution of Wind Farms" Asia-Pacific Power and Energy Engineering Conference 2015, 15-18 November, 2015, Brisbane, Australia.
- Mehdi Mosadeghy, Tapan K. Saha, Ruifeng Yan and Simon Bartlett, "Reliability Evaluation of Wind Farms Considering Generation and Transmission Systems" 2014 IEEE Power and Energy Society General Meeting, 27-31 July, 2014, Washington, DC, USA.

expected to be installed in Victoria and this state will have the highest wind capacity in Australia by 2020 [15]. The contribution of wind in NSW and Tasmania is not that high; nevertheless, similar to SA and VIC, their wind capacity is expected to grow significantly. Queensland has the lowest wind generation in the NEM and its wind capacity is not predicted to develop remarkably. Therefore, since there is not a significant amount of wind generation in QLD, this power system has not been considered in this study. Installed capacity of wind generation in different regions of NEM and their predicted capacity in 2020 are presented in Table 5.1.

In this chapter, the capacity value of wind power in South Australia, Victoria, New South Wales and Tasmania is calculated in two different reliability levels: HLI and HLII. In the HLI studies, the reliability assessment has been conducted at the generation level and the insufficiency of generators to supply demand and the contribution of wind power are investigated. At the composite system level or HLII, in addition to the generation shortages, transmission system's constraints and outages are taken into account in the reliability assessments. Therefore, evaluating the capacity value of wind generation in this level presents the effect of line outages and network limitations on the wind capacity value.

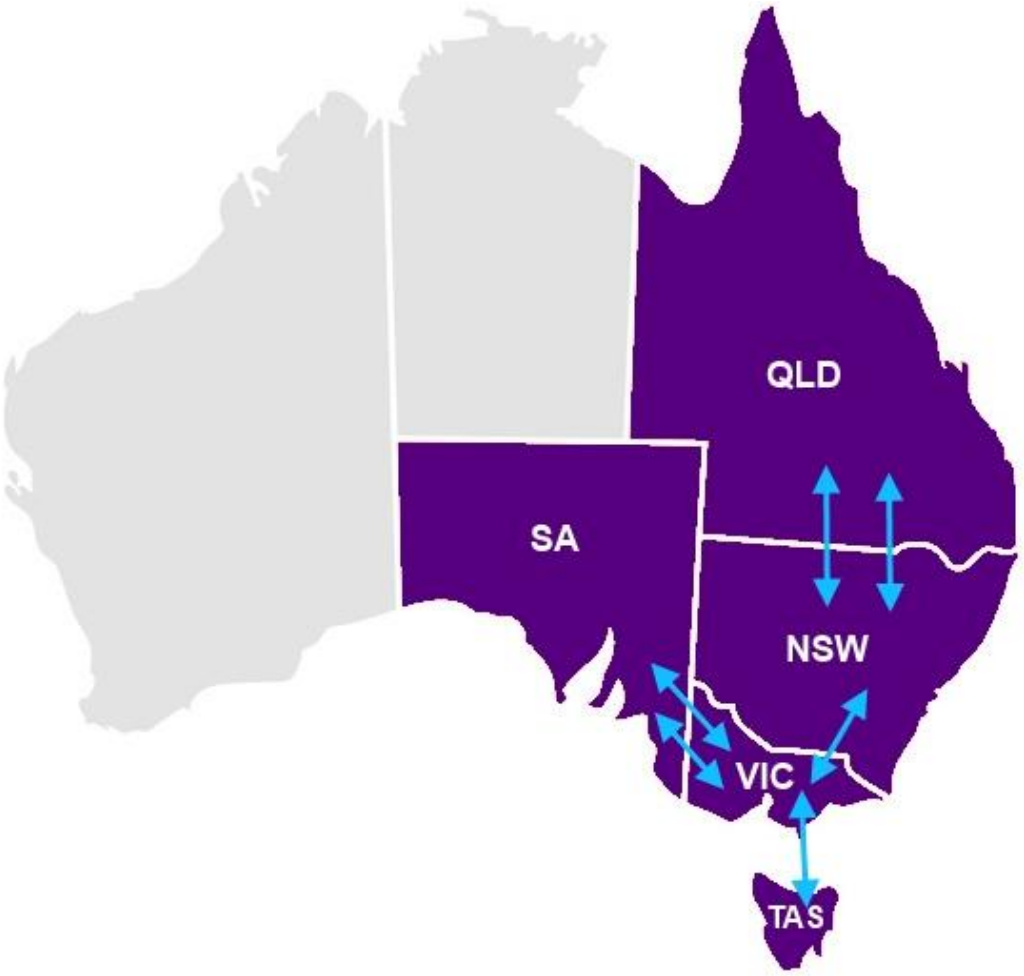

Figure 5.1. Regional map of national electricity market [111]

Table 5.1: Installed and predicted wind capacity of NEM regions [39], [15]

Region	2014 Wind (MW)	2020 Wind (MW)
New South Wales	281	2,382
Queensland	12	266
South Australia	1,473	2,555
Tasmania	308	1,368
Victoria	1,070	4,974

In order to calculate the reliability contribution of wind, the time-dependent approach that has been explained in Chapter 4 is utilized to model wind power, electricity demand and exchanged power through interconnections. The main reason for applying this methodology is its ability to capture the correlations between datasets and their time varying behaviours while keeping the assessment process simple and fast, particularly in the transmission level studies of large power systems such as NSW, SA and VIC, where the sequential methods might not be applicable and need significant computational time.

Furthermore, the impact of interconnections and interstate exchanged power on the ELCC of wind farms is evaluated. For this reason, the capacity value of wind farms in NSW and VIC power systems, which have several interconnections, has been calculated in island and connected modes. The significance of the tie-lines power flow on ELCC is assessed by comparing the results of these two modes.

Moreover, since Tasmania has a large hydro generation capacity, coordinating hydro units with wind farms to increase the capacity value of wind power is investigated. Different values are selected as the coordination capacity to analyse the impact of different coordination capacities on the ELCC of wind farms.

5.2. South Australia

5.1.1. South Australian Power System

South Australia (SA) is a Southern state in Australia and its capital city is Adelaide. The SA system has a substantial installed level of wind and solar generation, which can supply around 80% of its average load. Historical hourly load data of the SA system is extracted from [112]. The load profile of South Australia is depicted in Figure 5.2. In this diagram, the horizontal axis is the time of day in hours, the bottom and top of the boxes are the first and third quartiles, and the band inside the box is the second quartile (the median) of load data. The ends of the whiskers represent the variability outside the upper and lower quartiles and the minimum and maximum of all of the data. From this graph it can be observed that the overall electricity demand in SA is at low levels from midnight to early in the morning and this system has two peak periods: one in the morning and the other one in the evening. However, the highest peak (3,000 MW) occurs during the afternoon.

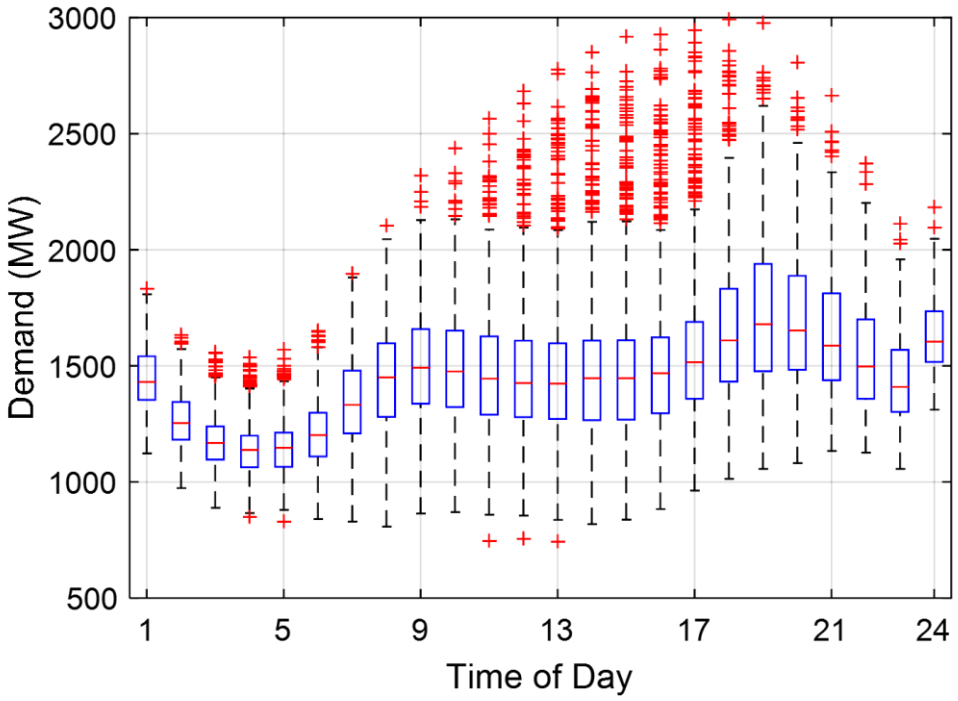

Figure 5.2. Box-and-whisker plot for hourly load data in South Australia for 2012-13 [112]

The generation profile of South Australia is a mixture of thermal and renewable generators. The total installed capacities of thermal and renewable generation of SA in 2013 were approximately 3,600MW and 1,700MW respectively [15]. Table 5.2 shows number, type and capacity of generators in South Australia.

Table 5.2: Generating unit data in 2013 [113], [114]

Type		Number of Units	Total installed Capacity (MW)
Conventional	Diesel	6	136.5
	Natural Gas	36	2716
	Brown Coal	6	770
Renewable	Wind	15	1202
	PV	(Distributed)	500

5.1.2. Wind Data

The total generated power of these wind farms in 2012 and 2013 is displayed in Figure 5.3. It shows that in those specific years, the maximum electricity generated by wind farms in SA was higher than 1,000MW [110]. The average value of total wind generation in South Australia during this period was 423MW and the standard deviation of its total hourly wind production was around 250MW.

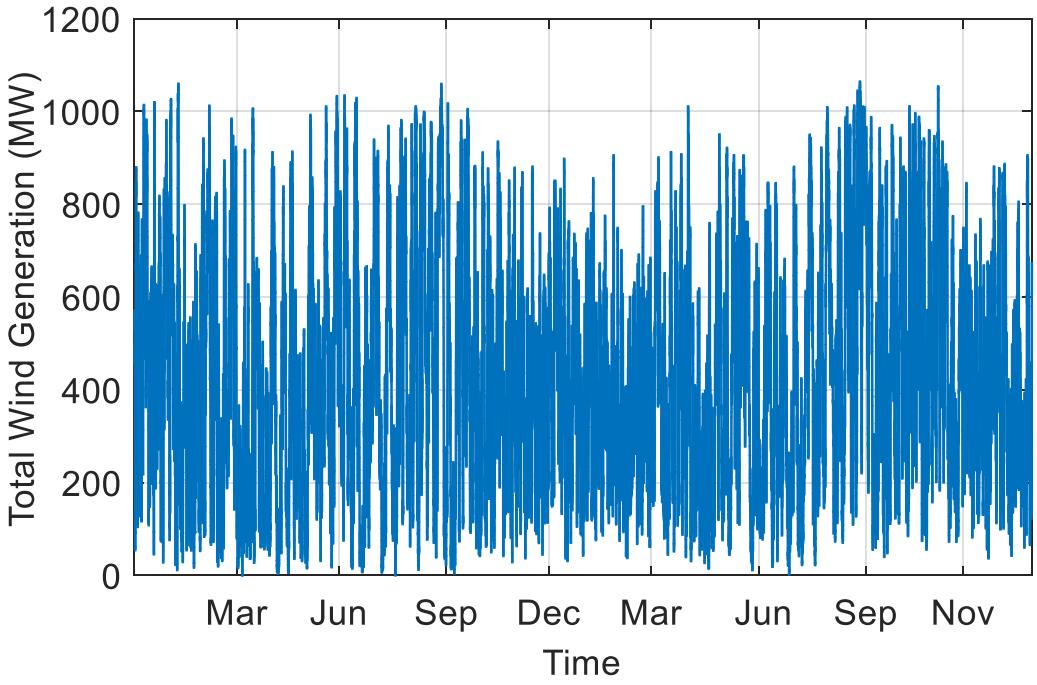

Figure 5.3. Total wind generation in South Australia 2012 and 2013 [110]

South Australia had fifteen wind farms with a total capacity of 1202MW in 2013. Table 5.3 gives the information of these wind farms [15]. Lake Bonney with the total installed capacity of 278.5MW is the largest wind farm and the North Brown Hill has the highest capacity factor in SA.

Table 5.3: South Australian wind farms [15]

Wind Farm's Name	Capacity (MW)	Capacity Factor
Canunda	46	0.3742
Cathedral Rocks	66	0.4081
Clements Gap	56.7	0.3855
Hallett (Brown Hill)	94.5	0.3975
Hallett Hill	71.4	0.3975
North Brown Hill	132.3	0.4115
Bluff Wind Farm	52.5	0.3835
Lake Bonney Stage 1	80.5	0.3452
Lake Bonney Stage 2	159	0.3364
Lake Bonney Stage 3	39	0.3408
Mount Millar	70	0.3934
Snowtown	98.7	0.4036
Starfish Hill	34.5	0.3786
Waterloo	111	0.3950
Wattle Point	90.75	0.3220

South Australia is connected to other states through two high voltage interconnections; Murraylink a 220 MW, ±150 kV HVDC light bipolar interconnector and Heywood a 275 kV HVAC with 460 MW capacity [115]. The average values of transferred power through these lines in 2012 and 2013 are illustrated in Figure 5.4 [110].

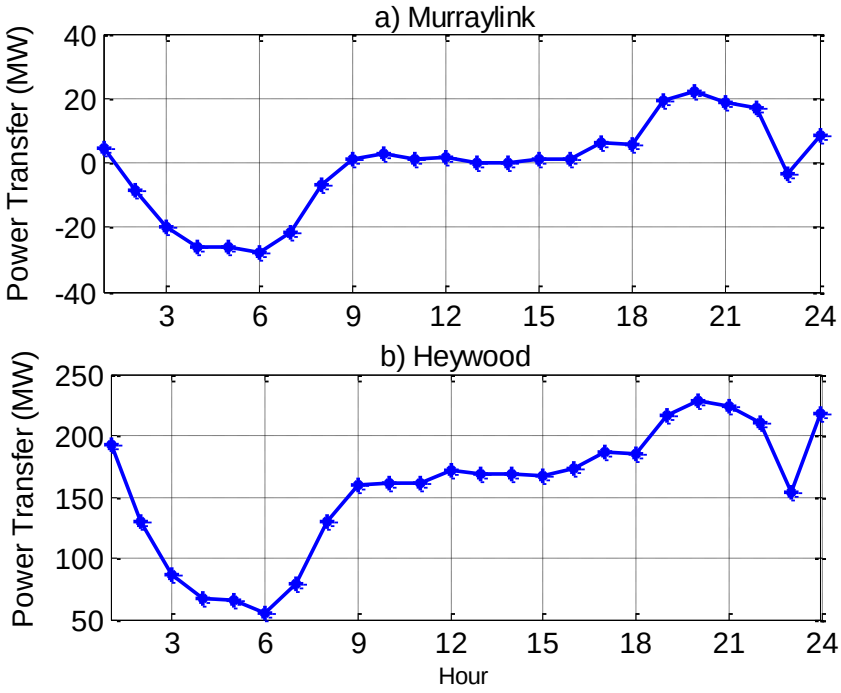

Figure 5.4. Mean value of power flow through tie-lines for 2012 and 2013 [110]

In this figure, when SA is importing power the transferred power is shown as positive and during exportation this value is negative. It can be seen that the average exchanged power through Heywood interconnection is toward South Australia and this system imports electricity through this link. The average amount of imported power is high during the evening peak time and is low in the early morning. On the other hand, there is a balance between imported and exported through Murraylink. The average exchanged power is positive during the evening period, while on average, South Australia exports electricity through this link in the morning and the mean value of exchanged power during this period is negative.

5.1.3. Simulation Results

In this study the output power of all South Australian wind farms, its hourly demand and transferred power through interconnectors have been modelled separately as hourly clusters using two years of historical data. Time-dependent clustered models of these input data sets have been created using the methodology explained in the previous chapter.

An hourly ten-cluster model of total demand in South Australia in per-unit value on the highest peak demand basis (2,991MW) is depicted in Figure 5.5. This model has captured the time dependency features of the demand. For instance, it shows that the electricity load is at its lowest level in the early morning and the highest peak can occur at midday. These features could be clearly seen from the historical data that has been displayed in Figure 5.2.

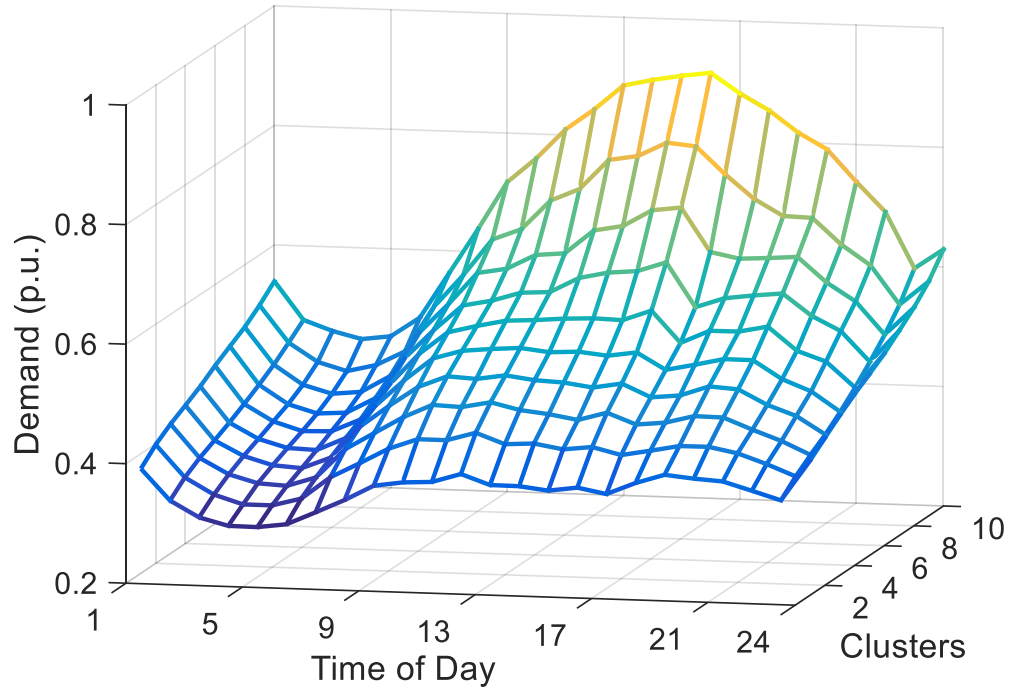

Figure 5.5. Time-dependent clustered model for electricity demand in South Australia

The same approach has been applied on all the wind farms and timely clustered models are created to represent their output power in the reliability studies. The time-dependent cluster model of the output power of the Clement Gap wind farm is presented in Figure 5.6. It shows that the generated power of this wind farm at each hour has ten different clusters (the appropriate number of clusters is obtained from the method explained in Section 4.5 of Chapter 4).

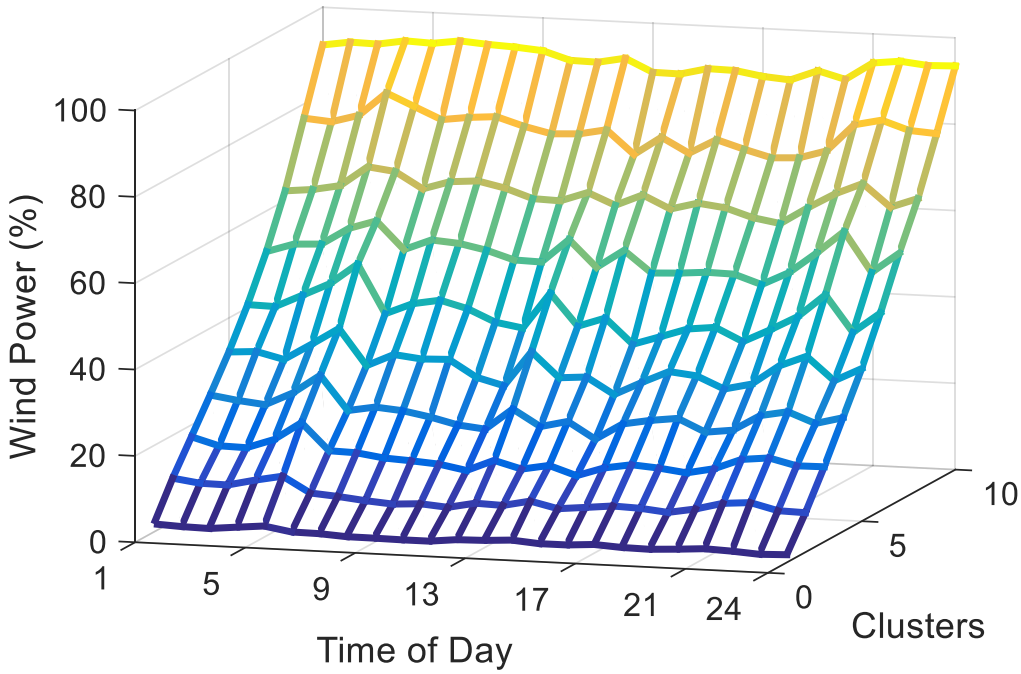

Figure 5.6. Time-dependent clustered model of Clement Gap wind farm

These clusters vary between 0 to more than 90 percent of the rated capacity. However, similar to load data, the probabilities of clusters are time-dependent and different for each hour. For instance, at 11:00am the probability of a low wind level for this wind farm (0.1% of the rated capacity) is around 32%, while the chance of a low level wind at 12:00am is around 12%. The probability of the clusters at each hour is presented in Figure 5.7.

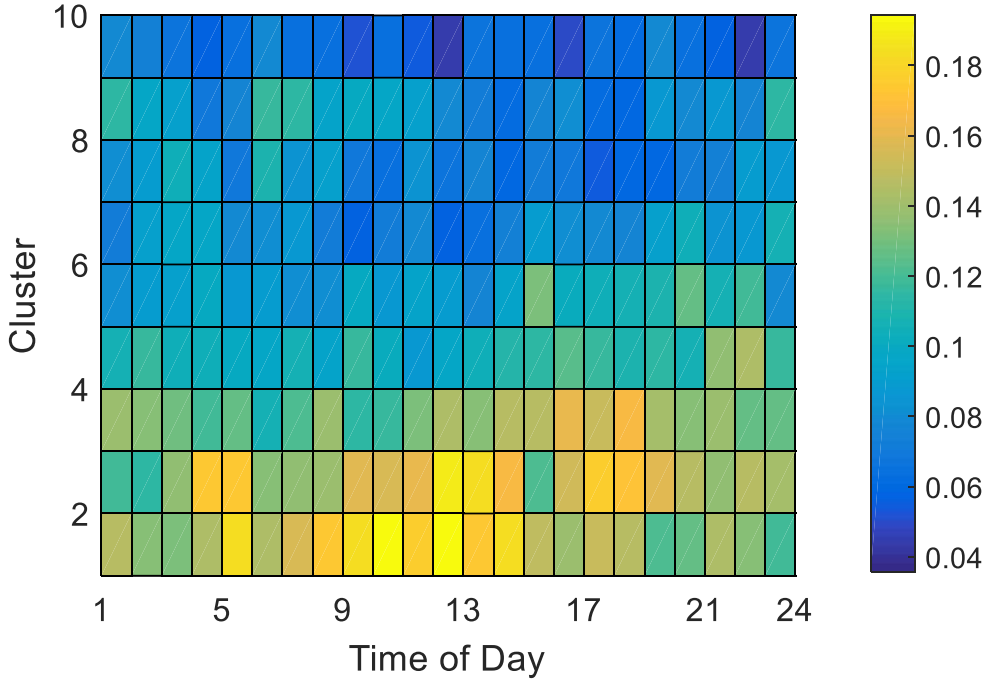

Figure 5.7. Probability of hourly clusters of the Clement Gap wind farm

The time-dependent model of this wind farm is also presented as a matrix in Table 5.4. In this table, columns represent clusters and rows are probability and value of each cluster for a specific time of day. For instance, at 8:00am the probability of having 24.8% wind power is 10% and the possibility of generating power with 91.4% of the nominal capacity is 8.8%.

Table 5.4: Time-dependent model of the Clement Gap wind farm

Time \ Cluster		1	2	3	4	5	6	7	8	9	10
1	Value (p.u.)	0.010	0.126	0.232	0.349	0.444	0.550	0.658	0.761	0.852	0.960
	Probability	0.150	0.118	0.108	0.109	0.081	0.082	0.088	0.083	0.115	0.066
2	Value (p.u.)	0.005	0.094	0.183	0.268	0.380	0.492	0.588	0.715	0.836	0.959
	Probability	0.157	0.079	0.085	0.090	0.116	0.096	0.085	0.092	0.135	0.064
3	Value (p.u.)	0.005	0.107	0.211	0.304	0.385	0.490	0.588	0.697	0.815	0.953
	Probability	0.167	0.103	0.082	0.088	0.108	0.079	0.088	0.093	0.126	0.067
4	Value (p.u.)	0.004	0.092	0.190	0.285	0.380	0.476	0.578	0.678	0.805	0.940
	Probability	0.179	0.096	0.103	0.082	0.074	0.077	0.114	0.070	0.119	0.088
5	Value (p.u.)	0.004	0.081	0.174	0.261	0.354	0.451	0.546	0.664	0.794	0.939
	Probability	0.185	0.092	0.083	0.089	0.086	0.089	0.089	0.075	0.129	0.083
6	Value (p.u.)	0.002	0.083	0.162	0.260	0.379	0.497	0.615	0.716	0.833	0.949
	Probability	0.187	0.083	0.116	0.094	0.109	0.107	0.062	0.093	0.083	0.064
7	Value (p.u.)	0.003	0.089	0.174	0.265	0.361	0.469	0.566	0.675	0.808	0.945
	Probability	0.181	0.108	0.111	0.090	0.086	0.086	0.083	0.092	0.092	0.071
8	Value (p.u.)	0.002	0.079	0.160	0.248	0.327	0.413	0.524	0.628	0.764	0.914
	Probability	0.208	0.094	0.100	0.100	0.089	0.090	0.085	0.068	0.078	0.088
9	Value (p.u.)	0.001	0.068	0.153	0.229	0.328	0.421	0.557	0.687	0.801	0.918
	Probability	0.224	0.120	0.098	0.101	0.096	0.101	0.074	0.059	0.068	0.057
10	Value (p.u.)	0.001	0.050	0.121	0.184	0.253	0.353	0.479	0.620	0.748	0.909
	Probability	0.246	0.116	0.096	0.086	0.088	0.090	0.078	0.066	0.075	0.059
11	Value (p.u.)	0.001	0.066	0.141	0.218	0.305	0.396	0.525	0.643	0.799	0.912
	Probability	0.324	0.114	0.103	0.083	0.073	0.067	0.056	0.064	0.057	0.059
12	Value (p.u.)	0.000	0.057	0.128	0.211	0.317	0.423	0.530	0.666	0.803	0.910
	Probability	0.319	0.122	0.096	0.077	0.093	0.068	0.059	0.055	0.055	0.057
13	Value (p.u.)	0.000	0.051	0.111	0.174	0.265	0.355	0.464	0.604	0.752	0.901
	Probability	0.278	0.122	0.090	0.082	0.085	0.077	0.067	0.060	0.074	0.066
14	Value (p.u.)	0.004	0.067	0.158	0.243	0.339	0.439	0.576	0.733	0.830	0.923
	Probability	0.260	0.135	0.142	0.096	0.067	0.071	0.078	0.049	0.053	0.048
15	Value (p.u.)	0.004	0.060	0.130	0.209	0.303	0.397	0.521	0.642	0.782	0.912
	Probability	0.223	0.112	0.108	0.115	0.079	0.071	0.086	0.070	0.079	0.056
16	Value (p.u.)	0.004	0.079	0.168	0.248	0.335	0.445	0.560	0.681	0.814	0.932
	Probability	0.242	0.124	0.115	0.067	0.077	0.100	0.083	0.071	0.081	0.040
17	Value (p.u.)	0.002	0.071	0.168	0.263	0.392	0.498	0.606	0.718	0.823	0.930
	Probability	0.252	0.112	0.103	0.111	0.081	0.079	0.082	0.067	0.071	0.042
18	Value (p.u.)	0.000	0.074	0.154	0.242	0.333	0.446	0.561	0.683	0.799	0.929
	Probability	0.271	0.094	0.081	0.083	0.070	0.090	0.103	0.067	0.083	0.057
19	Value (p.u.)	0.001	0.077	0.171	0.281	0.379	0.471	0.576	0.696	0.812	0.934
	Probability	0.250	0.107	0.073	0.096	0.078	0.094	0.086	0.063	0.092	0.062
20	Value (p.u.)	0.001	0.086	0.180	0.275	0.380	0.476	0.570	0.690	0.809	0.923
	Probability	0.197	0.108	0.085	0.100	0.101	0.081	0.085	0.085	0.089	0.070
21	Value (p.u.)	0.002	0.082	0.178	0.287	0.380	0.458	0.554	0.660	0.777	0.915
	Probability	0.161	0.082	0.096	0.104	0.083	0.090	0.089	0.101	0.104	0.089
22	Value (p.u.)	0.007	0.092	0.176	0.283	0.411	0.524	0.658	0.757	0.852	0.952
	Probability	0.142	0.089	0.093	0.096	0.109	0.119	0.094	0.085	0.101	0.071
23	Value (p.u.)	0.007	0.101	0.193	0.287	0.382	0.500	0.609	0.742	0.850	0.958
	Probability	0.134	0.098	0.092	0.085	0.101	0.085	0.093	0.116	0.122	0.074
24	Value (p.u.)	0.003	0.079	0.156	0.257	0.366	0.487	0.603	0.709	0.829	0.953
	Probability	0.126	0.078	0.081	0.096	0.103	0.100	0.096	0.098	0.141	0.082

After creating models for demand, wind farms and exchanged power, the reliability assessment has been conducted at two different levels: Generation level and Composite system level. At the generation level (HLI), the generation system adequacy in suppling demand is assessed and the reliability benefit of wind farms is evaluated regardless of transmission system. To investigate the contribution of wind power, first the reliability level of the original system without wind farms is calculated. As mentioned in the previous chapter, in the HLI studies, loss of energy expectation is utilized as the index to measure the reliability of the system. Figure 5.8 shows the LOEE of this system without wind generation for 2,000 sample years. It can be seen that LOEE of SA system is converging to 80 MWh/yr.

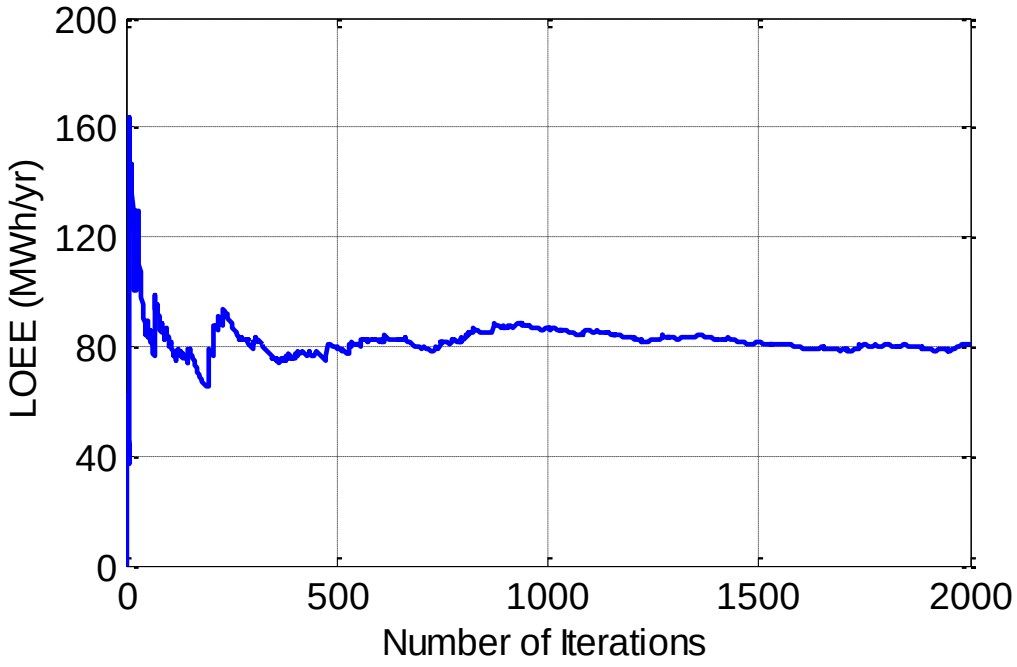

Figure 5.8. Loss of energy expectation of SA for 2000 sample years

In the next step, the LOEE of South Australia with wind generators has been calculated again for different extra loading levels. Figure 5.9 demonstrates the process of calculating capacity value of wind farms for SA at generation level. The red line is the LOEE of this system without wind units, which was shown in Figure 5.8. The blue line represents LOEE of SA system with 1202MW of wind farms. It can be seen that the capacity value of wind power in South Australia is around 385MW, which means wind units can supply 385 MW of extra loads while the reliability level of SA is not tolerated.

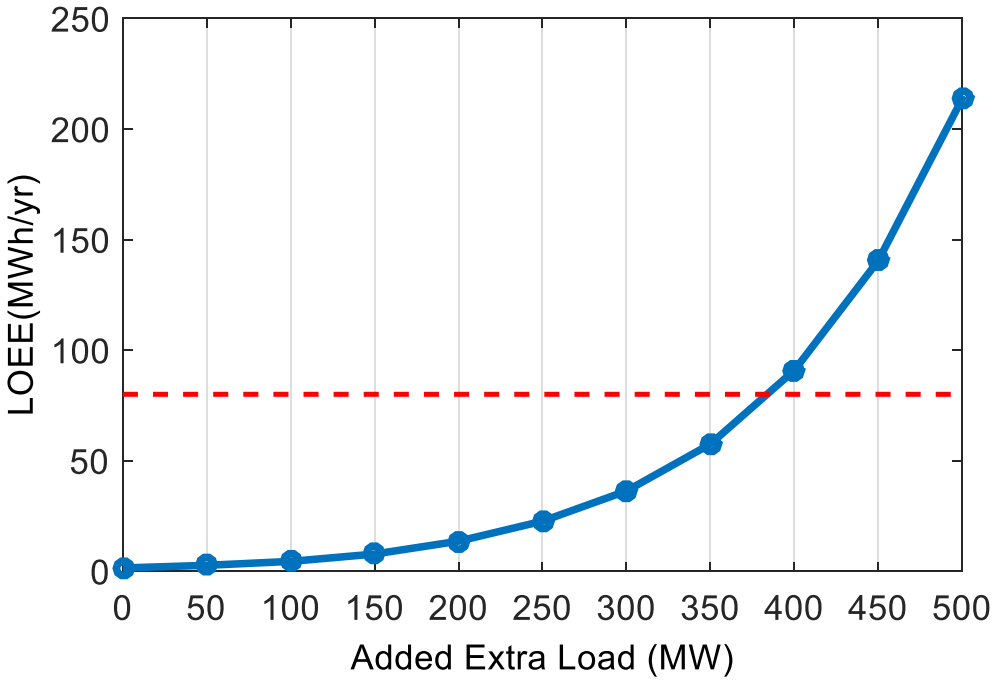

Figure 5.9. Reliability benefits of wind energy in SA

To investigate the impact of transmission network contingencies on the capacity value of wind, the proposed approach has been conducted on the SA system at the HLII level. At the transmission level, this system has around 400 high-voltage buses (66kV, 132kV and 275kV) and 89 high-voltage substations. The high voltage map of the South Australian power system is depicted in Figure 5.10. The SA system has a large network with about 5,600 route kilometres of transmission lines [116]. The Murraylink and Heywood interconnectors between SA and Victoria are on the East and the Southeast sides, respectively. Wind farms are distributed across this state thus, they have different wind regimes and there is no high correlation between most of the major wind farms. The correlation matrix between hourly generations of major wind farms in South Australia is presented in Table 5.5.

Table 5.5: Correlations between major wind farms production in SA

	Cathedral	North Brown Hill	Lake Bonney	Snowtown	Waterloo	Wattle Point
Cathedral	1.00	0.15	0.10	0.11	0.16	-0.01
North Brown Hill	0.15	1.00	0.39	0.70	0.75	-0.05
Lake Bonney	0.10	0.39	1.00	0.34	0.52	0.00
Snowtown	0.11	0.70	0.34	1.00	0.60	0.01
Waterloo	0.16	0.75	0.52	0.60	1.00	0.00
Wattle Point	-0.01	-0.05	0.00	0.01	0.00	1.00

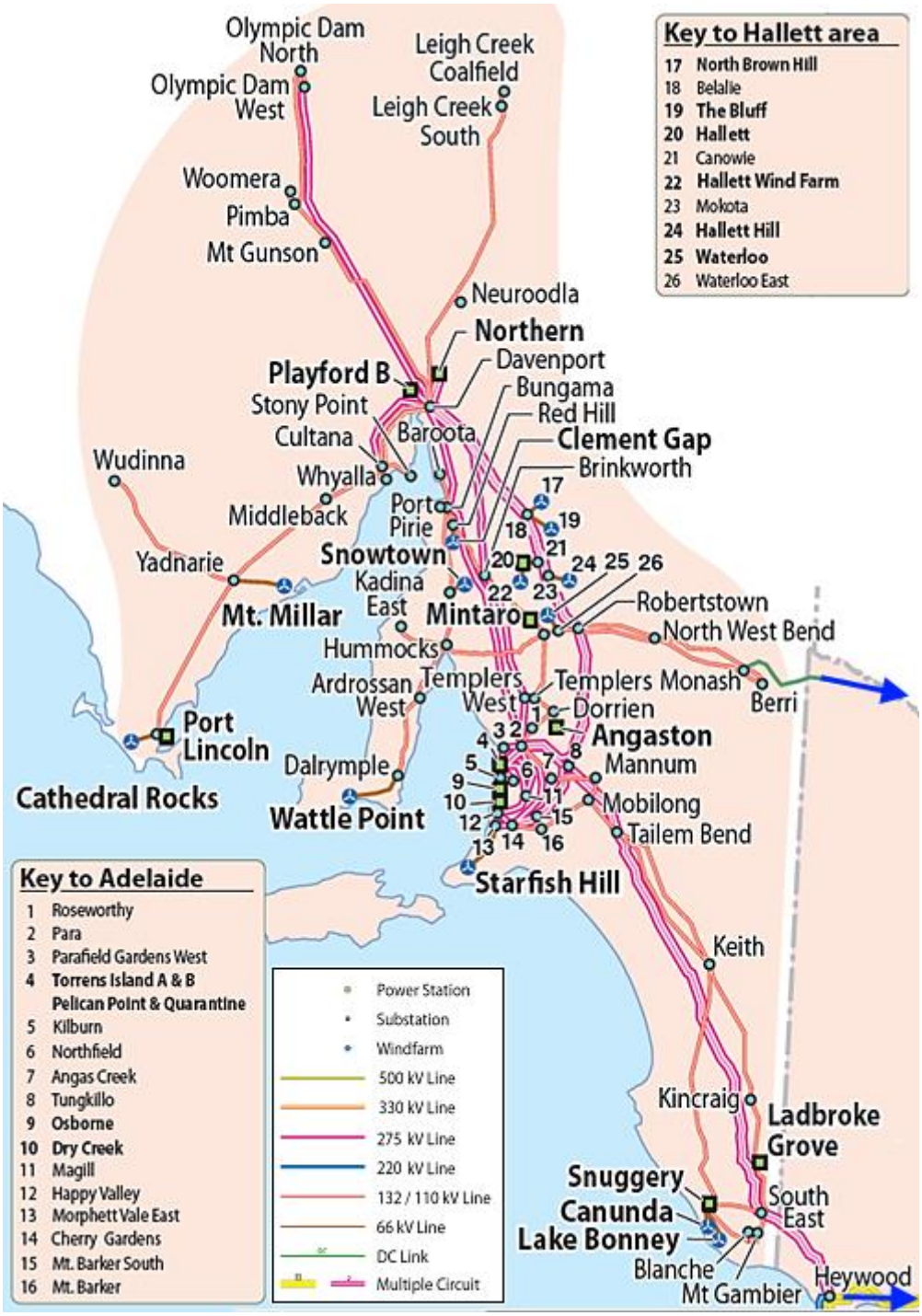

Figure 5.10. South Australian high voltage network [117]

In the HLII studies, the amount of curtailed load due to constraints or contingencies is recorded to calculate the reliability index of the system. First, a load flow analysis is conducted for each simulated system state to check if system constraints such as voltage limits and line flow limits are met. If these constraints are violated, corrective actions like generation rescheduling might be enough to avoid load curtailment. Otherwise, power outage has to be managed. An AC optimal power flow (OPF) in MATPOWER [109] has been used to minimize and record the total curtailed load due to any element outage(s). For this reason, an equivalent network was prepared with some

assumptions and approximations and the results can be considered as indicative but not exact. Hence, the outcomes presented in HLII may not reflect the exact composite system analysis of the SA particular system.

While sequential Monte Carlo requires a substantial amount of time to execute thousands of hourly load flow analysis for each of 2000 samples, the proposed approach only needs twenty-four load flows to be performed in each sample year. Because in the time-dependent clustering method, all data are categorized on an hourly basis and the reliability evaluation is conducted for each hour separately. Table 5.6 compares the ELCC of wind power in South Australia for the HLI and HLII levels calculated by means of the proposed method and the Sequential Monte Carlo technique.

Table 5.6: ELCC of wind energy in the SA System

Capacity Value	1202MW Wind	
	MW	%
HLI – Sequential Monte Carlo	385	32.0
HLI – Time-dependent Cluster	382	31.8
HLII – Sequential Monte Carlo	306	25.5
HLII –Time-dependent Cluster	312	26.0

This table shows that the reliability contributions of renewable resources at the HLII level have decreased due to transmission system insufficiency and contingencies. The ELCC of wind power has decreased around 70MW. It can be observed that results obtained from the time-dependent clustering technique in both HLI and HLII levels are accurate and close to the Sequential Monte Carlo method.

5.3. Victoria

5.1.4. Victorian Power System

Victoria is a Southern state of Australia between South Australia and New South Wales, and Melbourne is its capital city. Maximum demand in Victoria was about 10,000MW between 2013 and 2014 [112] while its generation capacity was around 12,000MW [118]. The Victorian electricity network has a mesh topology and is connected to three other states: New South Wales, South Australia and Tasmania via high-voltage interconnections.

Average demand in Victoria is around 5,400MW [112]. Figure 5.11 depicts the average and variability outside upper and lower quartiles of hourly electricity demand in this state from 2013 till the end of 2014 using box-and-whisker plot. These values, provided by Australian Energy Market Operator (AEMO), are net measured electricity demand [112], which is the total load minus production of rooftop photovoltaic (PV) systems at the distribution level. Installed capacity of rooftop PV in Victoria by the end of 2014 was around 700MW [114].

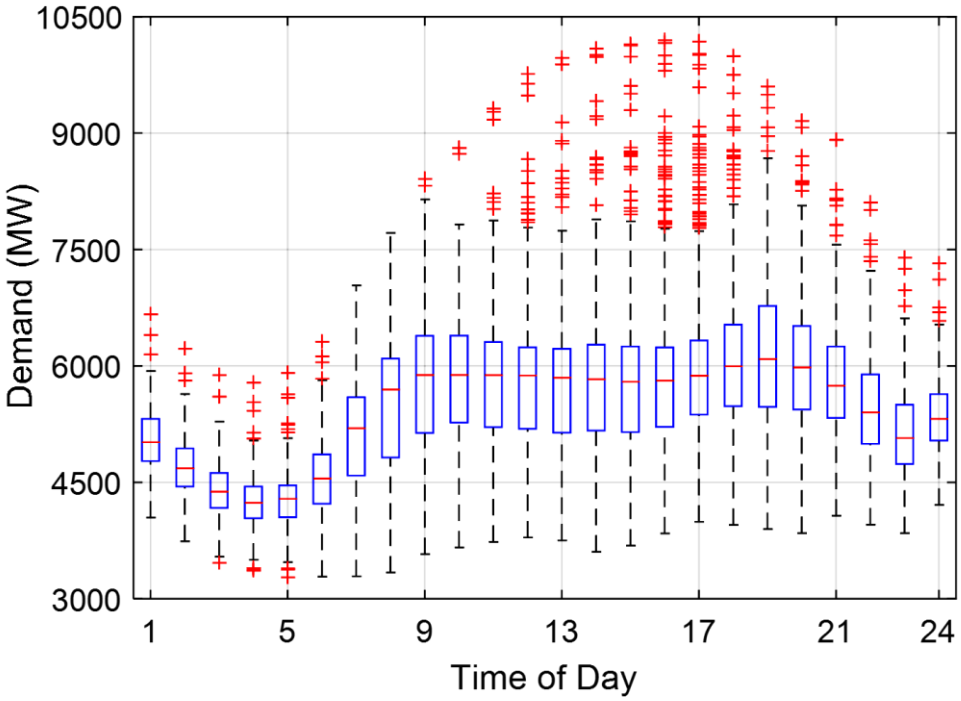

Figure 5.11. Box-and-whisker plot for hourly load data in Victoria for 2013-14 [112]

It can be seen that this load profile has two peaks: one in the morning and one in the evening. However, on some occasions high electricity demand has happened in the middle of the day. It also shows that the Victorian demand is low during midnight and early morning, and the minimum load value in these two years was around 3,200MW.

The generation portfolio of Victoria is displayed in Figure 5.12. Generators' contribution is shown in percentage value of total installed capacity. As it can be observed, the contribution of fossil fuel resources in this power system is around 72% with a majority of coal generators. Among renewable generators, hydro has the highest installed capacity. Wind power is the second highest renewable source of energy in Victoria with an installed capacity of 9%.

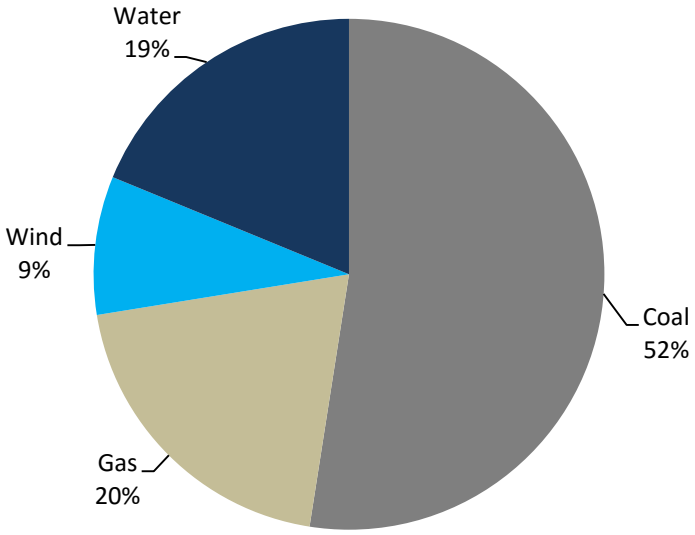

Figure 5.12. VIC installed capacity percentage by generation type [118]

Details of the generation system in the Victorian power system are given in Table 5.7. It shows that there are other types of renewable resources in this system, however, their contribution is insignificant. There is 53 MW of Biomass generation and solar power has the lowest capacity (1.5 MW). However, it should be mentioned that in this table, the solar term just stands for large size generators and the contribution of rooftop PV systems at the distribution level, which is around 800MW, has not been considered in this value.

Table 5.7: VIC existing and potential new developments by generation type (MW) [39]

Status / Type	Coal	CCGT	OCGT	Gas other	Solar	Wind	Water	Biomass	Other
Existing	6,410	21	1,904	516	1.5	1,070	2,296	53	0.8
Committed	0	0	0	0	0	154	0	0	0
Publicly announced	0	500	1,150	0	100	3,287	97	0	0
Withdrawn	189	0	0	0	0	0	0	0	0

The future of the role of wind power in this system is expected to become more significant since there are more than 3,000 MW of publicly announced projects for this renewable source. On the

other hand, the contribution of coal will decrease and 189 MW of coal generators will be withdrawn. Publicly announced proposals represent generation at an early stage of development that has met less than three of the following AEMO commitment criteria [25]:

- All land has been acquired.
- Contracts for supply of major components are finalised.
- All planning and environmental approvals have been obtained.
- Financing arrangements are finalised.
- Project construction has commenced or a date for commencing construction has been set.

As mentioned earlier, Victoria is connected to three other states (NSW, SA & TAS) through high voltage AC and DC interconnections. The connection between Victoria and NSW consists of 330kV and 220kV AC lines [115]. Victoria is connected to South Australia through one high voltage AC link (Heywood) and a HVDC interconnector (Murraylink). A HVDC interconnection (Basslink) transfers power between Victoria and Tasmania. The nominal capacity of these tie-lines is provided in Table 5.8 [115]. It can be observed that for some of these transmission links the capacity limit is different in each direction. For example, a maximum of 478MW can go from Victoria to TAS through Basslink, while this interconnection can transfer up to 594MW in the opposite direction.

Table 5.8: Nominal capacity of interconnections [115]

From	To	Nominal Capacity
Victoria	NSW	700 to 1600 MW
NSW	Victoria	400 to 1350 MW
Victoria	SA (Heywood)	460 MW
SA (Heywood)	Victoria	460 MW
Victoria	SA (Murraylink)	220 MW
SA (Murraylink)	Victoria	200 MW
Victoria	TAS (Basslink)	478 MW
TAS (Basslink)	Victoria	594 MW

The hourly variations of total exported power from Victoria to other states during 2013 till the end of 2014 is shown as a box-and-whisker plot in Figure 5.13 [110]. Positive values represent the amount of exported power from Victoria and negative numbers are the amount of imported power.

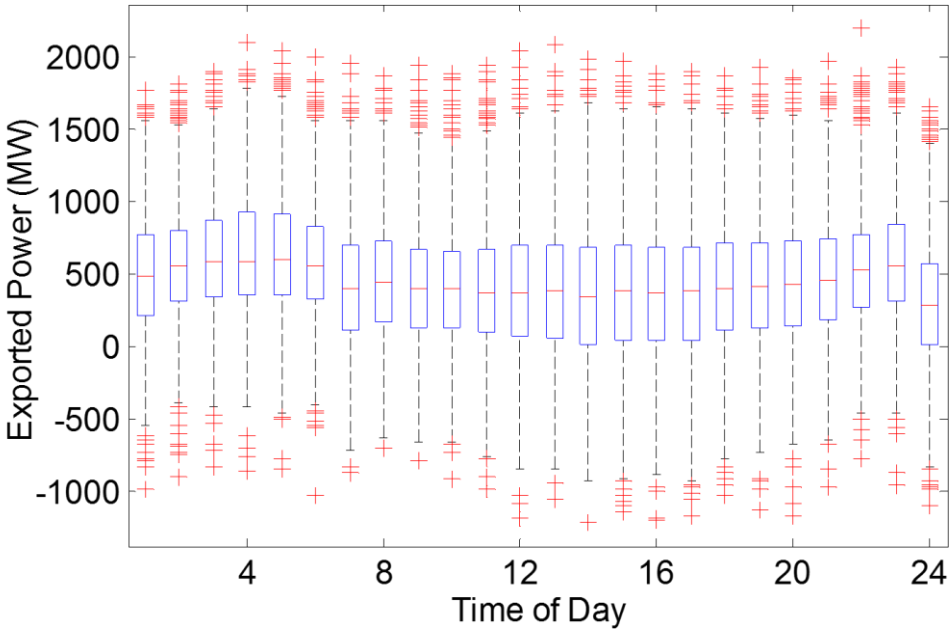

Figure 5.13. Box-and-whisker plot of hourly exported power from Victoria 2013-2014 [110]

The mean value of exchanged power is around 500MW which shows that during this period Victoria has mainly exported electricity through the tie-lines It can be seen that the highest amount of exported power is around 2,100MW, while this system has imported more than 1,000MW on some occasions.

5.1.5. Wind Data

By the end of 2014, there were seven large wind farms in Victoria with a total installed capacity of 1,070MW [15]. This state has the second highest installed wind capacity in Australia and by 2020 will become the highest with the addition of more than 4,000MW new wind farms [15].

Table 5.9: Existing Victorian wind farms [15]

Wind Farm	Installed Capacity (MW)	Capacity Factor (%)
Challicum Hills	53	34.08
Macarthur	420	36.62
Mortons Lane	20	36.62
Oaklands Hill	67	38.14
Portland	102	39.74
Waubra	192	38.48
Yambuk	30	39.74

Table 5.9 provides details of major Victorian wind farms that have been considered in this thesis. Macarthur with 420MW capacity is the largest wind farm not only in Victoria but also in the Southern Hemisphere. Amongst Victorian wind farms, Yambuk and Portland have the highest capacity factor, which is the ratio of average power production to the installed capacity.

Total hourly electricity production of these wind farms in 2013 and 2014 is illustrated in Figure 5.14. It shows that wind generators in Victoria could produce up to 850MW electricity in these years. However, on several occasions the total generated energy has fallen to zero megawatt. The mean value of total wind generation in this period is around 277MW and its standard deviation is about 214MW.

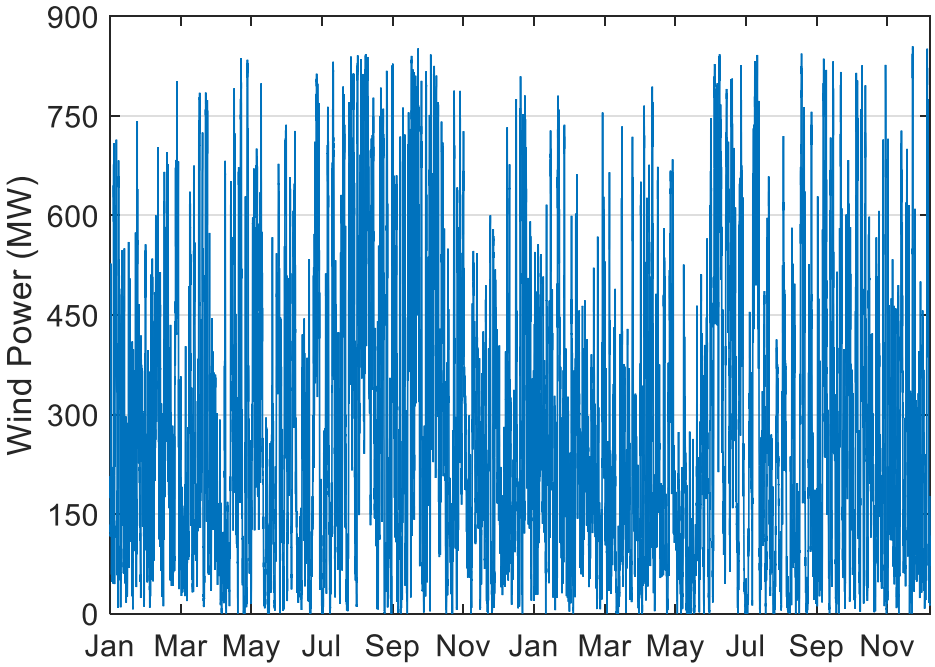

Figure 5.14. Total wind power production in Victoria in 2013 and 2014 [110]

5.1.6. Simulation Results

The first step to calculating the capacity value of wind power is to generate time-dependent cluster models for demand, exchanged power and wind datasets. Figure 5.15 depicts the demand model obtained from the methodology that has been explained in Chapter 4. This model is in per-unit values of the highest peak load in Victoria for 2013 and 2014 (10,196MW). A comparison between this model and the box-and-whisker plot of the VIC load (Figure 5.11) indicates that this model has captured the time dependency of the load profile. For instance, it can be seen that similar to the historical load profile, in this model the value of clusters during early morning is very low and the highest peak may happen around midday.

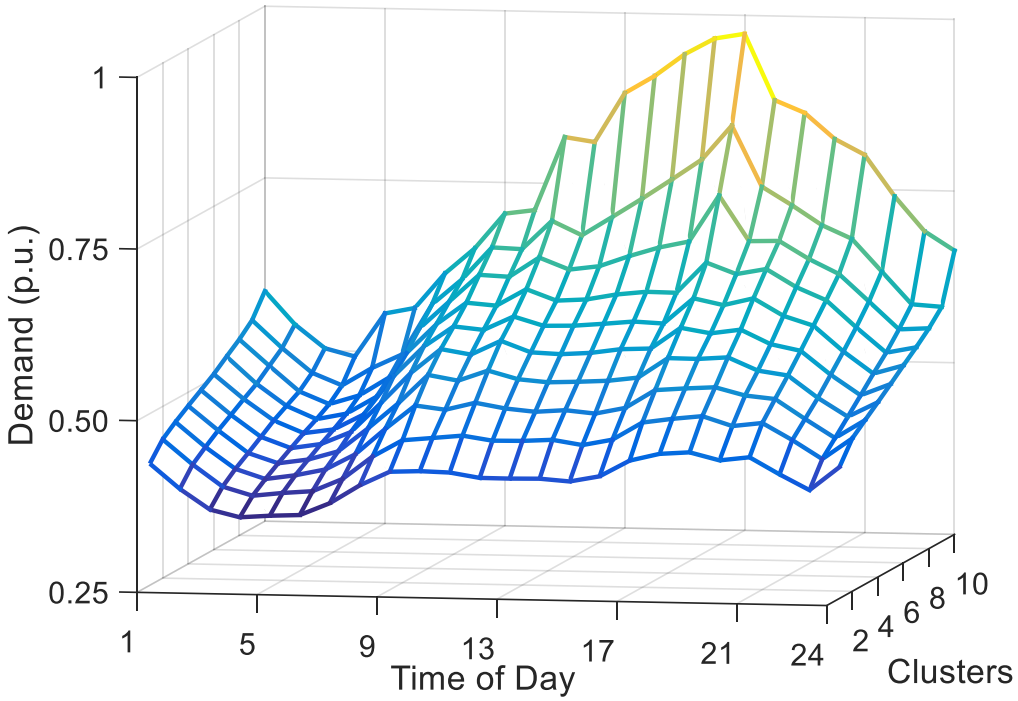

Figure 5.15. Time-dependent clustered model for electricity demand in Victoria

To measure the reliability contribution of wind energy in the power system and calculate the capacity value, in the first step, the reliability level of the system without wind power should be calculated. Loss of load expectation of Victoria without wind power for 20,000 sample years using the state sampling Monte Carlo method is illustrated in Figure 5.16.

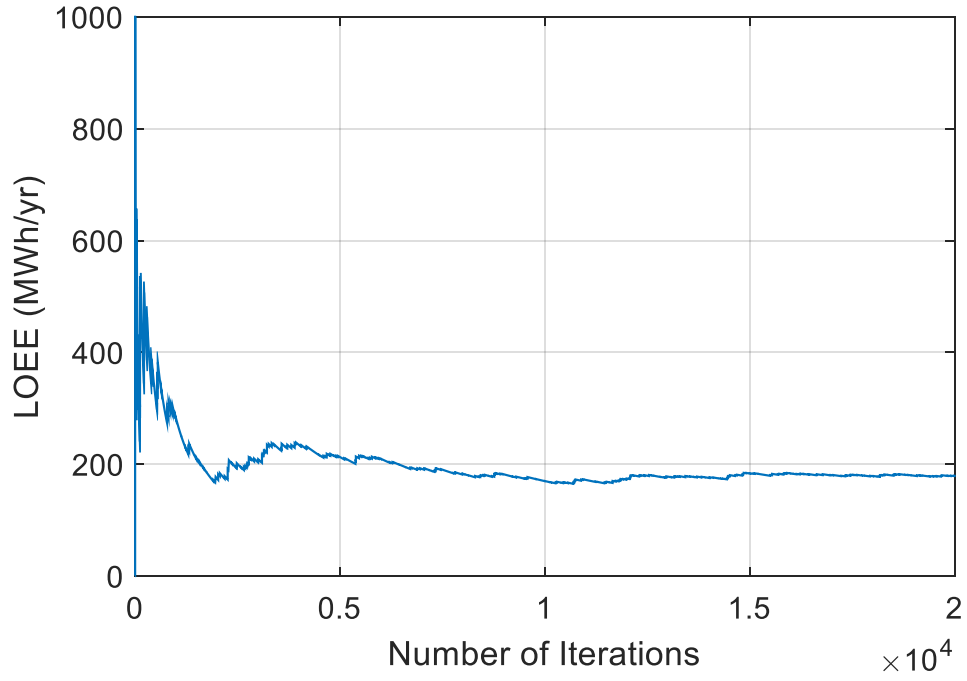

Figure 5.16. Loss of load expectation of Victoria for 20000 sample simulations

Then, this index is computed again for the VIC system with wind generation and with different levels of extra load added to its demand. Finally, the ELCC value is obtained based on the

comparison between the systems original reliability level and the LOEE in the presence of wind power. This process can be elaborated by means of Figure 5.17.

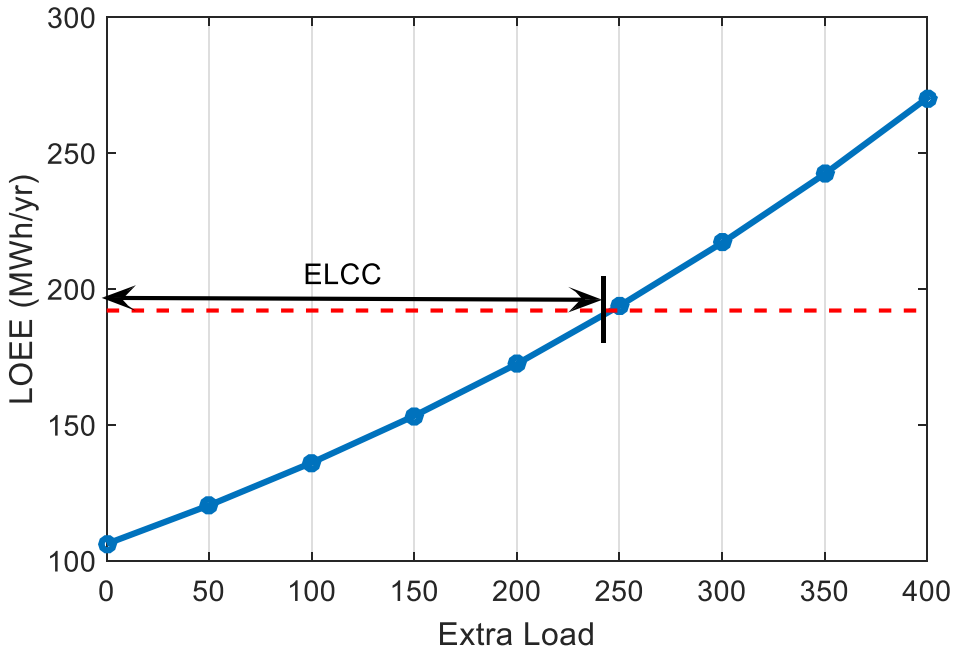

Figure 5.17. The process of calculating the ELCC of Victorian wind farms

From this figure it can be seen that the LOEE of Victoria without wind farms is around 192MWh/yr, which is considered as the system reliability level and is shown as the dashed red line. The blue line shows the LOEE of this system considering wind units and extra loads. It shows that by adding wind units, the system has become more reliable and LOEE has decreased to around 100MWh/yr. However, by increasing the load level, LOEE will increase and this system will become less reliable (blue line). The intersection between the blue line and original system's reliability level (red line) will be considered as the reliability contribution of wind power. Therefore, ELCC of the Victorian wind farms is about 247 MW. This value is less than 30% of the rated capacity of the wind farms and shows that the reliability contribution of wind in Victoria is small. There are several reasons for this issue. This system's high reliability, huge capacity of power exchange, analogous wind regimes and low correlations between wind power and load profile might be some of the main causes.

Unserved energy in Victoria as shown in Figure 5.16 is around 200MWh/yr. this value is less than 0.0005% of its annual energy consumption, which is much lower than the Australian minimum standard (0.002 %) [119]. This indicates that this network is highly reliable, which might be due to the meshed topology of the Victorian power grid and its huge generation capacity. Another reason can be the high capacity interconnectors between Victoria and other states, which allows this power system to import huge amounts of electricity during high demand periods or power shortage

incidents. For example, on 18 October 2014 at 9:30pm Victoria imported 2189MW electricity from its neighbouring power systems [110] which was about 34% of its demand at that time (6398 MW). Therefore, by importing a huge amount of electricity during shortages, this system stays highly reliable.

The uniform major wind regime of wind farms in Victoria might be another cause of the low ELCC. Figure 5.18 depicts the correlations between the output powers of large Victorian wind farms themselves and load data in 2013 and 2014. It shows that these wind farms generate electricity with a similar profile. Consequently, as they fluctuate simultaneously, they cannot compensate each other's variations and the total wind power is oscillating and in some occasions it may even drop to a very small value, which was shown in Figure 5.14, as well.

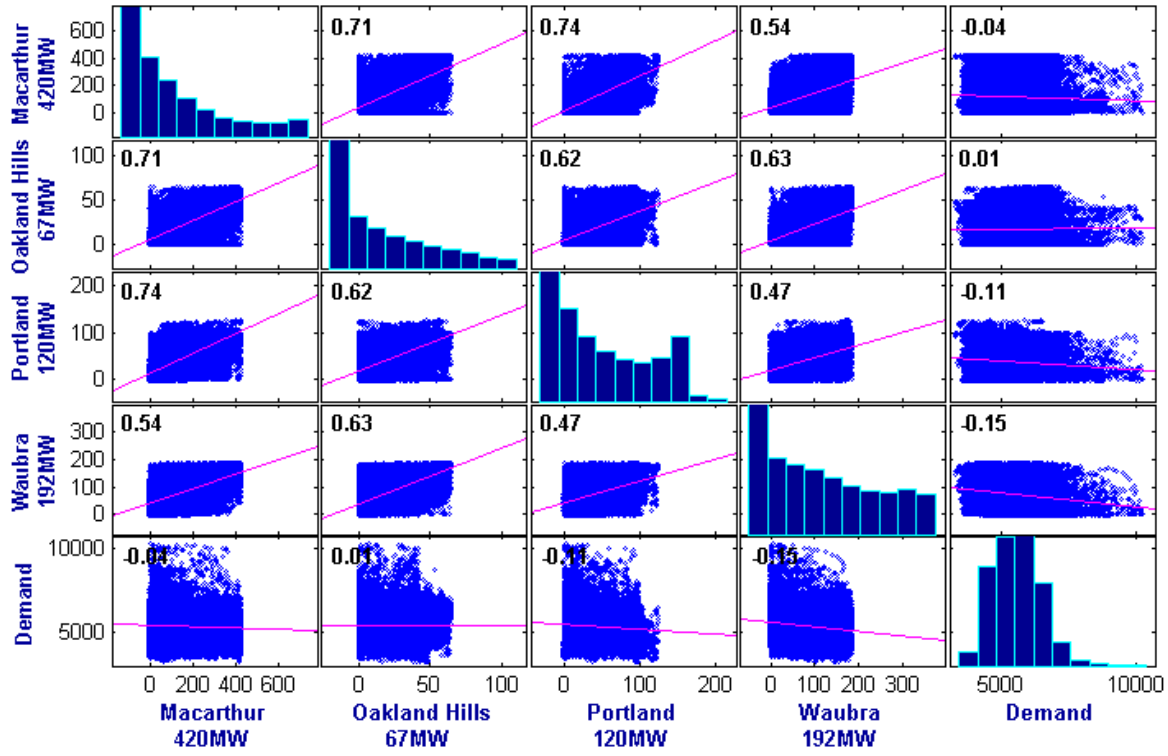

Figure 5.18. Correlations between generated power of wind farms and demand in VIC [110]

Figure 5.18 also illustrates the correlation between these wind farms and total demand in Victoria. It can be observed that the wind power and load profile in this state are almost uncorrelated. This means that during peak demand periods, when the chance of load curtailment and unreliability is high, the participation of wind units is low. Therefore, this may lead to a small contribution of wind power in the Victorian system's reliability.

The high voltage network of this power system contains around 312 buses and 450 transmission lines. This high voltage network carries electricity from power stations to electricity distributors across all of Victoria via 13,000 high voltage towers and approximately 6,500 kilometres of transmission lines [120]. The transmission grid of Victoria is depicted in Figure 5.19. This power

system from the West is connected to South Australia, from the South to Tasmania and from the Northeast to the New South Wales grid.

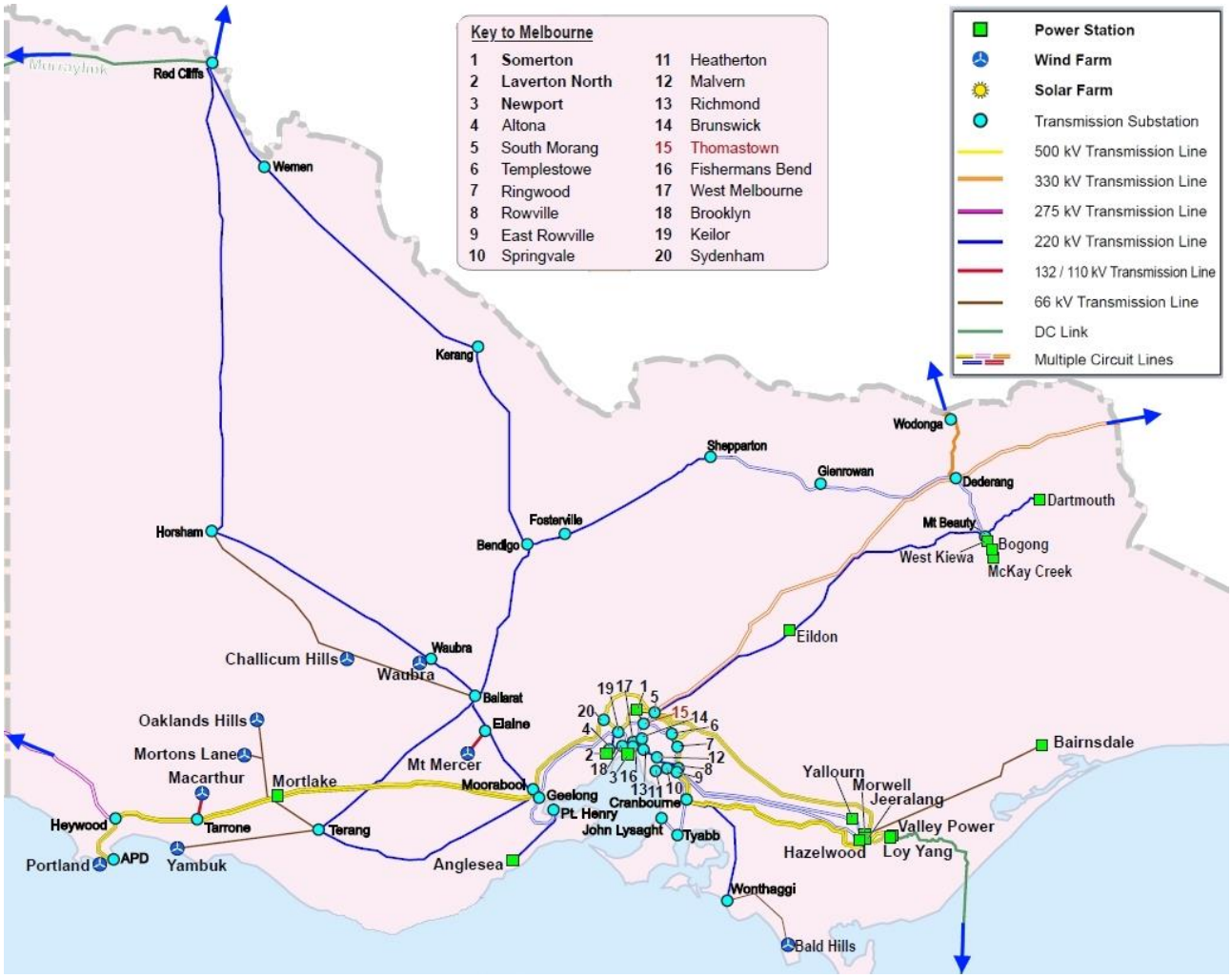

Figure 5.19. High voltage network of Victoria [117]

It can be seen that all the Victorian wind farms are located on the Southwest region of this network, which is the main reason for the high correlations between their wind regimes. Missing these correlations, as was mentioned in Section 4.5 of Chapter 4, will result in wrong models and the total wind generation model will not be accurate. For instance, the standard deviation of total historical wind power in Victoria, as mentioned before, is around 214 MW while the standard deviation value obtained from an uncorrelated model is about 134 MW. This lower fluctuation will result in higher capacity and overestimating the reliability contribution of wind energy.

The reliability assessment is conducted once again at the composite system level to evaluate the reliability contribution of wind generators considering transmission network constraints and outages as well. Capacity values of total wind power in Victoria at generation and composite system levels are given in Table 5.10.

Table 5.10: Capacity value of wind power in Victoria

Capacity Value	885 MW Wind	
	MW	%
Generation Level	247	27.9
Composite System Level	212	24.0

It can be seen that the impact of the transmission system on the ELCC value is around 4% and the capacity value has decreased from 247MW to 212MW. This reduction is much smaller than the 70MW decline in South Australia. The main reason is the mesh topology of the Victorian grid and thus, the low impact of line outages on the whole power system.

5.2. New South Wales

5.2.1. NSW Power System

New South Wales (NSW) has the highest population and is the largest electricity consumer network in Australia. This power system also has the largest generation level in Australia with a total generation capacity of 15,700MW in 2014. The majority of electricity in NSW is generated by coal power plants [39]. Figure 5.20 illustrates the contribution of different generator types in the total generation system of New South Wales and the detail of its generation portfolio is given in Table 5.11 [39]. It can be seen that the share of coal and gas generators in producing electricity in NSW is almost 80%. The installed capacity of hydro power plants is 2,745MW which is 16% of the total generation capacity and the contribution of wind power producers in NSW electricity generation is only 2% [118].

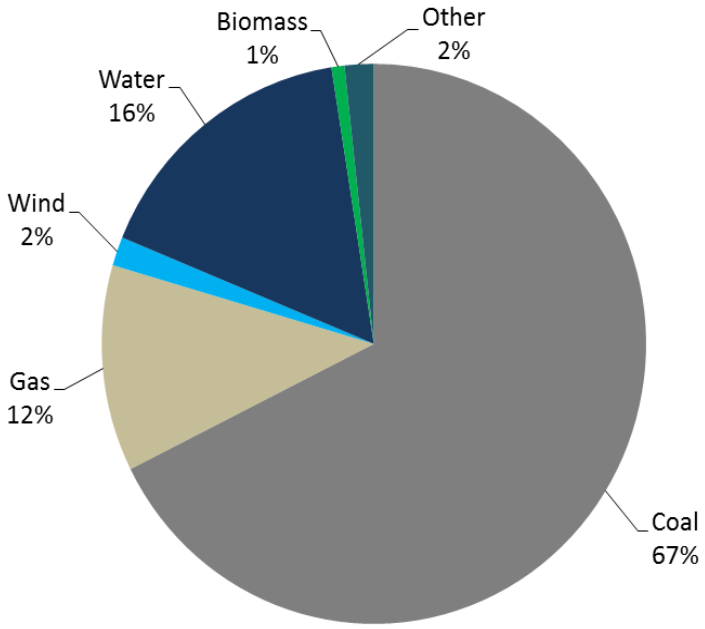

Figure 5.20. NSW installed capacity percentage by generation type [118]

Among all generators, the share of wind generation in publicly announced projects, which are expected to be constructed in the future, is the highest with around 5,000MW capacity. Solar energy is also expecting a significant growth with around 500MW committed and publicly announced development plans. For fossil fuel generators, the size of future projects is quite large as well, in particular for coal and open cycle gas turbine (OCGT) units. There are 2,000MW and 1,370MW publicly announced projects for coal and OCGT, respectively. However, a huge amount of coal power plants will be withdrawn in the near future (1,144MW).

Table 5.11: NSW existing and potential new developments by generation type (MW) [39]

Status / Type	Coal	CCGT	OCGT	Gas other	Solar	Wind	Water	Biomass	Other
Existing	10,240	598	1,388	25	0.1	281	2,745	129	291
Committed	0	0	0	0	175	385	0	0	0
Publicly announced	2,000	0	1,370	15	323	4,817	0	8	0
Withdrawn	1,144	0	0	0	0	0	0	0	0

As mentioned before, NSW has the highest demand in Australia and the average hourly demand in NSW from 2012 to the end of 2014 is around 8,000MW. The average value and variability outside upper and lower quartiles of hourly electricity loads in NSW from 2012 to 2014 is depicted in Figure 5.21 [112]. As can be seen, the average demand (boxes) in this system has two peak periods and the electricity consumption is low during midnight and early morning. Although the average value in the middle of the day is less than 9,000MW, on some occasions the highest peak demand occurs in this period (red crosses), probably due to summer air-conditioning. It can also be observed that the range of variations in NSW electricity consumption is from 5,000MW minimum demand to almost 14,000MW as the highest peak load [112].

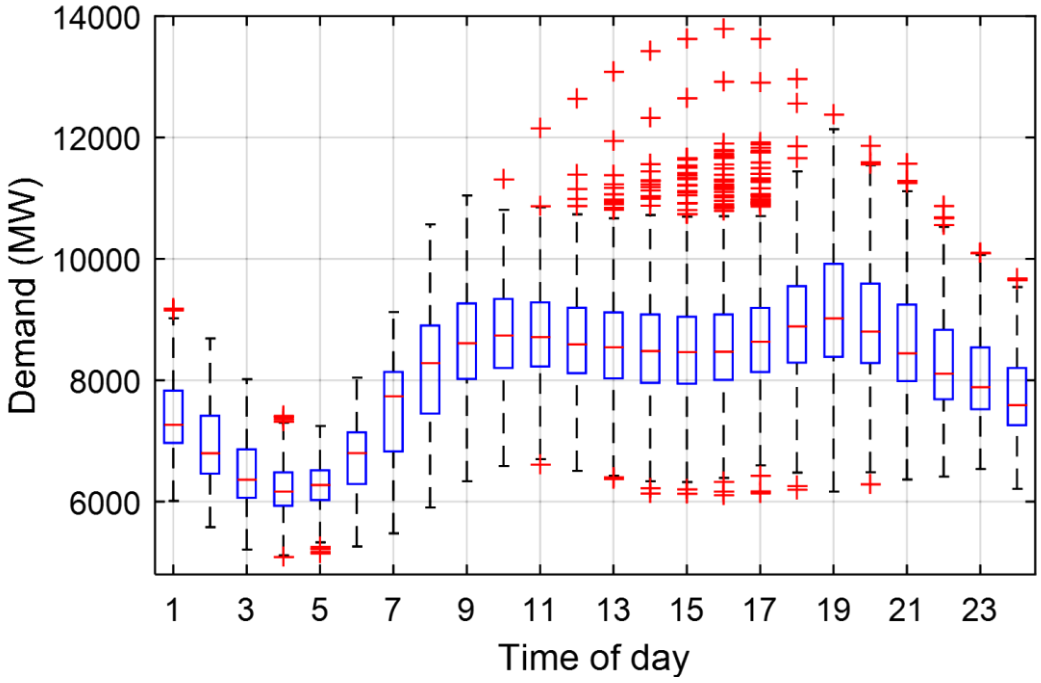

Figure 5.21. Box-Whisker plot of NSW demand for 2012-2014 [112]

The New South Wales network is connected to the Queensland and Victoria power systems through three interconnectors. From Terranora in NSW to Mudgeeraba in Queensland there are two

110 kV DC lines known as Directlink interconnector. The other tie-line is the Queensland to New South Wales (QNI), which is a 330 kV AC interconnection between Dumaresq in New South Wales and Bulli Creek in Queensland. Victoria to New South Wales interconnector (VNI) consists of 330 kV and 220 kV AC lines. Nominal capacities of these lines in each direction are presented in Table 5.12 [115].

Table 5.12: Nominal capacity of NSW interconnections [115]

From	To	Nominal Capacity
NSW (Directlink)	Queensland	107 MW
Queensland	NSW	210 MW
NSW (QNI)	Queensland	300-600 MW
Queensland	NSW	1078 MW
Victoria	NSW	700 to 1600 MW
NSW	Victoria	400 to 1350 MW

This table also shows that the capacity of these tie-lines in the NSW direction is higher, which is due to frequency, voltage, small signal and transient stability constraints. For example, the QNI connection can transfer up to 600MW from NSW to Queensland, while its capacity in the opposite direction is 1,078MW. The average hourly diagram of the total electricity transferred from NSW interconnections is illustrated in Figure 5.22. This value as seen in this diagram is negative all the time, which means most of the time NSW is importing power from other states through the interconnections. It can also be observed that the amount of exchanged power is time-dependent, for instance, the mean value of imported power during the early morning is almost double that of the imported electricity in the evening.

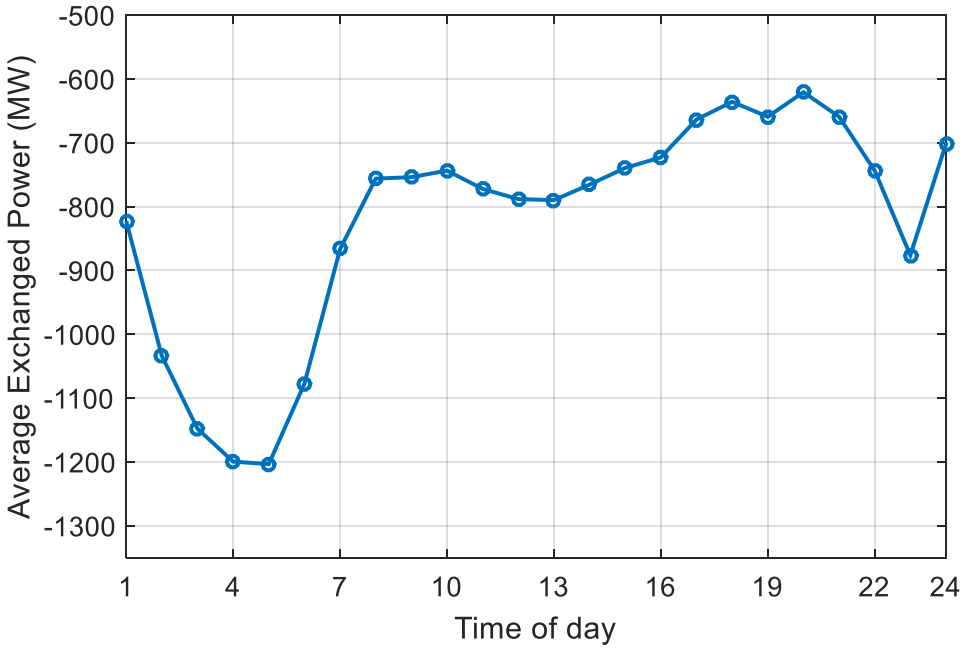

Figure 5.22. Average exchanged power of NSW with other states [110]

5.2.2. Wind Data

New South Wales does not have large installed wind capacity and only has four major wind farms. Details of these wind farms which have been considered in this study are presented in Table 5.13. The largest wind farm in NSW is Capital with 140MW and the smallest one is Cullerin wind farm (30MW), which has the highest capacity factor.

Table 5.13: Existing New South Wales wind generation [15]

Wind Farm	Capacity (MW)	Capacity Factor
Capital	140	0.3985
Cullerin	30	0.3997
Gunning	47	0.3751
Woodlawn	48	0.3985

Figure 5.23 demonstrates the total wind generation in NSW from 2012 till the end of 2014 [110]. It shows that the output of wind farms in NSW can vary from 0MW to 260MW. The mean value of the total hourly wind power is 84.72MW and its standard deviation is around 79MW.

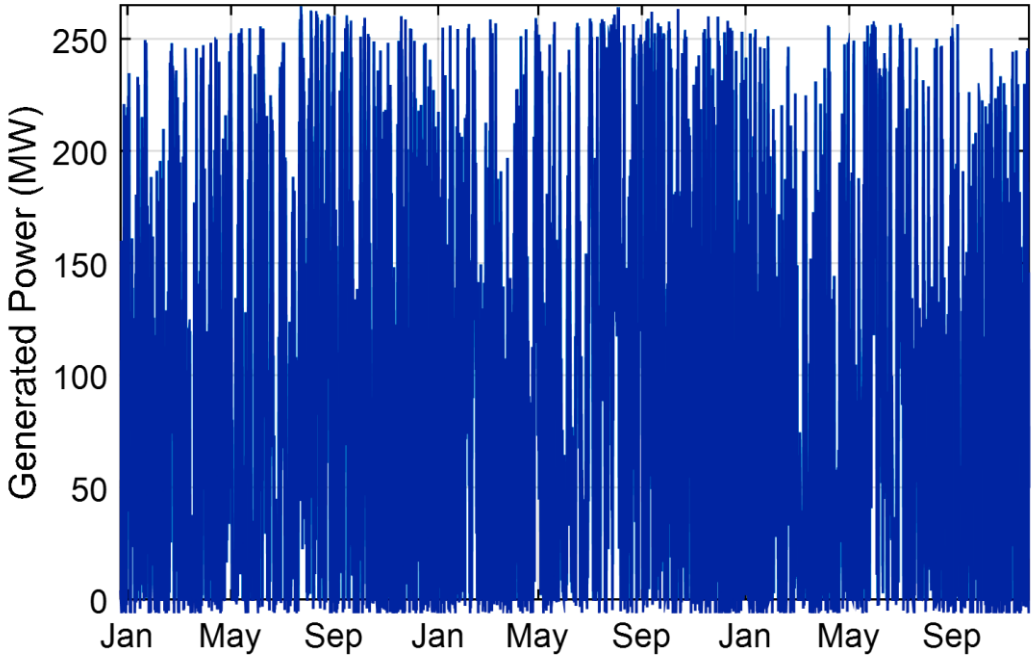

Figure 5.23. Total wind generation in NSW for 2012-2014 [110]

Correlations between outputs of the main NSW wind farms are shown in Figure 5.24. It can be observed that there is a high correlation between their generated powers. The highest correlation is between Capital and Woodlawn which is 90%. These correlations should be taken into account in the simulations; otherwise, the calculated ELCC will not be accurate.

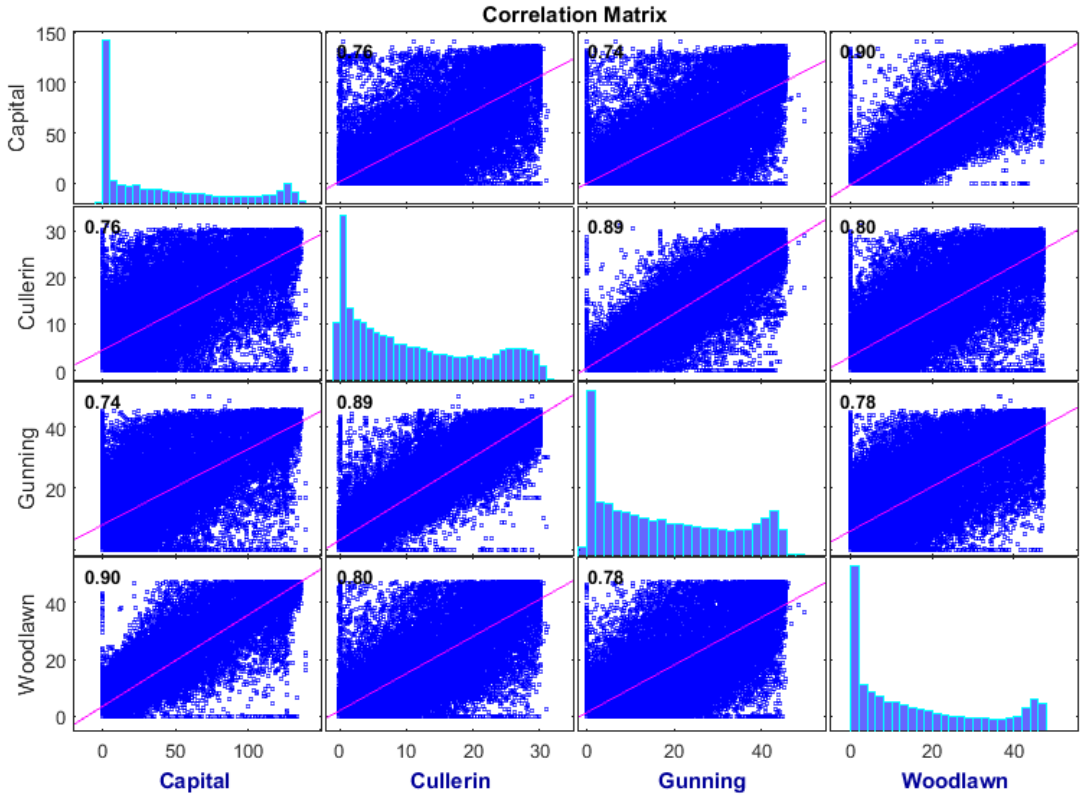

Figure 5.24. Correlation matrix between NSW wind farms

It can also be seen that the probability distribution functions of the electricity production in these wind farms (the diagonal elements) are similar as well. These high correlations and similarities in wind regimes are mainly due to the close vicinity of wind farm locations.

5.2.3. Simulation Results

To evaluate the reliability contribution of wind power in NSW, first, all historical data are classified into twenty-four groups and each group represents a specific time of the day. Then, by means of the Fuzzy C-mean method (explained in Chapter 4), data points in each of these 24 groups are clustered into a proper number of levels. The clustered model of the electricity consumption in New South Wales in per-unit of its highest peak demand (13,788MW) is demonstrated in Figure 5.25. As can be observed, for each hour there are 10 clusters to represent load value at that time. The number of clusters is obtained by using the elbow method which has been explained in Section 4.5.1 of Chapter 4.

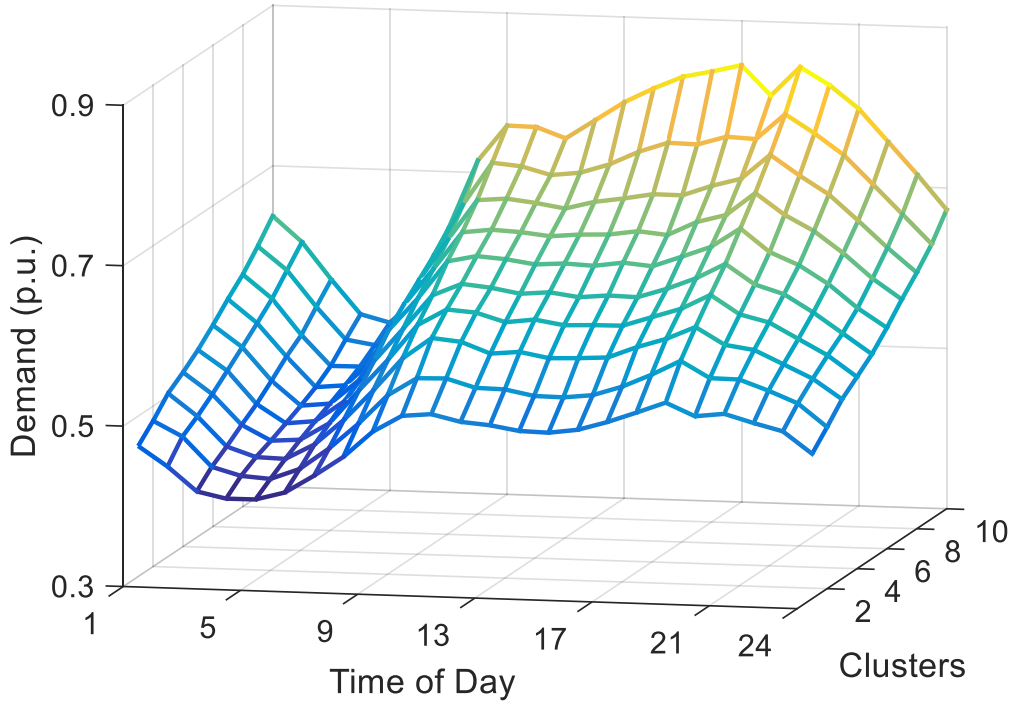

Figure 5.25. Time-dependent clustered model for electricity demand in NSW

Afterwards, these clusters are sorted successively in accordance with their cluster value. The time dependant model of Woodlawn wind farm is given in matrix form in Table 5.14. In this matrix, rows indicate the hour that clustering has been done for, and columns are the clusters representing wind power levels in per-unit and their probabilities at each hour. For example, the possibility of Woodlawn generating 96.5% of its nominal capacity at 1:00am is 8.6% and the probability of producing 0.9% of its installed capacity at the same time is 22.4%.

Table 5.14: Time-dependent model of Woodlawn wind farm

Time \ Cluster		1	2	3	4	5	6	7	8	9	10
1	Value (p.u.)	0.009	0.079	0.158	0.253	0.352	0.457	0.581	0.709	0.867	0.965
	Probability	0.224	0.140	0.131	0.104	0.083	0.061	0.063	0.054	0.055	0.086
2	Value (p.u.)	0.010	0.087	0.160	0.244	0.345	0.453	0.574	0.691	0.853	0.958
	Probability	0.264	0.145	0.110	0.095	0.081	0.056	0.049	0.045	0.056	0.099
3	Value (p.u.)	0.006	0.064	0.140	0.218	0.297	0.398	0.513	0.644	0.816	0.956
	Probability	0.251	0.130	0.115	0.091	0.078	0.074	0.046	0.053	0.053	0.110
4	Value (p.u.)	0.005	0.057	0.119	0.185	0.271	0.366	0.499	0.651	0.848	0.963
	Probability	0.253	0.120	0.106	0.074	0.091	0.080	0.058	0.058	0.069	0.089
5	Value (p.u.)	0.009	0.083	0.168	0.273	0.382	0.512	0.638	0.779	0.901	0.973
	Probability	0.304	0.148	0.118	0.083	0.068	0.051	0.049	0.047	0.061	0.071
6	Value (p.u.)	0.007	0.073	0.156	0.245	0.354	0.456	0.597	0.728	0.877	0.967
	Probability	0.283	0.154	0.115	0.072	0.068	0.070	0.048	0.053	0.055	0.082
7	Value (p.u.)	0.006	0.072	0.154	0.244	0.334	0.436	0.563	0.708	0.888	0.970
	Probability	0.282	0.151	0.092	0.088	0.076	0.072	0.054	0.057	0.059	0.070
8	Value (p.u.)	0.005	0.069	0.142	0.220	0.303	0.395	0.532	0.674	0.801	0.952
	Probability	0.307	0.120	0.098	0.073	0.070	0.073	0.062	0.054	0.035	0.109
9	Value (p.u.)	0.004	0.065	0.133	0.218	0.321	0.424	0.511	0.627	0.787	0.946
	Probability	0.313	0.111	0.108	0.083	0.068	0.064	0.047	0.040	0.056	0.110
10	Value (p.u.)	0.005	0.068	0.152	0.241	0.339	0.451	0.588	0.747	0.877	0.963
	Probability	0.328	0.104	0.108	0.082	0.065	0.070	0.047	0.053	0.062	0.081
11	Value (p.u.)	0.006	0.081	0.169	0.251	0.342	0.429	0.548	0.708	0.863	0.957
	Probability	0.343	0.098	0.088	0.079	0.053	0.053	0.055	0.064	0.059	0.109
12	Value (p.u.)	0.005	0.076	0.158	0.257	0.369	0.486	0.615	0.768	0.887	0.965
	Probability	0.328	0.105	0.080	0.080	0.067	0.049	0.066	0.065	0.060	0.100
13	Value (p.u.)	0.006	0.077	0.164	0.275	0.378	0.500	0.638	0.788	0.901	0.968
	Probability	0.318	0.101	0.094	0.070	0.061	0.060	0.058	0.061	0.075	0.100
14	Value (p.u.)	0.006	0.064	0.143	0.226	0.337	0.472	0.597	0.729	0.855	0.960
	Probability	0.307	0.097	0.083	0.068	0.064	0.053	0.061	0.059	0.068	0.139
15	Value (p.u.)	0.006	0.080	0.163	0.274	0.395	0.519	0.652	0.754	0.874	0.961
	Probability	0.291	0.139	0.068	0.072	0.066	0.065	0.039	0.054	0.075	0.131
16	Value (p.u.)	0.005	0.067	0.136	0.223	0.319	0.438	0.579	0.718	0.876	0.961
	Probability	0.234	0.119	0.094	0.063	0.063	0.077	0.067	0.073	0.085	0.127
17	Value (p.u.)	0.006	0.081	0.168	0.270	0.367	0.483	0.608	0.734	0.869	0.963
	Probability	0.224	0.101	0.104	0.096	0.064	0.069	0.067	0.062	0.083	0.130
18	Value (p.u.)	0.010	0.110	0.219	0.331	0.433	0.543	0.676	0.794	0.890	0.971
	Probability	0.199	0.119	0.113	0.103	0.074	0.078	0.065	0.064	0.087	0.099
19	Value (p.u.)	0.011	0.103	0.214	0.304	0.395	0.502	0.625	0.741	0.868	0.965
	Probability	0.147	0.120	0.106	0.102	0.103	0.080	0.070	0.084	0.087	0.100
20	Value (p.u.)	0.012	0.105	0.198	0.291	0.393	0.498	0.605	0.712	0.845	0.960
	Probability	0.142	0.106	0.111	0.120	0.108	0.084	0.069	0.088	0.062	0.110
21	Value (p.u.)	0.012	0.100	0.196	0.301	0.394	0.493	0.623	0.711	0.848	0.959
	Probability	0.149	0.133	0.122	0.110	0.094	0.107	0.063	0.062	0.058	0.101
22	Value (p.u.)	0.011	0.096	0.189	0.281	0.381	0.482	0.574	0.694	0.849	0.965
	Probability	0.154	0.127	0.122	0.105	0.111	0.071	0.080	0.077	0.057	0.095
23	Value (p.u.)	0.012	0.093	0.185	0.275	0.366	0.485	0.587	0.717	0.852	0.963
	Probability	0.185	0.130	0.118	0.109	0.110	0.081	0.069	0.046	0.057	0.093
24	Value (p.u.)	0.012	0.092	0.180	0.258	0.356	0.460	0.592	0.722	0.865	0.962
	Probability	0.221	0.141	0.099	0.113	0.089	0.084	0.056	0.057	0.057	0.084

In the next step, for each time-dependent clustered model, correlated uniformly random numbers between [0, 1] are generated for each hour and the cluster values with the probability related to these numbers are selected to represent the data at that specific time. This process should be conducted for all wind farms, demand and interconnector data sets. Simulated output power of Woodlawn for a sample day generated by means of the sampling technique (described in chapter 4) considering its correlations with other datasets is displayed in Figure 5.26. The output power of this wind farm can vary from 0MW to 48MW and the generated power at each hour is related to cluster values and their probabilities, generated random number and correlations with other wind farms at that time.

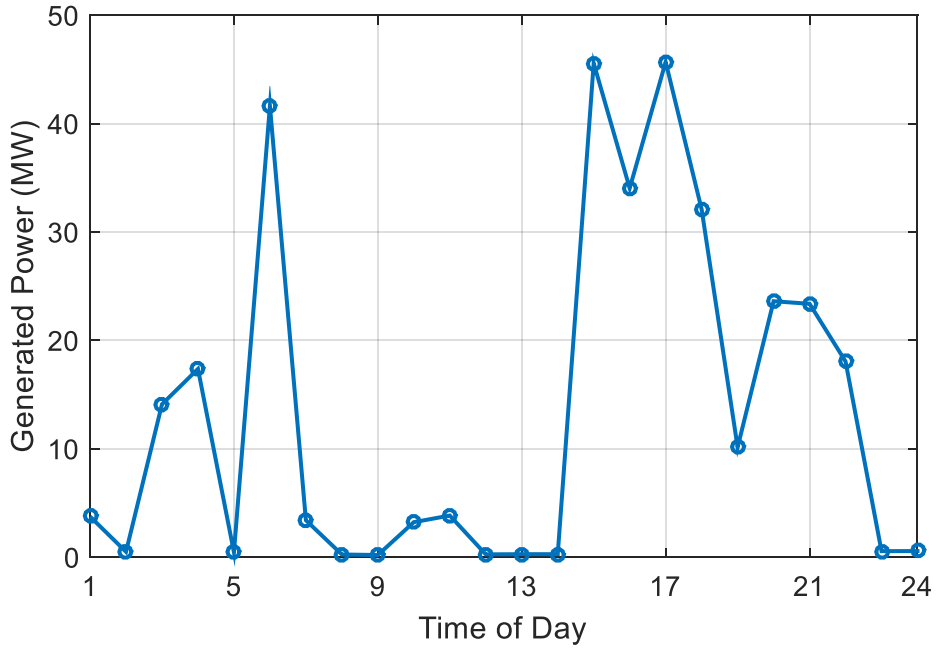

Figure 5.26. Simulated output power of Woodlawn for a sample day

Reliability of the NSW system is evaluated at generation and composite system levels using these time-dependent cluster models and the state sampling Monte Carlo technique. In the HLI study, all generators and electricity consumers are considered to be at one bus and the total generated wind power is deducted from the original demand minus the imported power plus the exported electricity. Then, the demand not supplied by the system is calculated on an hourly basis and the LOEE index is calculated for each hour. Finally, the overall loss of energy expectation is obtained by taking the average value of the hourly indices.

It should be mentioned that as NSW is highly reliable and its original LOEE at HLI level is very small, evaluating the impact of wind power on its original reliability level is not possible. Therefore, the NSW system has been modified and its load has been increased to reach the Australian standard of unserved energy level, which is 0.002% [121]. Then the load carrying capability of its wind power is calculated considering this new index. The LOEE of the modified NSW power system is

illustrated in Figure 5.27. This index is considered as a measure to calculate the reliability contribution of wind farms at the generation level.

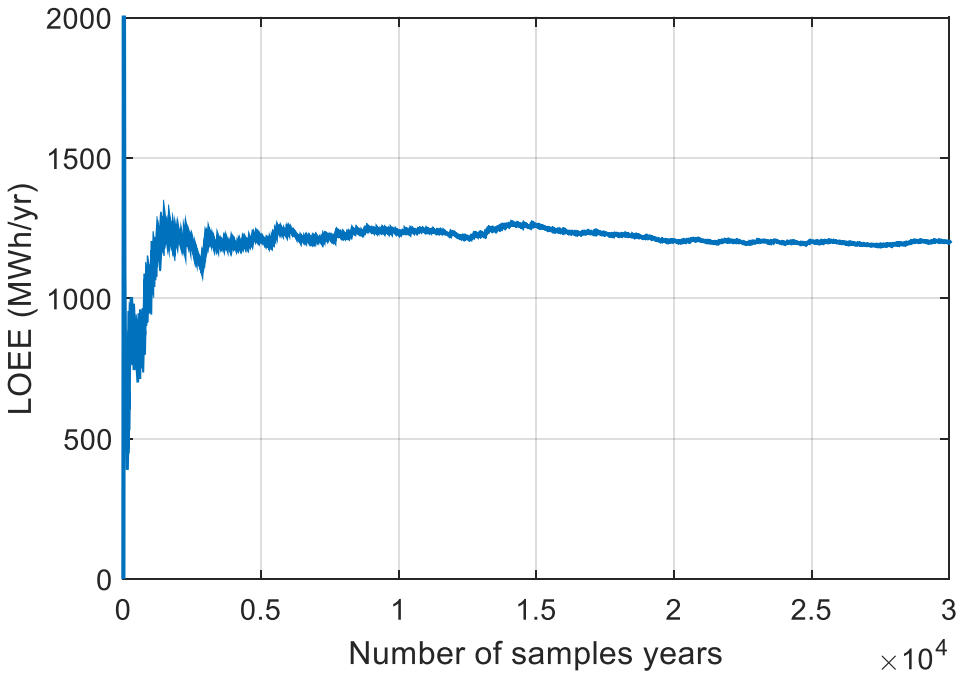

Figure 5.27. Loss of energy expectation of the modified NSW system

For the HLII study, all wind farms are modelled at their specific bus and the load flow analysis is conducted on an equivalent high-voltage network of NSW with some assumptions and approximations to evaluate the impact of transmission and generation system contingencies on the reliability contribution of wind farms. The amount of energy not supplied by the system without wind farms is used as the reliability level of the system and the amount of extra load that can be supported by wind farms without exceeding this level is measured as the expected load carrying capability of wind energy at this level.

The high-voltage network of NSW is shown in Figure 5.28. The NSW grid comprises 99 substations and around 13,000 kilometres of transmission lines. This transmission network operates at voltage levels of 500kV, 330 kV, 220 kV and 132 kV [122]. NSW, as mentioned earlier, has several connections with Victoria and Queensland networks.

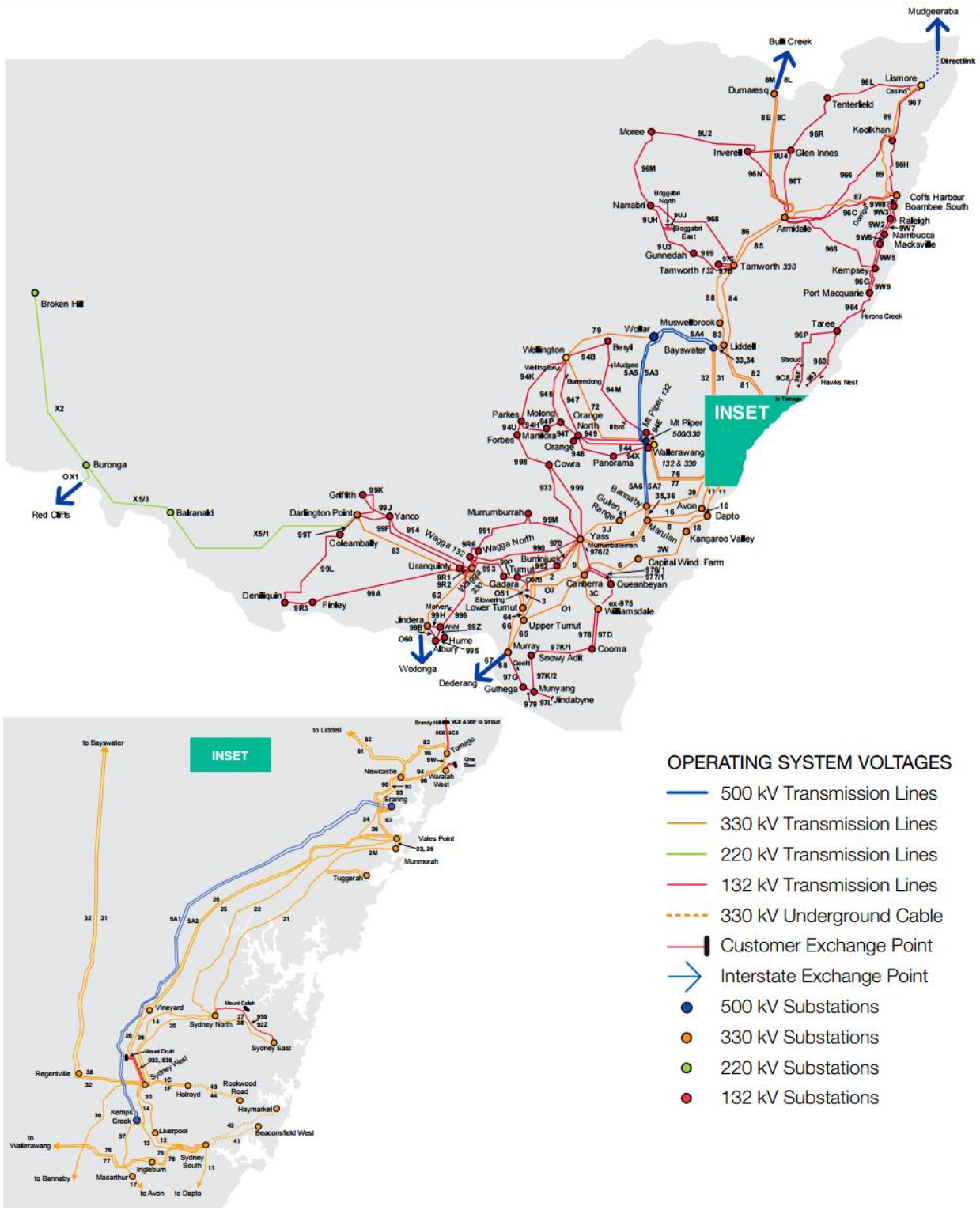

Figure 5.28. High voltage network of NSW [122]

The ELCC of wind farms in NSW at HLI and HLII are given in Table 5.15. It can be observed that the capacity value has decreased at the HLII level due to the transmission network constraints and contingencies. However, since NSW has a meshed network and wind farms are located in the middle of the network the impact of the transmission system is not that high compared to systems

like South Australia with large transmission networks and wind farms located at the edge of the system.

Table 5.15: Capacity value of wind power in NSW

Capacity Value	265 MW Wind	
	MW	%
Generation Level	93.05	35.24
Composite System Level	84.56	31.91

5.2.4. Impact of Interconnections on Capacity Value of Wind Farms

Victoria and New South Wales have several connections with other states and exchange a considerable amount of electricity through these tie-lines. Therefore, in this section, the impact of interconnections on the reliability benefits of wind energy in these power systems is investigated at the generation level. First, these networks are considered to work in islanded mode and no power is transferred through the interconnectors. Then, the results are compared with the ELCC of these two states considering the exchanged power through the tie-lines to investigate the impact of the interconnections on the reliability benefits of wind energy in these two states.

The loss of energy expectation indices of NSW and VIC in island mode are calculated. Then, the same index is calculated in the presence of wind energy by applying the approach that was explained in the previous sections. Figure 5.29 illustrates the ELCC calculation process for NSW wind farms in island mode.

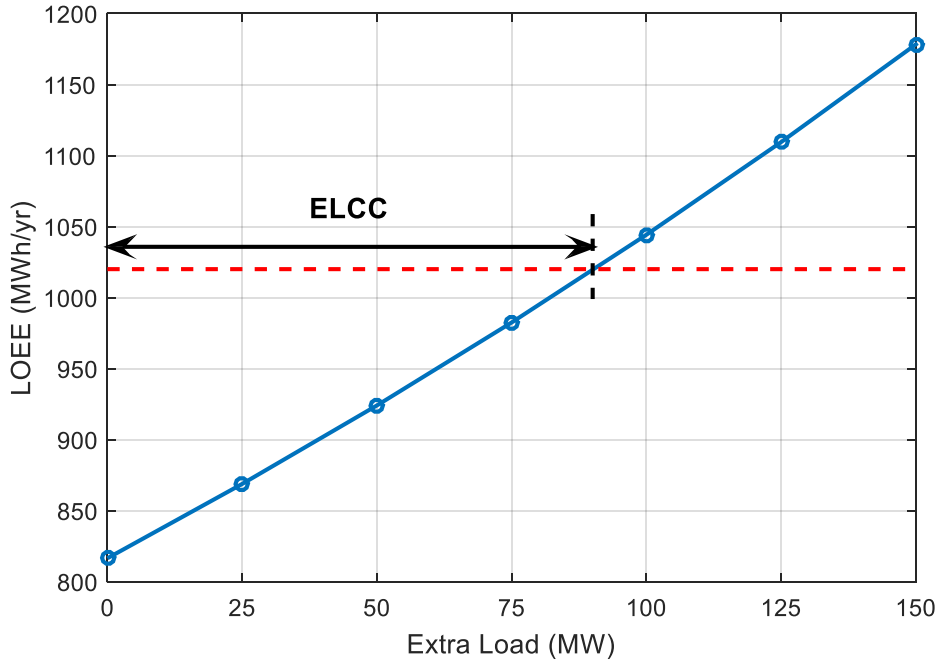

Figure 5.29. Capacity value of NSW wind farms in island mode

The ELCC of wind energy in New South Wales, as demonstrated in this figure is around 90MW. It means that this much extra load can be supplied with 265MW of installed wind farms in NSW while the reliability level of the system is unchanged. The same approach has been applied on the Victorian wind farms and the results of the study are presented in Table 5.16.

Table 5.16: ELCC of wind farms in NSW and VIC

From	ELCC (MW)	ELCC (%)
NSW (265MW)	90.20 MW	34.03
VIC (885MW)	219.8 MW	24.84

It can be observed that although the ELCC of wind farms in Victoria is higher in megawatt, its capacity value in percentage value is lower, due to its higher installed wind capacity. One reason might be the lower mean value or capacity factor of wind farms in Victoria (Table 5.9) in comparison to NSW wind farms (Table 5.13). The correlations between wind regime and load profile could be another reason. Table 5.17 compares the average hourly correlations between the NSW and VIC total wind power and their demand data in island mode. As can be seen, the correlation between wind generation pattern and load profile in Victoria is lower than in NSW.

Table 5.17: Average hourly correlations between wind power and load data in NSW and VIC

State	Correlation Coefficient
NSW	0.5986
VIC	0.3712

By comparing wind capacity values in the island mode with the ELCC values of NSW and VIC considering interconnections, which has been calculated in previous sections (Table 5.10 and Table 5.15), the impact of tie-lines can be investigated. The percentage values of the effective load carrying capabilities of wind power in NSW and VIC with and without interconnections are compared in Figure 5.30.

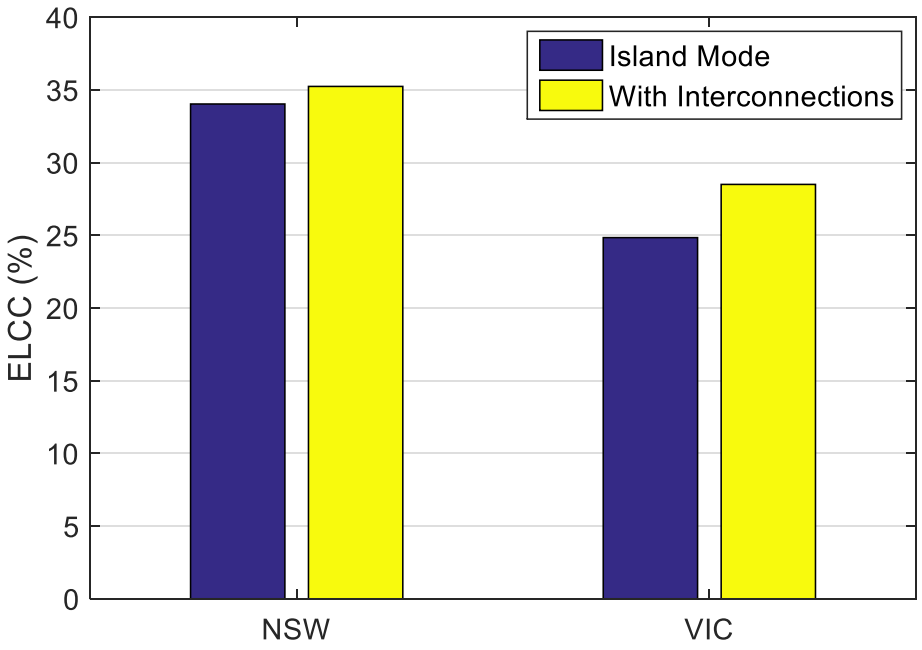

Figure 5.30. ELCC of NSW and VIC for different scenarios

As expected, it can be seen that in both systems, the ELCC of wind farms in the presence of tie-lines has increased. However, the increment in NSW is insignificant compared to the rise in the ELCC of VIC. The main reason for this might be the different role of the interconnectors in these two states. As it has been shown in Figure 5.13, Victoria exports electricity most of the time through these tie-lines and the average exported power for this system is positive. On the other hand, Figure 5.22 shows that NSW uses the interconnections mainly to import power. Therefore, as the tie-lines are considered and these networks are not islanded anymore, the VIC wind farms can export their generated power to other states when there is no need for them inside Victoria. Whereas, as NSW imports electricity, the contribution of wind is not changing that much and the impact of interconnections on its ELCC is negligible.

Therefore, it can be concluded that the impact of these power lines on the reliability benefits of wind farms can be different and depends on their roles in exporting or importing electricity. If tie-lines help to export power most of the time, the ELCC of wind energy may increase. However, if a system mainly imports electricity through them, their influences on ELCC might be insignificant.

5.3. Tasmania

5.3.1. Tasmanian Power System

Tasmania is an island state of Australia located South of Victoria. The majority of its power production is from renewable energy resources. This system is the smallest network in Australia and its maximum peak demand is around 1,800MW [112]. Electricity in Tasmania is currently almost entirely produced by hydro generation with a total installed capacity of 2,300MW [22]. Installed wind generation capacity is already around 308 MW with more than 1GW of projects publicly announced for future development. Tasmania is connected to mainland Australia via a single HVDC undersea link (Basslink) with an export capacity of 630 MW. Tasmania has the potential for high wind penetration levels [123]. Evaluating the contribution of wind generators in the system adequacy of the Tasmanian power system is essential due to the expected increase of wind power penetration levels in Tasmania.

Tasmania generates most of its electricity from hydro (77%) and has around 386MW of gas-fired generation as the second source of power production [22]. Currently, wind power has a 10% share of total generation capacity of this system. The proportion of different energy sources in the generation capacity of Tasmania is shown in Figure 5.31.

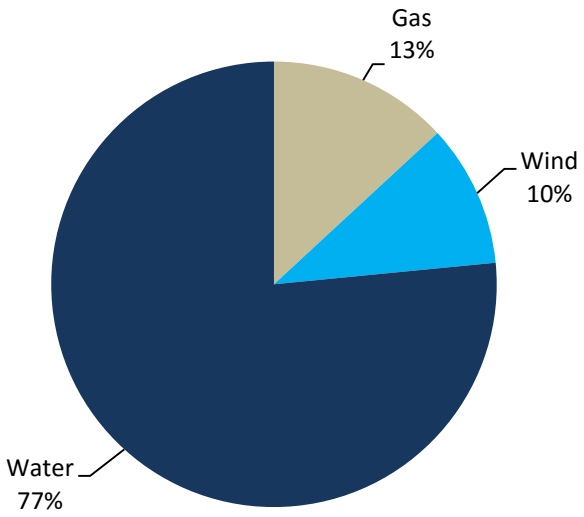

Figure 5.31. TAS installed capacity percentage by generation type [118]

Furthermore, future generation development in Tasmania is expected to be in the renewable sector as there are more than 1,300MW wind and 302MW hydro projects publicly announced. The details of the Tasmanian generation system and its future developments are given in Table 5.18.

Table 5.18: TAS existing and potential new developments by generation type (MW) [39]

Status / Type	CCGT	OCGT	Gas other	Wind	Water
Existing	208	178	5	308	2,281
Publicly announced	0	0	0	1,379	302

Unlike other states, in Tasmania peak load generally occurs during winter. Figure 5.32 shows the range of variations in the Tasmanian hourly load from 2011 to 2013 [112]. It can be seen that the hourly load profile varies from 650MW to more than 1,600MW and consists of two peak periods: one in the morning and the other in the evening.

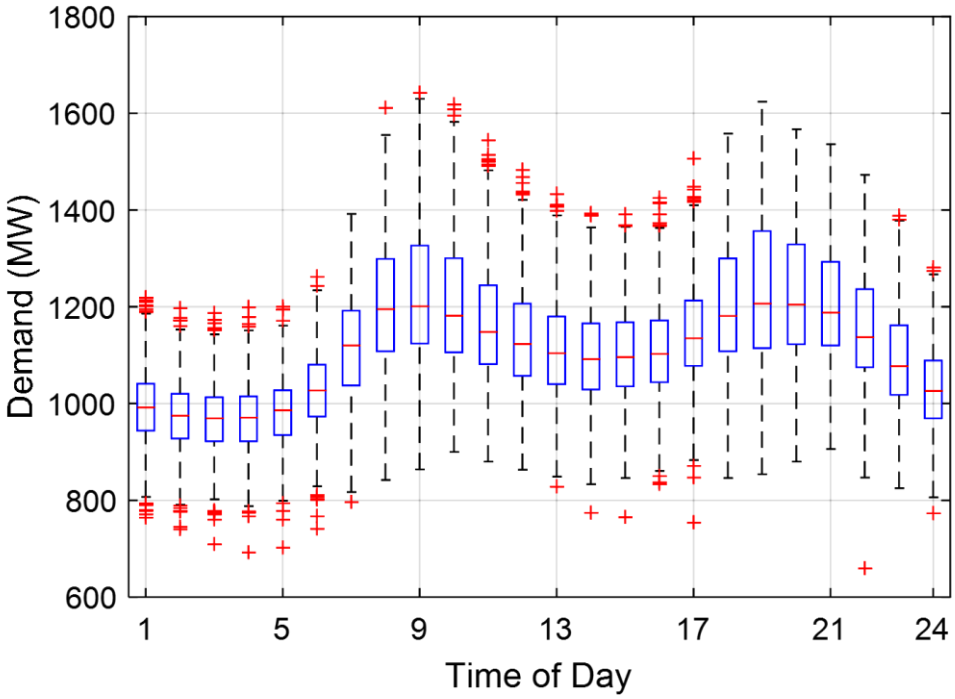

Figure 5.32. Box-and-whisker plot for hourly load data in Tasmania for 2011-13 [112]

It can be observed that the load profile of Tasmania is unique and different from other states. The average load in this system is low during midnight and midday, while in other states the highest peak demand happens during the midday period. This is mainly because of its mild weather in summer and very cold weather in winter [124]. Since the demand in winter is much higher than the summer load, the reliability evaluation for Tasmania is conducted only for the winter time (June, July and August), when this system may face some insufficiencies. The average seasonal demand of Tasmania in 2012 is depicted in Figure 5.33. It shows that the average electricity consumption in this state is the highest during winter and has the lowest peak in summer.

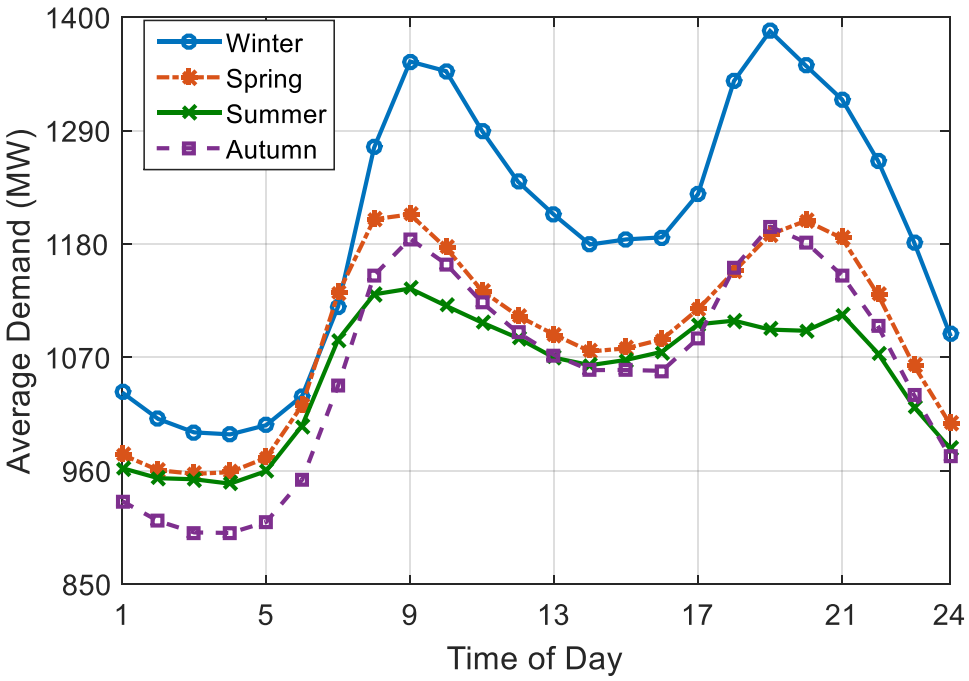

Figure 5.33. Average hourly demand of Tasmania for different seasons in 2012 [112]

5.3.2. Wind Data

Tasmania is geographically located within the 'Roaring Forties'; latitudes with some of the most reliable winds on Earth [123]. Tasmania currently has 140MW Woolnorth and 168MW Musselroe wind farms. This means the wind capacity in Tasmania might be able to supply around 17% of its peak demand (1,800MW). The statistical values of historical wind speed data of six years (2006 till 2012) for these sites provided by the Australian Bureau of Meteorology are presented in Table 5.19.

Table 5.19: Statistical data of Woolnorth and Musselroe sites wind speed [124]

Site	Mean (m/s)	Standard Deviation (m/s)
Woolnorth	9.73	4.94
Musselroe	6.80	3.65

It can be seen that the wind regime at the Woolnorth location is better than the one at the Musselroe site. However, it should be mentioned that for the Musselroe wind farm the BOM wind speed data of Eddystone Point weather station which is the nearest active weather station and is 30 kilometres distance from this wind farm was utilized.

5.3.3. Simulation Results

The process of calculating the capacity value of the Woolnorth wind farm for the winter period is shown in Figure 5.34. The dashed line in this figure illustrates the loss of energy expectation of Tasmania for different extra loads added to this power system. It can be seen that LOEE is around 200 MWh/yr for 1,800 MW peak load (no extra load). This index is computed once again considering wind farms and extra load levels. The solid line in Figure 5.34 depicts the LOEE of this system. Comparing these two lines, 44 MW extra load could be added to the Tasmanian power system supplemented by the Woolnorth wind farm without exceeding the existing LOEE level (200 MWh/yr.). This is equivalent to approximately 31% of the 140MW installed capacity of the Woolnorth wind farm.

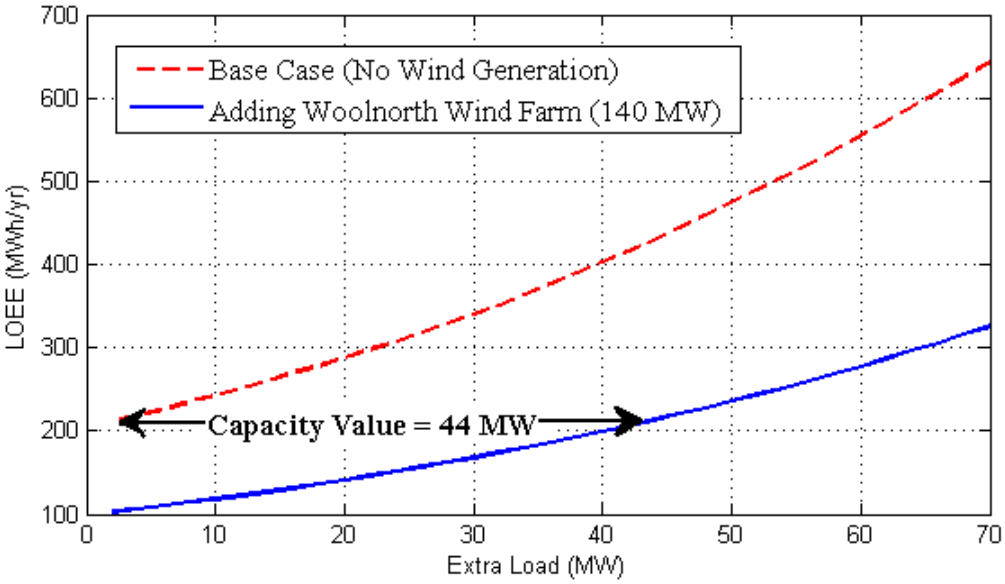

Figure 5.34. Capacity value of Woolnorth wind farm

Effective load carrying capability of Musselroe is investigated by applying the same process described before. The capacity value of this 168 MW wind farm is around 38 MW (23% of its installed capacity). Although this wind farm has a higher installed capacity than the 140MW Woolnorth wind farm, its capacity value is lower. This could be due to the lower wind speed in Musselroe compared with Woolnorth as has been shown in Table 5.19.

In order to calculate the impact of the transmission system on the capacity credit of wind farms, reliability assessment has been conducted at HLII. In this level, an equivalent network was prepared with some assumptions to study load flow analysis on the Tasmanian power system. The expected energy not supplied considering generation units and the transmission network has been calculated using the state sampling (non-sequential) Monte Carlo method. Figure 5.35 displays the high-voltage network of Tasmania and the location of Woolnorth and Musselroe wind sites. In Tasmania

the transmission network operates at voltages of 220 kV and 110 kV and consists of 3,577 circuit kilometres of transmission lines and underground cables, 49 transmission substations and 7 switching substations [125].

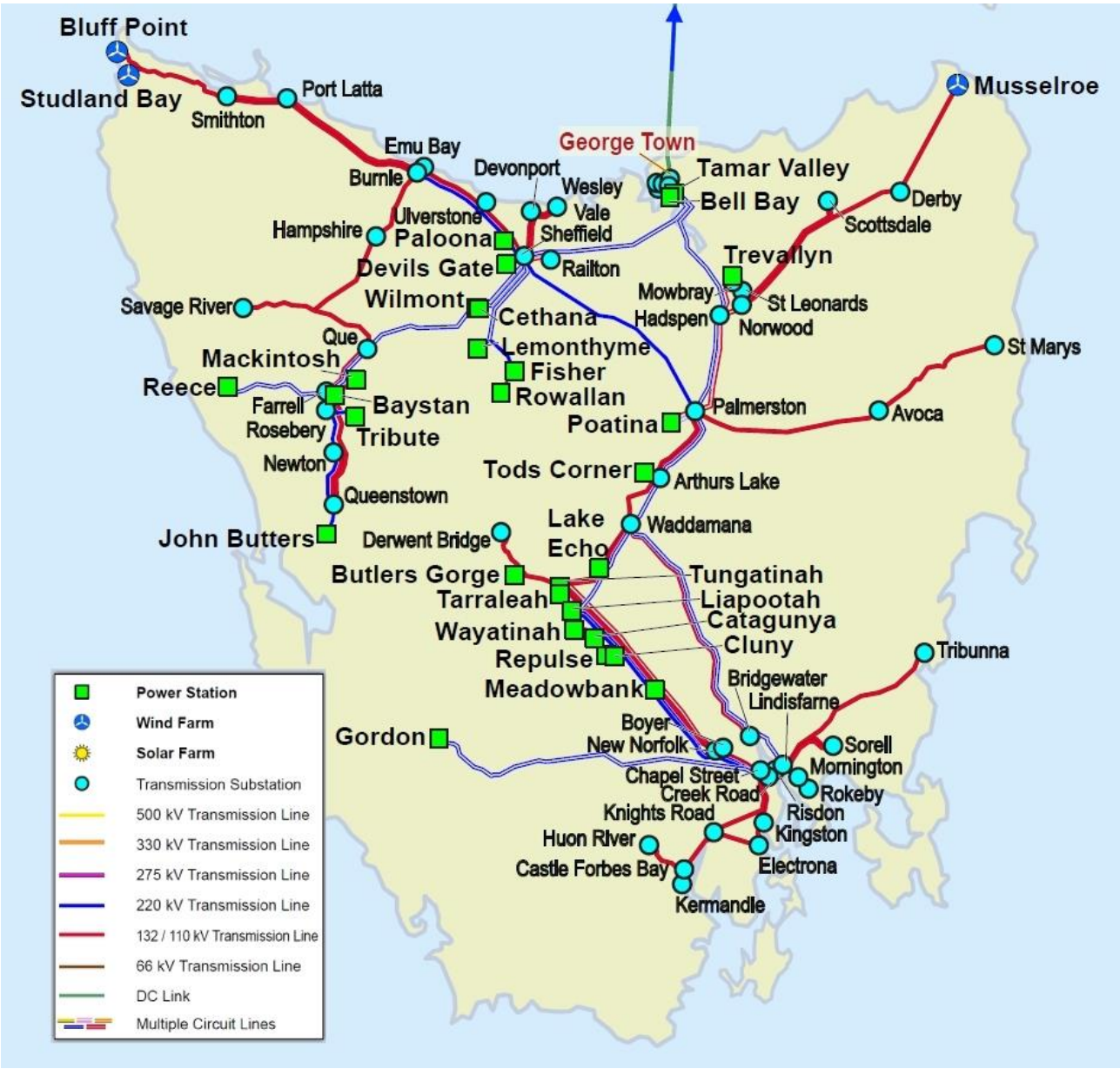

Figure 5.35. High voltage network of Tasmania [117]

Figure 5.36 depicts the EENS of the Tasmanian composite system during winter with and without wind generation. It can be seen that in all cases, by increasing system load the EENS is growing. However, adding wind generation can reduce this index and improve system reliability. But the amount of augmentation for each case is different. The ELCC of Woolnorth is around 35MW which is higher than Musselroe with 24MW capacity value and the load carrying capability of total wind generation in Tasmania is around 33MW.

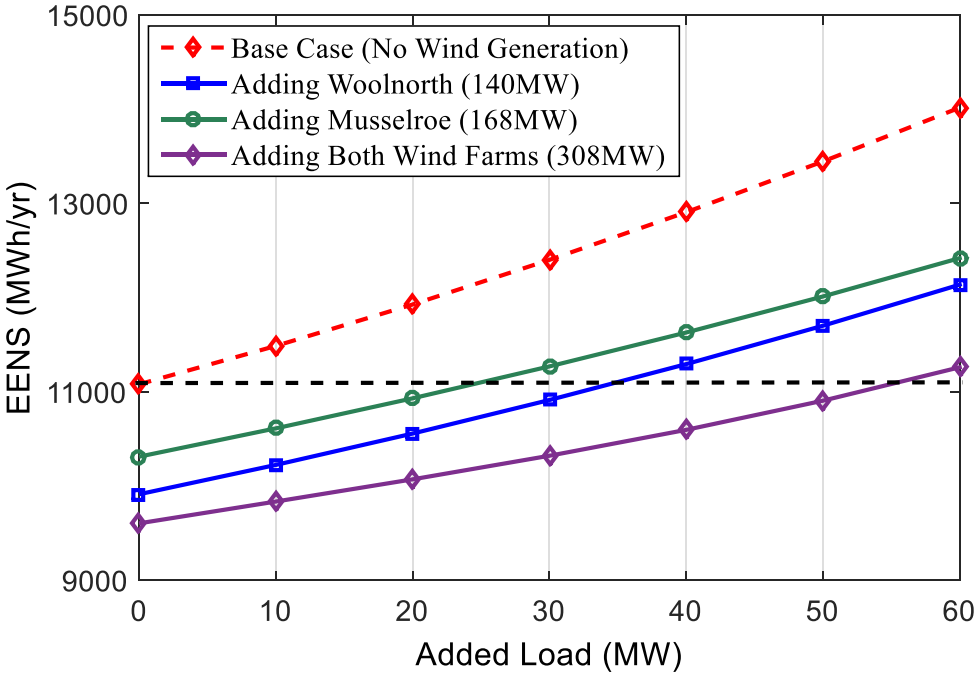

Figure 5.36. ELCC of wind farms in Tasmanian composite system during winter

Figure 5.37 compares the capacity value of wind farms at different reliability assessment levels. It shows that the reliability benefits of wind energy at HLII have decreased due to network constraints and transmission line contingencies. In this study, as wind farms are far from load centres, the effect of transmission system constraints is significant. Moreover, the amount of reduction in the ELCC of Musselroe is higher. Therefore, it can be concluded that transmission network reinforcement near this site might be more beneficial than near the Woolnorth site. However, economic analysis and more studies are required to verify this conclusion.

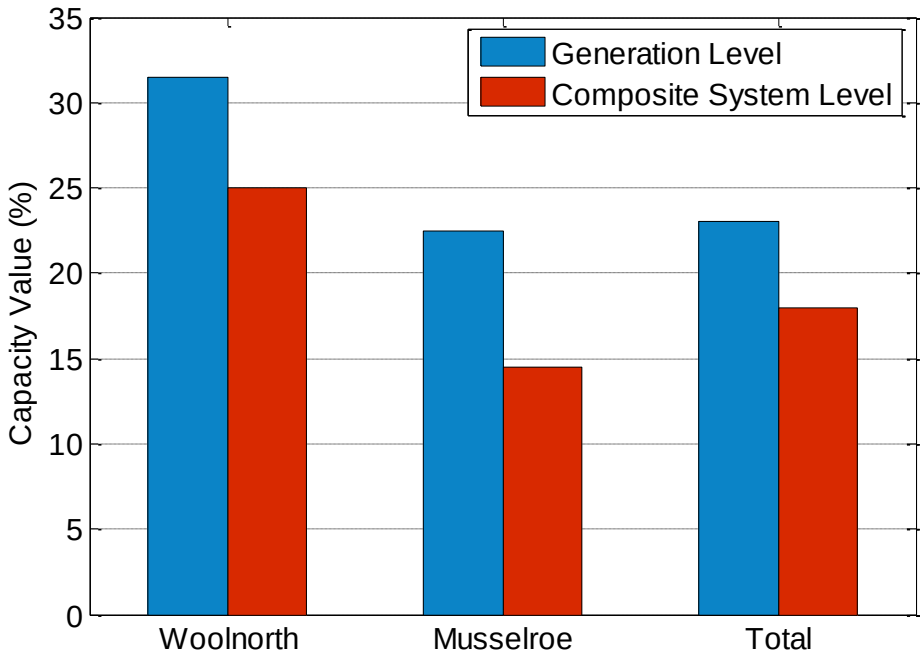

Figure 5.37. Capacity value of wind farms in two reliability assessment levels

5.3.4. Wind – Hydro Coordination

Hydroelectric power is the major source of electricity in Tasmania with 27 hydro power stations, generating around 10,000 GWh of electricity annually [123]. This presents an ideal opportunity for the Tasmanian power system to coordinate hydro-electric and wind power generation to balance wind power variations and maximize renewable energy utilization. Coordinating the output of some existing hydro units with wind farms can balance the wind power fluctuations and increase the benefits of wind farms. Power system reliability in the presence of wind-hydro coordination has been studied in [126] and [127]. Hydro units were considered as peak time generators in [126] and it was shown that coordinating wind and hydro can improve system adequacy when a proper number of hydro units are designated to support wind farms. Wind power is utilized in [127] to store water in hydro reservoirs during off peak periods, which can be used at a later time by the hydro station to produce its highest capacity during peak load times when electricity has a higher value.

For cooperation between hydro and wind generators, first, the coordination strategies such as energy storing inception and energy balancing should be determined. Energy inception policy specifies when the coordinated generator has to reduce its output and what the minimum required level of wind power to trigger the coordinated generator should be. Different values can be selected as the coordination criterion, which means the minimum required capacity of the wind to start preserving water in the storage [127].

In order to balance the stored and released water for hydro plants, the energy balancing strategy should be determined. Short-term and long-term policies can be considered as energy balancing policies. In these strategies, at the end of a specified operation cycle (e.g. 24 hours), all the stored water should be released. Although long-term policies are more flexible they may require a water management process and therefore, are more complicated.

Among Tasmanian hydro stations, the Gordon scheme located in the southern part of Tasmania is considered to be ideal for coordination with wind power. The Gordon station has the highest hydro installed capacity in Tasmania [22] comprising three 144MW units, which generates up to 432 MW of power. This hydro station is supplied with water from Lake Gordon and Lake Pedder [128]. Gordon hydro station is coordinated with Tasmanian wind farms in a daily energy balancing policy: during off peak periods the wind farm produces power and the hydro unit decreases electricity production which effectively stores water in its reservoir. During peak load periods, the Gordon hydro power station could generate additional power using the stored water to maximize its output when electricity usually has a higher value. The unused capacity of Gordon station during

peak time, which is around 30 MW, is utilized as an inception strategy. During off peak times when the wind farm power exceeds 30 MW, Gordon hydro unit stops producing power and retains its water level. This stored water can be used to obtain maximum power from this hydro station if it's required.

The coordination process between the Gordon hydro plant and Woolnorth for a sample day is illustrated in Figure 5.38. The dashed red line represents the inception strategy, the blue line is the power generation of Woolnorth and the shaded areas are the amount of energy that can be stored and utilized during peak times. For the cooperation process a day is divided into four periods: two off peak periods and two peak durations. The off peak times are from 11pm to 6am and 12pm to 5pm, while 6am to 12pm and 5pm to 11pm are considered the peak times.

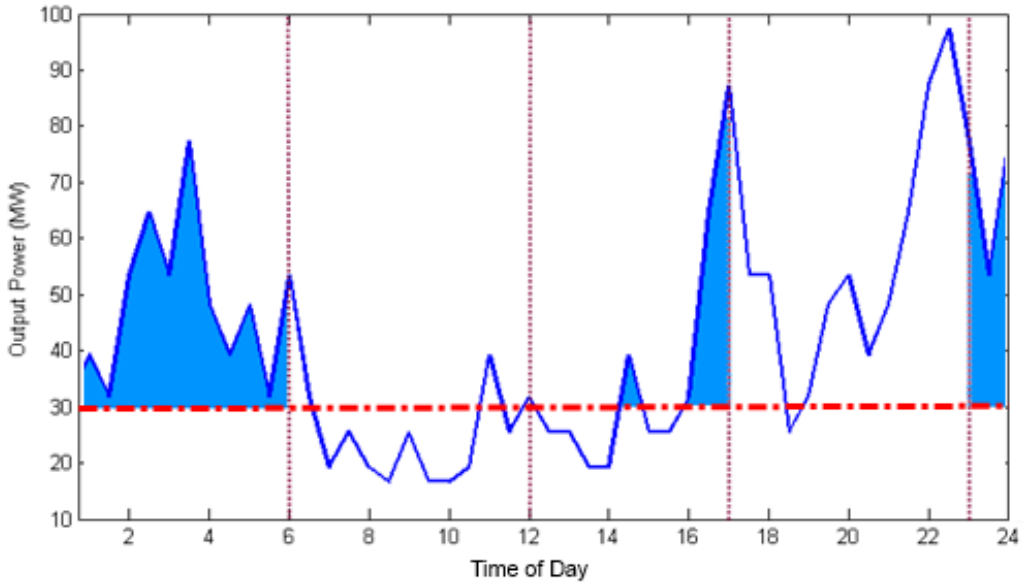

Figure 5.38. Coordination process between Gordon and Woolnorth for a sample day

The LOEE index of Tasmania has been calculated once again considering the cooperation. Then, by comparing this index with the original LOEE, the effective load carrying capability of wind farms coordinated with Gordon hydro station is calculated. The effect of this coordination on the capacity value of Woolnorth and Musselroe wind farms is displayed in Figure 5.39.

As is shown in Figure 5.39, the capacity values of Woolnorth and Musselroe have increased. This means that without using extra water and just by changing the power production plan of the Gordon hydro station, the load carrying capability of wind farms could be significantly increased. It should be noted that this increase depends on the wind regime of the wind farms. Taking Woolnorth as an example, coordinating 30 MW of hydro power has raised its capacity value from 31% to 46% or by 20 MW (from 44 MW to 64 MW). At Musselroe the same coordination has resulted in an increase from 23% to 33% or by 17 MW (from 38 MW to 55 MW).

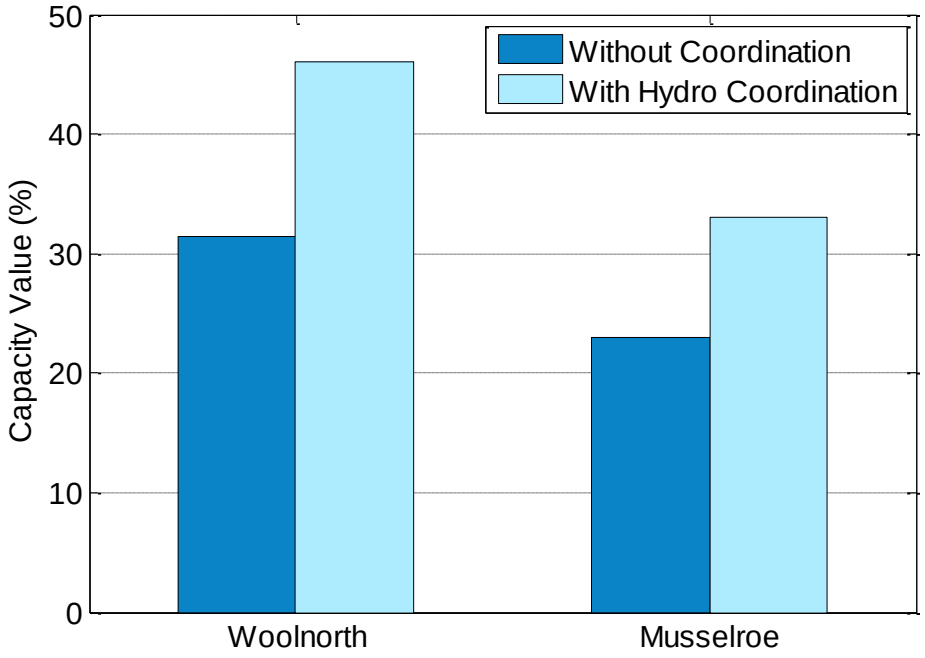

Figure 5.39. Capacity value of Tasmanian wind farms with and without hydro coordination

It is considered highly likely that the impact of coordinating on capacity value depends on wind speed regime at each wind farm, with larger increases occurring at wind farms with more consistent wind. Thus it is concluded that it would be better to use hydro units to support wind farms with higher wind speeds if the objective is to maximize the benefits from increased capacity value.

To assess the effect of a higher coordination criterion, the study was repeated with a 50 MW coordination capacity. In this simulation, the hydro unit could stop power production and retain its water when the output power of the wind farm is more than 50 MW during light load. Although this value is 20 MW higher, the results are similar to the previous study (coordinating 30 MW) and have not materially changed. It has increased the capacity value of Woolnorth and Musselroe wind farms by 21 MW and 18 MW, respectively.

Therefore, in order to investigate the impact of coordination inception strategy on the ELCC of wind farms, different values have been selected as the coordination capacity for the cooperation between Woolnorth wind farm and Gordon hydro unit. The results of this study are depicted in Figure 5.40. It can be seen that by increasing the coordination capacity, the ELCC of this wind farm is increasing. However, the increment rate decreases and the ELCC is saturated after 30MW coordination capacity. Lower probabilities of producing high levels of wind during off-peak and the constraint in the Gordon hydro reservoir are the main reasons. Therefore, selecting a higher coordination capacity may not improve the capacity value of wind farms significantly, and an optimum strategy should be selected according to hydro unit constraints and the output profile of wind farms.

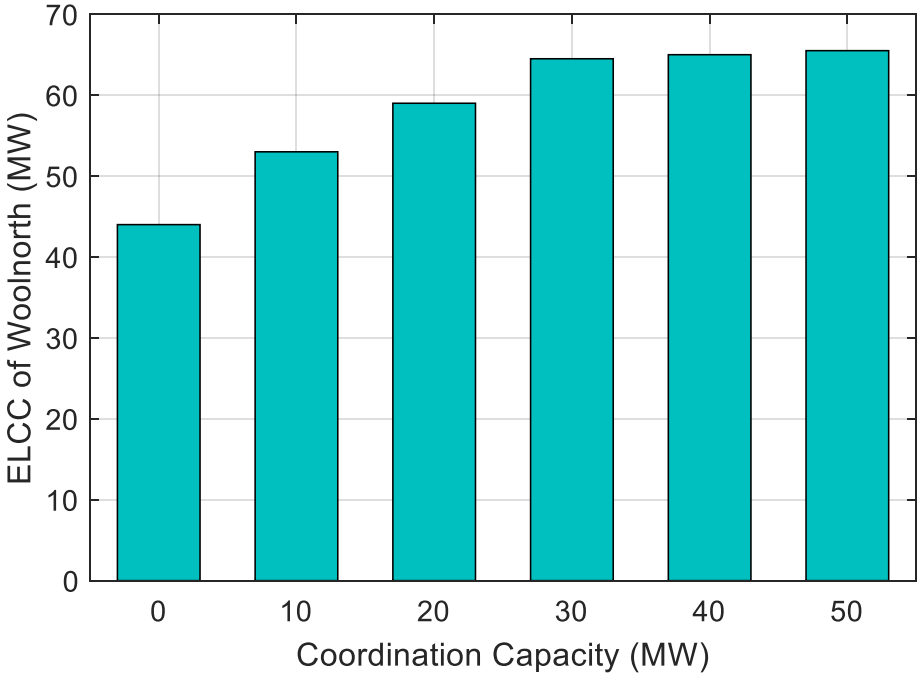

Figure 5.40. Capacity value of Woolnorth for different coordination capacities

5.4. Summary

Capacity values of wind farms in several regions of the NEM have been evaluated for hierarchical levels I and II in reliability studies. First, reliability contribution of wind energy in generation adequacy assessment has been investigated, where the capacity shortage of generators is important regardless of their location in the network. In the second level study, the impact of transmission system constraints and contingencies has also been taken into consideration. Because the location of generators and loads are important and will affect the result at this level, load flow study is also required in each iteration, which increases the computational time of current reliability assessment techniques significantly. Therefore, the proposed time-dependant clustering method, which has been explained in Chapter 4, has been applied to model wind generation, electricity consumption and exchanged power. This method is not only fast and simple but also is capable of keeping correlations and time properties of datasets and can be used in systems with a large number of renewable generators without losing its simplicity. In order to calculate the reliability benefits of wind generation, LOEE and EENS indices have been computed in the generation adequacy assessment level and composite system studies, respectively.

It is concluded that at the generation level, wind capacity value is related to wind regime of wind farms, their correlation with load profile, dependencies between wind patterns, generation capacity of the system, exchanged power through interconnections and the reliability level of the

studied system. While at the composite system level, in addition to these factors the topology of the transmission network, location of wind farms and transmission system constraints are affecting the ELCC of wind farms as well. By comparing the results of these two reliability assessment levels, it can be realized that reliability benefits of wind generation in the composite system assessment is lower. This can be due to transmission system constraints and outages. Hence, the amount of reduction in the ELCC of wind farms can be a criterion in network augmentation studies. Furthermore, results show that the impact of exchanged power through tie-lines can be dissimilar for different systems and is mainly related to the direction of the flowing power.

It is also concluded that wind-hydro coordination can improve the capacity value of wind farms regarding their wind regime and water constraints of the hydro unit. However, using different capacities to coordinate wind and hydro power indicates that coordinating with higher capacities may not result in a great increment in the capacity value of wind farms and the ELCC might be saturated after a certain level of coordination capacity.

Furthermore, there were many assumptions considered in this study with network information about different state networks. Hence the results presented in this chapter are the work of the candidate and do not reflect the views of the network companies or the Australian Energy Market Operator. To have an exact analysis, collaboration between the state electricity network companies, generators and AEMO is necessary.

Similar to wind power, the penetration level of solar power is increasing in the NEM regions. This growth, which is mainly due to the increment in the residential solar panels installations, will change the shape of the electricity consumption profile in power systems and consequently will affect the reliability level of systems and the capacity value of wind power. Since integration of photovoltaic systems is increasing, their role in supplying demand should be taken into account in reliability calculations. Therefore, in the next chapter the impact of solar energy on the reliability of power systems and its influence on the ELCC of wind farms are investigated.

Chapter 6

Impact of Solar PV on the Capacity Value of Wind Farms

6.1. Introduction[1]

Similar to wind energy, the photovoltaic (PV) penetration level is increasing in many countries power systems, which will affect not only the overall reliability of power systems, but also will affect the reliability benefits of wind farms. Several studies have proposed models for PV generators in reliability assessment and have evaluated electric systems reliability in the presence of solar energy [16]–[18]. However, these works haven't considered wind generation in their studies and the reliability assessment has been done just for PV panels.

A few works have addressed the reliability of systems with wind and solar PV generators [13], [19]. However, they have considered both wind and PV together and have not studied the impact of PV generation on the reliability benefits of wind farms. In Ref. [19] energy adequacy of a distribution system with renewable distributed generators (DG) has been evaluated and the reliability contribution of these small DGs during peak time is measured. Reliability evaluation of the IEEE reliability test system with large-scale wind and PV generation has been investigated in Ref. [13]. This work proposed a method to capture all correlations between wind speed, solar irradiation and load profile in the adequacy studies. It has concluded that these dependencies will affect the reliability indices, and by increasing the level of integrated renewable generators the impact of correlation will increase. To our best knowledge, little or no study has evaluated the reliability benefit of wind and solar in a realistic power system, and the influence of solar generation on the reliability contribution of wind energy has not been analysed.

[1] This chapter covers the following references:

- Mehdi Mosadeghy, Ruifeng Yan and Tapan K .Saha "Impact of PV Penetration Level on the Capacity Value of South Australian Wind Farms" Renewable Energy (Elsevier), Volume 85, January 2016, Pages 1135–1142.
- Mehdi Mosadeghy, Ruifeng Yan and T.K. Saha, "A Time Dependent Approach to Evaluate Capacity Value of Wind and Solar PV Generation" IEEE Transactions on Sustainable Energy, early access, DOI: 10.1109/TSTE.2015.2478518.

To address these gaps and investigate the influence of solar energy on reliability benefits of wind generators, the South Australia (SA) power system has been selected as a case study. Where the level of wind generation is the highest compared to demand in Australia, and this system has a high penetration level of solar energy [20]. The time-dependent clustering methodology, which has been explained in Chapter 4, is applied to model wind, PV and load data. Reliability indices of the SA system with and without renewable generators have been calculated at the generation level. Then, by comparing these indices, the impact of PV panels on the contribution of wind farms is analysed. Therefore, this research will provide a valuable methodology for system operators and planners to investigate the impact of solar energy while they are assessing the reliability contribution of wind farms. Because without considering this issue the reliability benefits of wind energy may be overestimated.

The rest of this chapter is organized as follows. A brief overview of solar power in the Australian National Electricity Market (NEM) is given. The methodology to model PV in reliability studies described. Then, the impact of solar power on the capacity value of wind has been evaluated. In addition, effects of seasonal dependencies and wind pattern correlations with PV profile on the capacity value of wind farms are discussed. Furthermore, the future contribution of renewable energies in the adequacy of the SA system is assessed by considering different scenarios for 2020. Finally, a summary of conclusions is given.

6.2. Solar Energy in the Australian NEM

Solar power is growing rapidly in many power systems around the world. At the end of 2014, around 177 GW of solar PV were installed all over the world, where more than 38 GW were installed in 2014 [129]. Total capacity of installed PV globally from 2000 to 2014 is illustrated in Figure 6.1. It can be seen that PV installation has increased significantly and solar power is expected to continue this growth strongly. A similar trend is happening in Australia and in 2014 around 900MW solar PV were installed in this country. Australian solar energy continues to develop steadily and its current annual growth rate is around 18% [42]. Most of the PV systems in Australia are small-scale rooftop installations; however there are a number of larger-scale PV power stations [130].

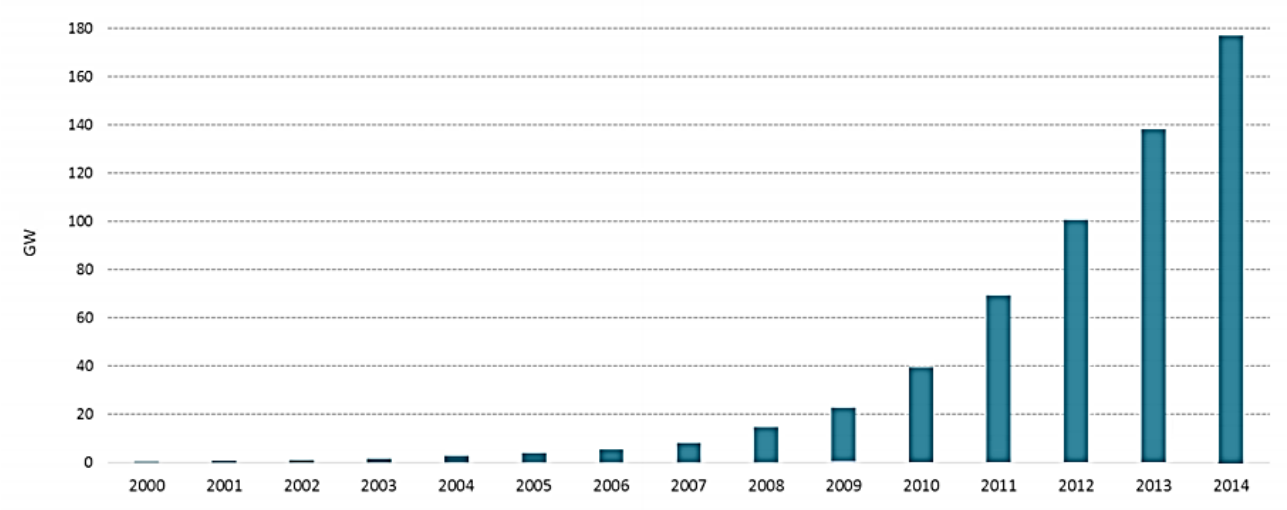

Figure 6.1. Evolution of global PV installation [129]

Australia has good potential for solar energy and currently there are more than 4,300 MW installed PV units, where the share of NEM is around 88% with 3,862 MW PV systems [40]. Australian PV installation density by postcode is depicted in Figure 6.2 [40]. It can be seen that the density in most of the major cities is high and this value in Brisbane and Adelaide is more than 45%.

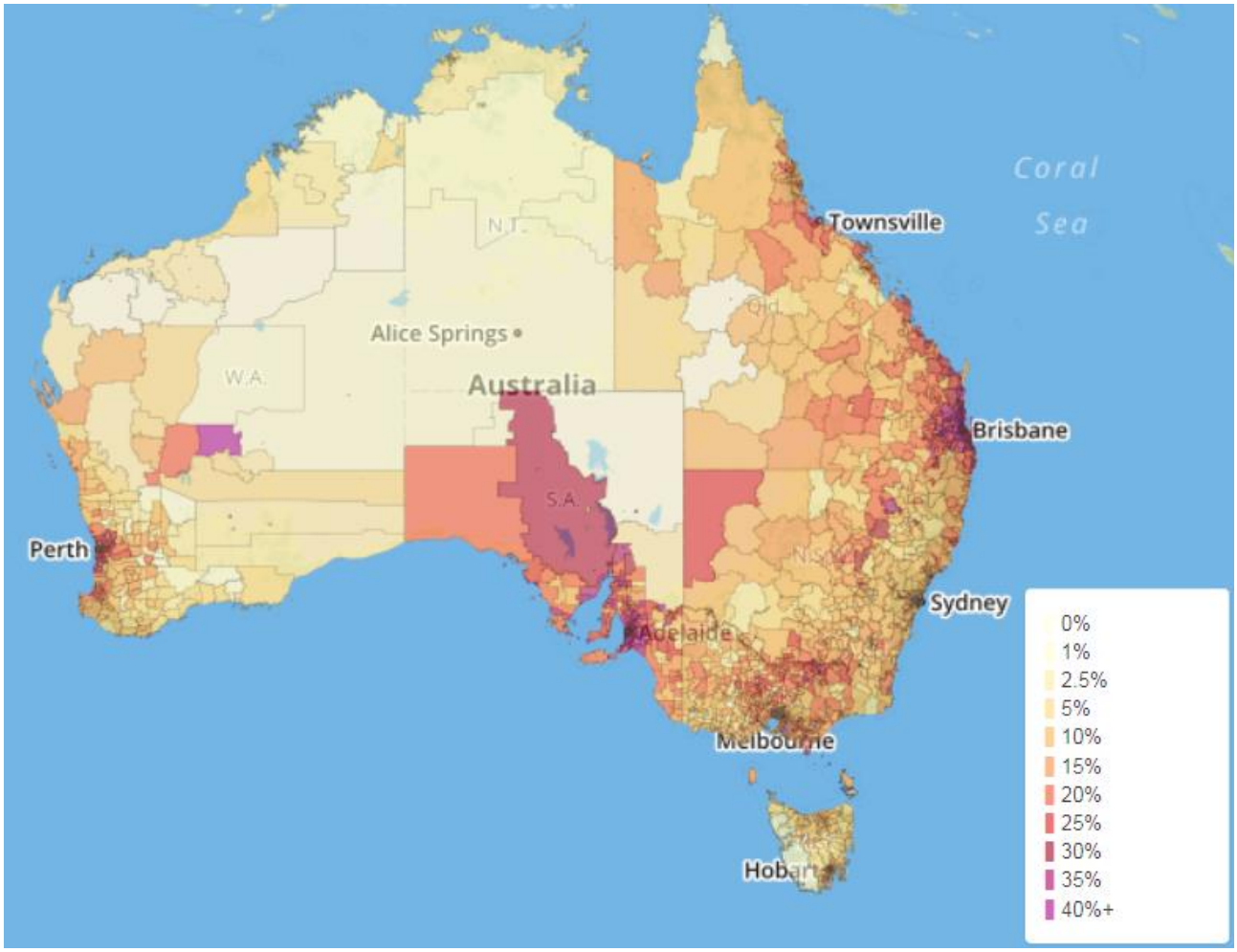

Figure 6.2. Australian PV installation density by postcode [40]

Among NEM regions, Queensland has the highest installed solar capacity with around 1,400 MW and New South Wales follows with almost 1,000 MW of solar generation. Victoria and South Australia are next with PV installed capacity of about 800 MW and 600 MW respectively. Currently, Tasmania has the lowest PV level with less than 100 MW of installed solar units. Total installed capacity of solar PV systems in NEM regions is presented in Figure 6.3 [40]. The maximum demand in most of these regions happens during the summer noon period [42]. Therefore, PV units can have a large impact on the reliability and generation adequacy of these systems since solar generation has a high output during that time and can contribute significantly to reduce the peak demand. Thus, in this research, the reliability contribution of solar power and its impact on the capacity value of wind farms is investigated.

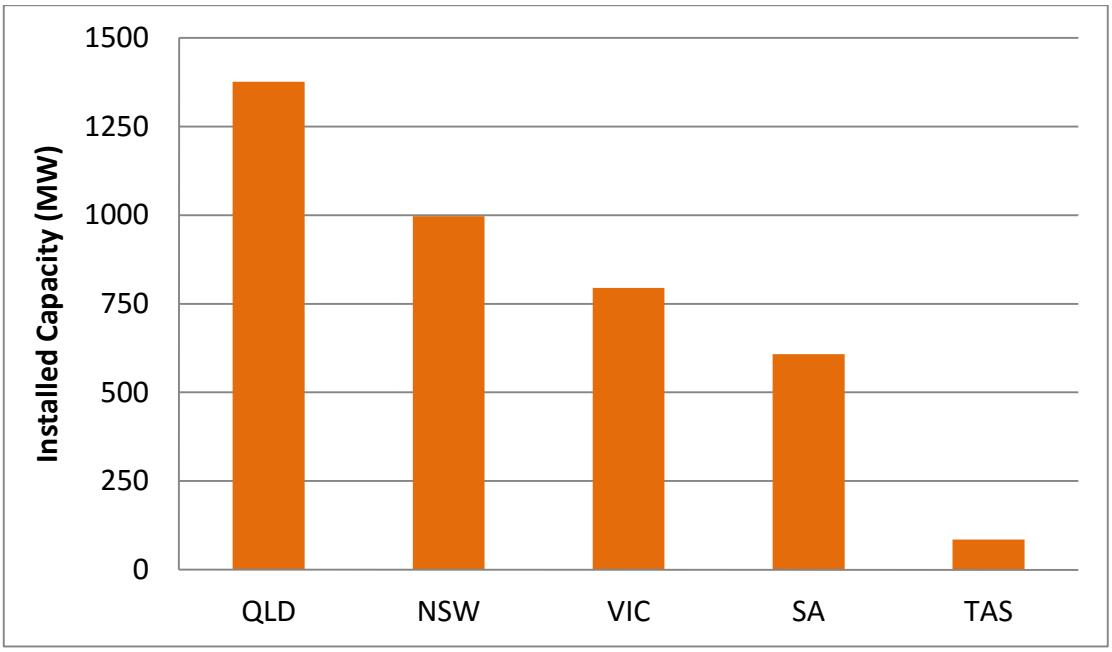

Figure 6.3. Installed PV generation capacity in NEM by State (Aug 2015) [40]

6.3. Solar Generation Model

South Australia is selected as the case study to evaluate the ELCC of its solar generation and the impact of solar energy on the capacity value of wind power. This system not only has the highest wind level in Australia but also has a significant amount of solar PV, which makes it an interesting case for this study. To obtain the output power of solar PV panels in South Australia, the total installed capacity of each suburb has been obtained from the Clean Energy Regulator [114]. Then, by implementing Global Horizontal Irradiance (GHI) data [124], the hourly generated power of PV panels in each suburb has been calculated using (6.1) [131].

$$P_M = P_M^* \frac{G_i}{G_j^*}\left[1-\gamma(T_c-25)\right] \tag{6.1}$$

where, P_M is cell output power (W), P_M^* denotes cell maximum installed power (W), G_i represents incident global irradiance (W/m^2) and G_i^* is standard incident global irradiance (1000 W/m^2). T_c denotes cell temperature and γ is cell maximum power temperature coefficient (˚C^{-1}).

By summarizing the output power of the photovoltaic panels in all suburbs, the total hourly solar generation of the SA system, which is shown in Figure 6.4, has been computed. As depicted in this figure, in 2013 PV panels in South Australia could produce up to 85% of their nominal capacity in the summer and around 55% during the winter. It should be mentioned that during this study, at the end of 2013 South Australia had around 500MW of PV panels [114].

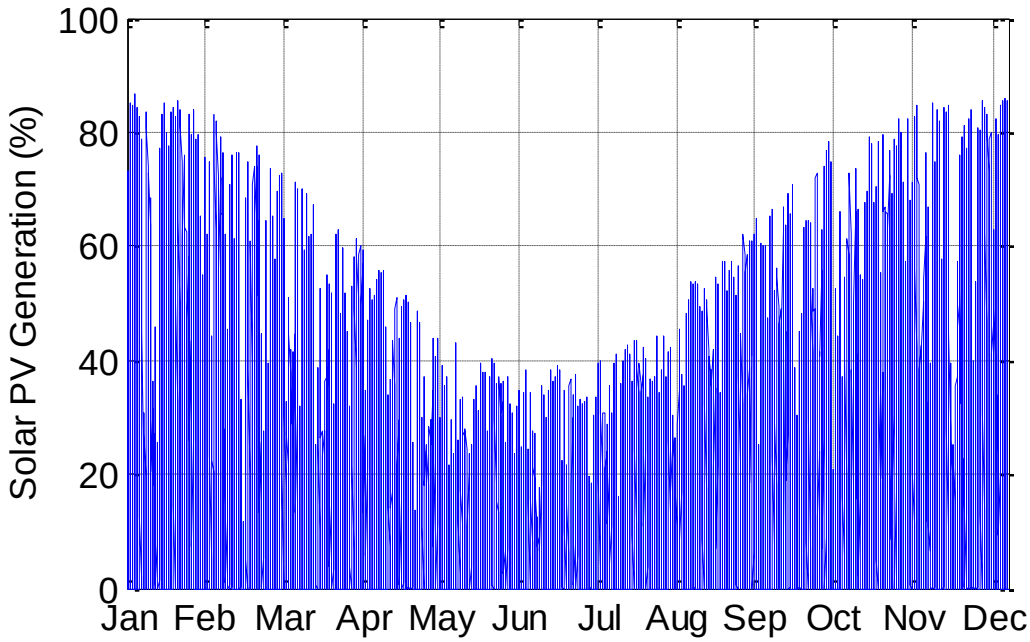

Figure 6.4. Total solar PV generation pattern in South Australia

In the next step, the hourly power data is transferred into time-dependent cluster model, which was explained in Chapter 4. The hourly 8-step model of per-unit PV generation is demonstrated in Figure 6.5. It shows that solar generation can have 8 different states for each hour, while these values are zero before sunrise and after sunset.

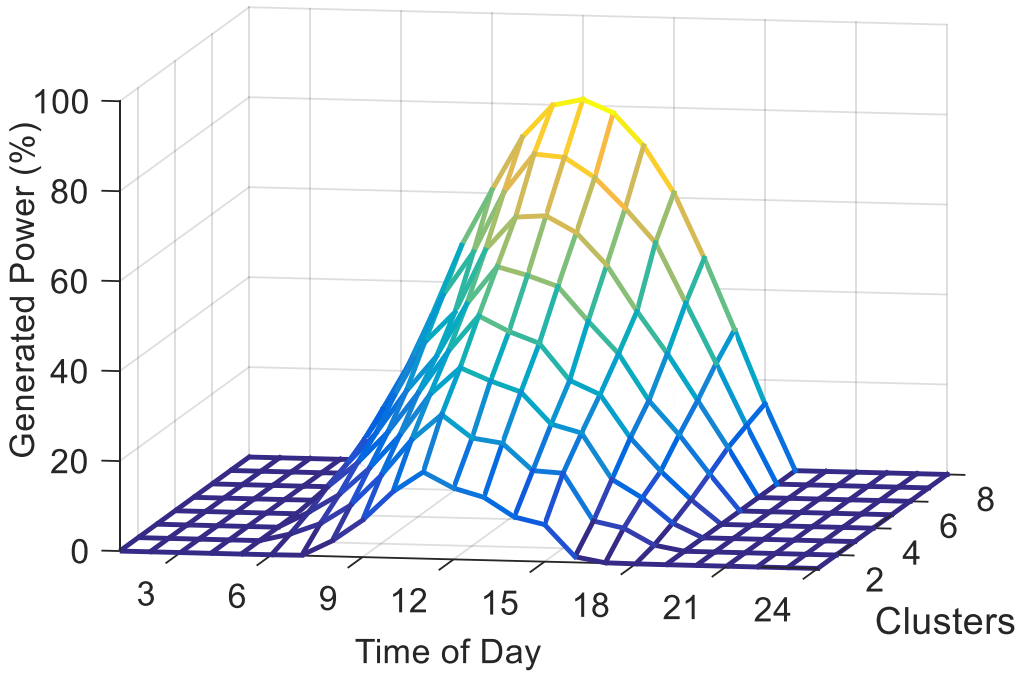

Figure 6.5. PV output model for South Australia

When time-dependent cluster model is created, to determine the hourly values of PV, wind and load from the clustered models, the correlated sampling approach (Chapter 4-Section 4.5.2) is utilized.

Figure 6.6 illustrates solar PV generation for a sample day created by this technique. The output value of each hour has been determined from time-dependent clusters using the sampling technique mentioned before.

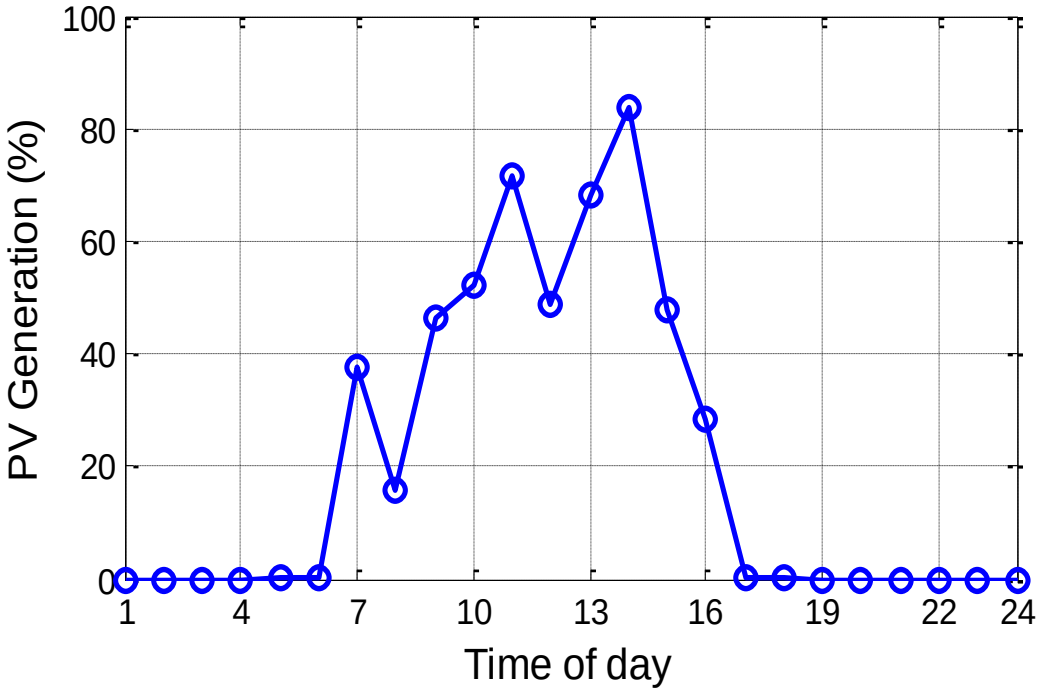

Figure 6.6. Hourly PV generation for a sample day obtained from the proposed technique.

To calculate the reliability index of the SA system, first the pure demand is calculated and by recording the events that demand exceeds the available generation capacity, the demand not supplied and consequently, the loss of energy expectations is determined. In order to obtain the amount of pure demand (D_t), which is a combination of system load, exchanged power, wind and PV generation, equation (6.2) is applied.

$$D_t = L_t + P_{\exp,t} - P_{imp,t} - P_{W,t} - P_{PV,t} \tag{6.2}$$

where, $P_{exp,t}$ and $P_{imp,t}$ are exported and imported power through the interconnectors at time t, and L_t denotes system load. $P_{PV,t}$ represents total power generation of solar PV and $P_{W,t}$ shows total wind power.

Historical hourly load data of the SA system is extracted from [112]. However, this data is not the actual demand and includes the output power of solar PV. Thus, to obtain the actual hourly load data, the total solar production in SA has been added to the given load data. The average daily load profile of South Australia with and without solar PV generation in 2012-2013 is depicted in Figure 6.7.

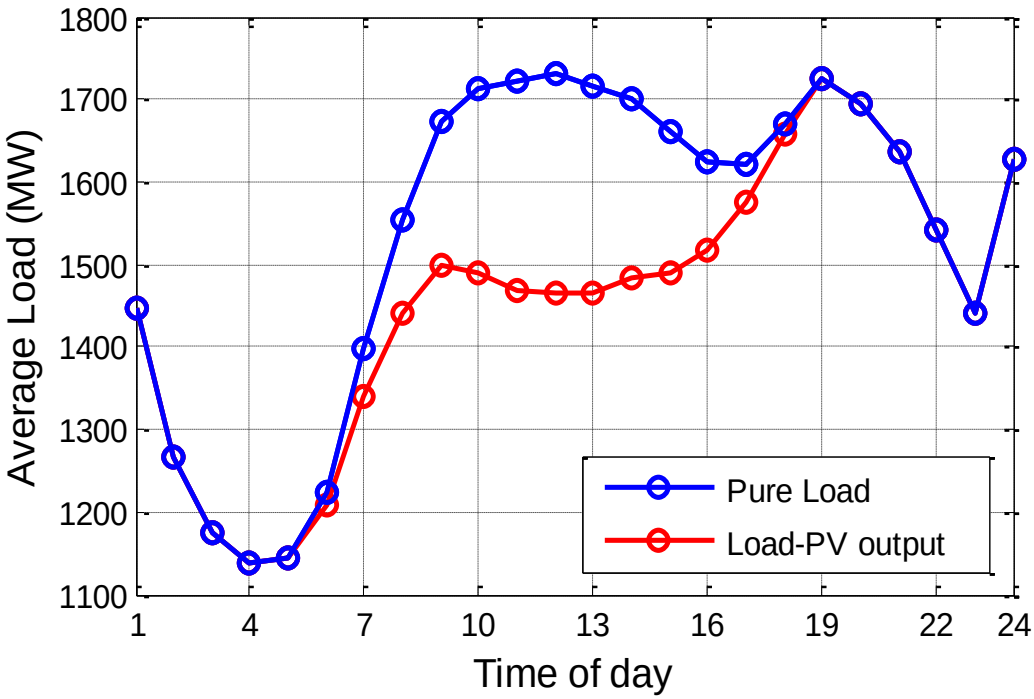

Figure 6.7. Average daily load profile of South Australia [112]

The red graph shows the SA demand obtained from AEMO database and the blue line is the actual load. The main difference is during midday when the generated power of solar units is high.

6.4. Impact of Solar Energy on the ELCC of Wind

To study the influences of solar generation, the capacity value calculation, mentioned in Chapter 4, is conducted again by incorporating PV generation. In the first step, to study the impact of solar generation on the reliability level of the SA system, LOEE of this system is calculated for a variety of PV installed capacities and different amounts of added load. Figure 6.8 depicts the result of this study. It can be seen that in all cases, by increasing PV capacity level, LOEE decreases and the system becomes more reliable, especially in the presence of higher amounts of added extra loads.

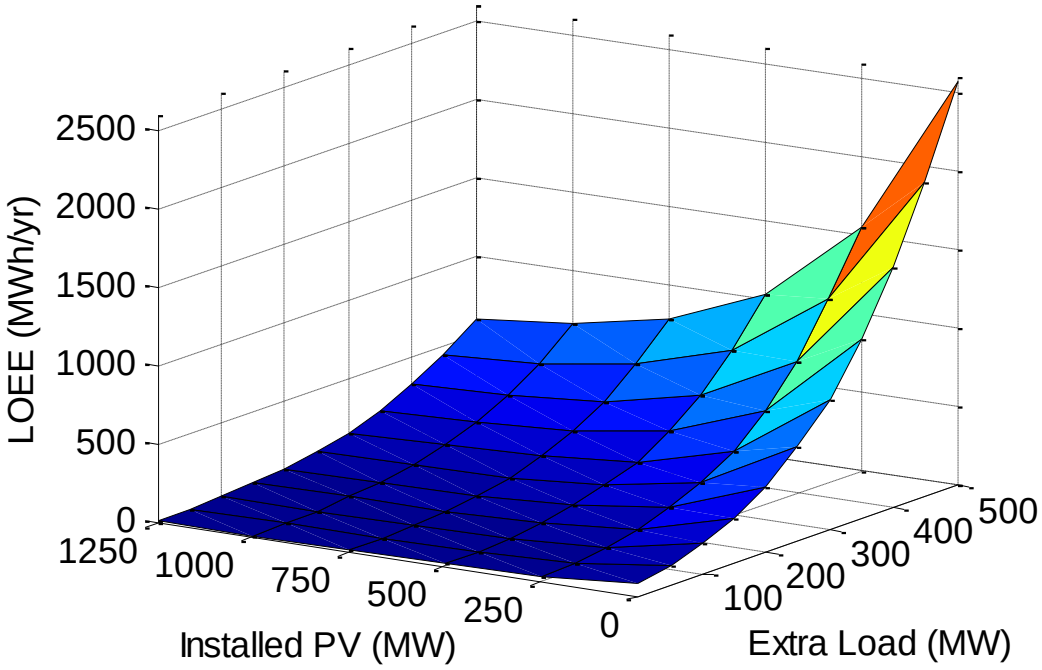

Figure 6.8. Sensitivity analysis of PV penetration level impact on LOEE

In the next step, in order to investigate the pure reliability benefits of solar energy, the ELCC of PV with different installation levels has been evaluated. Results are illustrated in Figure 6.9.

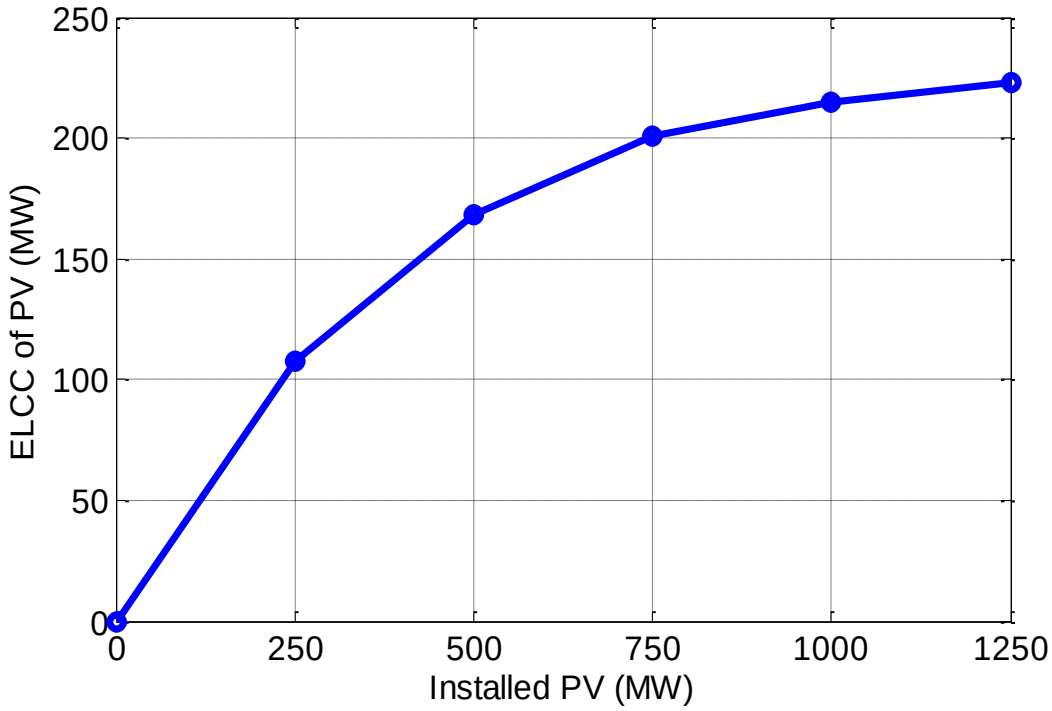

Figure 6.9. ELCC of different installed PV levels

As can be observed in this figure, by adding extra solar PV to the system the reliability contribution of solar energy will increase, however, the ELCC improvement rate will decline. For instance, the load carrying capability of 500MW solar generation is 168MW and by adding another 500MW PV this value will go up to 220MW, which means the extra 500MW PV has improved the ELCC of solar energy around 52MW. This can be due to the high generation to load ratio; as the PV level increases, total generation level of the system will grow and the reliability of the system will improve, as was shown in Figure 6.8. Therefore, the additional PV will have a lower reliability contribution.

Furthermore, to evaluate the reliability contribution of renewable energies in the SA system, the capacity value of wind and PV together in South Australia has been evaluated. Figure 6.10 compares the capacity value of wind farms, solar panels and wind - PV combined together in SA. It shows that the reliability benefit of PV is 168MW and wind power has a capacity credit of 385MW. However, the load carrying capability of wind and PV together is 497MW, which is less than the summation of those separately.

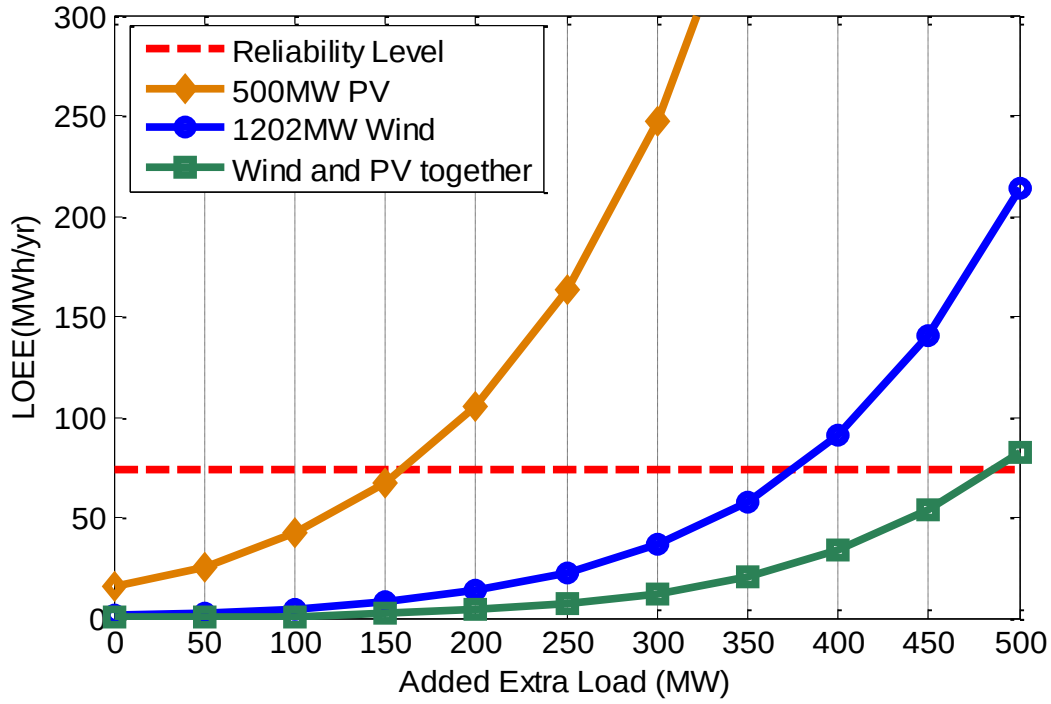

Figure 6.10. Reliability benefits of renewable energy generation in SA

The overlap between wind and PV generation during some periods of the day, as is shown in Figure 6.11, might be the reason. This figure shows that around midday both wind and solar generators are producing power and their total generation is high. Therefore, the reliability benefits of these sources together might be saturated and the system may face less reliability problems during that time of the day.

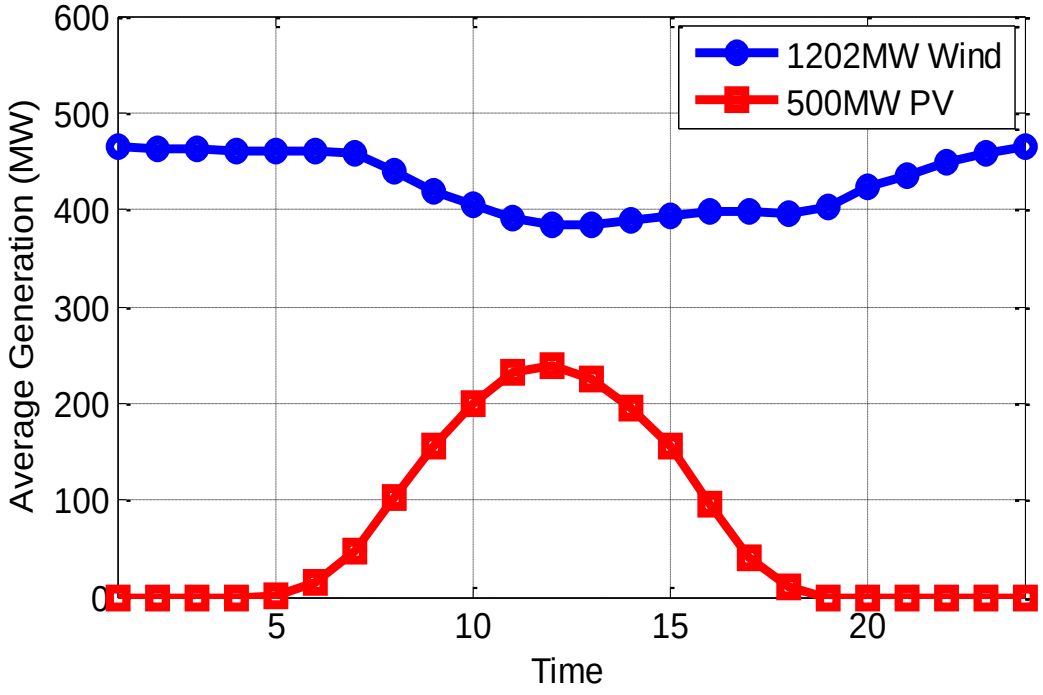

Figure 6.11. Average hourly output of renewable generators in SA

Moreover, to analyse the impact of this overlap and the influence of solar power on the reliability contributions of wind energy, the process described in Figure 6.10 has been repeated for 1202MW of wind and different levels of PV generation. Figure 6.12 displays the results of this study. This graph shows that as the level of PV generation increases the ELCC of renewable energy will grow, however, the growth rate will decline and the contribution will be saturated in high levels of PV and wind power. The main reason as mentioned in Figure 6.9 might be the higher ratio of generation to load.

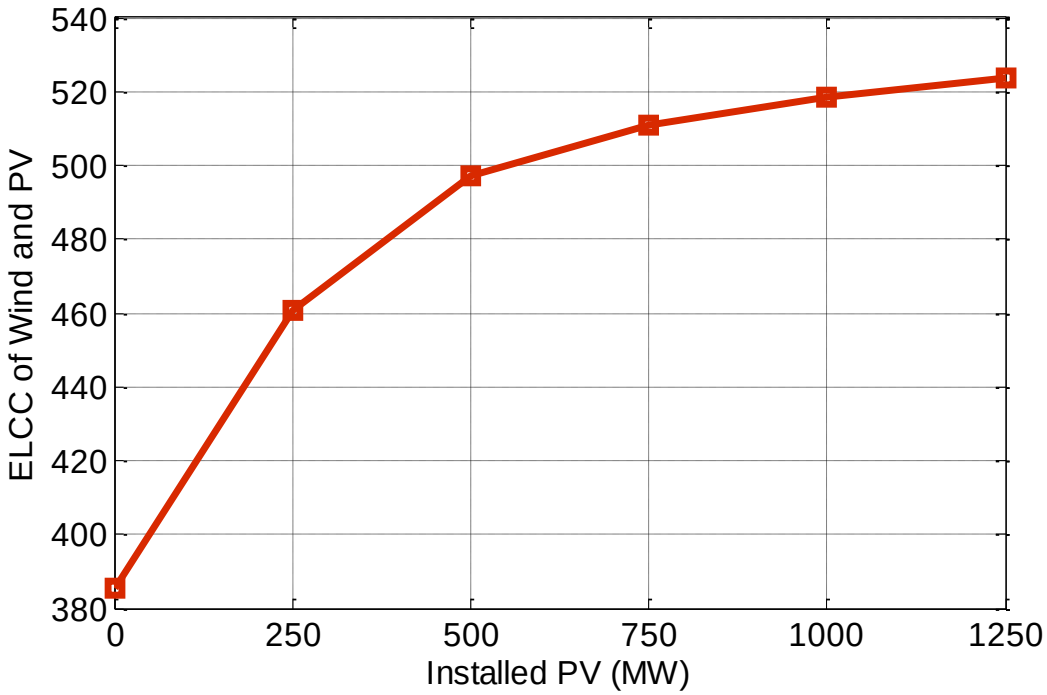

Figure 6.12. ELCC of renewable energy in SA for different levels of PV

By comparing Figure 6.9 and Figure 6.12, it can be noticed that by increasing solar PV levels, the impact of solar energy on the capacity value of wind energy increases, however the influence rate will decline and be saturated as the PV level increases. For example, ELCC of 500MW PV in Figure 6.10 is around 168MW and by adding 1202MW of wind generation this value raised to 497MW, while adding the same amount of wind power to the system with 1000MW PV panels has improved the ELCC from 220MW to around 520MW. One of the main reasons for this saturation as mentioned earlier, can be the growth in system generation level and the other one might be the higher overlap between PV and wind generation.

To demonstrate this impact clearly, the ELCC of wind farms for different penetration levels is presented in Figure 6.13. PV penetration level is considered as the peak value of solar generation divided by peak load. This graph shows that as the penetration level of PV increases the contribution of wind energy in the reliability of the system will decrease. It can also be understood that the impact of high solar PV penetration levels on the capacity credit of wind farms is higher;

however, the reduction rate of ELCC will decline as the PV generation level increases. For instance, if the PV penetration level changes from 0 to 15%, the ELCC of wind generation will decrease around 65 MW, but if PV level increases from 15% to 30%, capacity credit of wind farms will reduce another 20 MW.

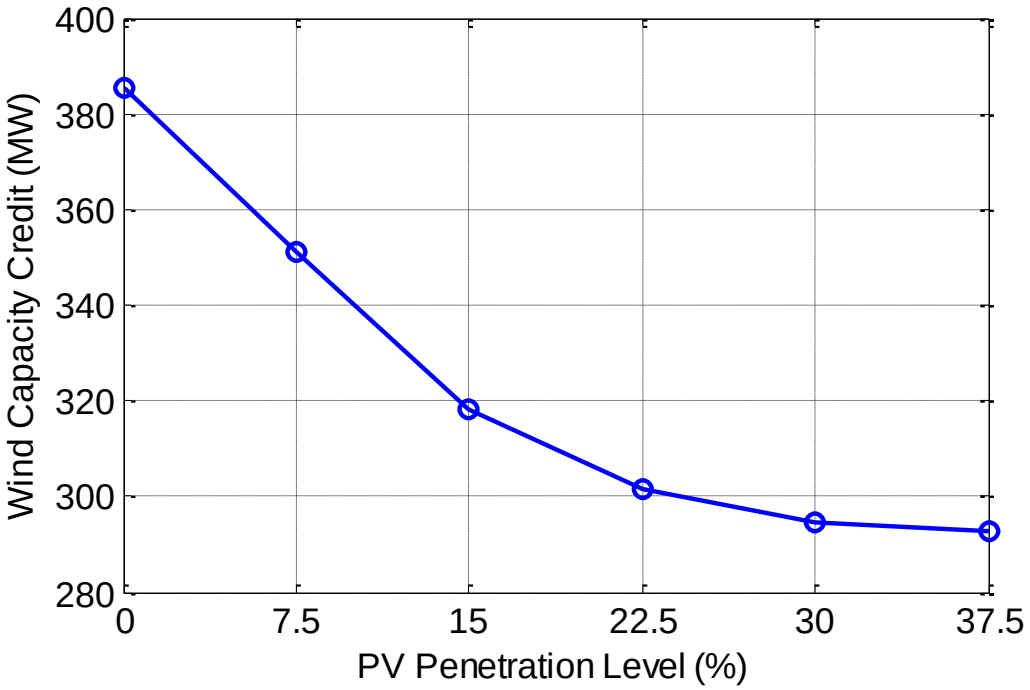

Figure 6.13. Wind capacity credit for different installed PV levels

6.4.1. Wind Profile Impact

As mentioned before, the impact of solar energy on the reliability benefit of wind farms can be related not only to the level of PV generation but also to the correlations between wind regime and PV profile. Therefore, in this section the effect of wind-load and wind-PV correlation on the capacity value of renewable resources has been investigated. For this reason, another wind regime has been assumed for South Australia. Figure 6.14 illustrates the median, quartiles, and extremes of the SA total wind generation data set using the box and whiskers plot and Figure 6.15 displays the probability of total wind generation under a new wind profile. The wind regime of the Macarthur wind farm in the state of Victoria has been selected as the new wind pattern [110].

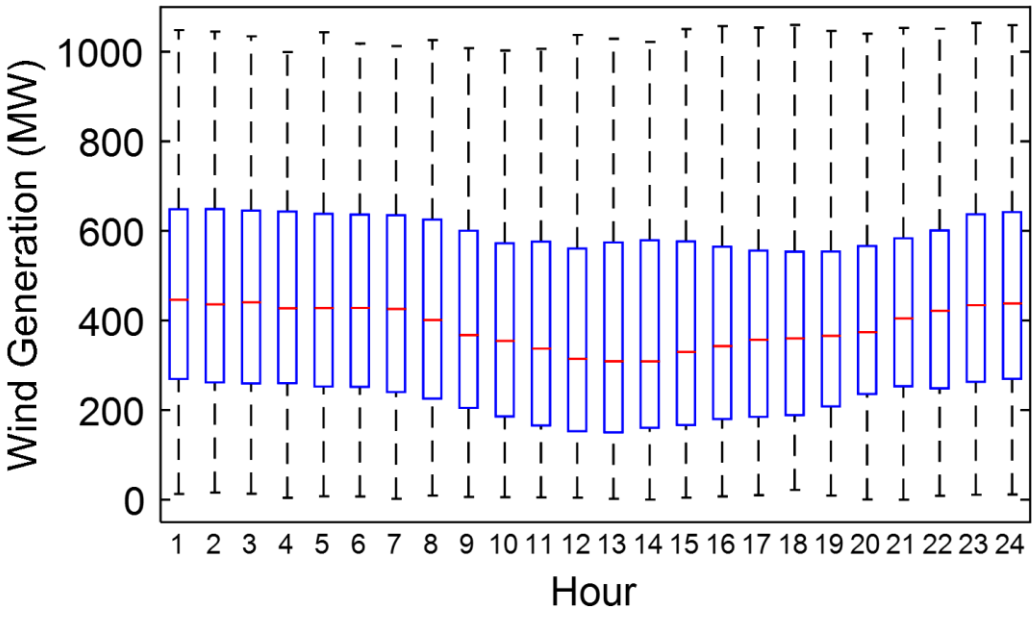

Figure 6.14. Box-and-whiskers plot for total wind generation in South Australia in 2013

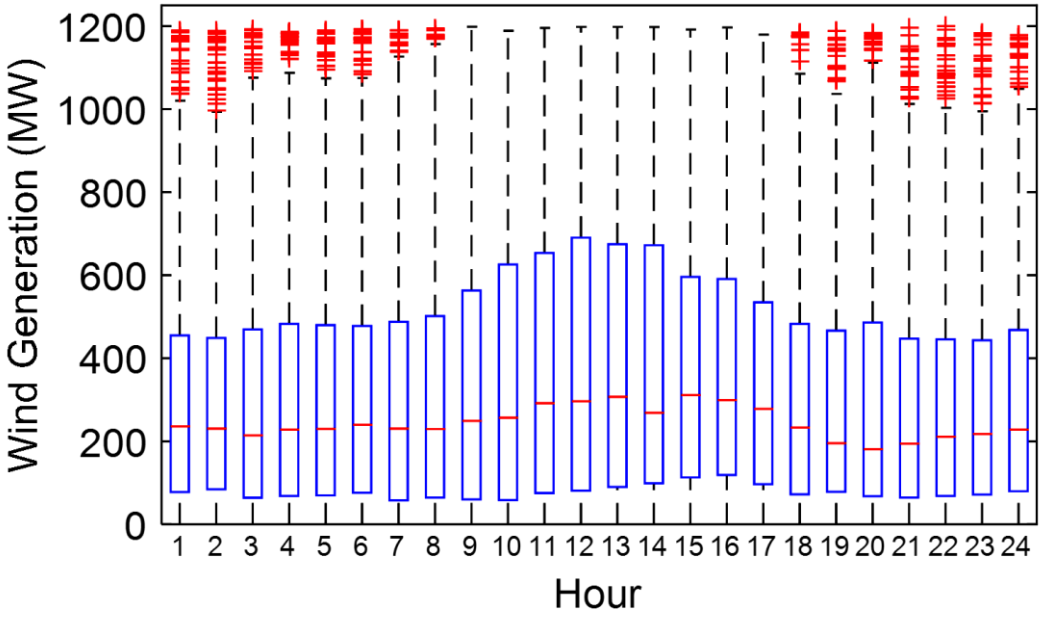

Figure 6.15. Macarthur wind power generation regime box-and-whiskers in 2013

Table 6.1: Wind regimes correlation with load profile on average monthly time scale

Correlation Coefficient	Load	Capacity Factor
SA Wind Regime	0.3141	0.384
Macarthur Wind Regime	0.2184	0.294

Table 6.1 demonstrates the capacity factor of these two wind regimes and their average monthly correlation with load profile. It can be noted that the SA wind regime has a higher capacity factor,

which means a higher mean value for its output, and this wind regime is more correlated to the system load.

The capacity value assessment method shown in Figure 6.10 has been applied to the new wind profile and results are given in Table 6.2. It shows that the effective load carrying capability of the SA wind profile is higher than the new one. The higher capacity factor of the SA wind regime can be one of the main reasons, and the higher correlation between this wind regime and load curve might be another cause. Therefore, it shows that the capacity value of wind farms not only depends on their power generation but also is related to their correlation with load profile.

Table 6.2: Effect of PV on ELCC of different wind regimes

ELCC of Wind Energy (MW)	0MW PV	500MW PV
SA Wind Regime	385	497
Macarthur Wind Regime	265	404

Furthermore, it can be seen that although the ELCC of combined wind and solar generations is higher in the SA wind profile, the added value of solar PV in the Macarthur regime is more; in this case, adding 500MW PV has improved the ELCC value by 112MW (from 385MW to 497MW), while in the second wind regime the added value of PV is 139MW. This is despite the expectation from correlation coefficient of solar generation and load data, given in Table 6.3.

Table 6.3: Average hourly correlation of PV generation and load for different wind regimes

Correlation Coefficient	**Load**	**Load- SA Wind**	**Load- Macarthur**
Solar PV	0.3652	0.4009	0.2329

This table shows correlations between PV output and the original SA load, original load minus SA wind power and original load minus wind power generated with the Macarthur regime. It was expected that due to higher correlation between PV and the second load profile (load minus SA wind), added benefit of PV should be higher in the SA wind regime, which is in contrary to the results in Table 6.2. The lower capacity factor of the Macarthur wind profile might be the main cause of this issue. As the average output power of Macarthur is lower, there will be more space for solar power to contribute to the system reliability and the added ELCC of solar energy in this case is higher. Therefore, it can be concluded that although the impact of PV generation on the reliability benefit of wind farms is related to the relation between wind profile and PV curve, the capacity factor of wind regime might affect the added value of solar generation as well.

6.4.2. Seasonal Correlation

Since the output power of solar generators is related to the season of the study, in some cases seasonal evaluations might be required. The proposed technique is also capable of capturing seasonal features of renewable resources and load data. In order to illustrate its effectiveness, a seasonal case study has been conducted for the South Australian network. Three different seasons are considered for this state: summer, spring-autumn and winter, and time-dependent cluster models for renewable generation systems, electricity demand, and exchanged power are created based on these seasons. Clustered models of the SA solar generation and load data in summer and winter are presented in Figures 6.16 - 6.19.

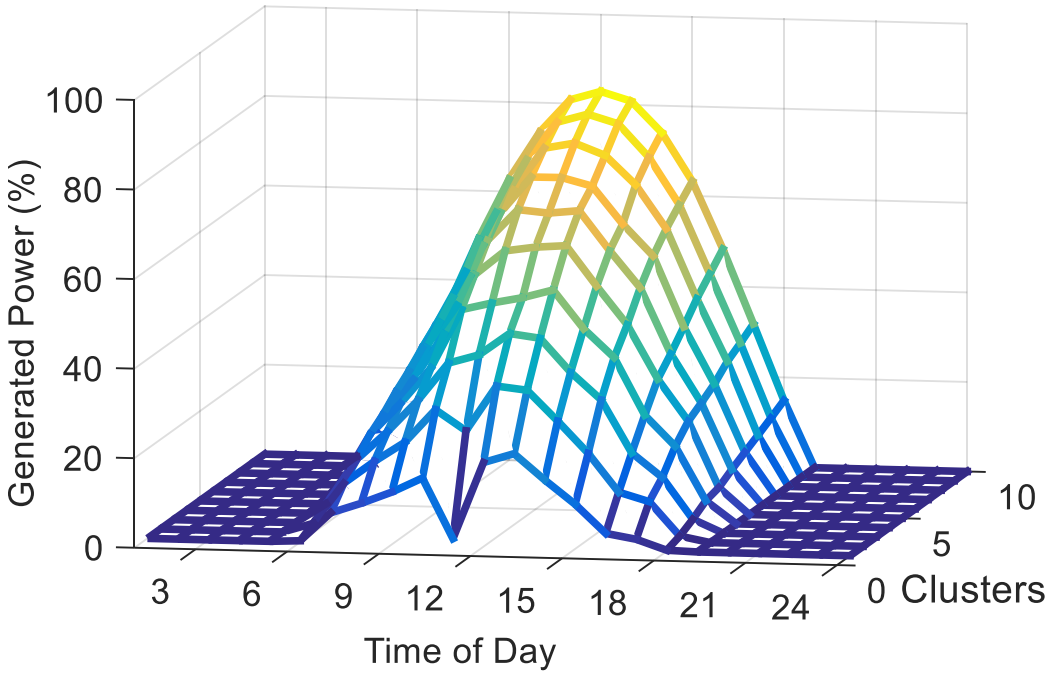

Figure 6.16. PV output model for South Australia in summer

From these figures it can be seen that load and solar generation have different profiles during summer and winter. For example, in Figure 6.16 the PV system can generate close to 85% of its installed capacity during solar peak time, while as shown in Figure 6.17, in winter its output power can go up to around 55%. In addition, these figures also show that the PV system generates power for a longer period in summer in comparison to winter. Furthermore, the range of hourly cluster values illustrates that the variation of solar energy in South Australia during summer is higher than that in winter. For instance, solar generation during midday in summer may change from 20% to 85% while in winter during the same period it varies from 15% to 55%.

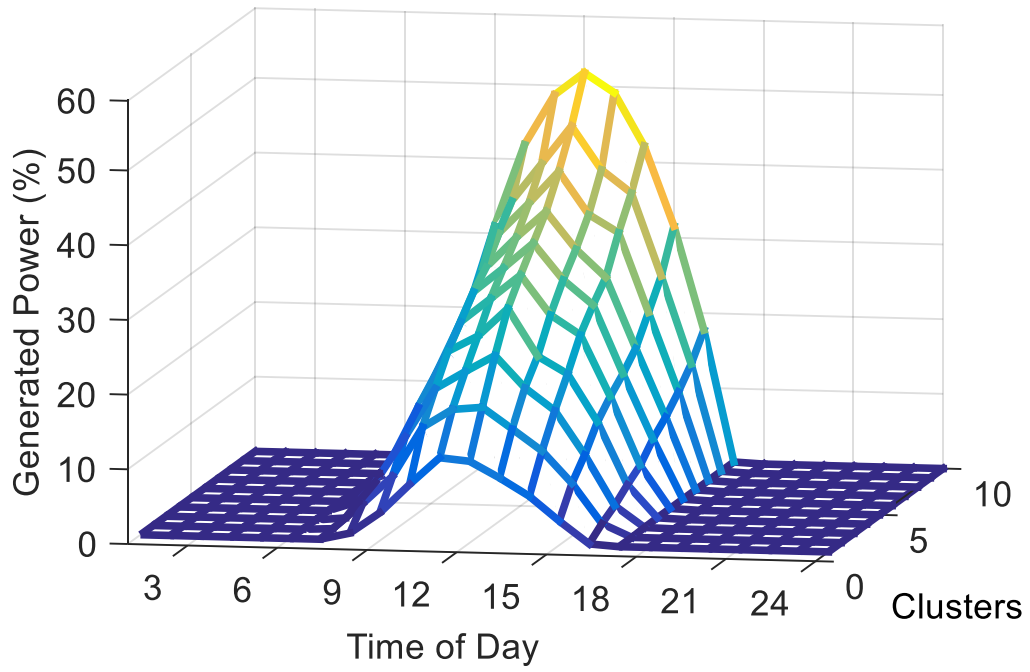

Figure 6.17. PV output model for South Australia in winter

This clustering technique is not only capable of capturing seasonal features of renewable resources but also can model seasonal patterns of electricity load. Figures 6.18 and 6.19 represent the SA load model during summer and winter. These figures show that the load patterns are different for hot and cold seasons. During summer, peak demand happens at midday, whereas the winter load model has two peak periods. The first peak is in the early morning and the second one occurs in the late evening. By comparing these two figures, it can also be concluded that the maximum demand during the hot season is generally higher than the winter period in South Australia.

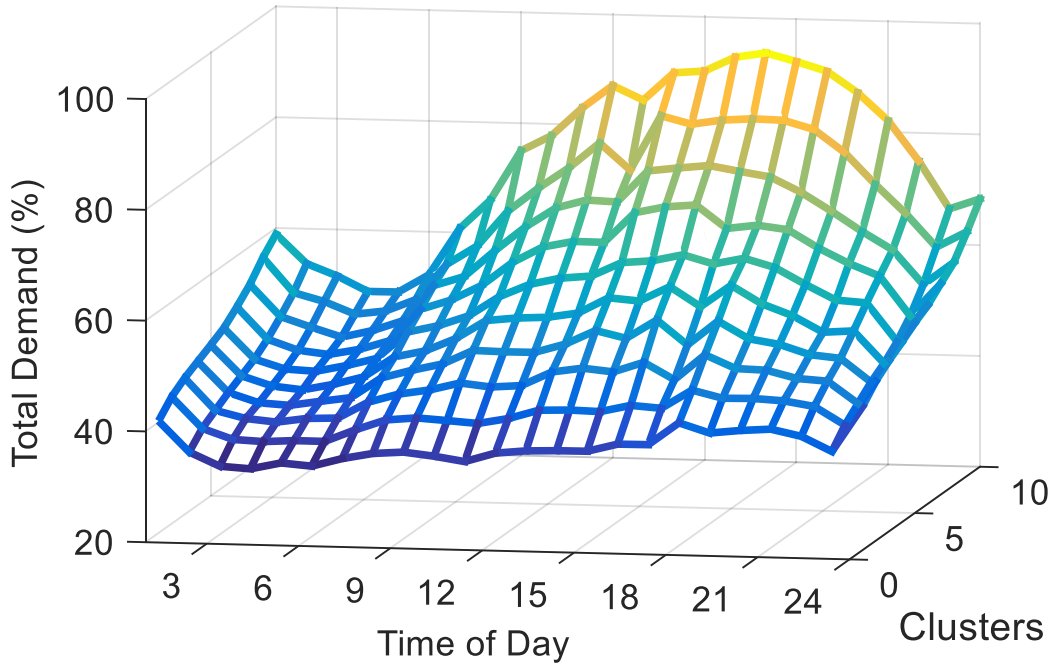

Figure 6.18. Load clustered model for South Australia in summer

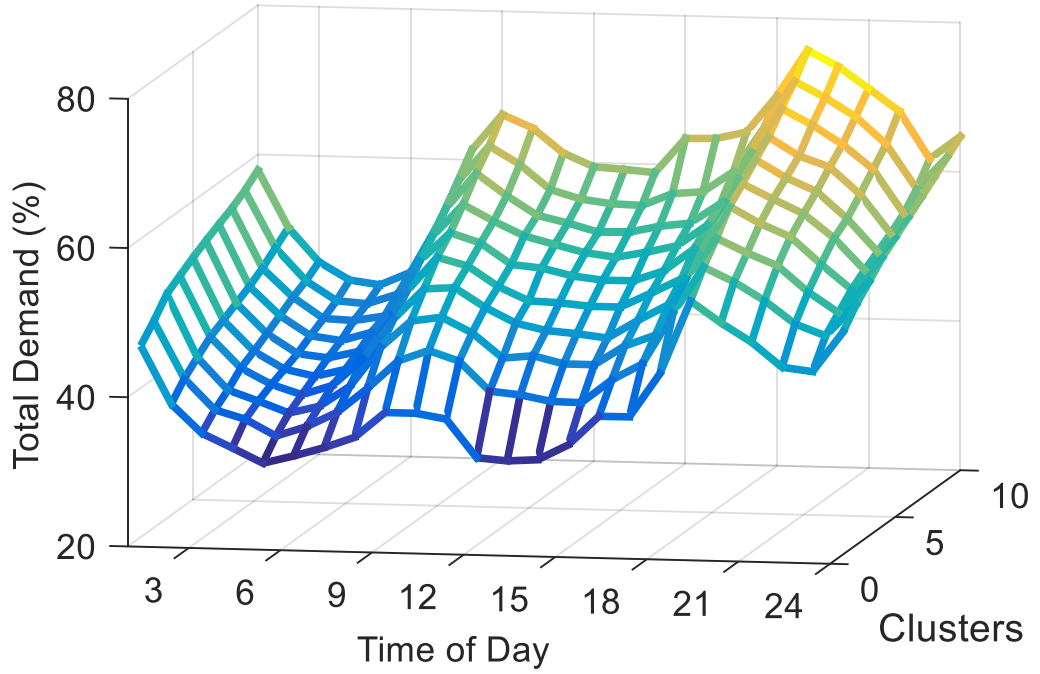

Figure 6.19. Load clustered model for South Australia in winter

After making seasonal clustered models for wind, PV, load and exchanged electricity, seasonal LOEE of the system is calculated and load carrying capabilities of wind and solar PV systems are evaluated based on the time-dependent clustering methodology proposed in Chapter 4. Results of the seasonal studies for South Australia using both the sequential Monte Carlo and the time-dependent clustering methods are summarised in Table 6.4.

Table 6.4: Seasonal reliability benefits of wind and PV generation in South Australia

ELCC (MW)		Summer	Spring-Autumn	Winter
1202MW Wind	Sequential Monte Carlo	403	338	392
	Time-dependent Cluster	391	333	409
	Error (%)	0.99	0.42	1.4
1202MW Wind + 500MW PV	Sequential Monte Carlo	561	390	415
	Time-dependent Cluster	550	382	429
	Error (%)	0.65	0.71	0.82

This table shows that the capacity value of wind farms during winter and summer is similar, while the added value of solar PV during summer is the highest and the load carrying capability of renewable resources during spring-autumn is the lowest. It can also be observed that the results of the clustering method are accurate and close to those of the sequential technique, which implies that the proposed approach is able to capture the seasonal features precisely.

6.4.3. Future Scenario

More renewable energy is projected to be integrated into the South Australian network in the near future. Table 6.5 gives an overview of the SA system in 2020. It has been predicted that the peak demand will grow to more than 3,700MW and the Heywood interconnector capacity will be expanded to 650MW. It also shows that more than 1,350MW new wind capacity is expected to be added to this system and its new solar capacity will be around 960MW by 2020 [15]. Therefore, to evaluate the future contribution of renewable energies in the generation adequacy of South Australia, two different scenarios have been studied for 2020. In the first scenario, there will be no thermal generation retirement and in the second one, 240MW of brown coal generation will be mothballed by 2020 [15].

Table 6.5: Projected 2020 South Australia System [15]

Wind (MW)	Rooftop PV (MW)	Utility PV (MW)	New Thermal (MW)	Heywood capacity (MW)
2555	560	400	321	650

Table 6.6 compares the capacity value of renewable generations for different scenarios. It can be seen that although the amount of capacity value in MW is higher in 2020, the percentage value of ELCC will be smaller than the existing system. Therefore, it can be concluded that as the penetration level of wind and PV increases, the percentage of their reliability contribution may decline. However, when thermal generators are retired this value may increase, but not as much as the mothballed capacity.

Table 6.6: Renewable energy capacity value in SA for 2020

ELCC	PV		Wind		Wind + PV	
	MW	%	MW	%	MW	%
2013 - Existing	168	33.6	385	32.1	497	29.2
2020 – No retirement	330	34.4	586	22.9	878	24.9
2020 - 240MW Brown Coal	352	36.7	641	25.1	922	26.2

It should be mentioned that the LOEE of the system increased after removing 240MW of brown coal generation, however it still meets the Australian reliability standard [121].

6.5. Summary

Like wind generation, solar PV penetration levels are growing fast in many power systems. Therefore, in order to have a proper evaluation of wind reliability contributions in systems like South Australia with fast growing PV, the impact of solar energy on the ELCC of wind farms needs to be investigated; otherwise the reliability benefit of wind energy might be overestimated. In this chapter, first, an overview of solar energy in the NEM is provided. Then the approach to model solar PV in reliability studies is explained and the impact of solar generation on the reliability contribution of wind energy at the generation level has been investigated. South Australia, which accounts for more than half of Australia's wind share and a rapidly increasing solar capacity is selected as the case study. Furthermore, the contribution of renewable generators in the future of the SA power system has been analysed and the impact of solar energy in 2020, when there are high levels of renewables integrated into this grid, is studied. In addition, seasonal impact and the influence of correlations between wind regimes and solar pattern are analysed.

It is concluded that integrating high levels of solar generation into the power system will reduce the ELCC of wind farms. However, the severity of this effect will decrease with further increases in PV generating capacity. It is also understood that as the level of wind and PV increases, the percentage value of their ELCC may decline. However, by retiring conventional generators this value may increase. In addition, it has been shown that although load carrying capability of wind farms is related to their wind profile and their dependencies with load curve, PV penetration level affects this value and the amount of influence depends on the capacity factor of wind farms and the correlation between wind and solar energy. Therefore, the correlation between wind regime, solar pattern and load profile should be considered in wind farm planning to obtain more reliability benefits from these sources of energy. However, as mentioned in previous chapters, other factors such as capacity factor, location of wind farm and transmission network constraints should be taken into account to have more accurate results.

Chapter 7

Conclusions and Recommendation for Future Research

7.1. Summary

In this thesis, wind characteristics are described and an overview of the global wind industry is provided. Wind markets in Denmark, Germany and USA, government policies, supporting targets and technical requirements for wind development in these countries are explained. In addition, an overview of the Australian wind industry is presented and the future of wind power in the Australian National Electricity Market is discussed.

Furthermore, basics of reliability assessment methods are briefly presented. Different models to represent wind power in reliability assessment and several reliability-based and estimation methods to calculate capacity value of wind are described. However, most of these methods are time-consuming or may not be able to keep the time relevancies and correlations among renewables and load datasets. Therefore, this thesis proposes a new approach to improve the existing methods and overcome their deficiencies. In the proposed framework, wind power and electricity demand are being modelled as time-dependent clusters. Fuzzy C-mean clustering method is utilized to create these clusters, which not only can capture time-dependent attributes of the datasets, but also are able to keep the correlations between them. Furthermore, a sampling method is developed based on the Cholesky decomposition and transformation techniques to select the proper hourly value from wind clusters while retaining the correlations. Afterward, the time-dependant models are applied with the state sampling Monte Carlo method to calculate the reliability indices of power systems with and without renewable generators. Then by means of these indices, the capacity value of wind is computed.

Afterward, the proposed methodology is applied to calculate load carrying capability of wind power in several regions of the NEM. First, reliability contribution of wind farms at the generation level of these systems is evaluated regardless of their transmission grid. Then, the impact of transmission system constraints and contingencies on the ELCC of wind is investigated. In addition,

the importance of interconnections and electricity exchange between these regions is studied. Moreover, coordinating hydro units with wind farms as an approach to increasing wind capacity value is assessed.

In addition, as the penetration level of solar generation is growing rapidly in the NEM regions, the shape of the electricity consumption profile in power systems and consequently the reliability level of systems are expected to change. These changes will affect the reliability contributions of wind power. Therefore, in this thesis the role of solar power in supplying demand is taken into account and the impact of solar energy on the capacity value of wind is investigated and the influence of correlations between wind regimes and solar pattern are analysed.

7.2. Main Findings and Contributions

- ***Time-dependent clustering approach***

In this thesis a time-dependent clustering method has been proposed to evaluate the reliability contribution of wind generators. This approach is not only much faster than the sequential technique but also is able to capture the time-dependent characteristics of wind units and the correlation between them. In order to demonstrate its effectiveness, this method has been applied on the IEEE reliability test system.

Results show that the new approach can estimate the ELCC of wind with an acceptable accuracy. It is also concluded that this method can be utilized for different penetration levels of wind and solar generators, and will provide precise results regardless of the wind profile and the size of renewable generators. Also, this approach is capable of capturing seasonal behaviour of power systems and renewable resources.

Furthermore, it is shown that this method is not only applicable at the generation adequacy assessment level but also can be employed in the composite system studies where the sequential techniques may require a huge amount of time and probabilistic and multistate models may not be able to keep the correlation between resources and capture their time dependencies. In addition, it is illustrated that the time-dependent clustering approach can be utilized in systems with several wind farms and solar generators without facing difficulties and losing its simplicity.

- ***Capacity value of wind power in NEM***

From the capacity value calculations, it is concluded that at the generation level, wind capacity value is related to the wind profile, correlations between wind power and electricity demand,

dependencies between wind regimes, exchanged power with neighbouring networks and the reliability level of the studied system. While, at the generation and transmission system level, in addition to these elements, topology of the transmission network, location of wind sites and transmission system constraints can affect the reliability contribution of wind farms as well. It can be realized that due to transmission system constraints and outages the reliability benefits of wind generation in this level is lower. Therefore, the amount of reduction in the capacity value of wind farms can be utilized as a criterion in network reinforcement studies. Furthermore, results show that considering tie-lines will increase the ELCC of wind units. This increment is mainly related to power flow direction and in systems with higher exportations ELCC grows more.

From hydro coordination studies, it is demonstrated that wind-hydro coordination can improve the capacity value of wind farms and the improvement is related to wind regimes and water constraints of the hydro unit. However, coordinating with higher capacities may not result in a great improvement and the capacity value of wind farms may become saturated after a certain level of the coordination capacity.

- ***Impact of solar power on the reliability contribution of wind***

The effectiveness of the proposed methodology to study the impact of solar energy is shown and it is concluded that integrating high levels of solar generation into the power system will reduce the ELCC of wind farms. However, the severity of this effect decreases with further increases in PV generating capacity and the amount of influence depends on the capacity factor of wind farms and the correlation between wind and solar energy. Therefore, considering solar generators in ELCC calculations is important, because without considering their role the reliability benefits of wind energy may be overestimated. It is also understood that as the level of wind and PV increases, the percentage value of their ELCC declines. However, by retiring conventional generators this value may increase.

It should be mentioned that there were many assumptions considered in this study with network information about different state networks. Therefore, the results presented in this thesis are the work of the PhD candidate and do not reflect the views of the network companies or the Australian Energy Market Operator. Further collaborations between the state electricity network companies, generators and AEMO is necessary to conduct an exact analysis.

All in all, since integration of wind and solar power into a power system is increasing the time-dependent methodology developed in this thesis, it can be a useful tool for power system engineers, in particular for planners to investigate the reliability contribution of these clean energies. The main

benefit of this method is its ability to keep the correlations between datasets, because without considering them the contribution of wind and solar power might be overestimated. Another advantage is its computational time. This method can be utilized by system operators to study several scenarios in a short amount of time. Although computational time may not be a critical issue in generation adequacy assessment, in transmission level studies of large systems it might become important, especially in systems with high levels of wind and PV systems. In addition, this research will provide a valuable methodology for system operators and planners to investigate the impact of solar energy while they are assessing the reliability contribution of wind farms. Because without considering this issue the reliability benefits of wind energy may be overestimated. Furthermore, this work provides an overview of wind contributions in different regions of the NEM which might be useful for Australian system operators and planners to have an estimation about how much they can rely on wind power in different states and can consider the results in future planning of renewable integrations. In addition, the methodology developed in this work can be a valuable asset for researchers working on renewable energies and can provide them an effective model to represent wind and solar power in their studies.

7.3. Future Research

A number of recommendations for future research are proposed as below:

- ***Electricity price impact***

The electricity price and the impact of market variations on the capacity value of wind can be analysed and the proposed approach can be modified to model electricity price variations in reliability assessments.

- ***A Model to consider reactive power***

New wind turbines can generate and contribute to provide reactive power in power systems. The reactive power can affect the reliability of power systems particularly at the transmission level. Therefore, a new model can be developed to represent wind farm reactive power generation and the impact of reactive power on the reliability contribution of wind farms should be investigated.

- ***Coordination with other generators***

Wind is being coordinated with hydro units in this thesis. However, other fast responding energy resources such as gas generators can also cooperate with wind farms and optimum coordination plans can be investigated to increase the ELCC value.

- ***Transmission reinforcement***

According to the result of reliability assessment, possible transmission reinforcement alternatives to improve the capacity value of wind farms can be investigated and the effective option to absorb more wind power can be specified. Moreover, the effect of applying Flexible Alternating Current Transmission System (FACTS) on the ELCC of wind farms, as another improvement option, can be assessed and an algorithm can be developed to obtain maximum reliability benefit from these devices.

- ***Congestion management***

Due to insufficiency of transmission grid capacity, congestions occur on the grid. Congestion management solutions can be studied to increase the transfer capability of the transmission system, avoiding wind energy curtailment and increasing reliability benefits of wind farms. Different congestion management schemes can be assessed to find proper methods to improve the ELCC of the wind farms in the NEM grid.

- ***Reliability-cost studies***

Reliability cost/worth assessment can be conducted for different reliability improvement plans. Then, in accordance with economic and technical constraints, some methodologies can be developed to increase the Australian wind capacity value in an effective way.

References

[1] Australian Energy Market Operator (AEMO), “Wind Integration In Electricity Grids : International Practice and Experience,” 2011.

[2] T. Ackermann and R. Kuwahata, “Lessons Learned From International Wind Integration Studies,” 2011.

[3] H. Pham, "*Handbook of Reliability Engineering*." Springer, 2003.

[4] A. Keane, M. Milligan, C. J. Dent, B. Hasche, C. D’Annunzio, K. Dragoon, H. Holttinen, N. Samaan, L. Soder, and M. O’Malley, “Capacity Value of Wind Power,” *IEEE Trans. Power Syst.*, vol. 26, no. 2, pp. 564–572, May 2011.

[5] B. Hasche, A. Keane, and M. O’Malley, “Capacity Value of Wind Power, Calculation, and Data Requirements: The Irish Power System Case,” *IEEE Trans. Power Syst.*, vol. 26, no. 1, pp. 420–430, Feb. 2011.

[6] R. Billinton and Y. Gao, “Multistate Wind Energy Conversion System Models for Adequacy Assessment Of Generating Systems Incorporating Wind Energy,” *IEEE Trans. Energy Convers.*, vol. 23, no. 1, pp. 163–170, Mar. 2008.

[7] R. Karki, P. Hu, and R. Billinton, “A Simplified Wind Power Generation Model for Reliability Evaluation,” *Energy Conversion, IEEE Transactions on*, vol. 21, no. 2. pp. 533–540, 2006.

[8] a Ghaedi, a Abbaspour, M. Fotuhi-Firuzabad, and M. Moeini-Aghtaie, “Toward a Comprehensive Model of Large-Scale DFIG-Based Wind Farms in Adequacy Assessment of Power Systems,” *Sustain. Energy, IEEE Trans.*, vol. 5, no. 1, pp. 55–63, 2014.

[9] A. P. Leite, C. L. T. Borges, and D. M. Falcão, “Probabilistic Wind Farms Generation Model for Reliability Studies Applied to Brazilian Sites,” *IEEE Trans. Power Syst.*, vol. 21, no. 4, pp. 1493–1501, 2006.

[10] W. Wangdee and R. Billinton, “Considering Load-Carrying Capability and Wind Speed Correlation of WECS in Generation Adequacy Assessment,” *IEEE Trans. Energy Convers.*, vol. 21, no. 3, pp. 734–741, Sep. 2006.

[11] R. Billinton and R. Karki, “Composite System Adequacy Assessment Incorporating Large-Scale Wind Energy Conversion Systems Considering Wind Speed Correlation,” *IEEE Trans. Power Syst.*, vol. 24, no. 3, pp. 1375–1382, Aug. 2009.

[12] H. Kim and C. Singh, “Three Dimensional Clustering In Wind Farms With Storage for Reliability Analysis,” *2013 IEEE Grenoble Conf. PowerTech, Powertech 2013*, 2013.

[13] Z. Qin, W. Li, and X. Xiong, “Incorporating Multiple Correlations Among Wind Speeds, Photovoltaic Powers and Bus Loads in Composite System Reliability Evaluation,” *Appl. Energy*, vol. 110, pp. 285–294, Oct. 2013.

[14] M. a. Abdullah, K. M. Muttaqi, A. P. Agalgaonkar, and D. Sutanto, “A Noniterative Method

To Estimate Load Carrying Capability Of Generating Units in a Renewable Energy Rich Power Grid," *IEEE Trans. Sustain. Energy*, vol. 5, no. 3, pp. 854–865, 2014.

[15] Australian Energy Market Operator (AEMO), "Integrating Renewable Energy - Wind Integration Studies Report," 2013. .

[16] G. Zini, C. Mangeant, and J. Merten, "Reliability of Large-Scale Grid-Connected Photovoltaic Systems," *Renew. Energy*, vol. 36, no. 9, pp. 2334–2340, Sep. 2011.

[17] R. M. Moharil and P. S. Kulkarni, "Reliability Analysis Of Solar Photovoltaic System Using Hourly Mean Solar Radiation Data," *Sol. Energy*, vol. 84, no. 4, pp. 691–702, Apr. 2010.

[18] P. Zhang, W. Li, S. Li, Y. Wang, and W. Xiao, "Reliability Assessment of Photovoltaic Power Systems: Review of Current Status and Future Perspectives," *Appl. Energy*, vol. 104, pp. 822–833, Apr. 2013.

[19] M. a. Abdullah, a. P. Agalgaonkar, and K. M. Muttaqi, "Assessment of Energy Supply and Continuity of Service in Distribution Network With Renewable Distributed Generation," *Appl. Energy*, vol. 113, pp. 1015–1026, Jan. 2014.

[20] R. Yan, T. K. Saha, N. Modi, N.-A. Masood, and M. Mosadeghy, "The Combined Effects of High Penetration of Wind And Pv on Power System Frequency Response," *Appl. Energy*, vol. 145, pp. 320–330, 2015.

[21] Global Wind Energy Council (GWEC), "Global Wind Report - Annual Market Update 2014," 2014.

[22] Australian Energy Market Operator (AEMO), "2011 Electricity Statement of Opportunities for The National Electricity Market," 2011.

[23] Department of the Environment, "The Renewable Energy Target (RET) Scheme." [Online]. Available: http://www.environment.gov.au/climate-change/renewable-energy-target-scheme. [Accessed: 01-Aug-2015].

[24] Australian Energy Market Operator (AEMO), "National Transmission Network Development Plan for The National Electricity Market," 2011.

[25] Australian Energy Market Operator (AEMO), "2012 Electricity Statement of Opportunities for The National Electricity Market," 2012.

[26] T. Ackermann, "*Wind Power in Power Systems*". John Wiley & Sons, 2012.

[27] "Aneroid Energy Website." [Online]. Available: http://energy.anero.id.au/. [Accessed: 01-Aug-2015].

[28] "Vestas Wind Systems." [Online]. Available: http://www.vestas.com/en/media/brochures.aspx. [Accessed: 01-Oct-2012].

[29] Global Wind Energy Council (GWEC), "Global Wind Statistics 2014," 2015.

[30] Global Wind Energy Council (GWEC), "Global Wind Energy Outlook 2014," 2014.

[31] Danish Wind Industry Association, “Statistics on The Development of Wind Power in Denmark 2005-2014.” [Online]. Available: http://www.windpower.org/en/knowledge/statistics/the_danish_market.html. [Accessed: 01-Jun-2015].

[32] A. Neslen, “Wind Power Keep It in The Ground,” *theguardian*, 10-Jul-2015.

[33] Danish Energy Agency, “Our Future Energy,” 2011.

[34] European network of transmission system operators for electricity (ENTSO-E), “Yearly Statistics & Adequacy Retrospect 2012,” 2013.

[35] Energy Matters, “Germany Exceeds 25% Renewable Energy.” [Online]. Available: http://www.energymatters.com.au/renewable-news/germany-25percent-renewables-em4621/. [Accessed: 01-May-2015].

[36] U.S. Energy Information Administration, “Electricity Data.” [Online]. Available: http://www.eia.gov/electricity/data.cfm. [Accessed: 01-Apr-2015].

[37] American Wind Energy Association, “U.S. Wind Industry Second Quarter 2015 Market Report,” 2015.

[38] U.S. Department of Energy, “Wind Vision: A New Era for Wind Power in The United States,” 2015.

[39] Australian Energy Market Operator (AEMO), “Regional Generation Information 2014.” [Online]. Available: http://www.aemo.com.au/Electricity/Planning/Related-Information/Generation-Information. [Accessed: 01-Jun-2015].

[40] “Australian PV Institute (APVI) Solar Map, Funded by The Australian Renewable Energy Agency.” [Online]. Available: pv-map.apvi.org.au. [Accessed: 25-Aug-2015].

[41] Australian Energy Market Operator (AEMO), “2012 National Transmission Network Development Plan,” 2012.

[42] Australian Energy Market Operator (AEMO), “2015 National Electricity Forecasting Report Overview,” 2015.

[43] Renewables SA, “Renewable Energy Resource Maps.” [Online]. Available: http://www.renewablessa.sa.gov.au/investor-information/resources. [Accessed: 10-Jun-2015].

[44] Clean Energy Council, “Renewable Energy Target.” [Online]. Available: http://www.cleanenergycouncil.org.au/policy-advocacy/renewable-energy-target.html. [Accessed: 01-Aug-2015].

[45] R. Billinton and W. Li, "*Reliability Assessment of Electric Power Systems Using Monte Carlo Methods"*. New York: Plenum Press, New York, 1994.

[46] M. Čepin, "*Assessment of Power System Reliability"*. London: Springer London, 2011.

[47] P. Hu, “Reliability Evaluation of Electric Power Systems Including Wind Power and Energy

Storage," University of Saskatchewan, 2009.

[48] L. M. De Carvalho, R. A. González-Ferńandez, A. M. Leite Da Silva, M. A. Da Rosa, and V. Miranda, "Simplified Cross-Entropy Based Approach For Generating Capacity Reliability Assessment," *IEEE Trans. Power Syst.*, vol. 28, no. 2, pp. 1609–1616, 2013.

[49] R. Billinton and R. N. Allan, "*Reliability Evaluation of Engineering Systems"*. Plenum Press, 1992.

[50] R. N. Allan and Billinton, "*Reliability Evaluation of Power Systems"*, vol. 11. Springer Science & Business Media, 2013.

[51] A. Calsetta, P. Albrecht, V. Cook, R. Ringlee, and J. Whooley, "A Four-State Model For Estimate of Outage Risk for Units in Peaking Service," *IEEE Trans. Power Appar. Syst.*, vol. PAS-91, no. 2, pp. 618–627, Mar. 1972.

[52] G. M. Masters, "*Renewable and Efficient Electric Power Systems*." Hoboken: Wiley, 2013.

[53] X. Li and M. Ding, "Load Model Based on Integrative K-means Clustering For Reliability Evaluation in Operational Planning," *2010 Asia-Pacific Power Energy Eng. Conf.*, pp. 1–4, 2010.

[54] J. C. Bezdek, R. Ehrlich, and W. Full, "FCM: The Fuzzy C-Means Clustering Algorithm," *Comput. Geosci.*, vol. 10, no. 2–3, pp. 191–203, 1984.

[55] N. Anuar and Z. Zakaria, "Cluster Validity Analysis For Electricity Load Profiling," *2010 IEEE Int. Conf. Power Energy*, pp. 35–38, Nov. 2010.

[56] S. Gilani, H. Afrakhte, and M. Ghadi, "Probabilistic Method for Optimal Placement of Wind-Based Distributed Generation With Considering Reliability Improvement And Power Loss Reduction," the 4th Conference on *Thermal Power Plants (CTPP),Tehran*, 2012.

[57] S. Bidoki, N. Mahmoudi-Kohan, and S. Gerami, "Comparison of Several Clustering Methods in The Case of Electrical Load Curves Classification," *2011 16th Conf. Electr. Power Distrib. Networks (EPDC), 19-20 April*, 2011.

[58] M. Masood Ahmad, A. Debs, and Y. Wardi, "Estimation of The Derivatives of Generation System Reliability Indices in Monte Carlo Simulation," *IEEE Trans. Power Syst.*, vol. 8, no. 4, pp. 1448–1454, 1993.

[59] R. Billinton and R. Karki, "Application of Monte Carlo Simulation to Generating System Well-Being Analysis," *IEEE Trans. Power Syst.*, vol. 14, no. 3, pp. 1172–1177, 1999.

[60] C. Borges and D. Falcao, "Power System Reliability by Sequential Monte Carlo Simulation on Multicomputer Platforms," *Vector Parallel Process. — VECPAR 2000*, pp. 242–253, 2001.

[61] R. Billinton and a. Sankarakrishnan, "A Comparison of Monte Carlo Simulation Techniques for Composite Power System Reliability Assessment," *IEEE WESCANEX 95. Commun. Power, Comput. Conf. Proc.*, vol. 1, no. 95, pp. 145–150, 1995.

[62] C. Grigg, P.Wong, P. Albrecht, R Allan, M. Bhavaraju, R. Billinton, O. Chen, C. Fong, S.

Haddad, S. Kuruganty, R. M. W. U, D. Patton, N. Rau, D. Reppen, K. Schneider, M. Singh, and Shaliidehpour. C., “The IEEE Reliability Test System - 1996,” *IEEE Trans. Power Syst.*, vol. 14, no. 3, pp. 1010–1020, 1999.

[63] A. K. Verma, A. Srividya, and D. R. Karanki, "*Reliability and Safety Engineering"*. Springer Series in Reliability Engineering, 2010.

[64] Y. Li, “Bulk System Reliability Evaluation in a Deregulated Power Industry,” University of Saskatchewan, 2003.

[65] W. Li, "*Risk Assessment of Power Systems: Models, Methods, and Applications*." Hoboken, NJ, USA: John Wiley & Sons, Inc., 2004.

[66] R. D. Zimmerman, C. E. Murillo-sánchez, and R. J. Thomas, “MATPOWER: Steady-State Operations, Planning, and Analysis Tools for Power Systems Research and Education,” *Power Systems, IEEE Transactions on*, vol. 26, no. 1. pp. 12–19, 2011.

[67] A. Sankarakrishnan and R. Billinton, “Sequential Monte Carlo Simulation for Composite Power System Reliability Analysis with Time Varying Loads,” *IEEE Trans. Power Syst.*, vol. 10, no. 3, pp. 1540–1545, 1995.

[68] C. D’Annunzio and S. Santoso, “Noniterative Method to Approximate the Effective Load Carrying Capability of a Wind Plant,” *IEEE Trans. Energy Convers.*, vol. 23, no. 2, pp. 544–550, Jun. 2008.

[69] M. Milligan and K. Porter, “The Capacity Value of Wind in the United States: Methods and Implementation,” *Electr. J.*, vol. 19, no. 2, pp. 91–99, Mar. 2006.

[70] R. Billinton, H. Chen, and R. Ghajar, “Time-Series Models for Reliability Evaluation of Power Systems Including Wind Energy,” *Microelectron. Reliab.*, vol. 36, no. 9, pp. 1253–1261, Sep. 1996.

[71] Z. Qin, W. Li, and X. Xiong, “Estimating Wind Speed Probability Distribution Using Kernel Density Method,” *Electr. Power Syst. Res.*, vol. 81, no. 12, pp. 2139–2146, Dec. 2011.

[72] Dan Ke, Wenhui Shi, Zhaohong Bie, Chun Liu, Xiaoxue Rong, and Wen Sun, “Probability Modeling on Multiple Time Scales of Wind Power Based on Wind Speed Data,” in *2014 International Conference on Power System Technology*, 2014, pp. 2590–2595.

[73] C. Sun, Z. Bie, M. Xie, and G. Ning, “Effects of Wind Speed Probabilistic and Possibilistic Uncertainties on Generation System Adequacy,” *IET Gener. Transm. Distrib.*, vol. 9, no. 4, pp. 339–347, Mar. 2015.

[74] Z. Qin, W. Li, and X. Xiong, “Generation System Reliability Evaluation Incorporating Correlations of Wind Speeds With Different Distributions,” *IEEE Trans. Power Syst.*, vol. 28, no. 1, pp. 551–558, 2013.

[75] L. Garver, “Effective Load Carrying Capability of Generating Units,” *IEEE Trans. Power Appar. Syst.*, vol. PAS-85, no. 8, pp. 910–919, Aug. 1966.

[76] P. E. O. Aguirre, C. J. Dent, G. P. Harrison, and J. W. Bialek, “Realistic Calculation of Wind Generation Capacity Credits,” in *Integration of Wide-Scale Renewable Resources Into the*

Power Delivery System, 2009 CIGRE/IEEE PES Joint Symposium, 2009, pp. 1–8.

[77] M. Milligan and K. Porter, "Determining the Capacity Value of Wind : An Updated Survey of Methods and Implementation," *Proc. AWEA Wind. 2008, Houston, TX*, 2008.

[78] R. Billinton and Dange Huang "Incorporating Wind Power in Generating Capacity Reliability Evaluation Using Different Models," *IEEE Trans. Power Syst.*, vol. 26, no. 4, pp. 2509–2517, Nov. 2011.

[79] A. S. Dobakhshari and M. Fotuhi-Firuzabad, "A Reliability Model of Large Wind Farms for Power System Adequacy Studies," *IEEE Trans. Energy Convers.*, vol. 24, no. 3, pp. 792–801, Sep. 2009.

[80] Y. Gao and R. Billinton, "Adequacy Assessment of Generating Systems Containing Wind Power Considering Wind Speed Correlation," *IET Renew. Power Gener.*, vol. 3, no. 2, p. 217, 2009.

[81] R. Billinton and Y. Cui, "Reliability Evaluation of Small Stand-Alone Wind Energy Conversion Systems Using A Time Series Simulation Model," *IEE Proc. - Gener. Transm. Distrib.*, vol. 150, no. 1, p. 96, 2003.

[82] R. Karki, S. Thapa, and R. B. Billinton, "A Simplified Risk-Based Method for Short-Term Wind Power Commitment," *IEEE Trans. Sustain. Energy*, vol. 3, no. 3, pp. 498–505, Jul. 2012.

[83] R. Billinton and W. Wangdee, "Reliability-Based Transmission Reinforcement Planning Associated with Large-Dcale Wind Farms," *IEEE Trans. Power Syst.*, vol. 22, no. 1, pp. 34–41, Feb. 2007.

[84] V. Lo Brano, A. Orioli, G. Ciulla, and S. Culotta, "Quality of Wind Speed Fitting Distributions for the Urban Area of Palermo, Italy," *Renew. Energy*, vol. 36, no. 3, pp. 1026–1039, Mar. 2011.

[85] N. Masseran, "Evaluating Wind Power Density Models and Their Statistical Properties," *Energy*, vol. 84, pp. 533–541, May 2015.

[86] M. D. Alexandrov and A. A. Lacis, "A New Three-Parameter Cloud/Aerosol Particle Size Distribution Based on The Generalized Inverse Gaussian Density Function," *Appl. Math. Comput.*, vol. 116, no. 1–2, pp. 153–165, Nov. 2000.

[87] R. Calif and F. G. Schmitt, "Modeling of Atmospheric Wind Speed Sequence Using a Lognormal Continuous Stochastic Equation," *J. Wind Eng. Ind. Aerodyn.*, vol. 109, pp. 1–8, Oct. 2012.

[88] E. C. Morgan, M. Lackner, R. M. Vogel, and L. G. Baise, "Probability Distributions for Offshore Wind Speeds," *Energy Convers. Manag.*, vol. 52, no. 1, pp. 15–26, 2011.

[89] P. Giorsetto and K. Utsurogi, "Development of a New Procedure for Reliability Modeling of Wind Turbine Generators," *IEEE Trans. Power Appar. Syst.*, vol. PAS-102, no. 1, pp. 134–143, Jan. 1983.

[90] S. H. Pishgar-Komleh, A. Keyhani, and P. Sefeedpari, "Wind Speed and Power Density

Analysis Based on Weibull and Rayleigh Distributions (A Case Study: Firouzkooh County of Iran)," *Renew. Sustain. Energy Rev.*, vol. 42, pp. 313–322, Feb. 2015.

[91] F. Vallee, J. Lobry, and O. Deblecker, "Impact of the Wind Geographical Correlation Level for Reliability Studies," *IEEE Trans. Power Syst.*, vol. 22, no. 4, pp. 2232–2239, 2007.

[92] F. Vallee, J. Lobry, and O. Deblecker, "System Reliability Assessment Method for Wind Power Integration," *IEEE Trans. Power Syst.*, vol. 23, no. 3, pp. 1288–1297, Aug. 2008.

[93] S. H. Jangamshetti and V. G. Rau, "Site Matching of Wind Turbine Generators: A Case Study," *IEEE Trans. Energy Convers.*, vol. 14, no. 4, pp. 1537–1543, 1999.

[94] J. Wang, S. Qin, S. Jin, and J. Wu, "Estimation Methods Review and Analysis of Offshore Extreme Wind Speeds and Wind Energy Resources," *Renew. Sustain. Energy Rev.*, vol. 42, pp. 26–42, Feb. 2015.

[95] W. Wangdee and R. Billinton, "Reliability Assessment of Bulk Electric Systems Containing Large Wind Farms," *Int. J. Electr. Power Energy Syst.*, vol. 29, no. 10, pp. 759–766, Dec. 2007.

[96] D. Gerbec, S. Gašperi, I. Mon, and F. Gubina, "Determining the Load Profiles of Consumers Based on Fuzzy Logic and Probability Neural Networks," *IEE Proc. - Gener. Transm. Distrib.*, vol. 151, no. 3, p. 395, 2004.

[97] M. Ghofrani, A. Arabali, M. Etezadi-Amoli, and M. Fadali, "Energy Storage Application for Performance Enhancement of Wind Integration," *IEEE Trans. Power Syst.*, vol. 28, no. 4, pp. 4803–4811, 2013.

[98] Y. Y.-Y. Hong and R.-C. R. Lian, "Optimal Sizing of Hybrid Wind/PV/Diesel Generation in a Stand-Alone Power System Using Markov-Based Genetic Algorithm," *IEEE Trans. Power Deliv.*, vol. 27, no. 2, pp. 640–647, Apr. 2012.

[99] D. J. Ketchen and C. L. Shook, "The Application of Cluster Analysis in Strategic Management Research: An Analysis and Critique," *Strateg. Manag. J.*, vol. 17, no. 6, pp. 441–458, 1996.

[100] J. Wen, Y. Zheng, and F. Donghan, "A Review on Reliability Assessment for Wind Power," *Renew. Sustain. Energy Rev.*, vol. 13, no. 9, pp. 2485–2494, Dec. 2009.

[101] D. A. Bechrakis and P. D. Sparis, "Correlation of Wind Speed Between Neighboring Measuring Stations," *IEEE Trans. Energy Convers.*, vol. 19, no. 2, pp. 400–406, Jun. 2004.

[102] A. Feijóo, D. Villanueva, J. L. Pazos, and R. Sobolewski, "Simulation of Correlated Wind Speeds: A Review," *Renew. Sustain. Energy Rev.*, vol. 15, no. 6, pp. 2826–2832, Aug. 2011.

[103] V. Madar, "Direct Formulation to Cholesky Decomposition of a General Nonsingular Correlation Matrix.," *Stat. Probab. Lett.*, vol. 103, pp. 142–147, Aug. 2015.

[104] C. Jinfu, C. Defu, S. Dongyuan, D. Xianzhong, and L. Gang, "Probabilistic Assessment of Available Transfer Capability Considering Spatial Correlation in Wind Power Integrated System," *IET Gener. Transm. Distrib.*, vol. 7, no. 12, pp. 1527–1535, Dec. 2013.

[105] L. Devroye, *"Non-Uniform Random Variate Generation"*. Springer-Verlag, 1986.

[106] M. Lovric, Ed., "*International Encyclopedia of Statistical Science*." Berlin, Heidelberg: Springer Berlin Heidelberg, 2011.

[107] W. Wangdee, W. Li, W. Shum, and P. Choudhury, "Assessing Transfer Capability Requirement for Wind Power Generation Using a Combined Deterministic and Probabilistic Approach," in *2009 IEEE Power & Energy Society General Meeting*, 2009, pp. 1–8.

[108] W. Wangdee and R. Billinton, "Probing the Intermittent Energy Resource Contributions From Generation Adequacy and Security Perspectives," *IEEE Trans. Power Syst.*, vol. 27, no. 4, pp. 2306–2313, Nov. 2012.

[109] R. D. Zimmerman, C. E. Murillo-sánchez, R. J. Thomas, L. Fellow, and A. M. Atpower, "MATPOWER : Steady-State Operations , Systems Research and Education," *IEEE Trans. Power Syst.*, vol. 26, no. 1, pp. 12–19, 2011.

[110] "NEMWEB database." [Online]. Available: www.nemweb.com.au. [Accessed: 01-Nov-2014].

[111] "Metering Dynamics Operating Regions." [Online]. Available: https://www.meteringdynamics.com.au/about-us/operating-regions/. [Accessed: 01-Sep-2015].

[112] Australian Energy Market Operator (AEMO), "AEMO Aggregated Price and Demand Data Files." [Online]. Available: http://www.aemo.com.au/Electricity/Data/Price-and-Demand. [Accessed: 01-Oct-2014].

[113] Australian Energy Market Operator (AEMO), "2013 Electricity Statement of Opportunities," 2013.

[114] Clean Energy Regulator, "Small-Scale Installations by Postcode." [Online]. Available: http://ret.cleanenergyregulator.gov.au/REC-Registry/Data-reports. [Accessed: 01-Oct-2014].

[115] Australian Energy Market Operator (AEMO), "Interconnectors Capabilities," 2014.

[116] "ElectraNet Network Maps and Statistics." [Online]. Available: http://www.electranet.com.au/network/network-maps-and-statistics/. [Accessed: 01-Sep-2015].

[117] "2015 NEM Regional Boundaries Map." [Online]. Available: http://www.aemo.com.au/Maps-and-Multimedia. [Accessed: 01-Sep-2015].

[118] Australian Energy Market Operator (AEMO), "Electricity Statement of Opportunities 2014," 2014.

[119] Australian Energy Market Commission Reliability Panel, "Reliability Standard and Reliability Settings Review 2010," vol. Final Repo, no. 30 April 2010, Sydney.

[120] "AusNet Electricity Network." [Online]. Available: http://www.ausnetservices.com.au/Electricity.html. [Accessed: 01-Sep-2015].

[121] Australian Energy Market Commission Reliability Panel, “Reliability Standard and Reliability Settings Review 2014,” 2014.

[122] TransGrid, “NSW Transmission Annual Planning Report 2015,” 2015.

[123] C. Potter and M. Negnevitsky, “Very Short-Term Wind Forecasting for Tasmanian Power Generation,” *IEEE Trans. Power Syst.*, vol. 21, no. 2, pp. 965–972, May 2006.

[124] “Climate Data Online - Bureau of Meteorology.” [Online]. Available: http://www.bom.gov.au/climate/data-services/. [Accessed: 01-Nov-2014].

[125] TasNetworks, “About TasNetworks.” [Online]. Available: http://www.tasnetworks.com.au/about-us/corporate-profile/about-tasnetworks. [Accessed: 01-Sep-2015].

[126] R. Karki, P. Hu, and R. Billinton, “Reliability Evaluation Considering Wind and Hydro Power Coordination,” *IEEE Trans. Power Syst.*, vol. 25, no. 2, pp. 685–693, May 2010.

[127] W. Wangdee, W. Li, and R. Billinton, “Coordinating Wind and Hydro Generation to Increase the Effective Load Carrying Capability,” in *2010 IEEE 11th International Conference on Probabilistic Methods Applied to Power Systems*, 2010, pp. 337–342.

[128] Hydro Tasmania, “Gordon Power Station Fact Sheets,” 2012.

[129] IEA-PVPS (International Energy Agency), “Snapshot of Global PV Markets 2014,” 2015.

[130] Australian Energy Market Operator (AEMO), “Rooftop PV Information Paper,” 2012.

[131] M. Fuentes, G. Nofuentes, J. Aguilera, D. L. Talavera, and M. Castro, “Application and Validation of Algebraic Methods to Predict the Behaviour of Crystalline Silicon PV Modules in Mediterranean Climates,” *Sol. Energy*, vol. 81, no. 11, pp. 1396–1408, Nov. 2007.

Appendix A:

IEEE Reliability Test System

Table A.1: General data of IEEE-RTS

Total Installed Capacity	Annual Peak Load
3405 MW	2850 MW

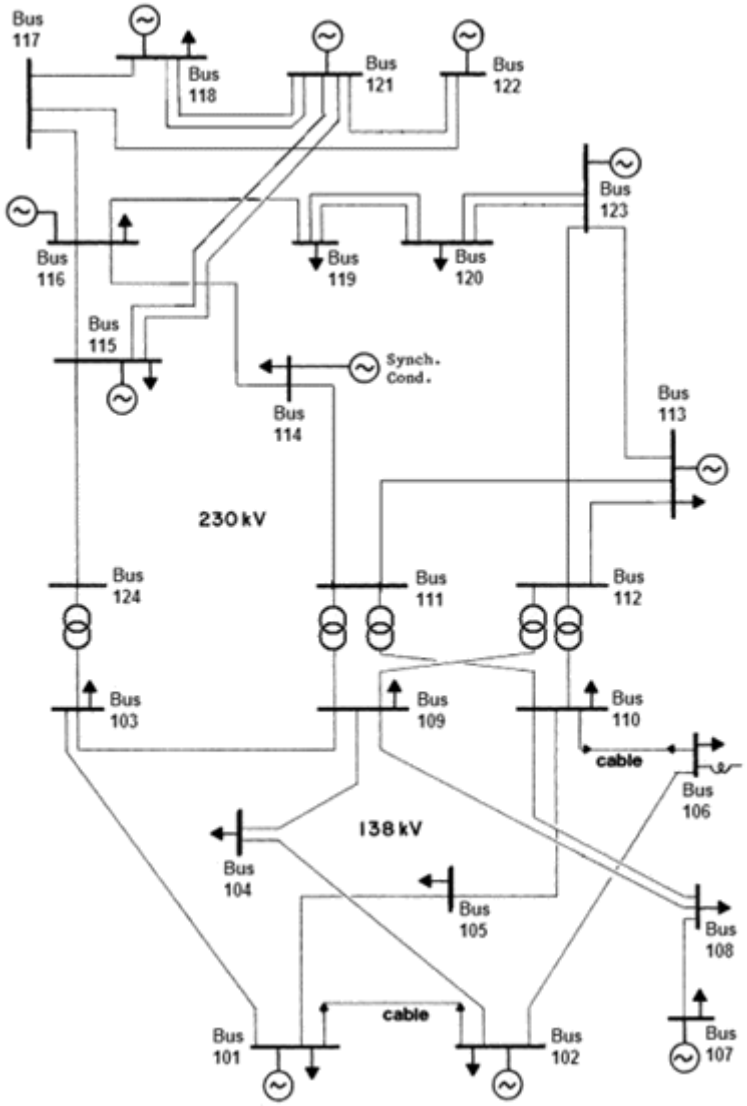

Figure A.1. IEEE reliability test system

Table A.2: Hourly Peak Load in Percent of Daily Peak

	winter weeks		summer weeks		spring/fall weeks	
	1 -8 & 44 - 52		18 -30		9-17 & 31 - 43	
Hour	Weekday	Weekend	Weekday	Weekend	Weekday	Weekend
12-1 am	67	78	64	74	63	75
1-2	63	72	60	70	62	73
2-3	60	68	58	66	60	69
3-4	59	66	56	65	58	66
4-5	59	64	56	64	59	65
5-6	60	65	58	62	65	65
6-7	74	66	64	62	72	68
7-8	86	70	76	66	85	74
8-9	95	80	87	81	95	83
9-10	96	88	95	86	99	89
10-11	96	90	99	91	100	92
11-noon	95	91	100	93	99	94
Noon-1pm	95	90	99	93	93	91
1-2	95	88	100	92	92	90
2-3	93	87	100	91	90	90
3-4	94	87	97	91	88	86
4-5	99	91	96	92	90	85
5-6	100	100	96	94	92	88
6-7	100	99	93	95	96	92
7-8	96	97	92	95	98	100
8-9	91	94	92	100	96	97
9-10	83	92	93	93	90	95
10-11	73	87	87	88	80	90
11-12	63	81	72	80	70	85

Table A.3:Daily load in Percent of Weekly Peak

Day	Mon	Tue	Wed	Thu	Fri	Sat	Sun
Peak Load	93	100	98	96	94	77	75

Table A.4: Weekly Peak Load in Percent of Annual Peak

Week	Peak Load	Week	Peak Load
1	86.2	27	75.5
2	90.0	28	81.6
3	87.8	29	80.1
4	83.4	30	88.0
5	88.0	31	72.2
6	84.1	32	77.6
7	83.2	33	80.0
8	80.6	34	72.9
9	74.0	35	72.6
10	73.7	36	70.5
11	71.5	37	78.0
12	72.7	38	69.5
13	70.4	39	72.4
14	75.0	40	72.4
15	72.1	41	74.3
16	80.0	42	74.4
17	75.4	43	80.0
18	83.7	44	88.1
19	87.0	45	88.5
20	88.0	46	90.9
21	85.6	47	94.0
22	81.1	48	89.0
23	90.0	49	94.2
24	88.7	50	97.0
25	89.6	51	100.0
26	86.1	52	95.2

Table A.5: Generation Unit Reliability Data

Unit Size (MW)	No. of Units	Unit Type	FOR	MTTF (Hour)	MTTR (Hour)
12	5	Oil	0.02	2940	60
20	4	Oil	0.10	450	50
50	6	Hydro	0.01	1980	20
76	4	Coal	0.02	1960	40
100	3	Oil	0.04	1200	50
155	4	Coal	0.04	960	40
197	3	Oil	0.05	950	50
350	1	Coal	0.08	1150	100
400	2	Nuclear	0.12	1100	150

Appendix B:

Papers Published During This Research

Impact of PV penetration level on the capacity value of South Australian wind farms
Mehdi Mosadeghy, Ruifeng Yan, Tapan Kumar Saha
Renewable Energy, Accepted 25 July 2015, DOI:10.1016/j.renene.2015.07.072
http://www.sciencedirect.com/science/article/pii/S0960148115301671

A Time-Dependent Approach to Evaluate Capacity Value of Wind and Solar PV Generation
Mehdi Mosadeghy, Ruifeng Yan, Tapan Kumar Saha
Sustainable Energy, IEEE Transactions on, Year: 2015, Volume: PP, Issue: 99, Pages: 1 - 10, DOI: 10.1109/TSTE.2015.2478518, IEEE Early Access Articles
http://ieeexplore.ieee.org/xpl/articleDetails.jsp?arnumber=7287758

The combined effects of high penetration of wind and PV on power system frequency response
Ruifeng Yan, Tapan Kumar Saha, Nilesh Modi, Nahid-Al Masood, Mehdi Mosadeghy
Applied Energy, Volume 145, 1 May 2015, Pages 320-330
http://www.sciencedirect.com/science/article/pii/S0306261915002214

Reliability evaluation of wind farms considering generation and transmission systems
Mehdi Mosadeghy, Tapan Kumar Saha, Ruifeng Yan, Simon Bartlett
IEEE PES General Meeting 2014, DOI: 10.1109/PESGM.2014.6939156,
http://ieeexplore.ieee.org/xpl/articleDetails.jsp?arnumber=6939156

Increasing wind capacity value in Tasmania using wind and hydro power coordination
Mehdi Mosadeghy, Tapan Kumar Saha, Ruifeng Yan
IEEE PES General Meeting 2013, DOI: 10.1109/PESMG.2013.6672585
http://ieeexplore.ieee.org/xpl/articleDetails.jsp?arnumber=6672585

Reliability evaluation with wind turbines and photovoltaic panels
Angel Andres Recalde, Tapan Kumar Saha, Mehdi Mosadeghy
Transmission & Distribution Conference and Exposition - Latin America (PES T&D-LA), 2014 IEEE PES, DOI: 10.1109/TDC-LA.2014.6955214
http://ieeexplore.ieee.org/xpl/articleDetails.jsp?arnumber=6955214